The interaction between HTLV-1 Tax protein and the proteasome

Joris Hemelaar

Thesis for the degree of

Doctor of Philosophy (D.Phil.)

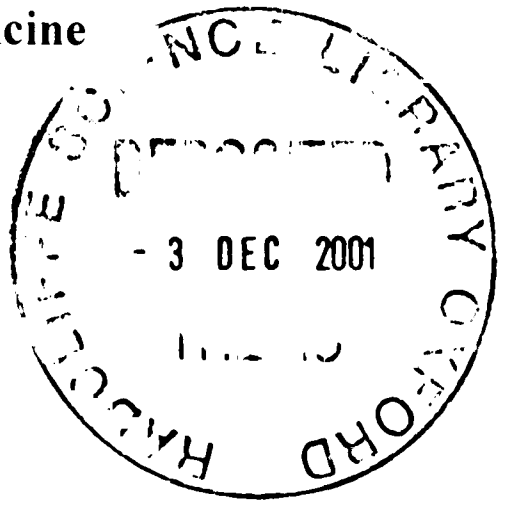
Trinity College

and

Nuffield Department of Clinical Medicine

University of Oxford

Trinity Term 2001



The interaction between HTLV-1 Tax protein and the proteasome

Joris Hemelaar, D.Phil thesis, Trinity Term 2001
Trinity College and Nuffield Department of Clinical Medicine
University of Oxford

This thesis presents studies on the interaction between the human T cell lymphotropic virus type 1 (HTLV-1) Tax protein and the 20S proteasome and the role of the interaction in cellular processes and the cytotoxic T cell (CTL) response against HTLV-1.

The rapid translocation of Tax into the nucleus is described. Tax accumulates in the nucleus and forms unique bodies involved in transcriptional activation.

It was further found that Tax associated with assembled nuclear 20S proteasomes and stimulated the chymotryptic and tryptic activities of the 20S proteasome, independent of the induction of the LMP2 and LMP7 proteasome subunits. Confocal microscopy revealed a partial colocalisation of Tax with nuclear proteasomes.

A panel of Tax mutants was generated and their subcellular localisation and association with the 20S proteasome analysed. This analysis revealed that both the N- and C-terminus of Tax play a role in proteasome binding of Tax and further showed that proteasome binding was not sufficient for nuclear localisation of Tax. Therefore, Tax probably translocates into the nucleus prior to and independent of proteasome association.

Tax specific CTL clones were generated and characterised using tetrameric MHC class I/peptide complexes. These CTL clones were used to investigate the requirements for processing and presentation of Tax for recognition by CTL. It was found that Tax was a metabolically very stable protein and that the presentation of the immunodominant Tax11-19 epitope was dependent on the transporter associated with antigen presentation (TAP), independent of the expression of LMP2 and LMP7 proteasome subunits and resistant to treatment with the proteasome inhibitor lactacystin.

It is proposed that the interaction between Tax and the 20S proteasome plays a role in Tax mediated transcriptional activation, leading to cellular activation and proliferation, and may not determine the immunodominance of Tax in the CTL response against HTLV-1.

Table of Contents

Authorship declaration 7

Acknowledgements 8

Chapter 1. Introduction 9

Preface 9
1.1. MHC class I antigen processing and presentation 10
1.1.1. Immunodominance in CTL response 10
1.2. 20S proteasome 11
1.2.1. 20S proteasome structure and assembly 12
1.2.2. Peptidase activities of the 20S proteasome 13
1.2.3. Proteasomal protein degradation and generation of peptide epitopes 14
1.2.4. Proteasome inhibitors 16
1.2.5. Other proteases implicated in antigen processing and presentation 17
1.2.6. Subcellular localisation of the proteasome 18
1.2.7. The DRiP hypothesis 20
1.3. Modulation and regulation of the proteasome 21
1.3.1. Immunoproteasome subunits LMP2, LMP7 and MECL-1 22
1.3.2. PA28 (11S) activator complex 23
1.3.3. 19S regulatory complex and the 26S proteasome 25
1.3.4. Ubiquitin conjugation 26
1.4. Viral interference with the class I processing and presentation pathway 28
1.4.1. Viral resistance to protein degradation 28
1.4.2. Interaction of viral proteins with the proteasome 29
1.5. NFκB/Rel family of transcription factors 31
1.5.1. NFκB/Rel transcription factors 31
1.5.2. IκB factors sequester NFκB in the cytoplasm 31
1.5.3. The IKK complex and NFκB activation 32
1.5.4. p105 34
1.6. Human T cell lymphotropic virus - type 1 35
1.6.1. HTLV-1 associated diseases 36
1.6.2. HTLV-1 mRNA splicing 36
1.6.3. HTLV-1 Rex protein 37
1.7. Tax 37
1.7.1. Subcellular localisation of Tax 38
1.7.2. Tax and CREB/ATF transcription factors 38
1.7.3. Tax and $p65^{SRF}$ 39
1.7.4. Tax and NFκB 39
1.7.5. Tax mediated NFκB activation by IKK complex activation 40
1.7.6. Physical interactions between Tax and NFκB/IκB factors 41
1.7.7. Tax mutants 42

1.8. Tax and disease 43
1.8.1. Tax mediated transformation 43
1.8.2. Tax in the immune response and in relation to TSP 44
1.9. Objectives of thesis 47

Chapter 2. Materials and Methods 48

2.1.General reagents 48
2.1.1. Buffers 48
2.1.2. Antibodies 49
2.2.DNA techniques 52
2.2.1. Bacterial strains and culture 52
2.2.2. Preparation of plasmid DNA 53
2.2.3. Recombinant DNA techniques 55
2.2.4. Mutagenesis 58
2.2.5. DNA sequencing 60
2.3.Tissue culture techniques 60
2.3.1. Maintenance of cell lines 61
2.3.2. Transfections 61
2.3.3. Vaccinia infection and titration 62
2.3.4. Pulse-chase metabolic labelling 64
2.3.5. Cytotoxic T cell tissue culture techniques 65
2.4.Protein techniques 68
2.4.1. Monoclonal antibody purification 68
2.4.2. Production of HLA-A2/β2m/Tax11-19 tetramer complexes 69
2.4.3. Expression and purification of Tax-6His 73
2.4.4. Separation of nuclear and cytoplasmic fractions 75
2.4.5. Immunoprecipitation 75
2.4.6. SDS-polyacrylamide gelelectrophoresis (SDS-PAGE) 76
2.4.7. Coomassie Brilliant Blue staining 78
2.4.8. Western blotting 78
2.4.9. Peptide cleavage assay 79
2.4.10. CATassay 80
2.5.Immunofluorescence techniques 80
2.5.1. FACS analysis 80
2.5.2. Indirect immunofluorescence confocal microscopy 81

Chapter 3. Nuclear localisation of HTLV-1 Tax protein 83

3.1. Introduction 83
3.2. Generation and specificity of rabbit anti-Tax sera 84
3.3. Tax expression and the effect of β-mercaptoethanol 85
3.4. Tax transactivates the HTLV-1 LTR, and the *c-fos* and IL-2Rα promoters 89
3.5. Tax is localised in the nucleus of transfected 293T cells 90
3.6. Tax colocalises with NFκB in nuclear bodies 92

3.7. Tax is only detectable in the nuclear fraction of 293T cells 94
3.8. Tax rapidly translocates into the nucleus after synthesis 96
3.9. Summary and discussion 98

Chapter 4. Interaction between HTLV-1 Tax protein and 20S proteasomes 105

4.1. Introduction 105
4.2. Purification of MCP21 antibody 106
4.3. Tax co-precipitates with 20S proteasomes 108
4.4. Tax co-precipitates with nuclear 20S proteasomes 111
4.5. Tax co-precipitated with 20S proteasomes has a slightly higher apparent molecular weight than Tax in total lysates 111
4.6. 20S proteasome fails to co-precipitate with Tax 114
4.7. Tax partially co-localises with proteasomes 116
4.8. Tax expression stimulates the chymotryptic and tryptic activities of the 20S proteasome 118
4.9. Tax does not induce LMP2 and LMP7 expression in 293T cells 122
4.10. Co-precipitation of Tax with 20S proteasomes from different cell lines 123
4.11. Expression and partial purification of recombinant Tax-6His 127
4.12. Summary and discussion 130

Chapter 5. Analysis of Tax mutants 138

5.1. Introduction 138
5.2. Generation of Tax mutants 139
5.3. Expression of Tax mutants 141
5.4. Subcellular localisation of Tax mutants 144
5.5. Analysis of proteasome binding of Tax mutants 147
5.6. Correlation between subcellular localisation, proteasome binding and transcriptional activation of Tax mutants 153
5.7. Summary and discussion 154

Chapter 6. Generation of Tax11-19 specific CTL clones 158

6.1. Introduction 158
6.2. Production of HLA-A2.01/β2m/Tax11-19 tetramer complexes 162
6.3. Generation of Tax 11-19 specific CTL clones from a CTL line 165
6.4. Analysis of CTL clones 166
6.4.1. HLA-A2/Tax 11-19 tetramer staining of CTL clones 166
6.4.2. Cytolytic activity of CTL clones 170
6.4.3. Characterisation of Vα and Vβ usage of Tax11-19 specific CTL clones 172
6.5. Summary and discussion 174

Chapter 7. Tax and MHC class I antigen processing and presentation 177

7.1. Introduction 177
7.2. Processing and presentation of Tax 182
7.2.1. Tax is a long-lived protein 182
7.2.2. Tax degradation is only marginally affected by treatment with proteasome inhibitor 184
7.2.3. Tax mobility on SDS-PAGE is affected by proteasome and isopeptidase inhibitors 186
7.2.4. Tax can be recruited to PML bodies during proteasome inhibition 188
7.2.5. Tax can be found to colocalise with proteasomes in perinuclear structures 191
7.2.6. Presentation of Tax11-19 epitope to CTL is dependent on the TAP transporter and independent of LMP2 and LMP7 proteasome subunits 193
7.2.7. Lactacystin does not block presentation of Tax 11-19 epitope to CTL 195
7.3. Tax has no apparent effect on the MHC class I antigen presentation pathway 198
7.3.1. Tax expression does not affect the degradation of influenza nucleoprotein 198
7.3.2. Tax does not affect the presentation of the 265-273 epitope of influenza nucleoprotein to CTL 200
7.3.3. Transient Tax expression in 293T cells does not affect MHC class I cell surface expression 202
7.3.4. Normal levels of MHC class I cell surface expression on HTLV-1 infected cell lines 204
7.4. Discussion 206

Chapter 8. Summary and discussion 213

8.1. Summary 213
8.2. Discussion 214
8.2.1. The role of Tax in HTLV-1 infection 214
8.2.2. Viral interference with the proteasome 219

Appendix A **Abbreviations** 222

Appendix B **Oligonucleotides** 224

Appendix C **Amino acid sequences of Tax mutants** 226

References 231

Authorship Declaration

I declare that this thesis represents my own work,

except where stated below.

It has never been submitted for any other degree.

Confocal microscopy studies were performed in collaboration with Dr. Françoise Bex at the Laboratory of Microbiology, Free University of Brussels, Brussels, Belgium.

Characterisation of Vα and Vβ usage of CTL clones was performed in collaboration with Dr. Judy Henwood, Molecular Medicine Unit, Level 6, Clinical Science Building, University of Leeds, Leeds.

Acknowledgements

Firstly, I would like to thank my mother and sister, mama and Majoie Hemelaar, for their support in difficult times. The same gratitude goes out to Bob Laterveer, for being such a good friend over a long distance.

Next I should thank Susan Daenke, who first accepted me in her lab with a Talents-grant from Holland. Did I live up to the descriptions in your "Attitudes of the Dutch"-book? I am very grateful for the trust you expressed in me by offering me the studentship to do a D.Phil. Although it was difficult at times, I never regretted accepting it. I wish you all the best in your new career!

Also many thanks go out to Andrew McMichael, for taking over supervision halfway through. Although it was sometimes hard to find a gap in your busy schedule to meet, it was always very helpful. I am also very grateful for the support you gave me in my plans for a future career.

For technical assistance and scientific discussions I have to thank numerous people in the Nuffield Department of Medicine and the Weatherall Institute of Molecular Medicine. In particular I would like to thank all the members of the Daenke-, Cerundulo-, Davis-, Phillips- and Klenerman-labs. I would like to mention here Sarah Booth, Bruce Booth, Uzi Gileadi and Simon Davis.

Financially, I should thank the Nuffic organisation and the Dutch Minister of Education for giving me the opportunity to come to Oxford. For support during my D.Phil I would like to thank the Medical Research Council, the British Society for Immunology and Trinity College.

This brings me to the Middle Common Room of Trinity College, which has been the centre of my social life over all these years. All those great people I met there over the years! Thank you all so much! I wouldn't have been writing these last words of my thesis without all of you. I would especially like to thank (in alphabetical order, as not to offend anyone!): Alun, Ben, Dougan, Filippo, Frank, Guy, Halvar, Jonas, Marina, Marisa, Murray, Naoko, Nick, Nicola, Raegan, Ryan, Sara, Sammy, Wei Yang, Wenke & Yuriy

Chapter 1

Introduction

Preface

The immune system can be divided into an innate (non-specific) and an acquired or adaptive (specific) arm. Innate immunity is a basic resistance to infectious diseases comprised of anatomical, physiological, phagocytic and inflammatory defensive barriers. Acquired immunity, on the other hand, is capable of specifically recognising and selectively eliminating foreign microorganisms and molecules. Acquired immunity consists of both humoral and cellular responses which possess the characteristics of specificity, diversity, memory and tolerance. Humoral immunity involves antibodies produced by B lymphocytes, which recognise antigens in the extracellular compartments, such as the blood or mucosa. Cellular immunity involves both $CD8^+$ T lymphocytes (cytotoxic T lymphocytes, CTLs), which monitor the intracellular compartment, and $CD4^+$ helper T lymphocytes, which assist in the priming and augmentation of both the humoral and the cellular immune responses (Kuby, 1994).

Viruses and other intracellular pathogens present a special challenge to the immune system, as the etiological agents are present within autologous cells. In general, antibodies appear to play a critical role in the defence against cytopathic viruses, whereas CTLs appear to be the crucial effector mechanism against noncytopathic viruses (Zinkernagel et al., 1996).

CTLs posses several effector functions aimed at destroying a target cell. CTLs can release perforin and granzymes, leading to target cell lysis. Furthermore, Fas ligand expression on the CTLs can induce Fas-dependent apoptosis in target cells. Lastly, CTLs can secrete cytokines (such as INF-γ and TNF-α) which can induce a set of antiviral mechanisms, including upregulation of the MHC class I pathway (Zinkernagel et al., 1996).

1.1. MHC class I antigen processing and presentation

MHC class I molecules present peptide epitopes on the cell surface for recognition by $CD8^+$ cytotoxic T lymphocytes (Germain, 1994; Rammensee et al., 1993; Townsend et al., 1986). The presented peptides (8-11 amino acids long) are generated by the degradation of endogenously synthesised nuclear and cytosolic proteins (Rock and Goldberg, 1999; Townsend et al., 1988; Townsend et al., 1985).

The multicatalytic proteinase complex called proteasome has been implicated in the degradation of most cellular proteins and the generation of the majority of the antigenic peptides (Rock et al., 1994). After their production the peptides are transported into the lumen of the endoplasmic reticulum (ER) by the transporter associated with antigen presentation (TAP) (Kelly et al., 1992; Momburg et al., 1994; Neefjes et al., 1993; Spies et al., 1992). Inside the ER the peptides form a complex with MHC class I molecules and β2 microglobulin (Townsend et al., 1989).

The current model for the assembly of MHC class I-peptide complexes is that newly synthesised class I heavy chains are bound by the chaperone calnexin. Upon binding of β2 microglobulin (β2m) to the heavy chain, calnexin is exchanged for calreticulin. Association of the class I-β2m-calreticulin complex with TAP is then mediated by tapasin. Peptide translocation by TAP eventually results in the formation of a class I-β2m-peptide complex, which dissociates from tapasin and calreticulin and is transported from the ER through the Golgi apparatus to the plasma membrane, where it is displayed for recognition by surveying CTL (Pamer and Cresswell, 1998).

1.1.1. Immunodominance in CTL response

Every pathogen contains numerous peptide epitopes that could potentially be presented to and recognised by $CD8^+$ T cells. However, only a small fraction of those potential peptides are functional *in vivo*. The restrictive selection of CTL epitopes is an aggregate effect of several steps in the MHC class I antigen processing and presentation pathway (Yewdell and Bennink, 1999).

Peptides, or suitable precursors, need to be liberated from their protein precursors, a task performed predominantly, but not exclusively, by the proteasome. During protein degradation, peptide epitopes can therefore be generated or destroyed (Beekman et al., 2000; Ben-Shahar et al., 1999; Dick et al., 1994; Luckey et al., 1998; Niedermann et al., 1995; Ossendorp et al., 1996; Yellen-Shaw et al., 1997).

Once generated in the cytosol or nucleus, the peptides need to be translocated into the ER by TAP. It has been shown that the TAP transporter is selective regarding the length and the sequence of the peptides it translocates (Momburg et al., 1994; Neefjes et al., 1993; Neisig et al., 1995).

After translocation into the ER, peptides need to bind to MHC class I molecules. The amino and carboxy termini of peptides (containing the 'anchor' residues) have to fit into the peptide-binding pockets of class I molecules. The affinity of peptides for class I molecules depends on MHC class I allele specific requirements for peptide binding motifs (Rammensee et al., 1993).

Finally the class I/peptide complex must be recognised by a T cell receptor (TCR) and trigger an immune response. This is dependent upon the diversity of the TCR repertoire, the numbers of precursor cells, their proliferative ability and their effector functions (Yewdell and Bennink, 1999).

Several comprehensive studies have indicated that all these processes contribute to the status of any given epitope in the hierarchy of immunodominance (Chen et al., 2000; Deng et al., 1997; Yewdell and Bennink, 1999).

1.2. 20S proteasome

As mentioned above, the multicatalytic proteinase complex called proteasome has been implicated in the degradation of most cellular proteins and the generation of the majority of the antigenic peptides (Rock et al., 1994).

1.2.1. 20S proteasome structure and assembly

The 20S proteasome is a multicatalytic proteinase complex (700 kDa) with a cylindrical shaped structure of 700 kDa composed of four rings, the outer two each containing seven structural α (alpha) subunits and the inner two each containing seven catalytic β (beta) subunits (Groll et al., 1997).

Only three of the seven types of β subunits, β1 (Y/delta), β2 (Z) and β5 (X/MB1) are proteolytically active. The β subunits are synthesised with an N-terminal propeptide. Proteasomes first assemble into 13-16S precursor complexes (Nandi et al., 1997). These half-proteasomes, consisting of one ring of α subunits and one ring of β subunits, remain inactive (even when the propeptides are genetically removed). The propeptide of β5 is needed for completion of proteasome assembly (combining of two half-proteasomes) and serves a chaperone-like function, which can be supplied separately. Proteasomes mature by auto-catalytically cleaving off the propeptides in a late stage of proteasome assembly, thereby exposing a catalytic threonine at the N-terminus (Baumeister et al., 1998; Chen and Hochstrasser, 1996; Yang et al., 1995). Maturation of the active subunits occurs by intrasubunit autolysis, whereas the inactive subunits are processed by the active subunits (Groll et al., 1999). The propeptides of β1 and β2 are dispensible for proteasome formation, but prevent N-acetylation, and thereby inactivation, of the catalytic threonine (Arendt and Hochstrasser, 1999). A short-lived chaperone, Ump1, is required for correct maturation of the proteasome, and is itself destroyed after activation of the proteolytic sites (Burri et al., 2000; Ramos et al., 1998). As completion of assembly and activation of the proteolytically active sites are tightly linked, this prevents formation of active sites before the hydrolytic chamber has been sealed off from the rest of the cell (Baumeister et al., 1998; Chen and Hochstrasser, 1996).

The proteasome β subunits appear prototypical of a new family of proteins referred to as the N-terminal nucleophile (Ntn) hydrolases, which are characterised by a single residue catalytic centre that is freed by the autocatalytic removal of the propeptide (Baumeister et al., 1998).

1.2.2. Peptidase activities of the 20S proteasome

The three different catalytically active subunits of the 20S proteasome are responsible for three different peptidolytic activities: β5 cleaves after hydrophobic residues (chymotryptic-like activity), β2 after basic residues (tryptic-like activity) and β1 after acidic residues (post-acidic activity; also referred to as peptidylglutamylpeptide hydrolysing (PGPH) activity and caspase-like) (Dick et al., 1998; Heinemeyer et al., 1997). Two other activities have been ascribed to the proteasome which perform cleavage after branched-chain amino acids (BrAAP activity) and after small neutral amino acids (SNAAP activity) (Orlowski et al., 1993). These cleavages are performed by one of the above three subunits depending on the context of the cleavage site (Dick et al., 1998; Heinemeyer et al., 1997). Cleavage by the 20S proteasome is ATP independent.

It was recently found that subunits of the proteasome allosterically regulate each other. Substrates of a chymotryptic-like site activated the other chymotryptic-like site and stimulated dramatically the post-acidic site. Moreover, substrates of the post-acidic site inhibited the chymotryptic-like site. As the chymotryptic-like activity is the rate-limiting activity in protein degradation, this latter effect can reduce the degradation of proteins by the 26S proteasomes. The authors proposed a "bite-chew" model in which proteins are initially cleaved by the chymotryptic-like site ("bite"), leading to activation of the post-acidic sites. This in turn leads to the temporary inhibition of the chymotryptic-like site and digestion of the fragment. When the fragments are small enough to diffuse out of the proteasome, the post-acidic site ceases to cleave and the chymotryptic-like site is reactivated and the cycle repeated (Kisselev et al., 1999). This view was subsequently modified by the finding that inhibition of the chymotryptic-like activity by a substrate for the post-acidic site did not require occupancy of the post-acidic site or hydrolysis of the substrate. These and other findings led to the

proposition of the existence of non-catalytic 'modifier' sites (Myung et al., 2001; Schmidtke et al., 2000).

Mutations in adjacent non-catalytic β subunits can affect the activity of the catalytic subunits, also indicating allosteric interactions within the proteasome complex (Baumeister et al., 1998).

1.2.3. Proteasomal protein degradation and generation of peptide epitopes

The 20S proteasome has a barrel shaped structure and the active sites of the β subunits are located inside the central chamber (Groll et al., 1997). As the openings at either end of the 20S cylinder as well as the central channel are small, protein substrates need to be unfolded and translocated into the central channel to reach the proteolytic sites (Groll et al., 2000; Ortega et al., 2000). *In vivo* the 20S proteasome core is therefore often found associated with a 19S regulatory particle which contains six ATPases (see below) (Glickman et al., 1998). Recently, direct evidence was provided that these ATPases promote substrate unfolding and translocation (Braun et al., 1999). The requirement of substrate unfolding and translocation, mediated by ATPases, explains the ATP dependency of protein degradation by the proteasome (see below).

An important aspect of proteasomal protein degradation is that it is progressive. In *in vitro* experiments, the relative amounts of the different peptide fragments generated remained the same over time, indicating that proteins were degraded progressively, without the release of protein digest intermediates (Akopian et al., 1997; Kisselev et al., 1999).

Inspection of the proteasomal cleavage fragments generated by the degradation of whole proteins showed that products range in length between 3 to 24 residues. This was the case for proteasomes from Thermoplasma acidophilum (which has 14 identical catalytic sites) as well as mammalian 20S and 26S proteasomes (which have three different pairs of catalytic sites). These results indicate a more random fashion of protein breakdown than predicted by the molecular ruler hypothesis, which assumed that the distance

between catalytic sites would determine fragment length (Akopian et al., 1997; Kisselev et al., 1999; Wenzel and Baumeister, 1995).

As proteasomal degradation produces peptide fragments, it is clear that other endo- and exo-proteases must function after the proteasome to complete the turnover of cell proteins into amino acids (Kisselev et al., 1998). Peptides have proven very hard to find in cell lysates, except for when they are associated with class I molecules (Falk et al., 1990).

Whereas the average product size after proteasomal cleavage was around 8 amino acid residues, it turned out that less than 15% of the products had the length of class I binding peptides (8-9 residues) and that two-thirds were too short to function in antigen presentation. The remaining 15% were larger than the required size of 8-9 residues and would require trimming in order to bind class I molecules (Kisselev et al., 1998; Kisselev et al., 1999).

The average size of 8 amino acids also indicated that only 10-15% of the peptide bonds were cleaved by the proteasome. It is obvious that the residue preceding the cleavage site does not alone determine where proteasomes cut larger substrates, but that it is strongly influenced by the context of the protein. Even sequences and structures far away from the actual cleavage site can have an effect (Rock and Goldberg, 1999).

Experiments in which synthetic 20-30 residue long peptides or whole proteins were subjected to cleavage by purified 20S proteasomes have shown that the proteasome is capable of directly generating antigenic peptides (Ben-Shahar et al., 1999; Dick et al., 1994; Niedermann et al., 1995). It has further highlighted the fact that the proteasome can also destroy potential epitopes (Luckey et al., 1998; Niedermann et al., 1995; Ossendorp et al., 1996) and that the sequences flanking epitopes can influence proteasomal cleavage (Beekman et al., 2000; Mo et al., 2000; Niedermann et al., 1995; Yellen-Shaw et al., 1997).

The ability of proteasomes to generate potentially immunocompetent peptides probably evolved well before the vertebrate immune system, as indicated by the ability

of yeast and insect proteasomes to generate several high copy ligands of MHC class I molecules (Niedermann et al., 1997).

1.2.4. Proteasome inhibitors

Several different types of low molecular weight inhibitors of the proteasome have been used to study proteasome function. C-terminal peptide aldehydes, such as N-acetyl-L-leucinyl-L-leucinyl-L-leucinal (LLnL; also known as Calpain Inhibitor I) and Cbz-L-leucinyl-L-leucinyl-L-leucinal (MG132), reversibly inhibit the proteasome and some other proteases such as lysosomal cathepsins and calpains (Lee and Goldberg, 1998; Rock et al., 1994). The natural *Streptomyces* metabolite lactacystin, more accurately its β-lactone derivative clasto-lactacystin-β-lactone, irreversibly binds and inhibits all active beta subunits, albeit with different efficiencies (β1, β2, β5, LMP2, LMP7, and MECL1) (Bogyo et al., 1997; Craiu et al., 1997; Dick et al., 1997; Fenteany et al., 1995).

Use of these inhibitors has shown that the proteasome is the major proteolytic activity responsible for degradation of short-lived, normal and abnormal proteins as well as long-lived proteins (Craiu et al., 1997; Rock et al., 1994). By blocking proteasome function, intracellular proteolysis can be reduced by 80-90%, whereas blocking lysosomal function at most decreases this process by 10-20%. Therefore, the proteasome constitutes the primary site for degrading proteins in mammalian cells (Rock and Goldberg, 1999).

Furthermore, use of these inhibitors has strongly implicated the proteasome as the main source of antigenic peptides for presentation to CTL (Benham and Neefjes, 1997; Cerundolo et al., 1997; Craiu et al., 1997; Rock et al., 1994).

1.2.5. Other proteases implicated in antigen processing and presentation

As described earlier, a significant proportion (around 15%) of the fragments generated by the proteasome are too long to bind to class I molecules. These fragments would require further trimming in order to bind MHC molecules. In addition, the class I-peptide complex formation or antigen presentation of certain epitopes could not be inhibited with proteasome inhibitors (Benham et al., 1998; Luckey et al., 1998; Schwarz et al., 2000; Vinitsky et al., 1997).

Several cytoplasmic and ER-resident proteases have recently been assigned a role in antigen processing and presentation, in addition to the proteasome. These proteases include tri-peptidyl peptidase II (TPPII) (Geier et al., 1999; Glas et al., 1998; Wang et al., 2000), puromycin-sensitive aminopeptidase (PSA) and bleomycin hydrolase (BH) (Stoltze et al., 2000), cysteine and metallo-proteases (Lopez and Del Val, 1997; Lopez et al., 2000) and leucine aminopeptidase (LAP) (Beninga et al., 1998). In many cases, these proteases have been proposed to play a role in post-proteasomal trimming of fragments. Several studies have indicated that the proteasome was required for the generation of the C-terminus of a peptide epitope, whereas the generation of the N-terminus was performed by another cytoplasmic protease (Beninga et al., 1998; Craiu et al., 1997; Mo et al., 1999; Stoltze et al., 2000). However, also proteasome independent trimming of the C-terminus of a relatively short peptide fragment has been reported (Yang et al., 1996). In addition, several studies have shown the involvement of ER-resident (amino-) peptidases in the trimming of antigenic peptides (Elliott et al., 1995; Snyder et al., 1994), which might even depend on the presence of the correct MHC class I molecule (Paz et al., 1999). In this respect it is important to note that the TAP transporter can translocate peptides up to 40 amino acids long (Momburg et al., 1994) and that trimming of at least 40 N-terminal amino acids in the ER has been reported (Elliott et al., 1995).

1.2.6. Subcellular localisation of the proteasome

Proteasomes are localised in both the cytoplasm and the nucleus at all phases of the cell cycle (Amsterdam et al., 1993; Palmer et al., 1994; Reits et al., 1997). Proteasomes diffuse rapidly within the nucleus and cytoplasm and are transported slowly and unidirectionally from the cytoplasm into the nucleus. When the nuclear envelope is disintegrated, during mitosis, the proteasomes move across the cell freely and can be contained within the nucleus upon nuclear membrane re-assembly (Reits et al., 1997). Changes in local distribution during the cell cycle have been reported, which correlated with time points of cyclin degradation (Amsterdam et al., 1993; Palmer et al., 1994).

1.2.6.1 MTOCs, PML bodies and aggresomes

Recently evidence has been accumulating about the role of centrosomes, or microtubule-organizing centres (MTOCs) and promyelocytic leukaemia (PML) oncogenic domains (PODs; also know as PML bodies) as sites of proteasomal degradation of cellular proteins (Anton et al., 1999; Fabunmi et al., 2000; Fabunmi et al., 2001; Garcia-Mata et al., 1999; Johnston et al., 1998; Mattsson et al., 2001; Wigley et al., 1999).

MTOCs are localised in the cytoplasm and have a central role in nucleating the assembly of most cytosolic microtubules. During mitosis, they organise the mitotic spindle to separate the chromosomes. However, overexpression of a misfolded protein or inhibition of proteasome activity leads to the accumulation of aggregates of misfolded protein at the MTOCs. These inclusions are stable, detergent-insoluble and have been called "aggresomes" (Johnston et al., 1998). They seem to originate from small aggregates that nucleate at the periphery of the cell and then move towards the centrosome, along microtubules, and accumulate in a pericentriolar region (Garcia-Mata et al., 1999; Johnston et al., 1998). Depending on the identity of the accumulated protein it might be polyubiquitinated, which might even occur at the MTOC. Furthermore, molecular chaperones (such as Hsp70) and, importantly, proteasomes can be found to localise at

these sites (Anton et al., 1999; Garcia-Mata et al., 1999; Johnston et al., 1998; Wigley et al., 1999). It appears that deposition of misfolded proteins at the MTOC (and possibly their ubiquitination) leads to the subsequent recruitment of proteasomes. In the case of an aggregation-prone form of influenza A nucleoprotein, the aggregates are destroyed once proteasomal inhibition is relieved (Anton et al., 1999). However, in Alzheimer's disease or Parkinson's disease, the accumulated inclusions also recruit proteasomes, but these substrates fail to be destroyed (Hirsch and Ploegh, 2000), and in fact impair the function of the ubiquitin-proteasome system (Bence et al., 2001).

PML bodies, on the other hand, are localised in the nucleus and contain several other proteins in addition to PML, such as Sp100, HAUSP and SUMO-1. PML bodies have been implicated in many different cellular functions such as transcriptional regulation, tumorigenicity and apoptosis. In addition, it was recently reported that PML bodies also perform a similar role in protein degradation as described above for the MTOCs, but they are expected to be limited largely to nuclear proteins (Anton et al., 1999). Misfolded proteins accumulate, form insoluble aggregates at the PML bodies and colocalise with molecular chaperones, polyubiquitin and proteasomes (Anton et al., 1999; Fabunmi et al., 2001; Mattsson et al., 2001).

Current evidence indicates that MTOC and PML bodies may be general sites of deposition of misfolded proteins and proteasomal degradation under basal conditions (Fabunmi et al., 2001; Garcia-Mata et al., 1999). These sites then become more visible when the system is overloaded with misfolded protein, either through overexpression of misfolded proteins, proteasome inhibition or by defects in the ubiquitin-proteasome pathway.

In addition to the role of MTOCs and PML bodies in protein degradation, there are also indications that they may be the sites of the generation of antigenic peptides for MHC class I restricted antigen presentation. Firstly, the proteasome regulator PA28, which has been implicated in antigen presentation (Groettrup et al., 1996; Preckel et al., 1999), was

shown to localise to both locales (Fabunmi et al., 2000; Fabunmi et al., 2001; Wigley et al., 1999). Furthermore, interferon-γ increased the number and size of PML and PA28 containing bodies and promoted the accumulation of immunoproteasomes at these bodies (Wigley et al., 1999). It was also reported that a correlation was found between the disappearance of a misfolded protein from MTOCs and PML bodies, and the cell surface expression of MHC class I bound peptide generated from the same protein (Anton et al., 1999). It is important to keep in mind that the nuclear envelope forms part of the ER and contains TAP transporters (Reits et al., 2000). It is therefore not necessary for peptides produced in the nucleus to be delivered to the cytoplasm before entering the ER for binding to MHC class I molecules. Lastly, it is interesting to note that the PML protein can induce the expression of the proteasomal LMP2 and LMP7 subunits as well as the TAP1 and TAP2 subunits of the TAP transporter, suggesting that PML bodies may play multiple roles in antigen presentation (Zheng et al., 1998).

1.2.7. The DRiP hypothesis

It was held for quite some time that peptides for MHC class I presentation were generated from mature proteins and that the rate of degradation (half-life) of the protein was an important determinant of the efficiency of epitope generation (Gileadi et al., 1999; Grant et al., 1995; Tobery and Siliciano, 1997; Townsend et al., 1988; Vijh et al., 1998). However, many immunodominant antigens, such as influenza NP and matrix proteins (Gileadi et al., 1999; Townsend et al., 1985) or HIV Gag protein (Schubert et al., 2000), are in fact long-lived proteins. In addition, several reports showed that the stability of endogenously synthesised antigens did not correlate with the generation of peptide/MHC complexes (Anton et al., 1998; Goth et al., 1996). This discrepancy was recently resolved by the demonstration that a large fraction of newly synthesised proteins are either not completely synthesised and are cotranslationally degraded (Turner and Varshavsky, 2000) or are completed but never attain their native structure and are rapidly degraded (Schubert et al., 2000). Both these classes of misfolded proteins are collectively called defective ribosomal products (DRiPs) (Yewdell et al., 1996). In

addition to this, it was elegantly shown that the majority of substrates for the TAP transporter are also derived from newly synthesised proteins (Reits et al., 2000). These data suggest that the majority of peptide epitopes may be derived from DRiPs rather than from native proteins.

1.3. Modulation and regulation of the proteasome

In vivo, 20S proteasomes are regulated by several proteins and protein complexes. Firstly, the catalytic β subunits allosterically regulate each other, as described above (Kisselev et al., 1999). In addition, cooperative incorporation of the γ-interferon inducible proteasome subunits LMP2, LMP7 and MECL-1 into newly assembled proteasomes (generating so-called immunoproteasomes) leads to altered cleavage patterns of the 20S proteasomes. Furthermore, expression of PA28 leads to preferred assembly of immunoproteasomes and the generation of an altered set of peptide fragments. Lastly, 19S regulatory complexes can associate with the 20S proteasome, enabling it to degrade ubiquitinated proteins and also changing the cleavage pattern.

From the crystal structure of the yeast 20S proteasome it is evident that the α and β subunits make many specific contacts with their neighbouring subunits (resulting in the fact that every subunit has a specific position in the complex) (Groll et al., 1997). Therefore it seems likely that the activation of certain subunits, the substitution of subunits and the docking of regulatory complexes will induce conformational changes in the whole 20S complex. These conformational changes could then result in altered peptidase activities and altered cleavage patterns. It is possible that conformational changes will change the internal surface of the 20S proteasome, in shape and/or electrocharge, resulting in a different movement of protein substrates through the lumen, leading to different cleavage patterns. Indeed, the crystal structure of PA28 with the 20S proteasome showed that PA28 binding resulted in opening of the gate in the ring of α subunits, possibly leading to the easier translocation of peptides into and out of the 20S proteasome (Whitby et al., 2000) (see below).

1.3.1. Immunoproteasome subunits LMP2, LMP7 and MECL-1

The catalytically active beta subunits β1 (Y/Delta), β2 (Z) and β5 (X/MB1) can be replaced upon γ-interferon stimulation by the (active) subunits LMP2, MECL1 and LMP7, respectively (Belich et al., 1994; Groettrup et al., 1996; Hisamatsu et al., 1996). The γ-interferon inducible subunits are mutually required for efficient proteasome assembly and maturation, generating so-called 'immuno-proteasomes'. Specifically, MECL-1 incorporation is dependent on the presence of LMP2 and uptake of LMP2 is strongly enhanced by MECL-1 expression. In addition, LMP7 is required for the efficient maturation of pre-proteasomes containing MECL-1 and LMP2 (Griffin et al., 1998; Groettrup et al., 1997).

The LMP2 and LMP7 genes were found to be localised in the class II region closely linked to the TAP1 and TAP2 genes, whose gene products are responsible for transport of peptides from the cytosol into the ER (Monaco, 1992).

Although LMP2 and LMP7 were shown not to be absolutely essential for antigen presentation (Arnold et al., 1992; Momburg et al., 1992), their incorporation into the proteasome increases the proteasome's capacity to cleave small peptides after hydrophobic residues (chymotryptic activity) and basic residues (tryptic activity) and reduces cleavage after acidic residues (post-acidic activity) (Driscoll et al., 1993; Gaczynska et al., 1993; Gaczynska et al., 1994). This was suggested to favour the production of the types of peptides found on MHC class I molecules on the cell surface, which terminate almost exclusively with hydrophobic or basic amino acids (Rammensee et al., 1993; Rammensee et al., 1995).

However, others have found that incorporation of LMP2 reduces cleavage of a chymotryptic substrate (LLVY) while not affecting the cleavage of a tryptic substrate (Boes et al., 1994), or that dual incorporation of LMP2 and LMP7 results in a reduction of cleavage of chymotryptic (LLVY) as well as an acidic substrate (Groettrup et al., 1995). Nevertheless, the general conclusion from this work was that incorporation of the LMPs alters the composition of the (types of) peptides generated by the

proteasome, while not affecting the rate of degradation of protein substrates (Boes et al., 1994; Gaczynska et al., 1993; Groettrup et al., 1995; Van Kaer et al., 1994).

The best evidence that LMP2 and LMP7 play a role in antigen processing and presentation came from the analysis of knock-out mice. LMP2 deficient mice had normal levels of MHC class I expression, a reduced number of CD8+ lymphocytes (indicating a role in intra-thymic selection) and their proteasomes had altered peptidase activities (reduced chymotryptic and tryptic-like and enhanced post-acidic). These mice also exhibited a reduced CTL response to influenza virus infection, which correlated with the less efficient presentation of an influenza nucleoprotein epitope (NP 366-374) (Van Kaer et al., 1994).

LMP7 knock-out mice exhibited reduced levels of MHC class I surface expression and presented the endogenous antigen HY inefficiently (Fehling et al., 1994).

Several groups have reported that LMP2 and LMP7 are required for presentation of specific epitopes to CTL (Cerundolo et al., 1995; Gileadi et al., 1999; Schwarz et al., 2000; Sibille et al., 1995). Interestingly, the generation of some epitopes required the incorporation of the LMP7 subunit, but not its catalytic activity (Gileadi et al., 1999; Sijts et al., 2000).

1.3.2. PA28 (11S) activator complex

The 20S proteasome can associate with the 200 kDa PA28 (11S) complex. The PA28 complex is built up of two γ-interferon inducible subunits, PA28α and PA28β, which form ring shaped complexes composed of three pairs of alternating α and β subunits that can bind to either end of the 20S proteasome (Ahn et al., 1996; Knowlton et al., 1997; Song et al., 1996).

PA28 was shown to enhance the efficiency of antigen presentation of certain epitopes without altering the degradation rate of the antigenic protein (Groettrup et al., 1996; Schwarz et al., 2000). The role of PA28 in antigen processing and presentation and the immune response was recently unambiguously confirmed by the analysis of $PA28^{-/-}$ mice (Preckel et al., 1999).

It was found that MHC class I molecules were less stable in PA28$^{-/-}$ cells, indicating acquisition of low affinity peptides. Indeed, a major shift in the spectrum of peptides presented by class I was detected by elution. The presentation of several exogenously provided and endogenously synthesised antigens was severely impaired in cells derived from PA28$^{-/-}$ mice, as measured in CTL assays. Furthermore, PA28 deficiency resulted in an impaired priming of CTL *in vivo* (Preckel et al., 1999).

Surprisingly, it was found that PA28 promoted immunoproteasome assembly, leading to the speculation that the phenotype observed was a consequence of a decreased cellular level of immunoproteasomes (Preckel et al., 1999). However, enhancement of antigen presentation by PA28, without affecting 20S proteasome subunit composition, was demonstrated by others (Schwarz et al., 2000).

The mechanism of PA28-mediated enhancement of antigen presentation remains uncertain. The PA28 complex has no proteolytic activity of its own, but stimulates the three peptidase activities of the 20S proteasome and alters the cleavage pattern of the 20S proteasome in such a way that the repertoire of peptides produced becomes larger (Groettrup et al., 1995; Song et al., 1997). Furthermore, PA28 did not enable the 20S proteasome to degrade whole proteins *in vitro* (Ma et al., 1992). The PA28 complex operates in an ATP independent way.

The crystal structure of PA28 with the 20S proteasome showed that PA28 binding resulted in opening of the gate in the ring of α subunits, possibly leading to the easier translocation of peptides into and out of the 20S proteasome (Whitby et al., 2000; Stohwasser et al., 2000). As two-thirds of proteasomal peptide products are normally too short to bind MHC class I molecules (Kisselev et al., 1999), opening of these gates could lead to the easier release of longer peptide products that could subsequently be trimmed and presented.

One report suggested that PA28 may induce coordinated double cleavages, thereby enhancing the presentation of dominant T cell epitopes (Dick et al., 1996).

1.3.3. 19S regulatory complex and the 26S proteasome

The bulk (80-90%) of short and long-lived proteins are degraded in an ATP dependent manner (Etlinger and Goldberg, 1977; Gronostajski et al., 1985). This was a surprising finding as peptide hydrolysis is a thermodynamically favoured reaction.

Use of proteasome inhibitors showed that the proteasome was responsible for the degradation of the bulk of both short and long-lived proteins (Craiu et al., 1997; Rock et al., 1994). The 20S proteasome cleaves peptide bonds without the requirement for ATP, but degrades whole proteins very inefficiently which makes it uncertain whether the 20S proteasome functions by itself in protein break-down *in vivo* (Rock and Goldberg, 1999).

In vivo the 20S proteasome therefore presumably functions mainly as the catalytic core of the 1,500 kDa 26S proteasome, which contains 19S regulatory complexes ('caps') attached to the ends of the 20S proteasome. The 26S proteasome renders proteolysis ATP dependent and is involved in the degradation of ubiquitinated proteins (Ciechanover, 1994). Degradation of short-lived and abnormal proteins generally requires the conjugation of ubiquitin (which is also an ATP dependent process). It is however still uncertain whether degradation of long-lived proteins also requires ubiquitin (Rock and Goldberg, 1999).

The 26S proteasome can however also rapidly hydrolyse some non-ubiquitinated proteins, for instance ornithine decarboxylase (Elias et al., 1995; Murakami et al., 1992). In addition, it was shown that a short-lived protein, $p21^{Cip1}$, could be found to be ubiquitinated, but that ubiquitination was not actually required for its rapid turnover (Sheaff et al., 2000).

The 19S cap is built up of around 20 different subunits (Baumeister et al., 1998). In yeast mutants this complex can be dissociated in a "lid" component and "base" that binds to the 20S proteasome. The base contains six distinct, but homologous, ATPases (and two non-ATPase subunits) which function to dissociate and unfold protein substrates and thread them into the 20S proteasome (Braun et al., 1999; Glickman et al.,

1998; Ortega et al., 2000). 20S proteasomes complexed with only the base component of the 19S cap had wild-type peptidase activity and were able to degrade a non-ubiquitinated protein substrate. Degradation of ubiquitinated substrates, however, did require the complete 19S cap (base + lid) (Glickman et al., 1998).

The lid contains a subunit (S5a) that has a high affinity for poly-ubiquitin (Deveraux et al., 1994). Although this subunit is involved in ubiquitin mediated degradation, it probably is not the only subunit of its type as indicated by the fact that a deletion mutant is viable (van Nocker et al., 1996). Also ubiquitin C-terminal hydrolases (isopeptidases), which ensure release and recycling of ubiquitin, have been found to be present in the 19S cap (Eytan et al., 1993; Papa et al., 1999).

1.3.4. Ubiquitin conjugation

Ubiquitin mediated protein degradation involves the covalent attachment of multiple ubiquitin molecules to proteins and the degradation of targeted protein with the release of free and reutilisable ubiquitin (Ciechanover, 1994). The ubiquitin system is involved in the degradation of short-lived and abnormal proteins (Ciechanover et al., 1984). As mentioned before, it remains unclear whether it has a role in the degradation of long-lived proteins. The system plays a crucial role in the degradation of transcriptional regulators MAT2α (Hochstrasser and Varshavsky, 1990), IκBα (Chen et al., 1995) and the processing of p105 to generate p50 (Lin et al., 1998; Orian et al., 1995; Palombella et al., 1994). Ubiquitin is also involved in cell cycle progression. The stage specific degradation of cyclins has been shown to be performed by the ubiquitin-proteasome pathway (Ghislain et al., 1993; Glotzer et al., 1991; Seufert et al., 1995). The ubiquitin pathway has further been implicated in the generation of MHC class I restricted epitopes from at least some antigens (Grant et al., 1995; Michalek et al., 1993). Major substrates in this process appeared to be defective ribosomal products (DRiPs), as discussed earlier (Reits et al., 2000; Schubert et al., 2000).

The conjugation of ubiquitin (a 72 amino acid protein) to protein substrates is conducted by a series of enzymes termed E1, E2 and E3. Firstly, the C-terminal glycine of ubiquitin is activated by the ubiquitin-activating enzyme E1. This is achieved by linking the C-terminal glycine to a cysteine in E1 via a high energy thiol ester bond, in an ATP dependent reaction. Ubiquitin is then transferred to a cysteine in one of the ubiquitin-conjugating enzymes (E2), which subsequently transfer the ubiquitin to the substrate that is bound to a ubiquitin-protein ligase E3. Together with E2, E3 is responsible for substrate recognition (Ciechanover, 1994).

The C-terminal glycine of ubiquitin becomes covalently linked to the ε-NH_2 group of a lysine in the target protein, via an isopeptide bond. Additional ubiquitin moieties are then conjugated to the first ubiquitin via linkage to the Lys-48 of ubiquitin, thereby generating a poly-ubiquitin chain (Chau et al., 1989). However, conjugation of ubiquitin to the N-terminus of a protein has also been reported (Aviel et al., 2000).

Recently, a new factor, E4, was described, that binds to ubiquitin moieties of preformed conjugates and catalyses the formation of multi-ubiquitin chains in conjugation with E1, E2 and E3. E4 is not essential for viability, but is involved in the multi-ubiquitination and degradation of a subset of proteins (Koegl et al., 1999). In this respect it is important to note that the minimal signal for efficient proteasomal targeting is formed by a tetra-ubiquitin (Thrower et al., 2000).

Probably only one (or possibly two) E1 protein exist, but multiple E2 and E3 molecules have been identified. As the E3 proteins bind protein substrates, they probably play a major role in the selection of proteins for degradation, although E2 proteins also play a role in this recognition (Ciechanover, 1994; Yaron et al., 1998).

The transient association of E2 and E3 enzymes with the 26S proteasome has been reported (Tongaonkar et al., 2000; Xie and Varshavsky, 2000) and it has been suggested that these interactions may be mediated by hPLIC proteins (Kleijnen et al., 2000). Therefore, E2 and E3 proteins could participate in the delivery of substrates to the proteasome by their physical association with the proteasome.

1.4. Viral interference with the class I processing and presentation pathway

Class I restricted $CD8^+$ cytotoxic T lymphocytes generally play an important role in the immune response against intracellular pathogens such as viruses. As the recognition of virus-infected cells by T lymphocytes relies on the cell surface expression of class I-β2m in association with virally derived peptides, many viruses have developed strategies to reduce or eliminate the cell surface expression of these complexes. Different viral products have been shown to affect various steps in the class I antigen processing and presentation pathway (Tortorella et al., 2000).

Many viral products have been shown to interfere with the transport of MHC class I molecules from the ER to the cell surface (Burgert and Kvist, 1985; Jones et al., 1996; Reusch et al., 1999; Wiertz et al., 1996; Wiertz et al., 1996; Ziegler et al., 1997).

In addition, viral proteins have been shown to block peptide transport by interacting with the cytoplasmic or luminal portion of the TAP transporter complex (Ahn et al., 1997; Hill et al., 1995; Tomazin et al., 1996).

There is also evidence that some viruses modulate the production of viral peptides by interfering with proteolysis. As these findings relate to the work presented in this thesis, they will be discussed in more detail below.

1.4.1. Viral resistance to protein degradation

Epstein-Barr Nuclear Antigen 1 (EBNA-1) of Epstein-Barr Virus (EBV) contains a glycine-alanine repeat that has been shown to inhibit, *in cis*, proteolytic degradation by the proteasome, thereby preventing EBNA-1 from being presented to and recognised by cytotoxic T lymphocytes. This gly-ala repeat also inhibits degradation when transferred to other proteins, like EBNA4 and IκBα (Levitskaya et al., 1995; Levitskaya et al., 1997; Sharipo et al., 1998).

1.4.2. Interaction of viral proteins with the proteasome

Other viral proteins appear to interact with the proteasome, often affecting its activity. The non-structural Hbx protein of hepatitis B virus (HBV) binds to two subunits of the 26S proteasome: 20S proteasome subunit PSMA7 (XAPC7; α4) and the PSMC1 (S4) ATPase subunit of the 19S regulatory complex (Fischer et al., 1995; Hu et al., 1999; Huang et al., 1996; Zhang et al., 2000). It was also shown that Hbx associated with the 26S proteasome *in vivo* and that Hbx caused a modest decrease in the proteasome's chymotryptic, tryptic and post-acidic activities. Furthermore, Hbx inhibited the hydrolysis of ubiquitin-lysozyme by the 26S proteasome *in vitro* (Hu et al., 1999). *In vivo* degradation of two well-established substrates of the ubiquitin-proteasome pathway was also inhibited (Zhang et al., 2000).

Proteasome inhibitors retarded Hbx degradation and increased the level of Hbx at steady state, indicating that Hbx is a substrate for the proteasome. Hbx sequences involved in its interaction with PSMA7 and PSMC1, were also important for its transcriptional activation function (Zhang et al., 2000). In addition, proteasome inhibitors blocked Hbx mediated transactivation of AP-1, AP-2 and SP1 site containing promoters, suggesting that proteasome function is required for the transactivation function of Hbx (Hu et al., 1999). The mechanism of this apparent proteasome requirement remains unknown.

It was further speculated that Hbx-mediated proteasome inhibition may stabilise other viral proteins and suppress antigen presentation *in vivo* (Hu et al., 1999).

HIV Tat protein has also been reported to interact with the 20S proteasome and the 19S regulatory complex. Presumably, Tat binds to the ring of α subunits of the 20S proteasome and to Tat-binding protein 1 and 7 (TBP1 and TBP7) in the 19S regulatory complex. This study was performed *in vitro* with recombinant and synthesised Tat and purified proteasome components (Seeger et al., 1997).

At low concentrations Tat appeared to potently inhibit cleavage of fluorogenic peptide substrates by the 20S proteasome, which was not due to competition by Tat.

Furthermore, Tat was able to inhibit PA28 complex (11S)-mediated activation of the 20S proteasome, by displacing the PA28 from the 20S proteasome.

When used at higher concentrations, Tat stimulated hydrolysis by the 26S proteasome, both of a fluorogenic peptide substrate as well as ubiquitin-lysozyme.

It is possible that Tat is displaced from the 20S proteasome by the 19S complex (similar to PA28 competition for binding) and that Tat, when bound to the 26S proteasome, acts on the 19S complex, perhaps the ATPases TBP1 (S5b) and TBP7 (S6). This would then lead to a moderate activation of the 26S proteasome (Seeger et al., 1997). Again, an effect of Tat on MHC class I antigen processing and presentation was suggested, but evidence is currently lacking.

HIV-1 Nef protein was reported to interact with the HsN3 (β7) proteasome subunit. However, most of this study was also performed in vitro, and the interaction could not be shown to occur in vivo. The possible function remained unknown (Rossi et al., 1997).

A further example of a viral protein interacting with the proteasome is type 5 adenovirus (Ad5) E1A protein (Turnell et al., 2000). The N-terminus of E1A was shown to bind 19S ATPase subunits S8 and S4 and to reduce ATPase activity. This correlated with a reduction in the ability of HPV16 E6 to target p53 for ubiquitin mediated proteasomal degradation. E1A interacted with proteasomes in the nucleus as well as in the cytoplasm. E1A was further shown to be a substrate for proteasome-mediated degradation, a process that was independent of ubiquitination but dependent on phosphorylation of a C-terminal PEST sequence (Turnell et al., 2000).

HTLV-1 Tax protein has been reported to physically associate with subunits HC9 (α3) and HsN3 (β7) of the 20S proteasome (Beraud and Greene, 1996; Rousset et al., 1996). The interaction between Tax and these subunits was studied by overexpressing single subunits and was not done in the context of the assembled proteasome. The functional significance of this association is uncertain, although a role in NFκB activation has been proposed. Tax reportedly tethers p105 and IκBα to proteasome subunits to enhance

their processing and turnover, respectively (Beraud and Greene, 1996; Petropoulos and Hiscott, 1998; Rousset et al., 1996). These initial findings formed the basis of the work presented in this thesis.

1.5. NFκB/Rel family of transcription factors

1.5.1. NFκB/Rel transcription factors

The NFκB/Rel family of transcription factors regulate a variety of genes involved in the inflammatory and immune responses, apoptosis and cellular proliferation. These transcription factors are activated by a variety of extracellular signals such as pro-inflammatory cytokines (TNFα, IL-1β), mitogens (LPS), and UV radiation (Baeuerle and Baltimore, 1996; Verma et al., 1995). Members of this protein family have a Rel-homology domain which mediates dimerization, nuclear localisation and DNA binding (Ghosh et al., 1995). Because of their abundance, the prototypical NFκB is a heterodimer of subunits known as p50 and p65 (RelA), which can bind to κB enhancer sequences in promoters. Other members of the NFκB family are p52, c-Rel, Rel B, p100 and p105, and most members can form homo- and heterodimers *in vitro*. p50 and p52 do not generally activate transcription as homodimers because they lack a transcriptional activation domain. However, p65, c-Rel and Rel B posses a potent C-terminal trans-activation domain. Depending on the presence or absence of an activation domain in the dimer, NFκB can act as an activator or repressor (Verma et al., 1995).

1.5.2. IκB factors sequester NFκB in the cytoplasm

NFκB/Rel factors are regulated post-transcriptionally by a family of cytoplasmic inhibitory proteins, termed IκBα, IκBβ, IκBε, IκBγ (p105 C-terminus), p105 and p100, which sequester NFκB in the cytoplasm (Baeuerle and Baltimore, 1988; Sun et al., 1994). These IκBs posses three to six so-called ankyrin repeats with which they bind the NFκB dimers and mask their nuclear localisation signals (NLS), thereby

preventing them from translocating into the nucleus. Each repeat of about 30 amino acids consists of two closely packed α helices, followed by a loop and a tight hairpin (Huxford et al., 1998; Jacobs and Harrison, 1998).

1.5.3. The IKK complex and NFκB activation

As mentioned before, in a resting cell the NFκB factors are sequestered in the cytoplasm by IκBs. Upon cellular activation NFκB is released from IκB and translocates to the nucleus, by virtue of its nuclear localisation signal, and activates transcription. The release of NFκB from IκB is caused by the subsequent phosphorylation, ubiquitination and proteasomal degradation of IκB (Chen et al., 1995; Palombella et al., 1994).

The signal-induced phosphorylation of IκBα takes place on serine residues 32 and 36 in the N-terminal signal response domain (SRD) (Brockman et al., 1995; Chen et al., 1995). This phosphorylation is performed by a 700-900 kDa IκB kinase (IKK) complex (Chen et al., 1996). The IKK-complex is built up around two kinase subunits, IKKα and IKKβ (also called IKK1 and IKK2) and several structural and regulatory subunits (DiDonato et al., 1997; Mercurio et al., 1997; Zandi et al., 1997). IKKα and IKKβ form heterodimers through their leucine zipper domains. Although both IKKs can phosphorylate IκBα, the two IKKs play crucial but distinct roles in early development with IKKα directing key stages in early skin and skeletal development and IKKβ by providing a TNFα induced anti-apoptotic signal (May and Ghosh, 1999).

A third member of the IKK complex, IKKγ (also called NEMO), which does not contain a kinase domain, associates with IKKα and (preferentially) IKKβ and is required for the activation of IKKα/IKKβ heterodimers in response to TNFα and IL-1β (Rothwarf et al., 1998; Yamaoka et al., 1998).

Another protein, IKK-complex-associated-protein (IKAP), has been found to associate with both IKKs and may function as a scaffold for the formation of a functional IKK complex (Cohen et al., 1998).

The activity of IKKα and IKKβ is regulated by several upstream kinases, NFκB inducing kinase (NIK), NFκB activating kinase (NAK), Akt and MEKK-1, through the phosphorylation of specific serine residues in the activation domains of IKKα and IKKβ. (May and Ghosh, 1999; Ozes et al., 1999; Tojima et al., 2000; Woronicz et al., 1997). MEKK1, originally identified as a component of the c-Jun activation pathway, can stimulate predominantly the IKKβ kinase activity in the IKK complex, leading to NFκB activation (Lee et al., 1997; Yin et al., 1998).

Phosphorylation of IκBα on Ser-32 and Ser-36 marks it out for ubiquitination on lysine residues 21 and 22 (Rodriguez et al., 1996; Scherer et al., 1995) and subsequent degradation by the 26S proteasome (Chen et al., 1995; Palombella et al., 1994). The receptor subunit of the ubiquitin-protein ligase (E3) that specifically recognises phosphorylated IκBα and promotes its ubiquitination was identified as β-TrCP, a member of the F-box family (Winston et al., 1999; Yaron et al., 1998).

One of the genes of which transcription is activated by NFκB is the IκBα gene. The newly synthesised IκBα can translocate to the nucleus, where it can bind to NFκB factors, inhibit their DNA binding and relocate NFκB to the cytoplasm (Arenzana-Seisdedos et al., 1995; Arenzana-Seisdedos et al., 1997). In this way IκBα downregulates NFκB activity and restores the autoregulatory loop (Beg et al., 1995; Brown et al., 1993; Sun et al., 1993). Similarly, it has been reported that p100 expression is induced upon NFκB activation (Sun et al., 1994).

In the absence of stimulation, IκBα undergoes continuous turnover. This basal degradation is independent of phosphorylation and ubiquitination, but does require the proteasome. It does not require the N-terminal SRD nor the C-terminal PEST domain, but solely depends on the core ankyrin domain (Krappmann et al., 1996).

1.5.4. p105

p105 is encoded by the NFκB1 gene, and the N-terminal portion of p105 corresponds to the p50 subunit of the prototypical NFκB complex. The C-terminus of p105 contains ankyrin repeats similar to IκBα (IκBγ; transcribed from an intronic promoter). A similar structural relationship exists between p100 and p52. p105 and p100 are able to form stable complexes with other NFκB factors (including p65 and c-Rel) and cause cytoplasmic retention of p65 and c-Rel, by means of their C-terminal IκB-like ankyrin domain (Mercurio et al., 1993; Naumann et al., 1993).

1.5.4.1. p105 processing

The p50 subunit is constitutively generated by processing of p105 by the ubiquitin-proteasome pathway. This was the first example of processing, rather than complete degradation, by the proteasome (Fan and Maniatis, 1991; Orian et al., 1995; Palombella et al., 1994). One report indicated that the generation of p50 from p105 can occur co-translationally by the 26S proteasome, indicating that p105 does not have to be fully synthesised before processing can occur (Lin et al., 1998).

A glycine rich region (GRR) at the C-terminal end of the p50 amino acid sequence separates the ankyrin repeat domain of p105 from the p50 domain of p105. This GRR is thought to play an important role in preventing p50 from being degraded by the proteasome during p105 processing (Lin et al., 1998; Lin and Ghosh, 1996). A similar domain, a glycine-alanine (gly-ala) repeat, in Epstein-Barr Nuclear Antigen (EBNA1) of Epstein-Barr virus (EBV) has been shown to inhibit, *in cis*, the proteolytic degradation by the proteasome (Levitskaya et al., 1995; Levitskaya et al., 1997; Sharipo et al., 1998).

1.5.4.2. Induced p105 degradation

TNFα induction leads to complete degradation of p105, while maintaining the constitutive generation of p50 by p105 processing. Induction of complete degradation of p105 will lead to the release of the NFκB factors that were previously associated with p105, resulting in nuclear translocation and transcriptional activation (Belich et al., 1999; Heissmeyer et al., 1999).

Signal induced degradation of p105 is mediated by IKKα and IKKβ, which are able to associate with the p105 C-terminus and phosphorylate p105 serine residues 921, 923 and 932. This phosphorylation marks p105 out for degradation, presumably by the ubiquitin-proteasome pathway, similar to IκBα (Heissmeyer et al., 1999).

1.6. Human T cell lymphotropic virus - type 1

Human T cell lymphotropic virus – type 1 (HTLV-1) is a persistent human retrovirus, infecting 10-20 million people worldwide. The virus is endemic in southern Japan, sub-Saharan Africa, the Caribbean and the South-East of the United States (Smith and Greene, 1991). It is spread vertically from mother to child, both perinatally and by breast-feeding, and horizontally by sexual contact and infected blood (transfusion or sharing of needles by drug abusers) (Bangham, 1993). Little or no free HTLV-1 particles are found in the plasma and transmission requires transfer of an infected cell. Within infected individuals, HTLV-1 spreads most efficiently by cell division and cell-to-cell contact, and free virions are poorly infectious (Daenke et al., 1999). HTLV-1 infects mainly $CD4^+$ cells *in vivo* (Richardson et al., 1990; Hanon et al., 2000), although it was recently shown that $CD8^+$ cells can also be infected (Hanon et al., 2000). The cellular receptor for HTLV-1 has been mapped to chromosone 17, but the identity of the receptor remains unknown (Sommerfelt et al., 1988; Daenke et al., 1999).

1.6.1. HTLV-1 associated diseases

Whereas the majority of HTLV-1 infected individuals remains healthy, 5% of HTLV-1 carriers develop either of two diseases: the neurological inflammatory disease HTLV-1 associated myelopathy or tropical spastic paraparesis (HAM/TSP) (Bangham et al., 1988; Gessain et al., 1985), or adult T cell leukaemia/lymphoma (ATL) (Uchiyama et al., 1977).

HAM/TSP is characterised by the progressive demyelination of regions in the spinal cord, leading to decreased muscle strength, spasticity and paralysis (Bangham et al., 1996; Gessain et al., 1985).

ATL is an aggressive and fatal malignancy of mature $CD4^+$ T lymphocytes. The period between infection and the onset of disease is typically quite long, ranging from 10 to 30 years. When ATL develops, the median survival of patients is 6 months (Bangham et al., 1996; Smith and Greene, 1991).

1.6.2. HTLV-1 mRNA splicing

HTLV-1 is a complex human retrovirus and its genome contains, besides the *gag*, *pol* and *env* encoding sequences, a so-called pX region between the *env* sequence and the 3' LTR. The pX region encodes two trans-regulatory proteins, termed Tax and Rex, that are both essential for viral replication (Chen et al., 1985; Inoue et al., 1987). Constitutive double splicing of the primary genomic transcript leads to the production of a small subgenomic mRNA containing the pX sequence, from which both Tax and Rex are translated from different, overlapping reading frames. Tax translation is initiated from the *env* AUG (Kinoshita et al., 1989; Kiyokawa et al., 1985; Nagashima et al., 1986; Smith and Greene, 1991).

It has further been reported that alternatively spliced mRNAs can be generated through the use of alternative splice acceptor sites in the pX region, which can lead to the expression of other proteins, Tof and Rof, for which until now no functions have been described (Ciminale et al., 1992; Koralnik et al., 1992).

1.6.3. HTLV-1 Rex protein

Rex is a 27kDa phosphorylated protein localised in the nucleus, and predominantly the nucleoli, of expressing cells. Rex functions to increase the expression of viral structural and enzymatic proteins by promoting the cytoplasmic accumulation of the incompletely spliced *gag/pol* (unspliced) and *env* (singly spliced) mRNAs, thereby allowing their translation (Hidaka et al., 1988; Smith and Greene, 1991).

In the absence of Rex, incompletely spliced viral mRNAs remain sequestered in the nucleus, where they are either spliced or degraded. Rex can bind to a large and stable RNA stem-loop structure in the 3' LTR, termed the Rex response element (RexRE). Rex acts by activating nuclear export of these incompletely spliced mRNAs. After mRNA export Rex shuttles back into the nucleus. Rex action also leads to a reduction of the expression of doubly spliced *tax/rex* mRNA (Hidaka et al., 1988).

The function of HIV Rev is analogous to HTLV-1 Rex. Although Rev and Rex proteins and their respective RNA response elements lack significant homology, HTLV-1 Rex can functionally replace Rev in an HIV system (Hanly et al., 1989).

1.7. Tax

The other protein encoded by the doubly spliced pX mRNA is Tax. Tax is a 40 kDa phosphoprotein that plays a central role in HTLV-1 infection and associated diseases. Tax is essential for viral replication (Chen et al., 1985) and potently activates transcription from the HTLV-1 long terminal repeat (LTR) (Sodroski et al., 1985). Tax also induces an array of cellular genes involved in T cell activation and proliferation.

Additionally, Tax has transformation properties and is likely to be responsible for the leukaemia (ATL) associated with HTLV-1 infection (Coscoy et al., 1998; Grassmann et al., 1989; Grossman et al., 1995). Tax is also the main target for the CTL response mounted against HTLV-1, and this is likely to play an important role in the control of HTLV-1 infection and in the development of TSP/HAM (Bangham, 2000; Bangham et al., 1996). These and other properties of Tax will be discussed in more detail below.

1.7.1. Subcellular localisation of Tax

HTLV-1 Tax is expressed predominantly in the nuclei of infected cells. Tax is distinguished from most other nuclear proteins by the absence of a short, highly basic nuclear localisation signal (NLS). Deletion of the amino acids 2 to 58 of Tax resulted in failure of Tax to localise to the nucleus (Gitlin et al., 1991). Furthermore, amino acid substitutions in the Tax N-terminus frequently led to the loss of nuclear localisation of Tax (Smith and Greene, 1990). Experiments with chimeras of Tax with β-galactosidase subsequently showed that the N-terminal 48 amino acids of Tax comprise a functional nuclear localisation domain (Smith and Greene, 1992).

The N-terminus of Tax contains multiple cysteine and histidine residues, which have been shown to be part of a zinc-binding domain (Semmes and Jeang, 1992). Although the zinc binding domain and the NLS-domain involve overlapping regions in the Tax N-terminus, substitution-mutations of Cys and His residues led to abrogation of Zn^{2+} binding but not abrogation of nuclear localisation, indicating that the two activities are functionally distinct (Semmes and Jeang, 1992; Smith and Greene, 1992).

1.7.2. Tax and CREB/ATF transcription factors

Tax is not itself a DNA binding protein and exerts its transactivation properties by modulating the function of various host transcription factors. Tax activates the HTLV-1 long terminal repeat (LTR) by interacting with members of the cAMP responsive element binding (CREB) / activating transcription factor (ATF) family of transcription factors. CREB/ATF factors can bind to three imperfectly repeated 21 bp enhancer sequences in the U3 region of the HTLV-1 LTR (Beraud et al., 1991; Suzuki et al., 1993; Zhao and Giam, 1992).

Crosslinking experiments have shown that Tax can form homodimers (Perini et al., 1995). It appeared that Tax can enhance the dimerisation of CREB/ATF factors by

interacting with their basic DNA binding domain, resulting in enhanced DNA binding (Baranger et al., 1995; Perini et al., 1995; Wagner and Green, 1993).

Tax remains bound to CREB/ATF when the dimer binds to the DNA, and Tax can then recruit the coactivator CBP (CREB binding protein), in a manner independent of CREB phosphorylation (Kwok et al., 1996). The Tax M47 mutant ($^{319}L^{320}L \rightarrow RS$) is incapable of binding CBP, providing a possible explanation for the lack of activation of the HTLV-1 LTR by this mutant (Bex et al., 1998).

1.7.3. Tax and $p65^{SRF}$

Among the genes involved in T cell activation and growth that are activated by Tax are the immediate early genes *c-fos*, *erg-1* and *erg-2*. These are activated by Tax binding to serum response factor $p65^{SRF}$, which binds to CArG boxes in the promoters of the respective genes (Fujii et al., 1988; Fujii et al., 1992; Suzuki et al., 1993).

1.7.4. Tax and NFκB

In addition to activating the genes described above, Tax activates transcription of the cytokine IL-2 and the α-subunit of its receptor (IL-2αR) by activating the NFκB pathway, ultimately resulting in nuclear expression of NFκB (Ballard et al., 1988; Inoue et al., 1986; Siekevitz et al., 1987). Activation of the HIV-1 LTR by Tax is also mediated by NFκB activation (Siekevitz et al., 1987). Other cellular proteins whose expression is induced by Tax via the NFκB pathway are TGF-β, GM-CSF, TNF-β, c-myc, GP34, vimentin, IL-6, IL-8, IL-15 and VCAM-1 (Yao and Wigdahl, 2000).

1.7.5. Tax mediated NFκB activation by IKK complex activation

Tax activates the NFκB pathway primarily by activating IKKα and IKKβ, leading to phosphorylation of IκBα and subsequent degradation of IκBα by the ubiquitin-proteasome pathway, as described above (Maggirwar et al., 1995; Sun et al., 1994).

IKKs are constitutively activated in Tax transfectants and HTLV-1 infected T lymphocytes (Chu et al., 1998; Geleziunas et al., 1998; Uhlik et al., 1998). It was recently revealed that Tax is recruited into the IKK complex by a physical interaction with IKKγ/NEMO, an essential regulatory component of the IKK complex, which appears to function as an adapter protein. Both the N- and C-terminal regions of IKKγ are required for recruitment of Tax to the IKK complex (Chu et al., 1999)(Harhaj and Sun, 1999)(Jin et al., 1999).

It was further shown that the Tax M22 mutant (Smith and Greene, 1990), which is selectively defective in NFκB activation (but not ATF/CREB mediated activation) did not bind IKKγ, whereas Tax M47 (NFκB competent, ATF/CREB deficient) did still associate with IKKγ, thereby suggesting that the defect of M22 lies in the docking of Tax to the IKK complex. M22 also failed to activate the IKK kinase activity, whereas M47 still did (Chu et al., 1999; Geleziunas et al., 1998; Harhaj and Sun, 1999).

Although it is not known at present exactly how Tax recruitment to the IKK complex triggers IKK activation, it is possible that Tax can bring upstream kinases like NIK and MEKK1 into the IKK complex (Chu et al., 1999; Harhaj and Sun, 1999; Jin et al., 1999). NIK has previously been shown to be involved in Tax mediated NFκB activation, as inactive forms of either IKKs or NIK attenuated Tax-mediated NFκB activation (Geleziunas et al., 1998; Uhlik et al., 1998). Tax also binds to the N-terminal domain of protein kinase MEKK1, thereby stimulating MEKK1 kinase activity, leading to increased activity of IKKβ and increased phosphorylation and degradation of IκBα (Yin et al., 1998).

Tax also induces phosphorylation and proteasome-mediated degradation of IκBβ. NFκB activation does not lead to enhanced transcription of the IκBβ gene, leading to

chronically downregulated expression of IκBβ in HTLV-1 infected T lymphocytes (McKinsey et al., 1996).

Moreover, Tax enhances constitutive turnover of IκBα. This is mediated by a phosphorylation and ubiquitination independent mechanism, whereby Tax tethers N-terminally hypophosphorylated IκBα to the proteasome (Krappmann et al., 1996; Petropoulos and Hiscott, 1998).

1.7.6. Physical interactions between Tax and NFκB/IκB factors

In addition to activating the NFκB pathway by inducing the phosphorylation and degradation of IκB, Tax physically interacts with many members of the NFκB family. Tax has been reported to interact with the DNA binding NFκB factors p50 (Bex et al., 1997; Suzuki et al., 1993), p52 (Beraud et al., 1994; Murakami et al., 1995), p65 (Suzuki et al., 1994) and c-Rel (Suzuki et al., 1994).

At least in some cases, Tax was shown to interact with NFκB factors when they were bound to κB enhancer sequences (Suzuki et al., 1993). Tax was also reported to localise in discrete nuclear foci containing splicing factors, RNApol II, CDK8 and NFκB factors p50 and RelA (Bex et al., 1997). In addition, Tax was found to recruit the coactivator p300 to this site. Tax mutant M148 (G148V) (Yamaoka et al., 1996) was incapable of interacting with p300, providing a possible explanation for its lack in NFκB activating properties (Bex et al., 1998). However, it has to be noted that the Tax M25 mutant (G148,149AS), was still active on both the HIV and the HTLV-1 promoter (Smith and Greene, 1990).

Therefore, in addition to inducing nuclear translocation of NFκB factors, Tax appears to interact with NFκB factors in nuclear transcriptional activation complexes.

Furthermore, Tax interacts with the inhibitory proteins IκBα (Suzuki et al., 1995) and IκBγ (Hirai et al., 1994), thereby preventing their interaction with NFκB factors. Also Tax binding to p105 (Hirai et al., 1992) and p100 (via its Rel homology domain) have been shown (Beraud et al., 1994; Murakami et al., 1995; Pepin et al., 1994).

Subcellular relocalisation of Tax as a result of overexpression of NFκB factors has been reported. p100, p105 and IκBα can relocate Tax to the cytoplasm, whereas p50, p52 and p65 enhance Tax nuclear localisation (Beraud et al., 1994; Pepin et al., 1994). However, it has to be noted that the reports on the interactions between Tax and NFκB factors are often contradictory and the functional significance of these apparently promiscuous interactions remains unclear.

1.7.7. Tax mutants

A series of double amino acid substitutions throughout the Tax protein was made (Smith and Greene, 1990). Five mutants were identified (one N-terminal: M1 (H3S) and four C-terminal: M45 (^{315}I^{316}P→RS), M46 (I317R), M47 (^{319}L^{320}L→RS), M48 (^{321}F^{322}N→RS) that selectively activated NFκB responsive promoters without activating CREB/ATF responsive promoters. Conversely, one mutant was identified that selectively activated the CREB/ATF promoter without being able to activate the NFκB responsive promoter (M22 (^{137}G^{138}L→AS) (Smith and Greene, 1990). However, the described phenotype of the M22 mutation was later reported to belong to a different mutation (^{130}G^{131}L→AS) (see erratum published (Smith and Greene, 1990)).

Similarly, Semmes and Jeang made single amino acid substitutions. They found that Tax residues exclusively important for HTLV-1 LTR transactivation were C29, C49, H52, S273, S274, S276, P316, L320 and for the HIV LTR C23, H41, H43, S113, S160, S258 (Semmes and Jeang, 1992).

Together, these data show that Tax activates both types of promoters via different signal transduction pathways and that Tax has at least two separate domains mediating transactivation (Smith and Greene, 1990). The C-terminal acidic domain (332-353), which is absent in Tax of HTLV-II, was shown not to be required for activation of either of the two types of promoters (Smith and Greene, 1990). Overall, Tax transactivation function has been shown to be very sensitive to single or double amino acid substitutions (Niewiesk et al., 1995; Semmes and Jeang, 1992; Smith and Greene, 1990).

The phosphorylation of serine residues 300 or 301 of Tax, has been reported to be required for Tax mediated activation of gene expression via both the CREB/ATF and NFκB pathways (Bex et al., 1999). In contrast to this, Semmes and Jeang reported that substitution of Ser 300 and 301 with alanines did not affect transactivation of an HIV promoter and only modestly reduced activation of the HTLV-1 LTR (Semmes and Jeang, 1992).

1.8. Tax and disease

1.8.1. Tax mediated transformation

HTLV-1 infection is etiologically associated with adult T cell leukaemia/lymphoma (ATL) (Uchiyama et al., 1977). ATL is an aggressive and fatal malignancy of mature $CD4^+$ T lymphocytes. A characteristic of ATL is the long period between infection and the onset of disease, which ranges from 10 to 30 years (Bangham et al., 1996; Smith and Greene, 1991).

The Tax protein has been implicated in the transformation of HTLV-1 infected cells. Tax was shown to immortalise (defined as inducing IL-2 dependent growth) and transform (IL-2 independent growth) primary T cells *in vitro* (Grassmann et al., 1989; Tanaka et al., 1990). Furthermore, mice transgenic for the Tax gene under control of a mature T-lymphocyte specific promoter developed large lymphocytic leukemia (Grossman et al., 1995).

The mechanism of Tax mediated transformation is not known. The current model includes an early period of Tax-induced polyclonal T cell proliferation. This polyclonal proliferation may in turn facilitate the occurrence of additional events leading to the completion of the transformation process and the monoclonal outgrowth of an IL-2 independent population of leukaemic T cells (Yoshida, 2001).

Tax activates the expression of a number of cellular genes involved in the regulation of cellular proliferation and also interacts directly with several cell cycle regulators. This

dysregulation of the cell cycle may eventually lead to immortalisation and transformation of the infected cell (Robek and Ratner, 1999; Yoshida, 2001). Whether Tax-mediated transactivation via the CREB/ATF or NFκB pathway, or both, is essential for immortalisation remains controversial (Robek and Ratner, 1999; Yamaoka et al., 1996). Tax was further reported to interact with MAD1, causing the loss of an M phase checkpoint in the cell cycle, providing a possible explanation for the HTLV-1 induced karyotypic abnormalities in ATL cells (Jin et al., 1998).

1.8.2. Tax in the immune response and in relation to TSP

HTLV-1 is etiologically linked to HTLV-1 associated myelopathy / tropical spastic paraparesis (HAM/TSP). HAM/TSP is a chronic inflammatory condition of the central nervous system (CNS) that is characterised by diffuse demyelination and mononuclear cell infiltrates in the CNS, consisting mostly of T cells (Bangham, 1993; Levin and Jacobson, 1997). However, the pathogenesis of HAM/TSP is still poorly understood. No evidence has been found that a specific strain of HTLV-1 is associated with HAM/TSP (Bangham et al., 1988; Daenke et al., 1990). Furthermore, infection of CNS cells by HTLV-1 and subsequent immune destruction of those cells by CTL does not seem to occur, as HTLV-1 provirus present in the CNS is found only in the invading lymphocytes, not in CNS cells (Levin and Jacobson, 1997; Matsuoka et al., 1998).

A hypothesis exists that an autoimmune response mediates HTLV-1 associated CNS damage. This would involve T lymphocytes activated by HTLV-1 infection, which migrate to the CNS and crossreact with self-antigens presented on cells in the CNS and so cause an inflammation reaction and tissue damage. However, in HAM/TSP no specific cell type is destroyed, but rather there is diffuse damage with both demyelination and neuronal loss, making this option less likely (Bangham et al., 1996; Levin and Jacobson, 1997). The most likely, remaining hypothesis is that activated invading lymphocytes cause bystander damage in the CNS (Bangham et al., 1996; Daenke and Bangham, 1994).

HAM/TSP patients as well as healthy carriers have a very strong, chronically activated cytotoxic T cell (CTL) response against the virus (Daenke et al., 1996; Jacobson et al., 1990; Parker et al., 1992). Controversy remains about whether the frequency of HTLV-1 specific CTL is (significantly) higher in HAM/TSP patients compared to healthy carriers (Bangham, 2000; Daenke et al., 1996; Elovaara et al., 1993; Jacobson et al., 1990; Jeffery et al., 1999; Kubota et al., 1998; Parker et al., 1992; Parker et al., 1994; Ureta-Vidal et al., 2001). This CTL response is mainly directed against the viral transcriptional activator protein Tax, of which multiple epitopes can be recognised simultaneously (Parker et al., 1994).

An important parameter in HTLV-1 infection is the proviral load, which generally is 10 to 100 fold higher in HAM/TSP patients than in healthy carriers (10% of PBMC in HAM/TSP patients can carry the HTLV-1 provirus) and is a strong determinant of the risk of developing HAM/TSP (Jeffery et al., 1999; Kubota et al., 2000). As a result of this higher proviral load, the anti-HTLV-1 antibody titre is typically higher in TSP/HAM patients (Lal et al., 1994).

The main question regarding HAM/TSP remains whether the CTL response against HTLV-1 is protective, causes tissue damage, or that it is involved in both (Bangham, 2000).

Several lines of evidence indicate that the MHC class I restricted T cell response is highly active in HTLV-1 infection *in vivo*. Firstly, chronically activated CTLs against the virus can be found (Daenke et al., 1996; Jacobson et al., 1990; Parker et al., 1992). It was further shown that autologous $CD8^+$ T cells rapidly kill $CD4^+$ cells naturally infected with HTLV-1, and expressing the Tax protein, by a perforin dependent mechanism (Hanon et al., 2000).

In addition, the CTL response was implicated in the selection for amino acid substitutions in Tax CTL epitopes, leading to abrogation of CTL recognition and severely impaired Tax transactivation function (Niewiesk et al., 1995). Overall, it appeared that Tax sequences were significantly more variable within and between

healthy carriers than TSP/HAM patients, indicating a stronger net positive selection for amino acid changes in healthy carriers (Niewiesk et al., 1994).

The most compelling evidence for a protective effect of the CTL response in HTLV-1 infection was recently provided by immunogenetic data. It was shown that the class I allele HLA-A2 was associated with a reduction of the risk of developing HAM/TSP and also with a 3-fold lower proviral load in healthy carriers (Jeffery et al., 1999). These data indicate that an efficient CTL response can reduce the HTLV-1 viral load and thereby reduce the risk of developing inflammatory disease.

On the other hand, there is evidence that anti-HTLV-1 CTLs might contribute to the inflammation in HAM/TSP. Tax specific $CD8^+$ T cells were found in the cerebrospinal fluid of some HAM/TSP patients, sometimes at a higher frequency than in peripheral blood (Elovaara et al., 1993; Greten et al., 1998). In addition, some clones of anti-HTLV-1 CTLs were shown to secrete the cytokines IFN-γ and TNF-α, the chemokines macrophage-inflammatory protein (MIP)-1α and –1β and IL-16 and the matrix metalloproteinase (MMP)-9. These factors may contribute to the migration of lymphocytes (MIP-1α and –1β, MMP-9) and inflammatory demyelination processes (IFN-γ and TNF-α) (Biddison et al., 1997; Kubota et al., 2000). However, whether the infiltrating T cells in HAM/TSP represent HTLV-1-specific CTL remains unknown.

It has been proposed that HAM/TSP patients have a less effective CTL response against the virus, resulting in a higher equilibium viral load. As it is known that cytokine secretion requires a higher concentration of antigen than target cell lysis (Hausmann et al., 1999), this higher antigen load might then stimulate the HTLV-1 specific CTL to secrete inflammatory mediators such as IFN-γ and TNF-α, which could cause tissue damage (Bangham, 2000). However, it also remains possible that the higher viral load in HAM/TSP, above a certain threshold (Jeffery et al., 1999), induces a more non-specific activation of T cells, which leave the circulation and establish foci of inflammation, thereby causing bystander damage (Bangham et al., 1996).

1.9. Objectives of thesis

HTLV-1 Tax protein had been reported to physically associate with subunits HC9 (α3) and HsN3 (β7) of the 20S proteasome (Beraud and Greene, 1996; Rousset et al., 1996). The interaction between Tax and these subunits was studied by overexpressing single subunits and was not done in the context of the assembled proteasome. Therefore, the functional significance of this association remained uncertain (Beraud and Greene, 1996; Petropoulos and Hiscott, 1998; Rousset et al., 1996).

The aim of the work presented in this thesis is to further characterise the interaction between the HTLV-1 Tax protein and the 20S proteasome, and to investigate the role of the interaction in cellular processes and the CTL response against HTLV-1.

The specific objectives therefore are (i) to determine the subcellular localisation of the Tax protein and the proteasome; (ii) to characterise the physical interaction between Tax and 20S proteasomes and the effect on the catalytic activity of the proteasome; (iii) to determine the regions of Tax involved in proteasome binding, nuclear localisation and transcriptional activation and the relationship between these properties of Tax; (iv) to investigate the role of the interaction in the processing and presentation of Tax for recognition by CTL.

Chapter 2

Materials and methods

2.1. General reagents

2.1.1. Buffers

TE (Tris/EDTA, DNA buffer):

10mM Tris-HCl (pH 8.0)

1mM EDTA

PBS (Phosphate buffered saline)

We used tablets (Sigma) dissolved in water. Final solution contained:

10mM phosphate buffer (pH7.4)

2.7mM KCl

137mM NaCl

LB (Luria-Bertani) medium (bacterial growth medium):

1 litre: 10g Bacto-tryptone

5g Bacto-yeast extract

5g NaCl

Adjust pH to 7.5 with NaOH and autoclave.

LB plates with antibiotics:

Add 15g agar to 1 litre of LB medium. Adjust to pH 7.0 with NaOH and autoclave. Allow the medium to cool to around 55 °C before adding antibiotics. Pour 20-25ml of medium into 85mm petri dishes. If necessary flame the surface of the medium with a Bunsen burner to eliminate bubbles and let agar harden. Store a 4°C for up to one month.

TBE (Tris/Boric acid/EDTA) buffer:

1 litre: 53.9g Tris base

27.5g Boric acid

3.72g EDTA

Adjust to pH8.3 with NaOH.

2.1.2. Antibodies

2.1.2.1. Antibodies for immunoprecipiation and Western blotting

Tax specific antibodies:

1135 TB: Terminal bleed of rabbit immunised with the synthetic C-terminal peptide of Tax (MISPGELEPPSEKHFRETEV), polyclonal.

1153 TB: Terminal bleed of rabbit immunised with the synthetic C-terminal peptide of Tax (MISPGELEPPSEKHFRETEV), polyclonal (different rabbit than 1135).

BR-76: Polyclonal rabbit anti-serum against the Tax C-terminus.

Y8: Mouse anti-Tax antibody. Tax epitope unknown.

mAb1316: Monoclonal mouse antibody against the Tax C-terminus (IgG2a subtype). Obtained from the NIH AIDS Research and Reagent Program.

Proteasome specific antibodies:

MCP21: Monoclonal mouse antibody against the HC3 α-subunit (α2) of the human 20S proteasome. IgG1 subtype (Hendil et al., 1995).

α-LMP2: Polyclonal rabbit antiserum against the LMP2 subunit of the human 20S proteasome (Belich et al., 1994). Gift of Dr. J. Trowsdale.

α-LMP7: Polyclonal rabbit anti-serum against the LMP7 subunit of the human 20S proteasome (Belich et al., 1994). Gift of Dr. J. Trowsdale.

Influenza nucleoprotein specific antibody:

4.7.18: Monoclonal mouse antibody against influenza nucleoprotein

Splicing factor specific:

mAb104: Monoclonal mouse antibody specific for a phospho-epitope in members of the SR family of nuclear pre-mRNA splicing factors (Roth et al., 1991). Gift of Dr. G. Screaton.

Secondary antibodies:

Anti-mouse: Goat anti-mouse IgG - horse radish peroxidase conjugated (HRPO) (Sigma)

Anti-rabbit: Goat anti-rabbit IgG - horse radish peroxidase conjugated (HRPO) (Sigma)

2.1.2.2. Antibodies for immunofluorescense microscopy

Tax specific antibodies:

mAb1314: Also known as α-Tax3. Monoclonal mouse antibody against the Tax C-terminus (IgG2a subtype). Obtained from the NIH AIDS Research and Reagent Program.

G38: Polyclonal rabbit anti-serum against the Tax C-terminus. Gift of Dr. Francoise Bex.

Proteasome specific antibody:

MCP21: Monoclonal mouse antibody against the HC3 α-subunit (α2) of the human 20S proteasome. IgG1 subtype (Hendil et al., 1995).

NF-κB/IκBα specific antibodies:

α-p65: Polyclonal rabbit antibody against the human NF-κB subunit p65. (Santa Cruz, sc-372)

Other antibodies:

α-HA: Polyclonal rabbit antibody against the HA-tag derived from influenza hemagglutinin. (Santa Cruz, sc-805)

α-PML: Polyclonal rabbit antibody against human PML protein. Gift of Dr. Francoise Bex.

Secondary antibodies:

anti-mouse-FITC: Goat anti mouse IgG conjugated to fluorescein isothiocyanate (Jackson Immunoresearch).

anti-rabbit-LRSC: Goat anti rabbit IgG conjugated to lissamine rhodamine sulfchloride (Jackson Immunoresearch).

anti-rabbit-Alexa: Goat anti rabbit IgG conjugated to Alexa Fluor 546 (Molecular Probes)

anti-mouse IgG2a-FITC: Goat anti mouse lgG2a conjugated to fluorescein isothiocyanate (Southern Biotechnologies)

anti-mouse IgG1-biotin: Goat anti mouse IgG1 conjugated to biotin (Southern Biotechnologies).

Streptavidin-Cy5: Streptavidin conjugated to Cy5 fluorochrome (Jackson Immunoresearch)

2.1.2.3. Antibodies for fluorescence activated cell sorting (FACS) analysis

CD8 specific antibody:

anti-CD8-tricolour: Mouse monoclonal antibody to human CD8 conjugated to Tri-colour (Caltag).

MHC class I specific:

W6/32: Monoclonal mouse antibody recognising a conformation specific epitope in the human MHC class I α chain.

Secondary antibody:

anti-mouse-FITC: Goat anti mouse IgG conjugated to fluorescein isothiocyanate (Jackson Immunoresearch).

2.2. DNA techniques

2.2.1. Bacterial strains and culture

For cloning purposes the bacterial strains JM109 and DH5α were used. They were grown either in LB solution or on LB-agar plates. Antibiotics were added depending on the resistance gene carried by the plasmid.

For mutagenesis of Tax the repair minus strain BMH 71-18 *mutS* was used.

For expression of recombinant Tax-6His protein in E.coli the strain BL21(DE3) was used in combination with pET-28c expression plasmid.

2.2.2. Preparation of plasmid DNA

2.2.2.1. Qiagen maxi plasmid isolation

This method for plasmid isolation was used to isolate large amounts (100µg upward) of plasmid DNA, which was mainly used to perform sequencing reactions and transfections.

Bacterial cells were transformed with the relevant plasmid, as described elsewhere. The next day a colony was picked and used to inoculate a 5ml overnight culture (LB with antibiotics). 1 ml of this culture was subsequently used to inoculate a 500ml overnight culture in a 2-litre flask.

To isolate the plasmid from the bacterial culture the following steps were followed:

1. The bacterial culture was transferred to a 1-litre container and centrifuged for in a JA4.2 Beckman rotor (30', 4000rpm, 4°C). Afterwards the supernatant was discarded completely.
2. The pellet was resuspended in 10ml resuspension buffer P1 (50mM Tris-Cl pH8.0, 10mM EDTA) and the suspension transferred to a 50ml Falcon tube. Subsequently, 10ml of alkaline lysis buffer P2 (0.2M NaOH, 1% SDS) was added after which the tube was inverted several times to mix the solutions. This mix was kept at RT for 5' to allow lysis. 10ml of cold neutralisation buffer P3 (3M KAc, pH5.5) was then added, immediately followed by horizontal shaking of the tube to allow quick mixing and denaturation of protein. The samples were kept on ice for 20' to allow renaturation of plasmid DNA and subsequently centrifuged in a Sorvall RT6000D table top centrifuge (25', 4000rpm, 4°C).
3. A QIAGEN–tip500 was equilibrated with 10ml QBT buffer (750mM NaCl, 50mM MOPS pH7, 15% ethanol, 0.15% Triton X-100). The supernatant from step 2 (containing the plasmid DNA) was applied to the column after filtering it through a 70µm cell strainer to prevent debris from blocking the column. The column was washed twice with 30ml QC buffer (1M NaCl, 50mM MOPS pH 7, 15% ethanol) and the plasmid eluted with 15ml elution buffer QF (1.25M NaCl, 50mM Tris-Cl pH8.5, 15% ethanol). The eluate was collected in Beckman polyallomer tubes and 0.7 volumes (10.5ml) isopropanol added and mixed with the eluate.

4. The samples were centrifuged in a Beckman JA-20 rotor (30', 20,000rpm, 4 °C). The supernatant was carefully removed (pellet can be loose), 1ml of 70% ethanol added and the whole mix transferred to one or two 1.5ml Eppendorf tubes. The tubes were centrifuged in a table top Eppendorf centrifuge (5', 13,000rpm, 4 °C). The supernatant was removed and the pellet either washed again with 1ml of 70% ethanol or left to air dry. Finally, the pellet was resuspended in 100-200µl of TE and stored at –20°C. The DNA concentration was determined by UV spectrophotometry.

2.2.2.2. Hybaid plasmid DNA isolation

This method was used to isolate plasmid DNA from small cultures (5 ml). The yield (~5µg) and purity were usually low and the plasmids were only used for analytical purposes, i.e. for analysis by restriction enzyme digestion.

The procedure was as follows:

1. 5ml of LB medium with antibiotics in a 20ml universal tube was inoculated with a single colony and incubated overnight at 37°C. The samples were centrifuged in a Sorvall RT6000D table top centrifuge (5', 2000rpm, RT). 4ml supernatant was removed and the pellet resuspended in the remaining medium. The suspension was transferred to a 1.5ml Eppendorf tube, centrifuged (1', 13,000rpm, RT) and the supernatant completely removed.
2. The pellet was resuspended in 210µl suspension solution (50mM Tris-Cl pH8.0, 10mM EDTA, 100µg/ml RNase). 210µl of cell lysis solution (200mM NaOH, 1% SDS) was added and the tube inverted to mix. After leaving the sample at RT for 5', 280µl of neutralisation solution (containing acetate and guanidine hydrochloride) was added and the tube shaken horizontally to mix. Subsequently, the samples were centrifuged in an Eppendorf centrifuge (10', 13,000rpm, RT).
3. The supernatant was taken and applied to a Hybaid spin column in a receiver tube. Samples were centrifuged (1', 13,000rpm, RT). The flow-through was discarded and 700µl of wash solution (containing ethanol, NaCl, EDTA, Tris-Cl) applied to the column. Samples were centrifuged twice (1', 13,000rpm, RT), with discarding of the flow-through after each time.
4. The column was placed in a 1.5ml Eppendorf tube without lid. 50µl distilled water was pippetted onto the membrane of the column and left to absorb for 1'. The

samples were centrifuged (2', 13,000rpm, RT) and the eluate (containing the plasmid DNA) transferred to a fresh Eppendorf tube and stored at –20°C. The DNA concentration was determined by UV spectrophotometry.

2.2.3. Recombinant DNA techniques

2.2.3.1. Polymerase chain reaction (PCR)

PCRs were usually performed in a final volume of 50µl with the following final concentrations of the components:

50mM	KCl
1.5mM	$MgCl_2$
10mM	Tris-HCl pH 8.3
200µM	dNTPs (Pharmacia)
2µM	Primer 1
2µM	Primer 2
1U	Taq polymerase (Bioline)

In this study only plasmid DNA was used as a template. Less than 100ng template DNA was added to each reaction. A drop of mineral oil was applied on top of the mix before the start of the thermocycling. The annealing temperature was usually chosen as 5°C under the lowest of the annealing temperature of the two primers. Primers were designed to have an annealing temperature of around 60 °C and to have a C or G nucleotide at the 3' terminus. The sequences of the primers used in this study are given in appendix B.

A typical programme for the thermocycling was as follows:

1 cycle:			30 cycles:		
5'	94°C	(denaturation)	45"	94°C	(denaturation)
1'	60-70°C	(annealing)	30"	60-70°C	(annealing)
1'	72°C	(extension)	1'	72°C	(extension)

After the last cycle the samples were kept at 4°C until they were removed from the machine and stored at -20°C.

2.2.3.2. DNA digestion using restriction enzymes

Restriction enzymes were purchased from New England Biolabs and used in combination with the buffers supplied by the manufacturer. 10U of enzyme was used per μg of DNA. Digestions were done at 37°C for 1-2 hours.

2.2.3.3. Klenow reaction

Sometimes the digestion of DNA with restriction enzymes had left a 5' overhang at the end of a DNA fragment and it was necessary for the next cloning step that this end was blunt. In this case the recessed 3' end at the same end of the DNA duplex was extended to the end of the 5' strand using the Klenow fragment of DNA polymerase I. The enzyme and buffer were purchased from New England Biolabs and used according to the manufacturer's instructions and in a final volume of 100μl. dNTPs (0.5mM final concentration) were purchased from Pharmacia. The reaction was performed at 37°C for 30'. Subsequently the Klenow enzyme was inactivated by heating the sample at 75°C for 10'.

2.2.3.4. Phosphatase treatment

To prevent the self-ligation of a linearised vector in a ligation reaction (which is an efficient process), the linearised vector was generally treated with alkaline phosphatase prior to the ligation reaction. The phosphatase will remove phosphates from the 5' end of DNA fragments, thereby rendering them unsuitable for ligation to the 3' end of another DNA strand. Alkaline phosphatase and the accompanying buffer were purchased from Boehringer and used according to the manufacturer's instructions.

Because the phosphatase remains very strongly attached to the DNA after the reaction and can inhibit the ligation reaction, it is necessary to remove the phosphatase by phenol extraction. The procedure is as follows:

Add 100μl of TE equilibrated phenol to the 100μl of the phosphatase reaction and vortex for 30". Spin in an Eppendorf centrifuge for 1' at 13,000rpm and transfer the top (aqueous) layer to a fresh Eppendorf tube. Add 100μl ether to the transferred liquid and vortex for 30". Spin in an Eppendorf centrifuge for 1' at 13,000rpm and transfer the

bottom layer to a fresh Eppendorf tube. Subsequently purify the DNA fragment using the Qiagen PCR purification kit.

2.2.3.5. DNA agarose gel electrophoresis

Samples of DNA (plasmids, restriction enzyme digests, PCR products) were analysed by TBE/agarose gel electrophoresis, using a Flowgen gel apparatus. 1x TBE buffer was made and 0.8-1.2 % (w/v) agarose added and the mixture heated in a microwave until boiling. When the agarose was completely dissolved, the mixture was cooled down under running water until touch-warm. Then ethidium bromide (<1µg/ml) was added to the mix and the mix poured into the gel container and left to solidify. TBE buffer was poured on top of the gel. The 6x DNA loading buffer was made up of the following: 15% (v/v) Ficoll-400, 0.25% (w/v) Bromo Phenol Blue. After running of the gel, the DNA fragments were visualised under UV light and pictures made with a Biorad gel documentation system (Gel Doc 2000).

2.2.3.6. Purification of DNA fragments

For purification of PCR products, DNA digestion products and DNA fragments from agarose gels the Qiagen PCR puification kit and the Qiagen Gel extraction kit were used. Procedures were performed according to the manufacturer's instructions and the DNA fragments eluted from the spin columns with 30µl of water.

2.2.3.7. DNA ligation

Ligations were performed using T4 DNA ligase with accompanying buffer (New England Biolabs). Approximately 100ng of vector and equimolar amount of insert were used. The final volume was always 10µl. Ligation reactions were performed either for 2 hours at room temperature for ligations involving sticky ends or overnight at RT or 14°C for blunt end ligations.

As controls, the insert was omitted form the reaction mix (to see amount of self ligation of vector) or both the insert and the T4 ligase were omitted (to see amount of uncut vector in preparation). Only if the control plates (after transformation) had considerably

fewer (5-10 times) colonies than the 'real' ligation, we proceded with the analysis of clones.

2.2.3.8. Transformation of bacteria with plasmid DNA

A 5ml LB culture of the relevant bacterial strain was incubated overnight at 37°C. The next day a 50 ml LB culture was inoculated with 0.5-1ml of the overnight culture and incubated at 37°C until the OD_{600} was between 0.35 and 0.55. The culture was transferred to a 50ml Falcon tube and centrifuged in a Sorvall RT6000D centrifuge (10', 3000rpm, RT). The supernatant was discarded and the pellet resuspended in 2ml of TSS solution. 14ml Propylene tubes were pre-chilled on ice and 100µl of the TSS suspension transferred to each tube. 10-100ng of plasmid DNA or 5µl of a ligation reaction was added to the cells and gently mixed. The tubes were left on ice for 30' before being transferred to a 42°C waterbath for 45". They were transferred back on ice for 2' and 900µl of LB was added. The suspension was incubated at 37°C for 1 hour, to allow expression of the antibiotic resistance gene. Then the suspension was transferred to an Eppendorf tube and pelleted (1', 13,000rpm, RT). Supernatant was removed and the pellet resuspended in 100µl LB. 20 and 80µl of resuspended cells were plated out on LB plates containing antibiotics to select for transformed bacteria.

100ml TSS solution:

90ml	LB
5ml	DMSO
5ml	1M $MgCl_2$
10g	PEG-6000/-8000

2.2.4. Mutagenesis

As part of the presented study, several mutants of Tax were generated using the GeneEditor™ *in vitro* site-directed mutagenesis system (Promega). This system uses antibiotic selection to obtain a high frequency of mutants. Together with the annealing of a mutagenic oligonucleotide to the Tax sequence, a selection oligo is annealed to the ampicillin resistance gene present on the pJFE-link plasmid. Subsequent synthesis and

ligation of the mutant strand links the two oligonucleotides. The selection oligo will alter the ampicillin gene on the newly synthesised mutant DNA strand in such a way that it will provide resistance to the GeneEditor^{TM} antibiotic selection mix (GEASM), while maintaining ampicillin resistance. Therefore, resistance to DEASM encoded by this mutant strand will facilitate selection of the desired mutation.

Alkaline denaturation of dsDNA

Approximately 2µg (0.5pmol) of pJFE-Tax was denatured by incubation with 200mM NaOH and 0.2mM EDTA for 5' at RT in a volume of 20µl. DNA was subsequently precipitated by addition of 2µl of 2M ammonium acetate and 75µl of 100% ethanol and incubation at -70°C for 30'. DNA was pelleted by centrifugation (15', 13,000rpm, 4°C), washed with 200µl 70% ethanol and the pellet air-dried. Finally, the DNA was taken up in 100µl TE buffer.

Hybridisation of oligos to template

The following mix was made:

Denatured template DNA	10µl (0.05pmol)
Phosphorylated selection oligo	1µl (0.25pmol)
Phosphorylated mutagenic oligo	1.25pmol
10x annealling buffer	2µl
Sterile distilled water	to final volume of 20µl.

This mix was heated at 75°C for 5' and allowed to cool down slowly (1.5°C per minute) to 37°C.

Mutant strand synthesis and ligation

The following components were added to the annealing reaction (in this order):

Sterile distilled water	5µl
10x synthesis buffer	3µl
T4 DNA polymerase	1µl (5-10U)
T4 DNA ligase	1µl (1-3U)

The samples were gently mixed and incubated at 37°C for 90'.

Transformation of BMH 71-18 mutS competent cells

The heteroduplex is then transformed into the repair minus BMH 71-18 *mutS* cells to prevent selection against the desired mutation. Competent cells were provided with the kit and transformation with 7.5µl (~50ng) of mutagenesis reaction was essentially as described in the previous section. After allowing expression of the antibiotic resistance gene by incubation of the cells in 1 ml of LB at 37°C for 60', 4ml of LB supplemented with 100µl GEASM was added and the culture incubated overnight at 37°C. GEASM should select for cells harbouring plasmids with the mutated ampicillin resistance gene and, thereby, the mutated Tax gene.

Transformation of JM109 cells and identification of mutants

Plasmid DNA was isolated from the overnight cultures of BMH 71-18 *mutS* cells, using the Hybaid method described elsewhere. 10-50ng of DNA was used to transform JM109 cells according to the protocol described before. Transformed cells were plated onto LB plates containing 150µl of GEASM and 250µg ampicillin per 20ml LB. Plates were incubated overnight at 37°C and colonies picked. Clones were initially analysed by performing minipreps and subsequent restriction enzyme analysis, as all mutagenic oligos introduced new restriction sites. When clones looked good after this analysis, a Qiagen maxiprep was performed and the Tax sequence completely sequenced.

2.2.5. DNA sequencing

Sequencing of pJFE-Tax and all the mutant constructs derived from it was done in the DNA Sequencing Facility of the Department of Biochemistry, University of Oxford. Sequencing was performed using ABI BigDye^{TM} dye terminator chemistry and an ABI 377 sequencer. The primers used were the JFE5-PRI and JFE3-PRI (unlabelled) primers which bind to sequences in pJFE-Tax upstream and downstream, respectively, of the Tax coding sequence.

2.3. Tissue culture techniques

Most tissue culture was performed under sterile conditions in Bio-mat2 Class II microbiological safety cabinets and cells were maintained in Heraeus instruments

incubators set at 37 °C and 5% CO_2. Work involving HTLV-1 infected cell lines was performed in a category 3 safety laboratory.

2.3.1. Maintenance of cell lines

293T cells (an SV40 transformed human embryonic kidney cell line) were maintained in D-10, which is DMEM (Dulbecco's Modified Eagle medium) supplemented with 10% foetal calf serum (FCS), 2mM L-glutamine and 100U/ml of both penicillin and streptomycin. The latter three are commonly called G/P/S).

Most other cell lines, such as B cell lines and hybridomas, were maintained in R-10 medium, which is RPMI (Rosell Park Memorial Institute medium) supplemented with 10% FCS and G/P/S. Live cells were counted using a 1:1 dilution of the cell suspension with Trypan blue (live cells exclude the blue stain) and an improved Neubauer cytometre.

Special cell lines used: 721.45: human B lymphoblastoid cell line. 721.174: 721.45 derivative with only one copy of chromosome 6 containing a deletion in the class II region of the MHC locus, thereby lacking TAP and LMP2 and LMP7 genes (DeMars et al., 1984). 721.174/TAPs: 721.174 cells stably transfected with plasmids containing the human TAP1 and TAP2 genes (Cerundolo et al., 1995). 721.174/TAPs/LMP7: 721.174/TAPs cells stably transfected with plasmid containing the LMP7b gene (Sewell et al., 1999).

721.174/TAPs cells were grown in the presence of 0.5mg/ml G418. 721.174/TAPs/LMP7 cells were grown in the presence of 0.5mg/ml G418 and 0.2mg/ml hygromycin.

2.3.2. Transfections

2.3.2.1. Easyfector transfection method

Most commonly, 293T cells were transfected using the Easyfector (Equibio) transfection reagent. The method described below will apply for the transfection of cells in 75cm^2 flasks, with the number between brackets indicating the amounts used when transfections were done in 6-well plates.

It was made sure that cells were between 50 and 70% confluent at the moment of transfection. 10 µg (2µg) plasmid DNA was diluted in 200µl (100µl) optiMEM (Gibco). 20µg (4µg) Easyfector was diluted in 180µl (100µl) optiMEM. Both solutions were mixed together and gently vortexed. The samples were left at RT until the cells were ready for transfection. The medium was removed from the cells. The cells were washed once with 8ml (3ml) optiMEM and 5ml (1ml) optiMEM was added to the cells. The 400µl (200µl) of DNA/Easyfector/optiMEM mix was then added dropwise to the medium. The medium was swirled to ensure good mixing. Cells were incubated at 37°C either during the day or overnight before 15ml (3ml) of D-10 was added to the flask (well). Cells were harvested 48-72 hours after transfection.

2.3.2.2. Ca^{2+}-phosphate transfection method

For transfection of 293T cells in 6 well plates the following protocol was used:
2 µg plasmid DNA was mixed into 100µl 0.25M $CaCl_2$. Subsequently 100µl of 2x HEPES buffer was added, while producing bubbles with a p1000 pipette. The samples were left at RT for 10' before adding the mix dropwise to the wells, where the cells were kept in 3ml D-10 (RPMI doesn't have the right pH). The medium was changed 6-12 hours later, and cells harvested 48-72 hours post-transfection.
500 ml 10x HBS (Hepes buffered saline) buffer was made as follows: 40g NaCl, 29.7g HEPES (not Na salt), 1g Na_2HPO_4. Make up volume up to 450ml with distilled water, adjust pH with 1M NaOH to 7.0 (around 23.1 ml) and make a final volume of 500ml with distilled water. 2x HBS was made by dilution and the pH checked. All solutions were filtered through a 0.2µm filter before use.

2.3.3. Vaccinia infection and titration

Recombinant vaccinia viruses were propagated in the human cell line tk143, which lacks the thymidine kinase (*tk*) gene. Recombinant vaccinia viruses have their *tk* gene disrupted due to homologous recombination of the recombinant gene into the *tk* gene. BUdR (5'bromo-2'deoxyuridine, 200x solution is 5mg/ml) is a reagent that will kill cells that express the *tk* gene. Therefore, this reagent will select for recombinant vaccinia

viruses and against wild type WR vaccinia viruses. BUdR is kept in the medium during expansion to maintain a pure population of recombinant viruses.

Expansion of recombinant vaccinia viruses:

1. The medium was removed from 80% confluent tk143 cells in 175 cm^2 flasks. The cells were washed with 8ml of DMEM and 5ml DMEM/0.1%BSA added on top of the cells. 1-2x10^7 pfu (plaque forming units) of the recombinant vaccinia virus was added and left for 1-2 hours to adhere to the cells. 25ml of D-10 containing 1x BUdR was added and the cells were left for 2-3 days.
2. Once a good cytopathic effect was visible (cells round up and detach), the cells were dislodged from the flask by tapping and the suspension transferred to a 50ml Falcon tube. Cells were pelleted by centrifugation (5', 2000rpm) and the supernatant removed.
3. The pellet was resuspended in 3ml of DMEM/0.1%BSA and subjected to 3 freeze-thaw cycles (alternating dry-ice and 37°C) with vortexing in between the cycles. Afterwards, samples were also sonicated 2 times 30", as well as before every time we would use the stock. The samples were aliquoted in 0.5ml portions into cryo-tubes, snap frozen on dry-ice and stored in liquid nitrogen.

Titration of recombinant vaccinia viruses:

1) Serial dilutions of the recombinant vaccinia virus stocks (sonicated before use) were made in DMEM/0.1%BSA. At least 1ml of the dilutions 10^{-2}, 10^{-4}, 10^{-6}, 10^{-7}, 10^{-8} and 10^{-9} were made. Wells of a 6-well plate containing 80% confluent tk143 cells were washed with 2ml DMEM/0.1%BSA and 0.5ml of each vaccinia dilution was added in duplicate to two wells. After 2 hours, 2.5ml of D-10 containing 1x BUdR was added to the wells and the cells left for 2-3 days.
2) When plaques had formed, cells were fixed with 4% formalin/PBS for 1 hour at RT. Subsequently, the fixative was removed and the cells stained with 1% crystal violet in water for 1-2 minutes. The staining solution was removed, the cells gently washed with water and left to air dry. Alternatively, the cells were fixed and stained simultaneously with a solution of 0.1% crystal violet and 20% methanol in PBS for 20". The number of pfu per ml of vaccinia stock solution

was determined by counting the plaques from 1 ml of dilution (the duplicate wells) and dividing it by the dilution factor.

2.3.4. Pulse-chase metabolic labelling

For certain experiments we labelled newly synthesised cellular proteins with ^{35}S-methionine and ^{35}S-cysteine. This was necessary to identify a cohort of proteins synthesised in a short period of time, that could then be followed with regard to movement within the cell (nucleocytoplasmic transport) or with regard to their intracellular degradation (to determine a protein's half-life).

Pulse-chase experiments on adherent cells were performed as follows:

1) Cells were taken 48 hours post-transfection. The medium was removed and the cells washed once with methionine/cysteine free RPMI. 5ml of methionine/cysteine free RPMI with 10% dialysed FCS (without methionine and cysteine) was added per 75cm^2 flask and the cells left for 1 hour to deplete the intracellular pool of methionine and cysteine.

2) The medium was then removed and replaced by 5ml of fresh methionine/cysteine free RPMI with 10% dialysed FCS. Then ^{35}S labelled methionine and cysteine was added (Promix, Amersham) at a concentration of 100µCi per 10^7 cells (or 20µCi/ml). Depending on the experiment this incubation lasted 1 to 2.5 hours.

3) After the labelling, the medium was removed, the cells washed once with 5ml of D-10 and either harvested immediately or 20ml of D-10 was added and the cells incubated at 37°C for the desired chase period. Cells were harvested by removing the medium and incubating the cells with 2-5mM EDTA in PBS for 5-10' (cells detach). The cells were pelleted (5', 1500rpm, 4°C) and the pellets frozen at -20°C.

For short pulse-chase experiments with adherent cells and suspension cells the protocol was slightly different:

1) Adherent cells were brought into suspension by incubation with trypsin/EDTA. Trypsin was subsequently inactivated by adding DMEM/20%FCS. The cell suspension was centrifuged (5', 1500rpm, RT) and the pellet washed with 2ml

methionine/cysteine free RPMI. Subsequently, the pellet was resuspended in 0.5ml methionine/cysteine free RPMI with 10% dialysed FCS per 10^7 cells and left for 1 hour.

2) After the starvation, ^{35}S labelled methionine and cysteine was added (Promix, Amersham) at a concentration of 100μCi per 10^7 cells and cells left to label for the required time.

3) After the labelling, 5ml of pre-warmed D-10, which contains excess unlabelled methionine and cysteine, was added to the samples. Samples were harvested by centrifugation (5', 1500rpm, 4°C) either immediately or after an incubation period at 37°C. The pellets were frozen at -20°C.

2.3.5. Cytotoxic T cell tissue culture techniques

2.3.5.1. Isolation of peripheral blood mononuclear cells (PBMCs) from blood

Peripheral blood mononuclear cells (PBMCs) were obtained from 20-60ml venous blood samples from volunteers, taken into tubes containing approximately 100μl of preservative-free Heparin (at 1000U/ml). Blood was diluted 1:1 with RPMI-1640 (Gibco). Then 6ml of Lymphoprep (Nycomed, Norway) was put in 20ml universal tubes and 15 ml blood/RPMI added carefully on top. Samples were spun at 1800rpm for 25', with the brake switched off. The white layer at the interface was carefully removed using a Pasteur pipette, taken up in a large volume of RPMI and spun at 2000rpm for 10'. Next the pellet was resuspended in 10ml of RPMI and spun at 1200rpm for 10'. The PBMCs (pellet) were either resuspended in cloning mix and irradiated for use as feeders for CTL lines and clones or resuspended in a small volume of FCS/10%DMSO for storage in liquid nitrogen.

2.3.5.2. Restimulation of CTL lines and clones

CTL lines and clones needed to be restimulated every 10-14 days in order to keep them proliferating. The restimulation mix consisted of the following components:

Irradiated PBMCs from 3 different donors	10^6/ml
Irradiated peptide pulsed HLA-matched B cell line	10^5/ml
PHA	1µg/ml
Human serum (HS)	5%
FCS (batch tested for T cell growth)	5%
RPMI medium (with P/S/G)	

IL-2 was added at day 3 at a final concentration of 10U/ml.

PBMCs were isolated from blood as described above. $2x10^7$ frozen PBMCs of 3 different donors were taken from liquid nitrogen. Because of the different haplotypes of the 3 donors, the mixed PBMCs will give rise to a so-called mixed lymphocyte reaction (MLR), producing cytokines which stimulate the T cells to proliferate. After thawing of the cells, they were washed twice with 30 ml of R-10. Finally the cells would be taken up in 30 ml of cloning medium (RPMI/HS/FCS/PHA) and irradiated for 12'.

3 $x10^6$ cells were taken of a growing EBV transformed B cell line with the restricting HLA allele for the relevant peptide epitope (HLA-A2 for Tax 11-19). Cells were pelleted by centrifugation (5', 1500rpm, RT) and resuspended in 1ml of R-10. Peptide was added at a final concentration of 10µM and the cells incubated at 37°C for 1-2 hours. Then 20ml RPMI was added and the cells pelleted by centrifugation. This wash was repeated once, the cells were taken up in cloning medium (RPMI/HS/FCS/PHA) and irradiated for 20'.

Finally, all the components were mixed together to produce the restimulation mix listed above. Approximately 1ml of the mix was added per well of a 24-well plate. On day 3, IL-2 was added to a final concentration of 10U/ml. CTL were kept at around 10^6 cells per well (depending on the proliferation/restimulation stage).

2.3.5.3. Cloning of CTL

The medium used for cloning was identical to the mix used for restimulating CTL lines and clones described in the previous section, i.e. RPMI/HS/FCS/PHA/PBMCs/BCL. In

this case a serial dilution of the CTL line to be cloned was made, in steps of 1:10 dilution. Finally, the CTL were mixed with the restimulation mix and 100µl of the resulting mix was distributed into each well of 96-well plates. Different dilutions of the CTL would be made, resulting in final concentrations of 0.3, 1 or 3 cells per well. On day 3, 100µl of cloning medium with 20U/ml IL-2 was added to each well (10U/ml final concentration). After 14 days growth of clones was checked microscopically and specificity of the candidate clones checked by tetramer staining. When tetramer staining indicated a positive clone, the clone was transferred to a 24-well plate well and restimulated as described in the previous section.

2.3.5.4. Chromium release CTL assay

Chromium release CTL assays were used to detect the presentation of class I restricted epitopes on the surface of infected cells. In short: target cells were infected with recombinant vaccinia virus expressing an antigen and labelled with ^{51}chromium. Epitope specific cytotoxic T cells are then added and CTL recognition of the relevant epitope on the infected target cell leads to lysis of this cell and the release of chromium into the medium.

Infection of target cells

Target cells used were typically B cell lines. $5x10^5$ cells per sample were taken and centrifuged (5', 1500rpm, RT). Supernatant was removed and cells washed with 3ml of RPMI/0.1%BSA. The pellet was loosened and the recombinant vaccinia virus added at multiplicity of infection of 5-10 pfu/cell. Cells were left for 90', washed with 2ml of RPMI and resuspended in 1ml of R-10. Typically cells were left overnight to express. In some cases expression was allowed for 2-3 hours before proceeding with the labelling and the rest of the CTL assay.

Labelling of target cells

Target cells ($5x10^5$/sample) were pelleted and the supernatant removed as much as possible. The pellet was loosened and resuspended in 30 µl of ^{51}Cr (=30µCi). 20 µM of peptide was added to the positive controls. Cells were incubated for 1 to 1.5 hours, during which time the CTL were prepared. After labelling, the cells were washed twice

with 4 ml of R-10 and taken up in 1 ml of R-10. The cells were counted, diluted to $5x10^4$ cells/ml and added to the CTL at 100µl ($5x10^3$ cells) per well. Each target was also plated in 4 extra wells: 2 for the spontaneous lysis control and 2 for the total release control. 100µl R-10 was added to these wells instead of CTL.

CTL preparation

During the labelling of target cells, the CTL were either thawed from liquid nitrogen or cultured cells taken from the incubator. Cells were counted, the total number of CTL determined and a decision made on the effector:target ratios to be tested. Dilutions of CTL were made and 100µl of cells per well distributed in 96-well round-bottom plates. Each experimental point was done in duplicate. After addition of the target cells, the plate was incubated at 37°C for 4-7 hours.

Harvesting

20µl of 20% Triton X-100 was added to the wells for the total lysis and mixed well with a p200 pipette. Harvesting was done by carefully pipetting 20 µl of the supernatant from the top side of each well into an Opti-plate. 200 µl Microscint (Packard) was added to each Opti-plate well, the plate sealed with a Topseal sticker and the plate shaken vigorously to mix before counting the samples in a Topcount microplate scintillation counter (Packard).

Specific lysis was calculated according to the following formula:
100 x (experimental lysis – spontaneous lysis) / (total lysis – spontaneous lysis)

Spontaneous lysis was always below 20% in the experiments presented in this thesis.

2.4. Protein techniques

2.4.1. Monoclonal antibody purification

For this study, the monoclonal antibodies MCP21 (anti-HC3 20S proteasome subunit) and mAb1316 (anti-Tax) were produced from B cell hybridomas and purified over a proteinA-sepharose (Sigma) column. Since both of these antibodies are of the mouse

IgG1 subtype, which has a relatively low affinity for proteinA, the antibodies were loaded onto the column in high salt (3.3M NaCl) and high pH (8.8) (Ey et al., 1978). Per batch of antibody purification, NaCl was dissolved in 300ml hybridoma supernatant to make a final concentration of 3.3M and 33ml of 1M Tris-HCl pH8.8 added (0.1M final).

The column consisted of 1 ml wet proteinA-sepharose which was equilibrated in a buffer of 0.1M Tris pH8.8/3M NaCl. The hybridoma supernatant (salt and pH adjusted) was applied to the column and allowed to pass through by gravity flow. The column was then washed sequentially by 10ml 50mM Tris pH8.8/3M NaCl and 10ml 10mM Tris pH8.8/3M NaCl. Antibody was then eluted with 7.5ml of 50mM citrate pH6.0 buffer in 0.5ml portions, which were collected in Eppendorf tubes containing 60µl 1M Tris pH8.0. The column was finally stripped with 7.5ml of 0.1M glycine pH3.0 buffer. Then the column was washed with 20ml 0.1M Tris pH8.0 and stored in 0.1M Tris pH8.0/ 20% methanol. Elution fractions were analysed by OD_{280} measurement and SDS-PAGE.

2.4.2. Production of HLA-A2/β2m/Tax 11-19 tetramer complexes

Protein expression

The HLA-A2.01 heavy chain and β2microglobulin were overexpressed in the BL21(DE3) strain of *Escherichia coli.* The methods for expression and inclusion body preparation are identical for the two proteins.

30ml LB with 100µg/ml ampicillin was inoculated with 1 colony from a plate or a scrape from frozen stock and incubated overnight at 37°C. The next day 6 flasks containing 1 litre of LB and 100µg/ml ampicillin each were inoculated with 2.5ml of the overnight culture. The cultures were grown until OD_{600} was 0.5 and at that time 0.5ml of 1M IPTG was added (0.5mM final). The cells were incubated at 37°C for another 4-5 hours to allow expression of the proteins. After that, the suspensions were transferred to 1-litre containers and bacteria pelletted by centrifugation in a JS4.2 rotor (30', 4200 rpm, RT). The supernatant was poured off and the pellets frozen at –20°C.

Protein purification

Cell pellets were thawed and each pellet resuspended in 15ml ice-cold PBS (90ml total for 6 flasks). The suspension was divided over three 50ml falcon tubes (30ml each) and

each tube was sonicated at maximum output for 7 times 1 minute. The lysates were transferred to 2 polyallomer 50ml tubes and centrifuged in a JA20 rotor for 10' at 15,000rpm and 4°C.

The supernatants were removed, each pellet loosened in 20ml ice-cold PBS and everything transferred to a (big) Dounce homogeniser. After homogenisation, the suspension was transferred to one fresh polyallomer tube. The tube was centrifuged as before and the top layer of the pellet (unlysed bacteria) scraped off. The bottom layer (white; inclusion bodies) was resuspended in 30ml ice-cold PBS, homogenised and again centrifuged in a propylene tube. The pellet, now nice and white, was resuspended and homogenised in 30ml ice-cold PBS for the last time and centrifuged as before. The supernatant was taken off and the pellet taken up in 20ml resolubilisation buffer and resuspended with a Dounce homogeniser. The mix was transferred to a fresh propylene tube and left on rollers overnight at 4°C for the protein to solubilise. The next day the tube was centrifuged for 10' at 15,000rpm and 4°C, and the supernatant taken. The supernatant was filtered through a 0.2µm filter and the protein concentration determined by measuring OD_{280}. 5 and 10µg of protein were checked for purity on a SDS-PAGE gel. Aliquots of 30mg HLA-A2 and 10mg of β2microglobulin were frozen and stored at -80°C.

Refolding, concentration and biotinylation

500ml refolding buffer was prepared and chilled on ice. 30mg HLA-A2 and 10mg of β2microglobulin were taken from -80°C and thawed. The heavy chain was taken up in 10ml of guanidine buffer. 10mg peptide was dissolved in 1 ml DMSO. The refolding buffer was placed on a stirrer in the coldroom and the following components were added in the described order: 1) 1ml of 0.1M PMSF; 2) 10mg β2microglobulin; 3) 30mg HLA-A2 in guanidine buffer and 4) 10mg peptide. All components were added slowly and dropwise. This mix was left stirring for 48-72 hours to allow refolding of HLA-A2/β2m/Tax 11-19 complexes.

The refolding mix was filtered through a 0.2µm filter and concentrated using a 10K cut-off membrane until a volume of 5ml was left. Subsequently, the buffer was exchanged and a biotinylation reaction performed as follows. The concentrate was centrifuged in Eppendorfs (2', 13,000rpm, 4 °C) and 2.5ml was loaded on a PD10 buffer exchange column (Pharmacia) that was equilibrated with 25ml of biotinylation buffer. 3.5ml of

biotinylation buffer was then applied to the column and the 'eluate' (containing the class I molecules in biotinylation buffer) collected. The following components were added to the protein sample (final concentrations in brackets): PMSF (0.1mM), pepstatin (5µg/ml), leupeptin (2µg/ml), ATP (5mM), biotin (714µM), biotin ligase (BirA) (5µg; Avidity). The biotinylation reaction was allowed to proceed overnight at RT.

Class I Complex purification

The sample was first run over a gel-filtration column (Superdex 75, XK26 column: Pharmacia) to isolate refolded class I complexes and to remove unrefolded heavy chain, β2m, peptide and excess components of the biotinylation reaction. The column was connected to a FPLC (fast performance liquid chromatography) system and 5ml fractions were collected. OD_{280} of the fractions was measured and the relevant fractions taken.
The biotinylated complexes were further purified over a HQ-10 ion-exchange column. Samples were loaded in the (low salt) FPLC buffer and eluted with a salt gradient. OD_{280} of the 1ml fractions was measured to see in which fractions the complex was.

ELISA

To determine which fractions contained the biotinylated complex, an ELISA (Enzyme-linked immunosorbent assay) was performed.
90µl of PBS was put per well of an ELISA plate, 3 wells for each fraction to be tested. 10µl of each fraction was added to one well, mixed and 10 µl transferred to the next well, mixed and once again 10µl was transferred, thereby making 1:10 dilutions of each fraction. The plate was left at 37°C for 1.5 hours to let the protein absorb to the plate. The wells were washed 6 times with excess PBS and 100µl of the following mix was added to each well: 1/2000 diluted Extravidin-peroxidase (Sigma) in PBS/0.5%BSA. The plate was incubated for 30' at RT and the wells washed 6 times with excess PBS. Finally, 100µl TMB reagent (3,3',5,5'-tetramethyl-benzidine; Biorad) was added to each well and the reaction allowed to take place (a blue colour develops). The reaction was quantified by measuring absorbance at 405nm. The positive fractions were taken and their purity checked on an SDS-PAGE gel. The complexes were aliquoted at 60µg per vial, snap frozen in dry-ice and stored at -80°C.

Tetramerisation

An aliquot of 60µg biotinylated class I complex was thawed and transferred to a brown glass vial (to protect it from light). 5 aliquots of 19µl Extravidin-phycoerythrin (PE) (Sigma) were added to the complex, leaving at least 1 hour between each two additions. The final concentration of (monomeric) complex per µl was calculated and the tetramer stored at 4°C.

Solutions:

LB:

Per 1 litre: 10g Bactotryptone
5g Yeast extract
5g NaCl

IPTG (isopropyl-β-D-thiogalactoside):

1M (2000X) = 0.238 g/ml

Urea resolubilisation buffer:

8M urea
0.1M NaH_2PO_4
10mM Tris-Cl pH8
0.1mM EDTA
0.1mM DTT (stored at -20°C)

Refolding buffer (500ml):

400mM L-arginine
100mM Tris pH 8.0
2mM EDTA
5mM reduced glutathione
0.5mM oxidised glutathione
0.1mM PMSF Check pH=8.0

Guanidine buffer (10ml):

6M guanidine-HCl

200mM NaCl

100mM Tris pH 8.0

10mM EDTA

Check pH= 8.0

Biotinylation buffer (100ml):

20mM Tris pH 8.0

50mM NaCl

7.5mM $MgCl_2$

Before reaction add the following (final conc.):

0.1mM PMSF

5µg/ml pepstatin

2µg/ml leupeptin

5mM ATP

714µM biotin.

Biotin stock:

Make up 25mM stock in 200mM Tris base and store frozen.

FPLC buffer:

20mM Tris pH 8

50mM NaCl

Filtered through a 0.2µm filter before use.

2.4.3. Expression and purification of Tax-6His

Expression system

The Tax open reading frame was extended with a sequence coding for 1 lysine residue followed by 6 histidine residues and cloned into the pET28c vector. Expression of Tax-6His is under control of a T7*lac* promoter and the plasmid carries the *lac* repressor gene (*lacI*) under control of its natural promoter. As a host the *E.coli* strain BL21(DE3) was chosen. This strain carries a lysogen of bacteriophage DE3, which harbours the T7 RNA polymerase under control of a *lacUV5* promoter.

Without induction, the *lac* repressor will suppress transcription from both the T7*lac* promoter and the *lacUV5* promoter. However, when IPTG is added to the medium, expression of the T7 RNA polymerase will be induced through the *lacUV5* promoter.

The T7 RNA polymerase will in turn strongly activate transcription from the T7*lac* promoter, leading to expression of Tax-6His.

Expression of Tax-6His

1 litre of LB+30µg/ml kanamycin was inoculated with 2.5ml of overnight culture and incubated until OD_{600} was 0.6. IPTG was added to a final concentration of 1mM and the culture incubated for a further 3 hours. The bacteria were collected by centrifugation (30', 4200rpm) in a JS4.2 rotor), the supernatant removed and the pellet frozen.

Lysis and binding to Ni^{2+}-NTA matrix

The cell pellet was resuspended in 30ml binding buffer supplemented with protease inhibitors per 2 litre of culture. The suspension split into 2 and each fraction was sonicated on ice 5 times for 1 minute. The suspension was transferred to a polyallomer tube and centrifuged in a JA20 rotor (10', 15,000rpm, 4°C). The supernatant was taken off and filtered through a 0.45µm filter.

5ml of wet Ni^{2+}-NTA was incubated overnight in 100mM $NiSO_4$, washed 2 times with 10ml of water and 2 times with 10ml binding buffer. The Tax-6His containing supernatant and the prepared Ni^{2+}-NTA were mixed and incubated overnight on rollers at 4°C.

Column washing and elution.

The next day, the suspension was poured into a column holder and the flow-through collected. The column was washed with 20ml of binding buffer and 20ml binding buffer containing 5mM imidazole and the protein eluted with 10ml of binding buffer containing 100mM imidazole. 1ml fractions were collected and analysed for the presence of Tax-6His protein.

Binding buffer:

500mM NaCl

20mM Tris-Cl pH8.3

Protease inhibitors (final con.):

PMSF (1mM)

PepstatinA (20µg/ml)

Leupeptin (20µg/ml)

Aprotinin 1% (v/v)

2.4.4. Separation of nuclear and cytoplasmic fractions

$3x10^7$ transfected 293T cells were used per sample. Cells were spun down and resuspended in 500µl 15mM Tris HCl (pH7.5), 60mM NaCl, 1mM EDTA, 14mM β-mercaptoethanol, 1x protease inhibitor cocktail (Boehringer) (Buffer 1) with 7.5% PEG-6000 and 0.05% NP40 and left on ice for 30' to allow lysis of the plasma membrane. Nuclei were pelleted by centrifugation (30", 13,000rpm, 4°C) and the cytosolic supernatant fraction transferred to a fresh Eppendorf tube. The cytoplasmic fraction was centrifuged (5', 13,000 rpm, 4°C) to remove all insoluble material and transferred to a fresh Eppendorf tube. The nuclei were washed by resuspension in 500µl Buffer 1 with PEG-6000 (but without NP-40) and spun down again (30", 13,000 rpm, 4°C). Nuclei were then lysed by resuspension in 500 µl Buffer 1 containing 1%SDS. The release of chromosomal DNA required brief sonication of the samples and lysates were centrifuged (5', 13,000 rpm, 4°C) to remove insoluble material. Supernatants were transferred to fresh tubes and either used immediately or stored at -20°C.

2.4.5. Immunoprecipitation

Typically, $3x10^7$ transfected 293T cells were used per sample. Cells were resuspended in 1ml of lysis buffer (150mM NaCl, 50mM Tris-HCl pH7.5, 0.5% NP-40, 0.5% Triton-X100, 1x protease inhibitor cocktail (Boehringer)) and allowed to lyse on ice for 40'. Samples were centrifuged (5', 13,000 rpm, 4°C) and the supernatant transferred to a fresh Eppendorf tube. If nuclear and cytoplasmic fractions were prepared this lysis step was replaced by the separation protocol described in the previous section.

100µl of fixed *Staphylococcus aureus* organisms (Sigma) were taken per sample and washed 3 times with 1ml of wash buffer (150mM NaCl, 50mM Tris-HCl pH7.5, 1mM EDTA). After the last wash, the *S. aureus* was taken up in the same volume as at the start (100µl/sample), added to the samples and the samples tumbled at 4°C for 4 hours or overnight (pre-clearing of sample of proteins binding to proteinA non-specifically).

The *S. aureus* was completely removed by centrifugation (13,000 rpm, 10', 4°C). The supernatant was transferred to a fresh Eppendorf tube and 1/10 volume of 10%BSA added together with the antibody for the immunoprecipitation. Samples were incubated overnight at 4°C.

20µl proteinA-sepharose (Bioprocessing Ltd.) per sample was taken and washed 3 times with 1ml of wash buffer. Finally, it was taken up in 50µl wash buffer per sample and added to the samples. Samples were rotated for 1.5 hours at 4°C. ProteinA-sepharose was collected by centrifugation (5', 13,000 rpm, 4°C) and washed 4 times with 1ml of wash buffer. Finally, 20µl of 2x SDS-sample buffer was added to each pellet and the samples frozen at -20°C until they were loaded on a SDS-PAGE gel.

2.4.6. SDS-polyacrylamide gelelectrophoresis (SDS-PAGE)

To separate proteins according to molecular weight, SDS-polyacrylamide gelelectrophoresis was performed using a discontinuous buffer system, as previously described (Laemmli, 1970). The mini-gel system used (Mini protean II dual slab cell) was purchase from Biorad and used according to the manufacturer's instructions.

In short the procedure of running a SDS-polyacrylamide gel was as follows:
The gel components were assembled according to the manufacturer's instruction. The separating gel mix was prepared and poured between the 2 glass plates. A layer of water or butanol was added on top to ensure a straight top of the gel and the gel allowed to polymerise for at least 30'. The water/butanol layer was carefully removed before the stacking gel was poured on top and the comb inserted. The stacking gel was also allowed to polymerise for at least 30' before the combs were removed, the gels transferred to the electrophoresis apparatus and 1x running buffer poured into the container. Protein samples in 1x SDS-sample buffer were boiled in a heat block set at 95°C for 5', spun down briefly to collect the sample (30", 13,000rpm) and loaded into the wells. The gel was run at 200 Volts until the Bromophenol Blue dye reached the end of the gel (approximately 40').

The separating gel varied in acrylamide content between 7.5 and 15% depending on the protein of interest. The stacking gel was always set at 4%. Ready made Protogel mixture (30% acrylamide, 0.8% bisacrylamide; National Diagnostics) was used. Polymerisation was initiated by adding ammonium persulphate (APS) and TEMED.

Mixes for the *separating gels* (0.375M Tris pH 8.8) were made as follows (10ml):

	7.5%	10%	12%	15%
Dist. water	4.85ml	4.05ml	3.35ml	2.35ml
1.5 M Tris-Cl pH8.8	2.5ml	2.5ml	2.5ml	2.5ml
10% SDS	0.1ml	0.1ml	0.1ml	0.1ml
30% acryl/bis	2.5ml	3.3ml	4.0ml	5.0ml
10% APS	50µl	50µl	50µl	50µl
TEMED	10µl	10µl	10µl	10µl

The *stacking gel* (4% acrylamide, 0.125M Tris pH 6.8) was made as follows (10ml):

Dist.water	6.1ml
0.5M Tris-Cl pH 6.8	2.5ml
10% SDS	100µl
30% acryl/bis	1.3ml
10% APS	50µl
TEMED	10µl

4x SDS-sample buffer(8ml):		*Final concentration:*
Dist. water	4.2ml	
0.5 M Tris-Cl pH 6.8	1.0ml	62.5mM
Glycerol	0.8ml	10% (v/v)
10% SDS	1.6ml	2% (w/v)
β-mercaptoethanol	0.4ml	0.7M
Bromophenolblue	0.32mg	0.004% (w/v)

5x Running buffer(1 litre):		
Tris base	15 g	125mM
Glycine	72g	1M
SDS	5g	0.5%

2.4.7. Coomassie Brilliant Blue staining

After running of the gel, the gel was either used to proceed with Western blotting (see next section) or stained with Coomassie Brilliant Blue R-250 (CBB), as described here. The gel was taken out of the gel apparatus and soaked in staining solution (40% methanol, 10% glacial acetic acid, 0.2% (w/v)CBB) for 1-3 hours. The gel was subsequently destained with destaining solution (40% methanol, 10% glacial acetic acid). Once the destaining was judged sufficient, the gel was soaked into a solution of 7% acetic acid for 10' before transferring the gel into Whatman paper, overlaying the gel with Saran-wrap. The gel was then dried in a vacuum-pump heated dryer (SE1160; Hoefer Scientific Instruments) for 2 hours. If proteins were labelled with radioactivity, the gel would be exposed to X-ray film.

2.4.8. Western blotting

An SDS-PAGE gel was run as described above. The proteins were transferred onto a nitrocellulose membrane (Amersham) using a 'wet' transfer method (Biorad). A "sandwich" was made consisting of 2 transfer buffer soaked Whatman papers, the gel, wet nitrocellulose and 2 more soaked Whatman papers. Care was taken that no air bubbles would remain between the layers. The sandwich was positioned in the transfer apparatus in such a way that the gel was on the anode (-) side and the nitrocellulose on the cathode (+) side. The negatively charged SDS-covered proteins would therefore move from the gel onto the nitrocellulose. The transfer took place at 100V for 1 hour. After the transfer, the sandwich was disassembled, the membrane briefly washed in PBS and then transferred into blocking buffer. The membrane was incubated in blocking buffer and gently shaken for at least 1 hour. The membrane was washed twice for 10' in washing buffer and the membrane transferred to a plastic bag. The primary antibody was diluted in blocking buffer (usually at 1/400) and added to the membrane after which the bag was sealed. The membrane was incubated with the primary antibody for 1 hour at RT or at 4°C overnight. The membrane was washed in washing buffer 3 times for 10' after which it was incubated with horse-radish peroxidase (HRPO) conjugated secondary antibody (usually diluted 1/500-1/1000 in washing buffer) for 1 hour at RT. Again the membrane was washed 3 times 10' with washing buffer. Detection of proteins was

performed using the Enhanced ChemiLuminescence kit (ECL, Amersham). Films were exposed to the membrane for times ranging from seconds to several minutes.
In certain cases the bound antibodies were stripped off the membranes by incubating the membrane in stripping buffer (100mM 2-mercaptoethanol, 2% SDS, 62.5mM Tris-HCl pH6.7) for 30' at 50°C) with occasional agitation. Membranes were then extensively washed with large volumes of washing buffer and incubated in blocking buffer for at least 1 hour. Hereafter, the membranes were ready again to be probed with primary antibodies (see above).

Transfer buffer(1 litre):	*Final conc.:*
3.03g Tris base	25mM
14.4g Glycine	200mM
Make up to 800ml with water, dissolve	
and add 200ml methanol.	20%

Washing buffer:

PBS with 0.05% (v/v) Tween-20 (Sigma)

Blocking buffer:

Washing buffer with 5% (w/v) Marvel (dried milk).

2.4.9. Peptide cleavage assay

Peptidase activity of immunoprecipitated proteasomes was determined using synthetic substrates N-succinyl-LLVY-AMC (LLVY) and N-cbz-GGR-AMC (GGR) (Sigma), which assay the chymotryptic and tryptic activities of the proteasome, respectively. Cleavage of these substrates after the Y and R, respectively, will lead to the release of the AMC group, which is fluorescent. Substrates were kept in 10mM stocks in DMSO (-20°C) and diluted to 100μM in 20mM Tris HCl (pH 7.5). Proteasome inhibitors lactacystin and calpain inhibitor I (LLnL) were included at 25μM and 200μM final concentration, respectively, where indicated. Proteasomes were immunoprecipitated with MCP21 or W6/32 (negative control), using $2x10^6$ cell equivalents per sample, and 70-250μl diluted substrate added to the immunoprecipitates. After 1-2 hours incubation at

37°C, 50µl samples were taken and transferred to a 96-well flat-bottom plate. Fluorescence of duplicate samples was measured at 370nm $\lambda_{excitation}$, and 460nm $\lambda_{emission}$ on a spectrofluorimeter (CytoFluor 2350 Fluorescence Measurement System (Millipore)). Values of the negative controls were substracted and activity was quantified relative to the amount of proteasome in the immunoprecipitated proteasome preparation. This was determined by densitometry of SDS-PAGE Western blots with MCP21

2.4.10. CATassay

To measure the activation of a promoter, the promoter was placed in front of a chloramphenicol acetyltransferase (CAT) gene. Subsequently the expression of CAT was measured by the transfer of the acetyl group from acetyl-coenzymeA to chloramphenicol. A microversion of the CAT assay, relying on the diffusion of reaction products into scintillation fluid, was used (Niewiesk et al., 1995). Transfected cells were scraped from the bottom of the wells and transferred to 1.5ml Eppendorf tubes. Cells were spun down (1', 13,000 rpm) and supernatant removed. Pellets were resuspended in 50µl of cold lysis buffer (0.1M Tris pH8, 1% glycerol) and lysed by freeze-thawing 3 times. Cell debris was spun down (5', 13.000 rpm) and supernatant transferred to a fresh tube. Supernatants were heat inactivated at 65°C for 20'.

7µl of cell lysate was placed into a well of a 96-well plate along with 2µl chloramphenicol (1.6mg/ml, diluted in 0.1M Tris pH7.8) and 2µl ^{3}H-Acetyl CoA (0.1 µCi/µl, NEN Research products). The mixture was overlayed with 100µl of Betascint (Packard), covered with a sticker and incubated at 37°C for 1 hour. The amount of acetylated chloramphenicol that had diffused into the Betascint was measured with a Topcount microplate scintillation counter (Packard).

2.5. Immunofluorescence techniques

2.5.1. FACS analysis

The analysis of expression of molecules on the surface of cells was carried out using a FACScan flow cytometer (Becton-Dickinson) and CellQuest computer software.

FACS analysis was mostly performed to analyse the specificity of T cell lines and clones by tetramer staining for which the following protocol was used:

Using 96-well round bottom plates, 1-1.5x10^5 cells were plated per well. The plate was centrifuged (5', 1500rpm, RT) and most supernatant removed from the wells. 1 μg of tetramerised class I complexes (tetramer; PE-labelled) was added to the relevant samples, mixed and the plate incubated at 37°C for 20'. Cells were washed 3 times with 200μl of PBS/well. After the last spin, most supernatant was removed and 1 μl anti-human CD8-tricolour conjugate (Caltag) was added to the relevant samples and the plate incubated on ice (and in darkness) for 20'. Cells were washed 3 times with 200μl of PBS/well and finally each sample was taken up in 400μl FACS-fix (2% paraformaldehyde & 2% FCS in PBS) and transferred to a 4ml FACS-tube. Samples were stored at 4°C and in darkness until analysed by flow cytometry.

When other surface molecules were analysed, cells were incubated with primary antibodies at 4°C for 30', the cells washed, incubated at 4°C with fluorochrome-conjugated secondary antibodies for 30', washed again and fixed.

2.5.2. Indirect immunofluorescence confocal microscopy

293T cells were grown on coverslips and fixed either 48 hours post-transfection or after overnight infection (m.o.i. of 5 pfu/cell) with recombinant SFV (Semliki Forest Virus). Fixation and permeabilisation were performed either concurrently by incubation of coverslips in cold (-20°C) methanol for 6' or by sequential incubation in 4% paraformaldehyde in PBS for 10 minutes (fixation) and 0.05% Triton X-100 in PBS for 10 minutes (permeabilisation) at room temperature. The samples were saturated with PBS containing 0.5% gelatin and 0.25% BSA (blocking buffer) for 1 hour at RT, followed by an incubation with a dilution of primary antibodies in the blocking buffer for 1 hour at RT. The samples were then washed 3 times with PBS containing 0.2% gelatin (washing buffer) and incubated for 1 hour at RT with a dilution of fluorochrome conjugated secondary antibodies in blocking buffer. When a biotinylated secondary antibody was used, fluorochrome conjugated streptavidin was used as a tertiary 'antibody'. The procedure of incubation of the cells with streptavidin was identical to that used for the secondary antibodies. The samples were finally washed 3 times in washing buffer, mounted onto slides with Dabco mounting solution and the coverslips

sealed with nailvarnish. Slides were stored at -20°C and analysed on a Zeiss LSM510 laser scanning confocal microscope in collaboration with Dr. Françoise Bex (CERIA, Brussels, Belgium).

Chapter 3

Nuclear localisation of HTLV-1 Tax protein

3.1. Introduction

The Tax protein of human T cell lymphotropic virus type 1 (HTLV-1) activates the HTLV-1 long terminal repeat and key regulatory proteins involved in inflammation, activation and proliferation. Tax is a 40kDa phosphoprotein, which has been reported to be localised predominantly in the nucleus (Bex et al., 1997; Slamon et al., 1988; Slamon et al., 1985; Smith and Greene, 1990). Tax does not contain a highly basic nuclear localisation signal, but instead its N-terminal 48 amino acids comprise a functional nuclear localisation domain (Smith and Greene, 1992).

In order to study the properties of the Tax protein, we expressed Tax in 293T cells by transiently transfecting the cells with pJFE-Tax (Niewiesk et al., 1995) (controls were transfected with the empty vector pJFE-link). The advantage of using transfectants compared to HTLV-1 infected cell lines (see below) is that it allows the study of the Tax protein in isolation, without interference of other viral factors and processes. In addition it allows the expression of mutant Tax proteins (Chapter 5) and does not require category III microbiological safety measures. Attempts were made to establish stable transfectants but these attempts failed, probably due to the induction of apoptosis by Tax expression, as observed by others (Chlichlia et al., 1995).

Expression of Tax from the pJFE-Tax vector is under control of the SRα promoter, which is composed of the simian virus 40 (SV40) early promoter and the R-U5 segment of the HTLV-1 LTR long terminal repeat (Takebe et al., 1988). 293T cells are an SV40 transformed human embryonic kidney cell line. Expression of the large T antigen from the SV40 virus in the 293T cells ensures replication of the transfected plasmid, (which contains the SV40 origin of replication) leading to relatively high levels of expression (Takebe et al., 1988).

In this chapter the expression, detection, transcriptional activation properties and subcellular localisation of Tax expressed in 293T cells are presented.

3.2. Generation and specificity of rabbit anti-Tax sera

In order to study the Tax protein, it was necessary to have antibodies against Tax, with which we would be able to detect the Tax protein. A Kyte-and-Doolittle hydrophobicity/hydrophilicity plot indicated that the C-terminus of Tax was hydrophilic (data not shown) and therefore likely to be exposed on the surface of the protein and available for antibody recognition. Hence, a synthetic peptide representing the Tax C-terminus (MISPGELEPPSEKHFRETEV) was made and used to immunise two rabbits. Immunisations were performed at Genosys Biotechnologies.

In Figure 3.1. total lysates of 293T cells transfected with pJFE-Tax and control transfectants were separated on SDS-PAGE gels and immunoblotted with the pre-immune and immune sera (the terminal bleeds (TB)) of the rabbits. Expression of the 40kDa Tax protein in the Tax transfectants could be readily detected with the immune sera from both rabbits. There was little crossreactivity with proteins in the control transfectants. Similarly, pre-immune sera displayed low background staining.

Other Tax C-terminus specific antibodies used in this study were BR-76 rabbit antiserum and monoclonal mouse antibody mAb1316. The epitope of the Y8 anti-Tax antibody was not known (see Materials and methods).

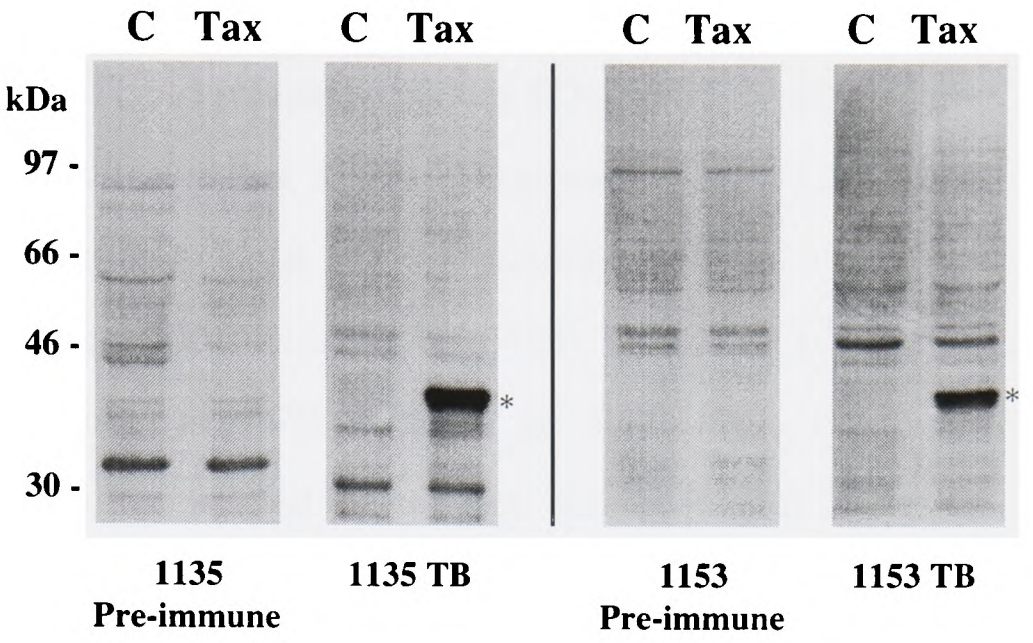


Figure 3.1. Specificity of rabbit anti-Tax anti-sera.

Equal amounts of total cell lysates of Tax- and control (C) transfected 293T cells were separated by SDS-10%PAGE, transferred to nitro-cellulose and probed with the indicated pre-immune and immune (TB; Terminal bleed) sera of rabbits 1135 and 1153.

Asteriks indicates Tax protein.

3.3. Tax expression and the effect of β-mercaptoethanol

The expression of Tax in transfected 293T cells and HTLV-1 infected cell lines was compared.

MT-2, MT-4(P) and MT-4(S) are HTLV-1 transformed cell lines that were generated by cocultivation of human cord lymphocytes with an adult T cell leukaemia (ATL) cell line (Harada et al., 1985; Miyoshi et al., 1981; Yoshida et al., 1982).

Expression of the 40kDa Tax protein could easily be detected in transfected 293T cells (Figure 3.2A, lanes 2 and 6). The transfection efficiency was 30-40%, as determined by immunofluorescence microscopy (data not shown). Whereas 293T Tax transfectants and the MT-4(P) cells expressed only the 40kDa Tax protein (Figure 3.2B, lane 5), the MT-2 cells also expressed a ~64kDa protein that reacted with the anti-Tax antibody (Figure

3.2B, lane 3). MT-4(S) cells appeared negative for Tax expression (Figure 3.2B, lane 7). The expression level of 40kDa Tax in 293T transfectants was in the range observed for the Tax expressing HTLV-1 infected cell lines MT-2 and MT-4(P) (Figure 3.2A and B).

A literature search indicated that the 64-kDa protein species in MT-2 cells that reacted with the anti-Tax antibody most likely represented a fusion protein of Env and Tax (Lemasson and Nyborg, 2001; Miwa et al., 1984). However, Tax is also known to form homodimers (Baranger et al., 1995; Chun et al., 2000; Perini et al., 1995; Wagner and Green, 1993). Since we wanted to exclude the possibility that the 64kDa band represented a disulfide-linked Tax-dimer, we also harvested cells in SDS sample buffer without β-mercaptoethanol.

It was a surprise to find that the 40kDa Tax band disappeared from all the lysates (293T transfectants, MT-2, MT-4(P)) when β-mercaptoethanol was not included in the SDS sample buffer (compare Figure 3.2B lanes 1 with 2, 3 with 4 and 5 with 6). Instead, a smear appeared in the 35-40kDa range, which was more apparent when the level of Tax expression was higher (Figure 3.2B, lane 6). The fact that the omission of β-mercaptoethanol had such an effect on the mobility of Tax in a SDS-PA gel suggests that intra-molecular disulfide bonds are present in Tax. Several (8) cysteine residues are present within Tax. Therefore, when β-mercaptoethanol is not included in the SDS sample buffer, the disulfide bond(s) may not be broken and Tax may not completely unfold, leading to the retention of some structure and a different (in this case higher) mobility in the SDS-PA gel.

In addition, the omission of β-mercaptoethanol from the sample buffer led to the appearance of high-molecular weight aggregates in MT-2 lysates (Figure 3.2B, lane 4), part of which was insoluble (at start of stacking gel) and part of which was soluble (at top of separating gel) (Figure 3.2B, lane 4). This suggests that the env-Tax protein can form intermolecular disulfide bonds. These high molecular complexes may represent covalently (S-S) linked env- Tax multimers or the covalent linkage of env-Tax to other unknown proteins.

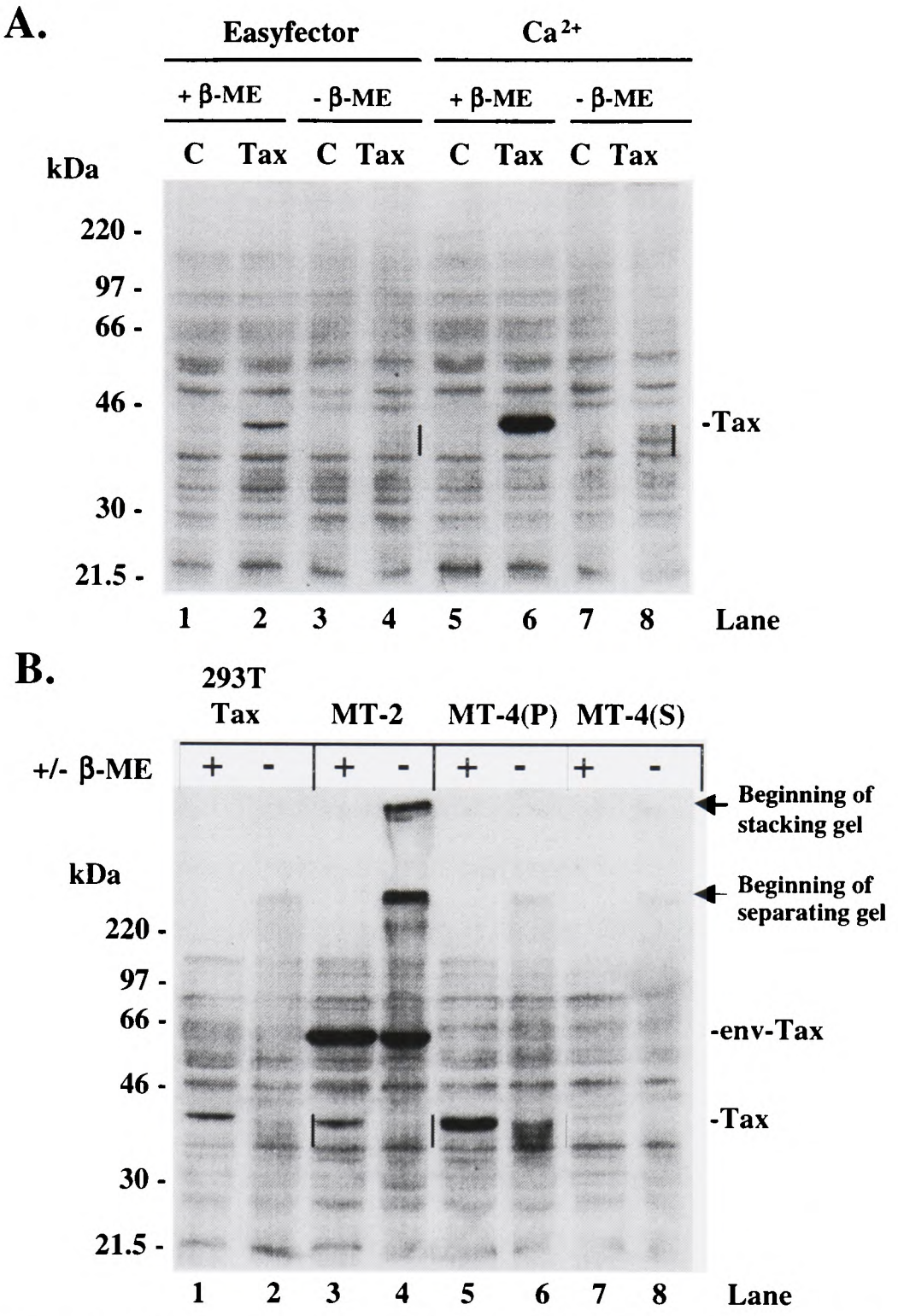


Figure 3.2. Tax expression in transiently transfected 293T cells and HTLV-1 infected cell lines and the effect of β-mercaptoethanol .

Cells were harvested directly in SDS-sample buffer with (+) or without (-) β-mercapto-ethanol (β-ME), as indicated. Equal amounts of protein were loaded in each lane. Samples were separated by SDS-PAGE and subjected to Western blotting with the monoclonal anti-Tax antibody mAb1316. **Figure A**: 293T cells transfected with pJFE-Tax (Tax) or empty control vector (C) using either the Easyfector method or Ca^{2+}/phosphate precipitation method. **Figure B.**: MT-2, MT-4(P) and MT-4(S) are HTLV-1 infected and transformed cell lines. The bar indicates the position of the Tax protein in the absence of β-mercaptoethanol.

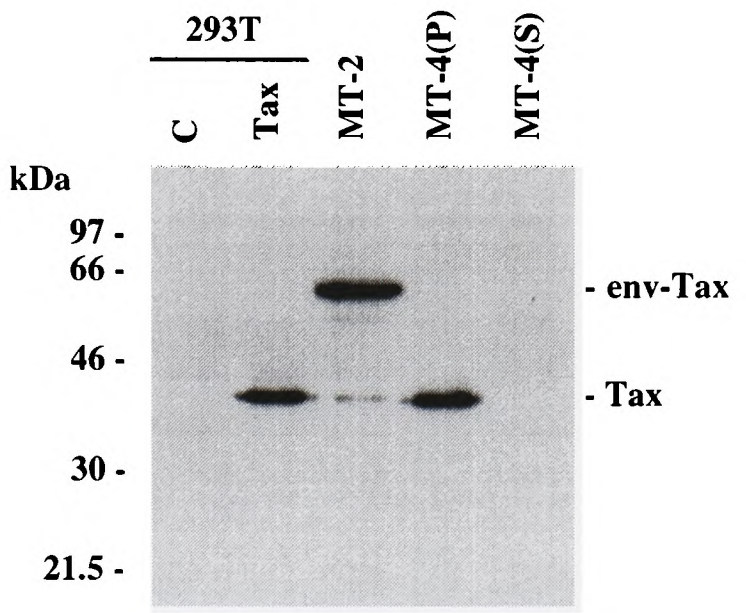


Figure 3.3. Anti-Tax immunoprecipitation

Total cell lysates of the indicated cell types were subjected to immunoprecipitation with anti-Tax serum 1135TB. Precipitates were separated by SDS-PAGE and subjected to immunoblotting with anti-Tax monoclonal antibody mAb1316.

293T cells were transfected with pJFE-Tax (Tax) or empty control vector (C). MT-2, MT-4(P) and MT-4(S) are HTLV-1 infected and transformed cell lines.

The 40kDa Tax protein from all cell lines and the 64kDa env-Tax from MT-2 could be immunoprecipitated with the 1135TB anti-serum (Figure 3.3). The same result was obtained with an immunoprecipitation with the monoclonal anti-Tax antibody mAb1316 (data not shown). These data show that the C-terminal epitope of native Tax and native env-Tax can be recognised by both the 1135TB antiserum and mAb1316.

3.4. Tax transactivates the HTLV-1 LTR, and the *c-fos* and IL-2Rα promoters

The previous data have shown that Tax is expressed in transiently transfected 293T cells at levels comparable with the levels seen in HTLV-1 infected cell lines. It is well established that Tax can transactivate the HTLV-1 long terminal repeat through its interaction with CREB/ATF factors and CREB binding protein (CBP) (Beraud et al., 1991; Bex et al., 1998; Kwok et al., 1996; Suzuki et al., 1993; Zhao and Giam, 1992). In addition, Tax can activate transcription from the IL-2Rα promoter via the NFκB pathway (Ballard et al., 1988; Inoue et al., 1986; Siekevitz et al., 1987) and activate transcription from the *c-fos* promoter through its interaction with serum response factor $p65^{SRF}$ (Fujii et al., 1988; Fujii et al., 1992; Suzuki et al., 1993).

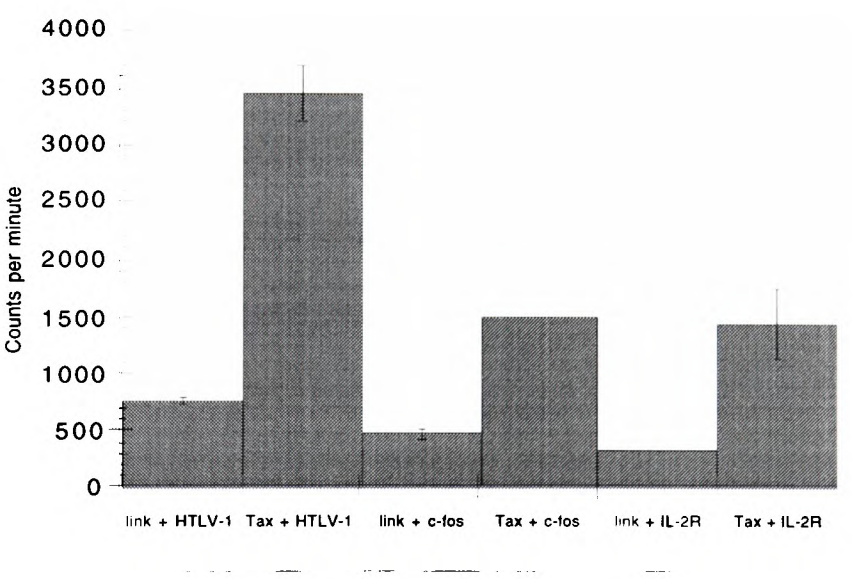


Figure 3.4. Tax transactivates the HTLV-1 LTR and the c-fos and IL-2Rα promoters.

293T cells were transiently co-transfected with either pJFE-Tax or pJFE-link (empty vector) and one of the promoter-CAT constructs: HTLV-1 LTR-CAT, c-fos-CAT or IL-2R-CAT.

CAT activity was measured as described (Niewiesk et al., 1995). Measurements were done in duplicates.

As single or double amino acid mutations can dramatically impair Tax transactivation function (Niewiesk et al., 1995; Semmes and Jeang, 1992; Smith and Greene, 1990), we wished to establish whether the Tax sequence that was present in pJFE-Tax encoded a Tax protein that was fully transcriptionally active. To this end, plasmid constructs were used in which the HTLV-1 LTR and the *c-fos* and IL-2Rα promoters were driving expression of a chloramphenicol acetyltransferase (CAT) gene (Niewiesk et al., 1995). Subsequently, a CAT-assay was performed on lysates from 293T cells co-transfected with pJFE-Tax (or empty vector) and one of the three promoter-CAT constructs. This confirmed that Tax was indeed capable of transactivating the HTLV-1 LTR and the *c-fos* and IL-2Rα promoters, and was therefore completely functional (Figure 3.4).

3.5. Tax is localised in the nucleus of transfected 293T cells

Tax is a 40kDa phosphoprotein, which has been reported to be localised predominantly in the nucleus (Bex et al., 1997; Slamon et al., 1988; Slamon et al., 1985; Smith and Greene, 1990). Tax does not contain a highly basic nuclear localisation signal, but instead its N-terminal 48 amino acids comprise a functional nuclear localisation domain (Smith and Greene, 1992). In addition, many amino acid substitutions, especially in the N-terminal domain, lead to loss of nuclear localisation capacity of Tax (Smith and Greene, 1990).

Using immunofluorescence microscopy we confirmed that, in transiently transfected 293T cells, Tax was localised in the nucleus (Figure 3.5). Tax was present in nuclear bodies and also as more diffuse nuclear staining. The nuclear bodies have been previously described and were reported to contain splicing factors, NF-κB, p300 coactivator, the largest subunit of RNA polymerase II and the cyclin-dependent kinase CDK8 (Bex et al., 1997). These structures were proposed to play a role in Tax mediated activation of gene expression via the NFκB pathway (Bex et al., 1997; Bex et al., 1998).

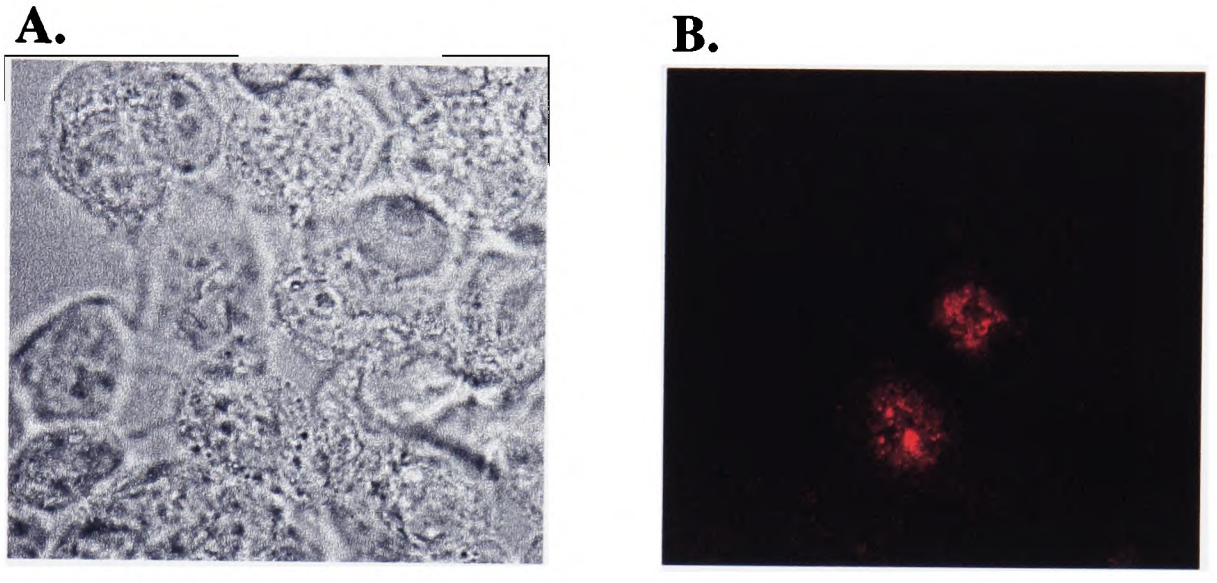


Figure 3.5. Tax is localised in nuclear bodies

Immunofluorescence microscopy. 293T cells were infected with SFV-Tax expressing Tax fused to an HA-tag. After 18 hours the cells were fixed and Tax was detected with an anti-HA antibody and a secondary LRSC-conjugated antibody. **A.** Differential interference contrast (DIC) picture. **B.** Immunofluorescent Tax detection.

3.6. Tax colocalises with NFκB in nuclear bodies

We subsequently performed confocal microscopy to determine the localisation of Tax and NFκB factor p65 (RelA) in 293T cells. We observed that NFκB was almost exclusively cytoplasmic in cells that did not express Tax (Figure 3.6). However, in transfected and Tax expressing cells, NFκB was no longer confined to the cytoplasm and was also found in the nucleus. In fact, it colocalised with Tax in the nuclear bodies. These results confirm that Tax is able to mobilise NFκB from the cytoplasm to the nucleus and that it colocalises with NFκB in bodies that are likely involved in transcriptional activation.

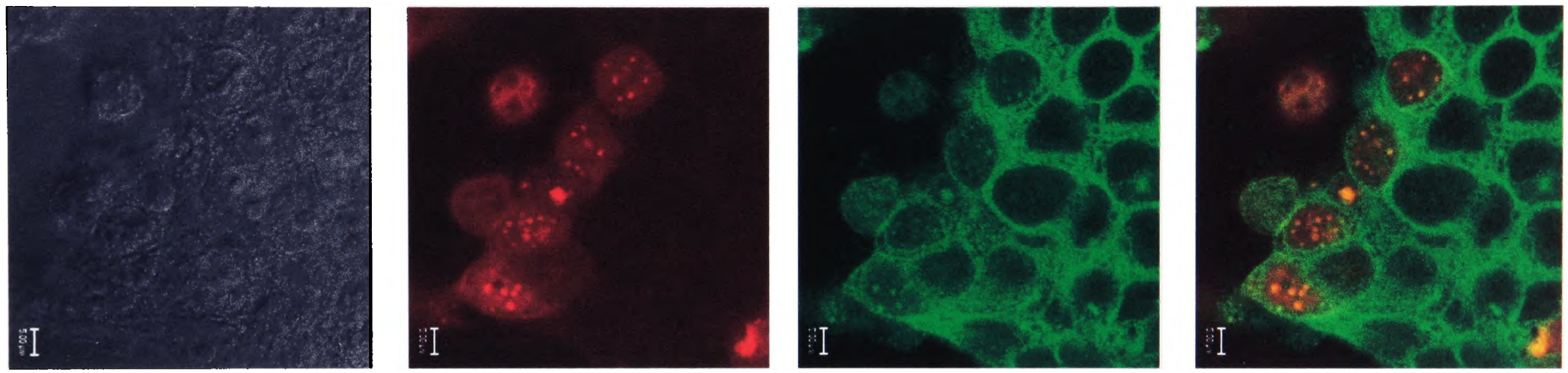


Figure 3.6. Tax colocalises with NFκB in nuclear bodies.

Immunofluorescence confocal microscopy on transiently transfected 293T cells, as described in materials and methods. A monoclonal mouse antibody against the Tax C-terminus and a polyclonal rabbit antibody specific for the p65 subunit of NFκB were used. DIC: differential interference contrast picture; Tax: Tax detection (red); NFκB: NFκB detection (green); Tax/NFκB: detection of Tax and NFκB and overlap (yellow)

3.7. Tax is only detectable in the nuclear fraction of 293T cells

In order to study nucleo-cytoplasmic transport of Tax we established a protocol to separate cytoplasmic and nuclear fractions of transfected 293T cells. The plasma membrane was lysed with 0.05% NP-40 in the presence of 7.5% PEG-6000 and after a wash the nuclei were lysed with 1% detergent. Immunoblotting of fractionated material with anti-Tax antibody showed that Tax was abundantly present in the nuclear fraction, whereas it could not be detected in the cytoplasmic fraction (Figure 3.7A). Separation of nuclear and cytoplasmic fractions was confirmed in two ways. Coomassie Brilliant Blue staining of an SDS-PA gel with samples from both fractions showed that histones were only present in the nuclear fraction (Figure 3.7B) (Slamon et al., 1988). Furthermore, a Western blot on lysate fractions was performed using a monoclonal antibody mAb104, which recognises nuclear SR pre-mRNA splicing factors (Gui et al., 1994; Roth et al., 1991). Splice factors could easily be detected in the nuclear fraction and no signal could be detected from the cytoplasmic samples (Figure 3.7C), even after longer exposure (data not shown). Although no Western blot with an antibody specific for a cytoplasmic protein was performed, abundant protein was present in the cytoplasmic fraction. As this did not react with the splicing factor specific antibody it was presumed that it represented cytoplasmic protein.

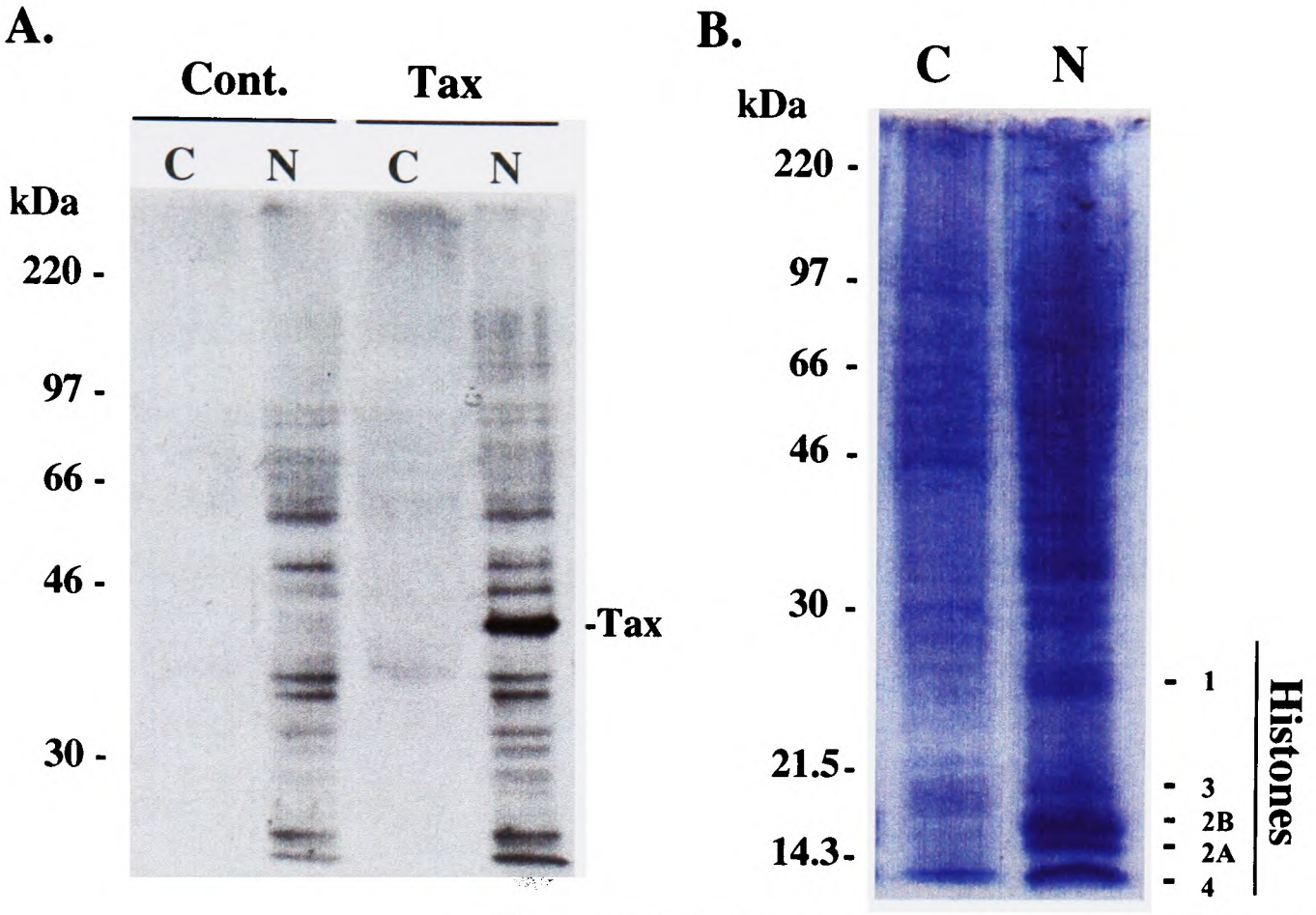
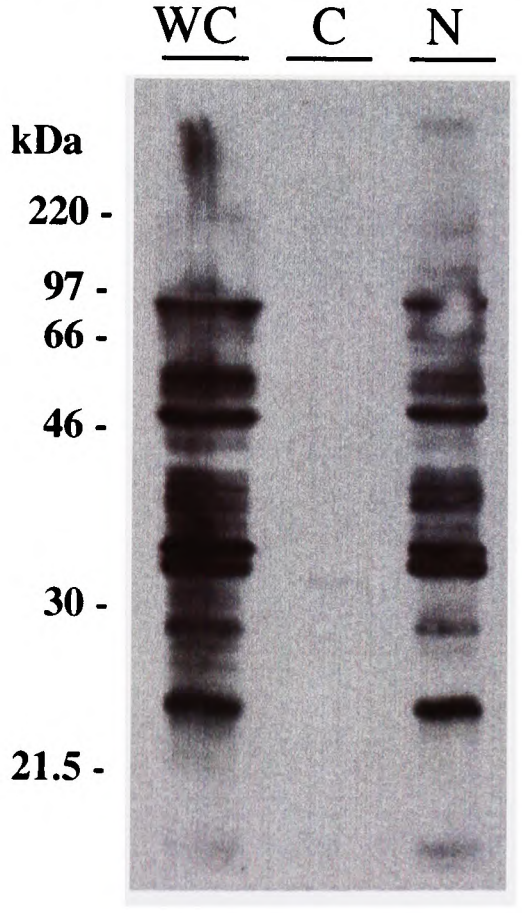


Figure 3.7. A. At steady state Tax is only detectable in the nuclear fraction. Nuclear and cytoplasmic fractions of transiently transfected 293T cells were separated by SDS-PAGE and Western blotted with a polyclonal rabbit antibody against the Tax C-terminus (1135TB). C= cytoplasmic fraction, N= nuclear fraction, Tax= Tax transfectants, Cont.= control transfectants.

B. Histones are present only in the nuclear fraction. Nuclear and cytoplasmic fractions of 293T cells were separated by SDS-PAGE and the gel stained with Coomassie Brilliant Blue. The bands of the histone proteins are indicated on the right (Slamon et al., 1988).

C. SR splicing factors are present only in the nuclear fraction. Whole cell lysates (WC), cytoplasmic (C) and nuclear (N) fractions of 293T cells were separated by SDS-PAGE and Western blotted with mAb104 specific for a phospho-epitope in members of the SR family of nuclear pre-mRNA splicing factors (Roth et al., 1991).



3.8. Tax rapidly translocates into the nucleus after synthesis

To determine how quickly after synthesis Tax translocated into the nucleus, we performed a pulse-chase metabolic labelling experiment. Cells were incubated with ^{35}S labelled methionine and cysteine, which were incorporated into newly synthesised proteins. Subsequently, nuclear and cytoplasmic fractions were prepared and Tax immunoprecipitated from both fractions. Immunoprecipitates were separated by SDS-PAGE and the dried gel exposed to an X-ray film. After 15 minutes of metabolic labelling, significant amounts of labelled Tax could already be found in the nuclear fraction (Figure 3.8A, lane 5). During the 10 minutes of the chase, more Tax was transported from the cytoplasm (compare lanes 2 and 3) into the nucleus (compare lanes 5 and 6). Analysis of steady-state levels of Tax in both fractions by immunoblotting revealed abundant Tax in the nuclear fraction, whereas Tax was undetectable in the cytoplasmic fraction (Figure 3.8B).

These data show that Tax is transported into the nucleus very rapidly (<15 minutes) after synthesis in the cytoplasm. These results are consistent with results obtained with the HTLV-1 infected cell line SLB-1 (Slamon et al., 1988).

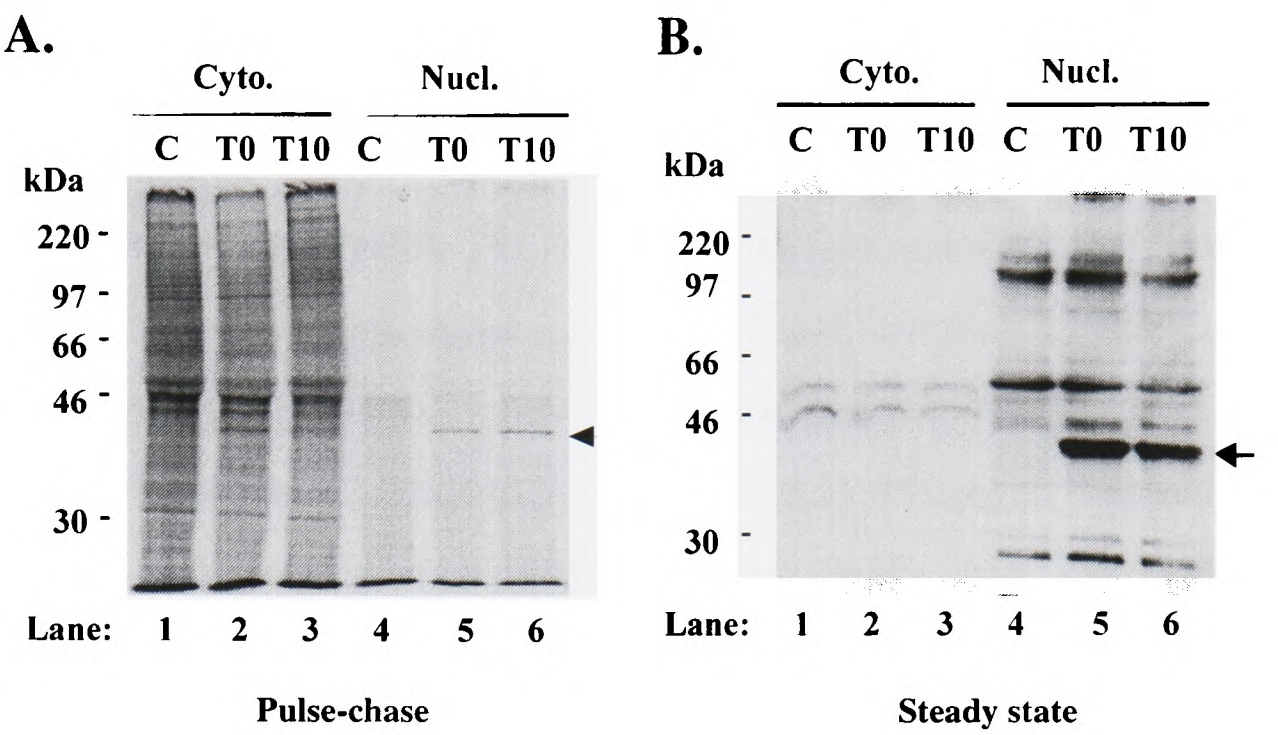


Figure 3.8. Tax rapidly translocates into the nucleus after synthesis.

A. Newly synthesised Tax moves from the cytoplasm to the nucleus.

293T cells transiently transfected with Tax were metabolically labelled for 15 minutes and either harvested immediately (T0) or chased with excess cold medium for another 10 minutes (T10). Nuclear and cytoplasmic fractions were separated and Tax immuno-precipitated with a polyclonal rabbit anti-Tax antibody (BR-76). An autoradiograph of the immunoprecipitates separated by SDS-10%PAGE is shown.

B. At steady state Tax is only detectable in the nuclear fraction.

Equal amounts of protein of the cell fractions from figure (A.) were separated by SDS-10%PAGE, blotted onto nitrocellulose and Tax protein detected with Y8 anti-Tax antibody. Cyto= cytoplasmic fraction, nucl= nuclear fraction and C= control transfectants, T= Tax transfectants. The arrow indicates the Tax protein.

3.9. Summary and discussion

Summary

In this chapter we have characterised the expression, by transient transfection, of the HTLV-1 Tax protein in 293T cells. The 40kDa Tax protein was specifically recognised by polyclonal rabbit antibodies raised against the Tax C-terminus (Figure 3.1). The expression level of the Tax protein in 293T cells was equivalent to the level seen in HTLV-1 infected cell lines MT-2 and MT-4(P) (Figure 3.2). Moreover, Tax translocated into the nucleus very quickly after synthesis and at steady state Tax was almost exclusively present in the nucleus (Figure 3.8). Within the nucleus, Tax was found to localise predominantly in nuclear bodies where it colocalised with NFκB (Figure 3.6). Furthermore, we showed that Tax was able to transactivate the HTLV-1 LTR, and the *c-fos* and IL-2Rα promoters (Figure 3.4).

We therefore conclude that expression of Tax in 293T cells by transient transfection resembles Tax expression in HTLV-1 infected cells with respect to expression level, subcellular localisation and transcriptional activation properties.

Nuclear localisation of Tax

Nucleocytoplasmic transport of macromolecules takes place through nuclear pore complexes (NPCs). The NPC is composed of between 50 and 100 distinct proteins called nucleoporins and resides in the nuclear envelope. Nucleocytoplasmic transport is an active, signal mediated process and the functional pore size is around 25 nm in diameter (Feldherr et al., 1984; Mattaj and Englmeier, 1998). Active transport is mediated by nuclear transport receptors, which can bind substrates on one side of the nuclear envelope, transport them through the NPC and release the substrate on the other side. The unloaded receptor will then shuttle back through the NPC for another cycle of transport. Directionality of nucleocytoplasmic traffic is imposed by the small GTPase Ran, which is mostly GTP bound in the nucleus, and GDP-loaded in the cytoplasm

(reviewed in (Mattaj and Englmeier, 1998; Nakielny and Dreyfuss, 1999; Ohno et al., 1998).

The nuclear localisation of Tax and the rapid translocation of Tax into the nucleus after synthesis (Figures 3.5 & 3.8) are consistent with previous reports (Bex et al., 1997; Slamon et al., 1988; Slamon et al., 1985; Smith and Greene, 1990). However, Tax does not contain a highly basic nuclear localisation signal, but instead its N-terminal 48 amino acids comprise a functional nuclear localisation domain. This region was able to confer nuclear localisation when expressed as an N-terminal extension of a large cytoplasmic protein (Smith and Greene, 1992). Deletion of the amino acids 2 to 58 of Tax resulted in failure of Tax to localise to the nucleus (Gitlin et al., 1991). In addition, many amino acid substitutions in Tax, especially in the N-terminal domain, lead to loss of nuclear localisation capacity of Tax (Smith and Greene, 1990).

The N-terminus of Tax contains multiple cysteine and histidine residues, which have been shown to be part of a zinc-binding domain (Semmes and Jeang, 1992). Although the defined zinc binding domain and the nuclear localisation domain overlap, substitution mutations of Cys and His residues lead to abrogation of Zn^{2+} binding but not (abrogation of) nuclear localisation, indicating that the two activities are functionally distinct (Semmes and Jeang, 1992; Smith and Greene, 1992).

The nuclear localisation signal of Tax is distinguished from most previously described NLSs by its large size, weak basic amino acid composition and abundance of cysteine and histidine residues. It is unknown whether the domain as a whole is required or whether there are smaller (interdependent) subregions or a bipartite NLS that are responsible for nuclear localisation (Mattaj and Englmeier, 1998; Nakielny and Dreyfuss, 1999; Smith and Greene, 1992).

In short, it is not known what the defining element in the N-terminal domain of Tax is and how it is recognised by a nuclear import receptor. In addition, several amino acid substitution mutations in Tax outside the N-terminal nuclear localisation domain have been shown to abrogate nuclear localisation (Bex et al., 1998; Smith and Greene, 1990). This indicates that there are other regions in the Tax protein that contribute to Tax nuclear localisation. It remains a good possibility that Tax enters the nucleus by some

indirect mechanism, i.e. its association with some other protein which bears a nuclear localisation signal, as has been shown for adenovirus encoded DNA polymerase (Smith and Greene, 1992; Zhao and Padmanabhan, 1988).

Furthermore, it is unlikely that Tax localisation in nuclear bodies is static, as it has recently been shown that nuclear proteins, although appearing compartmentalised in subnuclear regions, are highly mobile, moving in and out of their preferred locale (Phair and Misteli, 2000). In addition, it was recently reported that Tax can shuttle between the nucleus and cytoplasm (Burton et al., 2000). However, the balance clearly lies on the side of the nucleus and the functional significance of this finding remains unknown (Burton et al., 2000).

In any case, Tax protein has adapted very well to the cellular nuclear import machinery, as indicated by its very efficient translocation into the nucleus after synthesis (Figure 3.8). This is likely an important property, as it will speed up viral gene expression and replication (see below).

Nuclear localisation and Tax transactivation

Tax is not a DNA binding protein and exerts its transactivation properties by modulating the function of various host transcription factors. Consequently, nuclear localisation of Tax is important for several of its functions.

Nuclear localisation of Tax is required for activation of the *c-fos*, *erg-1* and *erg-2* genes, which is mediated by Tax binding to serum response factor $p65^{SRF}$ which binds to CArG boxes in the promoters of the respective genes (Fujii et al., 1988; Fujii et al., 1992; Suzuki et al., 1993).

Furthermore, nuclear localisation is important for Tax mediated activation of the HTLV-1 LTR. Tax activates transcription from the viral LTR by binding to members of the CREB/ATF family, thereby enhancing their dimerisation and DNA binding (Baranger et al., 1995; Perini et al., 1995; Wagner and Green, 1993; Zhao and Giam, 1992). Tax remains bound to CREB/ATF (Beraud et al., 1991; Suzuki et al., 1993; Zhao and Giam, 1991) and recruits the coactivator CREB binding protein (CBP) to the transcription site

in a manner independent of CREB phosphorylation (Kwok et al., 1996; Yan et al., 1998). Consequently, Tax can be found to colocalise with CREB/ATF and CBP in the nucleus (Bex et al., 1998).

Additional evidence came from a Tax mutant with a deletion of amino acids 2 to 58 which failed to localise to the nucleus. This deletion strongly decreased the Tax mediated transactivation of the HTLV-1 and it was also able to act *in trans* on full length Tax, possible by sequestering full length Tax in the cytoplasm by forming heterodimers (Gitlin et al., 1991).

Tax and NFκB

The role of nuclear localisation of Tax in mediating NFκB activation is less straightforward.

In a resting cell, NFκB dimers are sequestered in the cytoplasm by their interaction with members of a family of inhibitory proteins, most notably, IκBα which mask their nuclear localisation signals (Figure 3.6) (Baeuerle and Baltimore, 1988; Jacobs and Harrison, 1998). Upon induction by a variety of extracellular signals IκBα is phosphorylated on specific serine residues by a large (700-900 kDa) cytoplasmic IκB kinase (IKK) complex (Chen et al., 1995; Karin and Ben-Neriah, 2000). This phosphorylation marks it out for polyubiquitination and subsequent degradation by the proteasome. IκBα degradation leads to release of NF-κB, which then translocates to the nucleus to activate transcription (Palombella et al., 1994).

HTLV-1 infected and Tax expressing cells demonstrate constitutive nuclear expression of NF-κB (Figure 3.6) (Chu et al., 1998; Yin et al., 1998). Tax appears to act at multiple levels to initiate and maintain NF-κB activation. Probably most importantly, Tax induces increased IκBα phosphorylation and degradation. Tax can be recruited to the IKK complex by its physical association with IKKγ/NEMO, an essential regulatory component of the IKK complex (Chu et al., 1999; Harhaj and Sun, 1999; Jin et al., 1999). This recruitment of Tax leads to activation of the IKKα and IKKβ kinases, probably with the involvement of upstream kinases MEKK1 and NIK (Geleziunas et al., 1998;

Uhlik et al., 1998; Yin et al., 1998). However, it remains unclear in which cellular compartment this takes place. The IKK complex is localised predominantly in the cytoplasm and nuclear IκBα is protected from normal signal induced degradation (Rodriguez et al., 1999). Tax, on the other hand, is present predominantly in the nucleus (Figures 3.5 & 3.6) (Bex et al., 1997; Bex et al., 1998).

One group reported that nuclear localisation was not required for NF-κB activation by Tax, which suggests that Tax acts on the cytoplasmic IKK complex. Specifically, N-terminal deletion mutants ΔN81 and ΔN109 were defective for CREB/ATF and SRF mediated transactivation and nuclear localisation, while still capable of activating κB reporter constructs (Nicot et al., 1998). This implies that the little (wild-type) Tax found in the cytoplasm plays a crucial role in NF-κB activation.

On the other hand, it was shown by others that a cytoplasmic Tax mutant (F1) induced nuclear RelA expression but nevertheless failed to activate a NF-κB dependent promoter (Bex et al., 1998). This indicated that induction of gene expression by Tax via the NF-κB pathway is probably dependent on both Tax mediated nuclear localisation of NF-κB and the direct interaction of Tax with NF-κB and p300 in nuclear bodies (Bex et al., 1998; Suzuki et al., 1993).

Other mechanisms may also play a role in Tax mediated NF-κB activation. IκBα can translocate to the nucleus where it can bind to NF-κB factors, inhibit their DNA binding and relocate NF-κB to the cytoplasm (Arenzana-Seisdedos et al., 1995; Arenzana-Seisdedos et al., 1997). Tax has been shown to bind directly to the ankyrin domain of IκBα, thereby preventing its interaction with NF-κB factors (Suzuki et al., 1995). In addition, one group has argued that phosphorylation and proteasome dependent IκBα degradation can occur in the nucleus, suggesting that the IKK complex is also present in the nucleus, making it an easy target for Tax (Renard et al., 2000). However, evidence for this latter mechanism is currently lacking.

Env-Tax and disulfide bonds

One complete provirus and seven defective proviruses were detected in MT-2 cells (Kobayashi et al., 1984). The detection of the 64kDa form of Tax in MT-2 cells, presumably a fusion protein of env and Tax (env-Tax) (Lemasson and Nyborg, 2001; Miwa et al., 1984), should raise some concern about the use of this cell line as a model for HTLV-1 infection. We have shown that the env-Tax is expressed at much higher levels than the 40kDa form of Tax in MT-2 cells (Figure 3.2). Therefore, when detecting Tax in MT-2 cells with antibodies in an experimental setting where the size of the protein cannot be determined, i.e. with immunofluorescence or FACS analysis, one cannot assume that what is detected is 40kDa Tax, as it will be mostly 64kDa env-Tax.
We do not know what activities this env-Tax possesses, but it seems likely that it is cotranslationally inserted into the ER, folded inside the ER and subsequently expressed on the cell surface. Indeed, when performing immunofluorescence microscopy on MT-2 cells using Tax specific antibodies, significant amounts of staining were observed at the plasma membrane and in the ER (Bex et al., 1997; Bex et al., 1998; Miyoshi et al., 1981). Similarly, when MT-2 cells are used for the intracellular detection of Tax expression by flow cytometry, one is likely to be detecting mainly the env-Tax fusion protein, which is more abundant than the 40kDa Tax protein (Hanon et al., 2000).

A remarkable finding was the effect of the omission of β-mercaptoethanol from the SDS-PAGE sample buffer on the mobility of Tax and env-Tax in a SDS-PA gel (Figure 3.2). The 40kDa Tax band disappeared from all the lysates when β-mercaptoethanol was not included in the SDS sample buffer. Instead, a smear appeared in the 35-40kDa range (Figure 3.2). The fact that the omission of β-mercaptoethanol had such an effect on the mobility of Tax in a SDS-PA gel suggests that intra-molecular disulfide bonds are present in Tax. Several (8) cysteine residues are present within Tax. However, disulfide bonds are normally only formed in the ER and it remains unclear how disulfide bonds could be formed in Tax as the cytoplasmic and nuclear environments are reducing (Rietsch and Beckwith, 1998). Whatever the structural and/or functional significance of this finding, it

highlights the importance of ensuring that β-mercaptoethanol is present in the SDS-sample buffer when you want to detect the Tax protein by Western blot.

In addition, the omission of β-mercaptoethanol from the sample buffer led to the appearance of high-molecular weight aggregates in MT-2 lysates (Figure 3.2), part of which was insoluble (at start of stacking gel) and part of which was soluble (at top of separating gel) (Figure 3.2B, lane 4). This indicated that the env-Tax protein can form intermolecular disulfide bonds. These high molecular complexes may represent covalently (S-S) linked env-Tax multimers or the covalent linkage of env-Tax to other unknown proteins. As this fusion protein is presumably co-translationally inserted into the ER and folded inside the ER, it is possible that disulfide bond formation is catalysed by the ER resident protein disulfide isomerase (PDI, (Rietsch and Beckwith, 1998)). It remains unknown whether covalent disulfide linkage of envelope proteins plays a role in particle formation.

Chapter 4

Interaction between HTLV-1 Tax protein and 20S proteasomes

4.1. Introduction

The proteasome is a multicatalytic proteinase complex implicated in the degradation of most cellular proteins (Rock and Goldberg, 1999; Rock et al., 1994). The catalytic core of the proteasome is formed by the 20S proteasome, which has a cylindrical structure composed of four rings, the outer two each containing 7 structural α-subunits and the inner two each containing 7 β-subunits, of which only 3 are proteolytically active (Baumeister et al., 1998; Groll et al., 1997). Proteasomes have three important regulatory functions: the removal of abnormal proteins; the recognition and degradation of proteins involved in transcription regulation, cell cycle and signal transduction processes and the proteolytic processing of proteins for presentation by the MHC class I pathway (Rock and Goldberg, 1999). In mammalian cells, proteasomes are localised in both the nucleus and the cytoplasm (Reits et al., 1997).

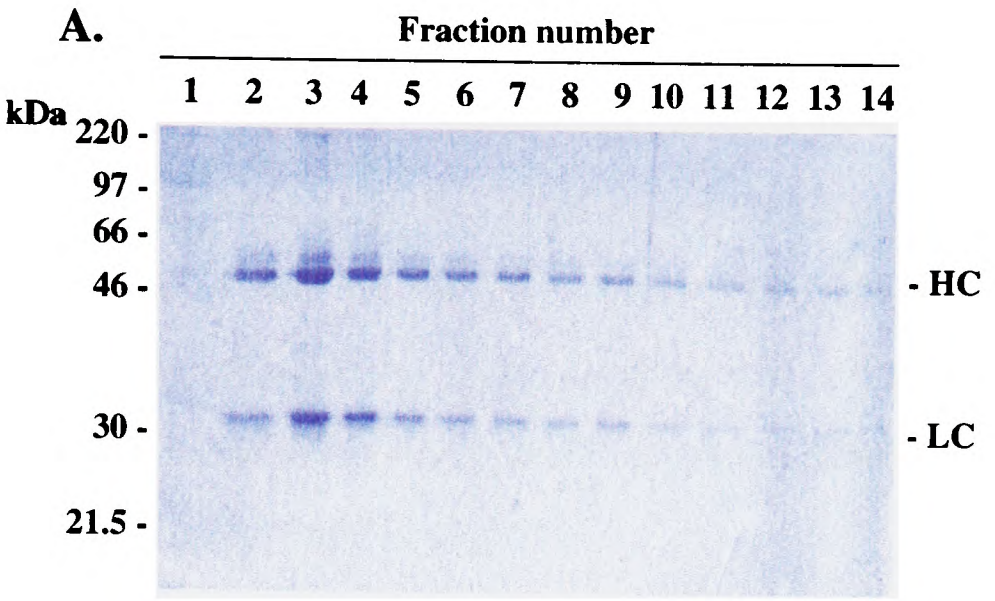
Previous studies had shown that Tax can bind to the proteasomal α-subunit HC9 (α3) and (non-catalytic) β-subunit HsN3 (β7) (Beraud and Greene, 1996; Petropoulos and Hiscott, 1998; Rousset et al., 1996). These studies were performed with the yeast two-hybrid system and by ectopically expressing these subunits and Tax in the cytosol of COS7 monkey cells. It remained unclear from these studies whether the expressed subunits were incorporated into mature 20S proteasomes and whether Tax binding to assembled proteasomes occurred. Hence, the physiological relevance of these findings remained uncertain.

To better understand the physical association of Tax with proteasomal subunits and the consequences of this interaction for cellular processes, we investigated the ability of Tax to bind to intact cellular proteasomes and studied the resulting proteolytic activity of the complexes. The implications of our findings will be discussed.

4.2. Purification of MCP21 antibody

In order to study the human 20S proteasome, we obtained the hybridoma for the mouse MCP21 antibody. Monoclonal antibody MCP21 recognises an epitope in the HC3 (α2) α-subunit of the human 20S proteasome, both in a Western blot as well as in immunoprecipitations, in the latter case immunoprecipitating assembled 20S proteasomes (Hendil et al., 1995).

MCP21 was purified from hybridoma supernatant over a proteinA-sepharose column. Because MCP21 is of the IgG1 subtype, it has a relatively low affinity for proteinA. Therefore, the pH of the hybridoma supernatant was adjusted to pH 8.8 and salt dissolved to 3.3M final concentration to increase MCP21 binding to the proteinA. Antibody was eluted with a low pH and low salt buffer (Figure 4.1) (Ey et al., 1978). Elution fractions were run on an SDS-PA gel to assess the purity and OD280 measurements were taken to determine the protein concentration.



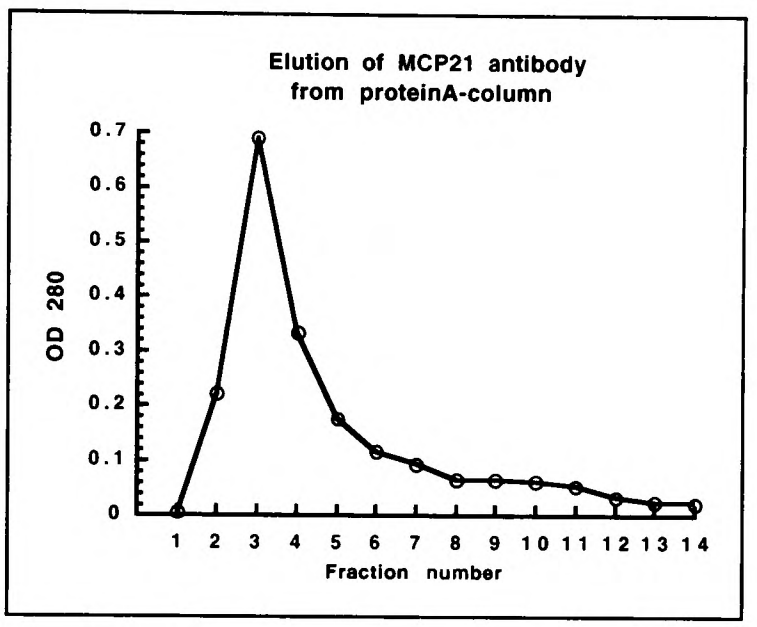


Figure 4.1. MCP21 purification.

Hybridoma supernatant containing MCP21 antibody was adjusted to pH 8.8 (100mM Tris) and 3.3M NaCl and applied to a 1 ml proteinA-sepharose column. MCP21 antibody was eluted with 50mM citrate buffer of pH 6.0 and 0.5 ml fractions were collected.

A. 2 µl of each elution fraction was loaded per lane. Samples were separated by SDS-10%PAGE and the gel stained with Coomassie Brilliant Blue. HC=heavy chain, LC=light chain.

B. OD280 of the fractions was measured, using 50mM citrate buffer as a blanc.

4.3. Tax co-precipitates with 20S proteasomes

To investigate the possible interaction between Tax and assembled proteasomes, we immunoprecipitated proteasomes from Tax-transfected or control-transfected 293T cell lysates using the proteasome antibody MCP21. The immunoprecipitated proteasomes were electrophoresed and subsequently immunoblotted with a Tax-specific antibody. Tax protein was clearly detected in proteasome immunoprecipitations from whole cell lysates of Tax-transfected cells (Figure 4.2A).

As a specificity control, immunoprecipitations were performed with W6/32 antibody, a MHC class I molecule specific mouse antibody, followed by a Western blot with an anti-Tax antibody (Y8) (Figure 4.2.B). No Tax was detected in these immunoprecipitates, indicating that immunoprecipitation is not due to non-specific interaction of Tax with the proteinA or the MCP21 antibody. One caveat in the interpretation is that the W6/32 antibody, although an IgG, is of a different subtype (IgG2a) than MCP21 (IgG1).

Immunoprecipitation of intact proteasomes by MCP21 antibody was confirmed in metabolically labelled cell lysates by the presence of a characteristic stack of proteins of 22-32kDa, which is typical of the 20S proteasome (Peters, 1994), and indicated an equivalent efficiency of proteasome recovery from Tax-transfected and control cells (Figure 4.2C).

Identical results were obtained when using lysates from 293T cells infected overnight with a recombinant vaccinia virus expressing Tax (vac-Tax, (Parker et al., 1992)), indicating that vaccinia virus infection does not prevent binding of Tax to the proteasome (Figure 4.3).

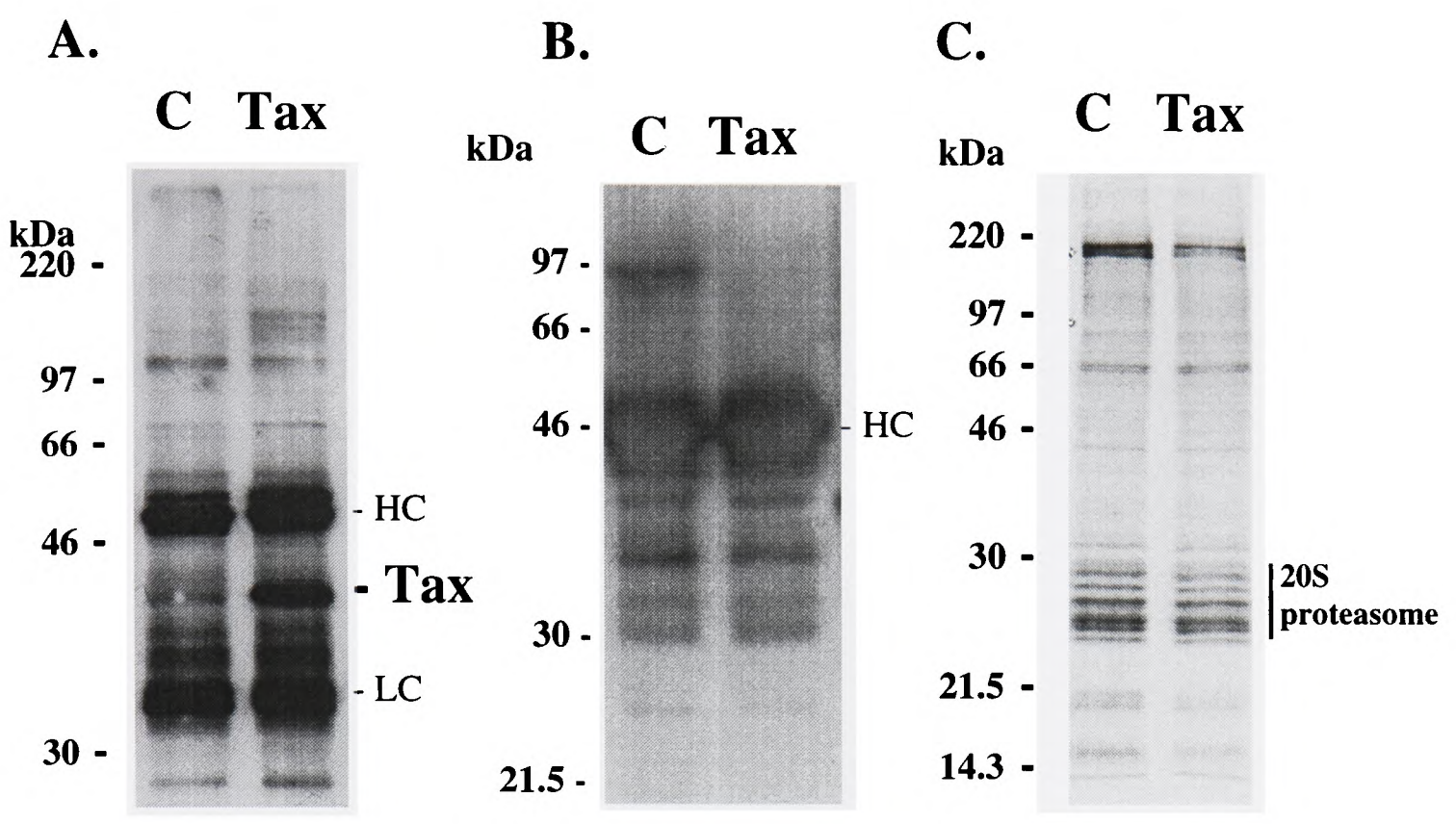


Figure 4.2. Tax co-precipitates with 20S proteasomes.

A. Immunoprecipitation of 20S proteasomes from whole cell lysates with MCP21 (monoclonal mouse antibody specific for HC3 α subunit), followed by a Western blot using a mouse anti-Tax antibody (Y8).

B. Immunoprecipitations from whole cell lysates using W6/32 antibody (mouse monoclonal antibody specific for human MHC class I molecules), followed by a Western blot using the Y8 anti-Tax antibody.

C. Immunoprecipitation of 20S proteasome with MCP21 antibody from whole cell lysates of cells metabolically labelled for 2.5 hours. An autoradiograph of the immunoprecipitates separated by SDS-12%PAGE is shown.

C= 293T control transfectants, Tax= 293T Tax transfectants, HC= IP-antibody heavy chain, LC= IP-antibody light chain.

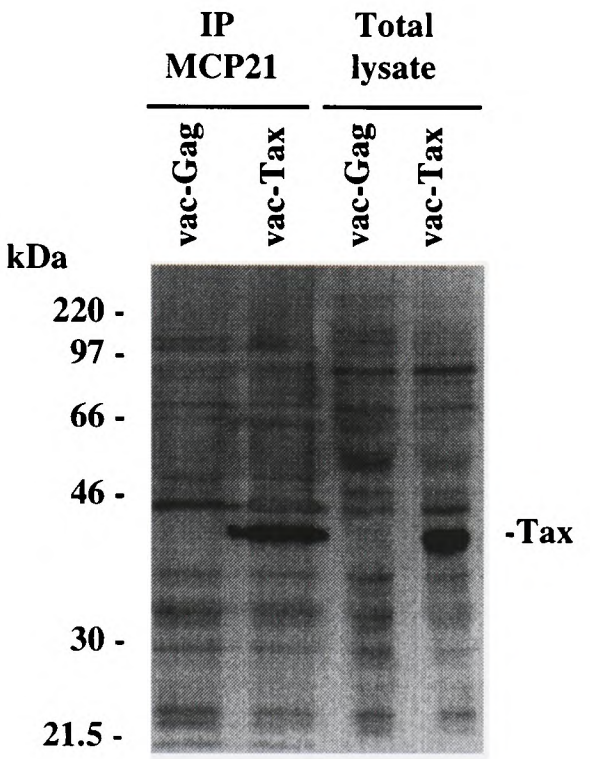


Figure 4.3. Tax expressed from vac-Tax co-immunoprecipitates with 20S proteasomes.

293T cells were infected with vac-Tax or vac-Gag (control) at a M.O.I of 3pfu/cell and left to express overnight. $2x10^7$ cells were lysed and subjected to immuno-precipitation with MCP21. Immunoprecipitates and total cell lysates (10^5 cells/lane) were separated by SDS-PAGE and immunoblotted with anti-Tax serum 1135TB.

4.4. Tax co-precipitates with nuclear 20S proteasomes

As Tax is predominantly a nuclear protein (Chapter 3), we predicted that Tax would be bound to nuclear proteasomes. We therefore prepared nuclear and cytoplasmic fractions from transfected cells and repeated the proteasome immunoprecipitations on fractionated material. Immunodetection of these preparations with Tax-specific antibody showed that Tax was restricted to proteasomes from the nuclear fraction (Figure 4.4A). Western blotting of the immunoprecipitates with MCP21 confirmed that proteasomes from both fractions were immunoprecipitated (Figure 4.4B).

4.5. Tax co-precipitated with 20S proteasomes has a slightly higher apparent molecular weight than Tax in total lysates

We observed that the Tax protein detected after immunoprecipitation of proteasomes had a slightly higher apparent molecular weight, as determined by SDS-PAGE, than Tax detected in a total lysate (Figure 4.5). This was true both for Tax expressed by transient transfection (Figure 4.5A) as well as for Tax expressed from a recombinant vaccinia virus (Figure 4.3). Moreover, the same was seen when Tax was co-precipitated with nuclear proteasomes (Figure 4.5B). The shift in size is approximately 1-2 kDa and is consistent with a post-translational modification such as phosphorylation or dephosphorylation. Although the nature of this proposed modification remains unknown, it may play an important role in the binding of Tax to the proteasome and may have a regulatory function (see discussion).

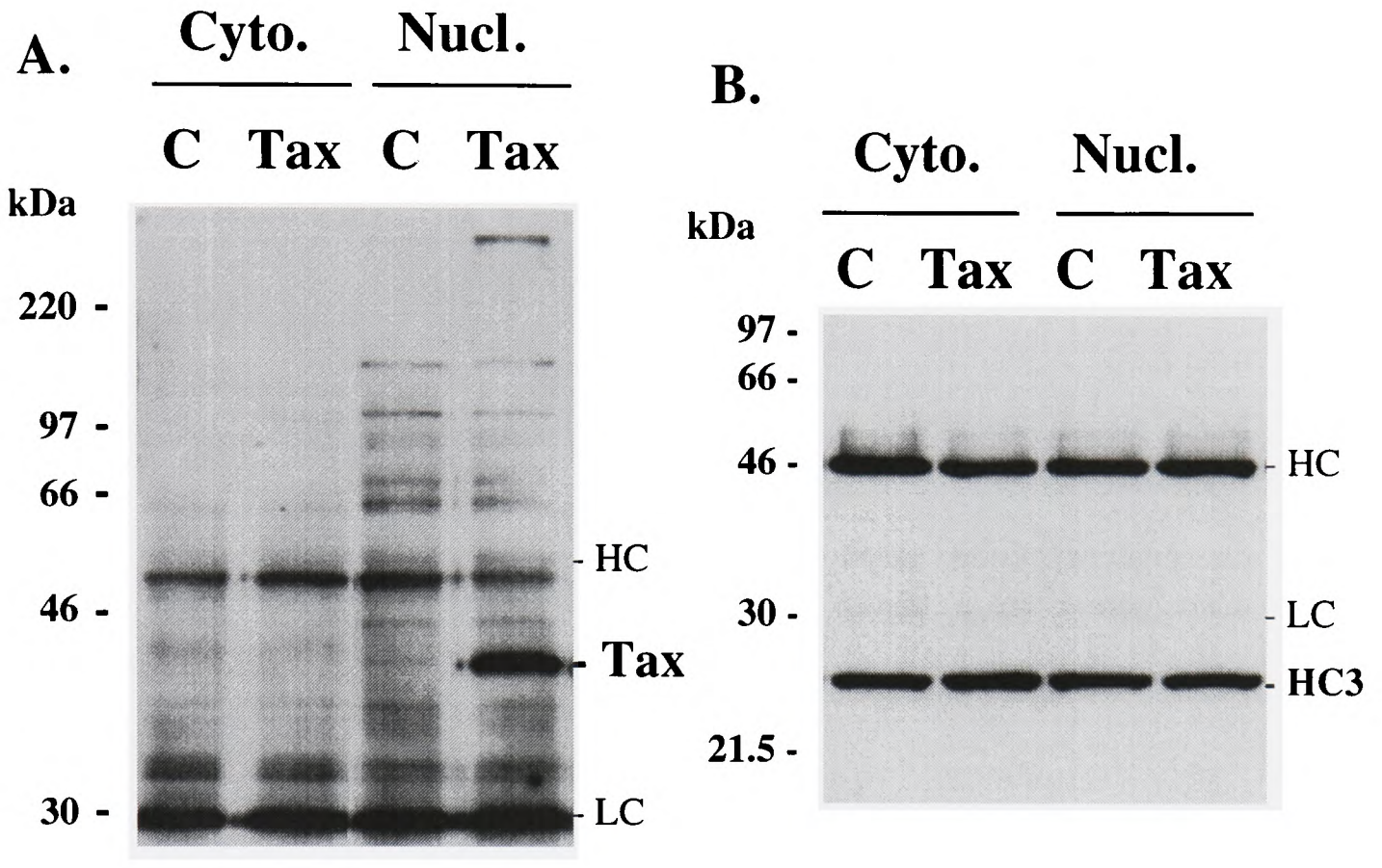


Figure 4.4. Tax co-immunoprecipitates with nuclear 20S proteasomes.

A. Immunoprecipitation of 20S proteasomes from cytoplasmic and nuclear fractions with MCP21 antibody, followed by a Western blot using a mouse anti-Tax antiserum (Y8).

B. Immunoprecipitates from (A.) were probed in a Western blot with MCP21 antibody to detect the HC3 proteasome subunit. This shows that equal amounts of proteasome were immunoprecipitated from all fractions. The secondary antibody used was Fc specific, hence the light chain was not recognised.

C= 293T control transfectants, Tax= 293T Tax transfectants, HC= IP-antibody heavy chain, LC= IP-antibody light chain, cyto= cytoplasmic fraction, and nucl.= nuclear fraction.

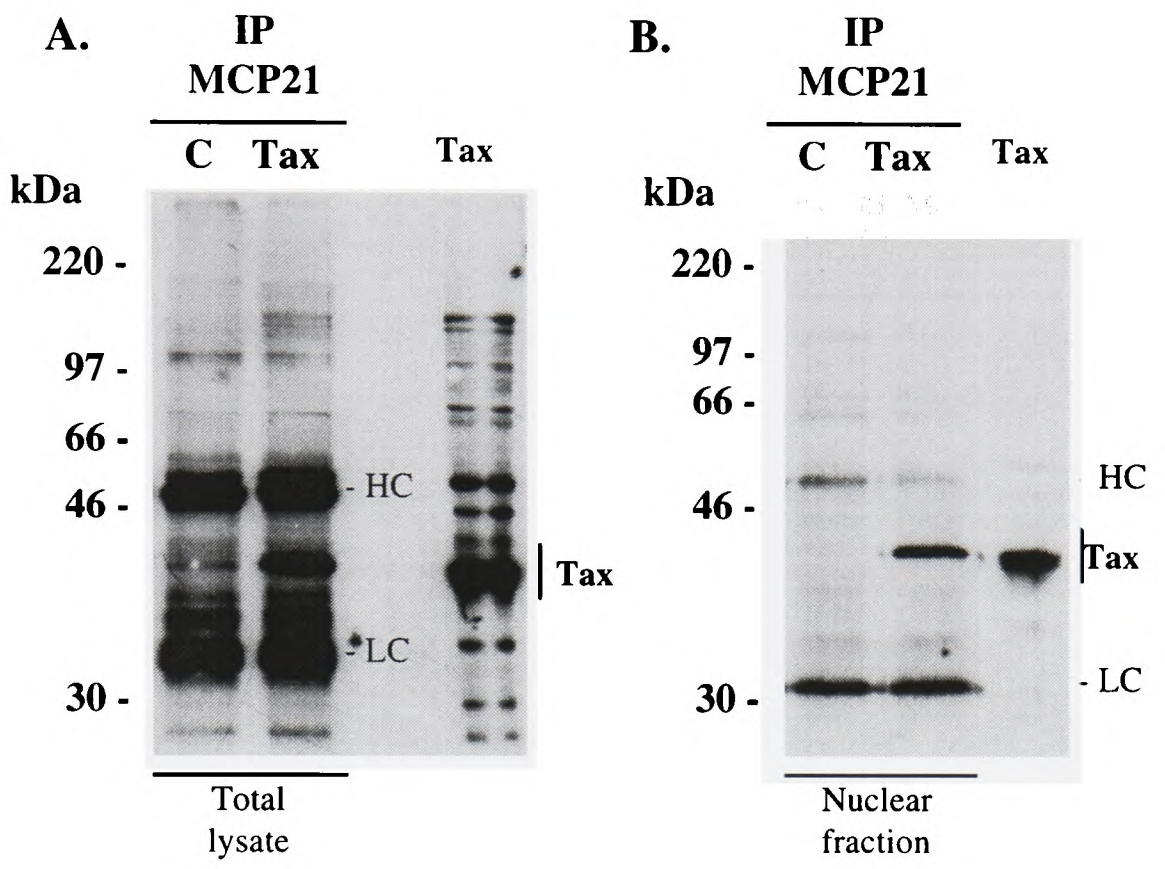


Figure 4.5. Tax co-precipitated with 20S proteasomes has a slightly slower mobility than Tax in total lysates.

A. Immunoprecipitation of 20S proteasomes from whole cell lysates ($3x10^7$ transfected 293T cells) with MCP21 (proteasome specific monoclonal mouse antibody), followed by a Western blot using a mouse anti-Tax antiserum (Y8). Total lysate of Tax transfected 293T cells was used as a control (right lane, $2x10^5$ cells/lane).

B. Immunoprecipitation of 20S proteasomes from nuclear fractions of transfected 293T cells, followed by a Western blot using a mouse anti-Tax antiserum (Y8). Total lysate of Tax transfected 293T cells was used as a control (right lane).

C= 293T control transfectants, Tax= 293T Tax transfectants, HC= IP-antibody heavy chain, LC= IP-antibody light chain.

4.6. 20S proteasome fails to co-precipitate with Tax

Reciprocal immunoprecipitation experiments on whole cell lysates revealed that proteasome proteins were not detected in Tax immunoprecipitates (Figure 4.6). Antibody binding of Tax may be incompatible with proteasome association of Tax, and as the Tax-specific antibodies 1135TB and 1153TB were raised against a C-terminal peptide in Tax, this would suggest that Tax binds the proteasome via its C-terminal domain. Alternatively, it may indicate that only a small proportion of the total amount of proteasomes is bound to Tax. The amount of HC3 immunoprecipitated with MCP21 from $2x10^6$ cells was still detectable (see right lane of figure 4.6 A.). This and other experiments have indicated that the detection limit lies around $1x10^6$ cells (data not shown; see also legend figures 4.8 and 4.9). As the anti-Tax immunoprecipitations were performed on lysates from $2x10^7$ cells and we could not detect any HC3, this would suggest that Tax-immunoprecipitations bring down less that 1/20 of total proteasomes. However, the efficiencies of the immunoprecipitations are unknown and these considerations should therefore be treated with caution.

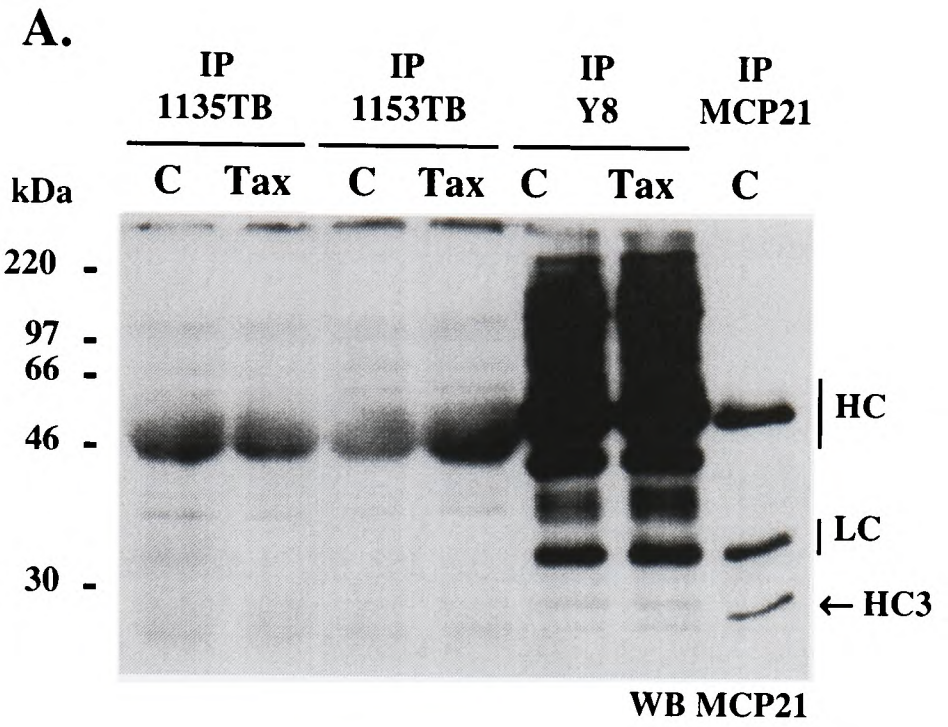


Figure 4.6. 20S proteasome fails to co-precipitate with Tax.

A. Immunoprecipitation with various anti-Tax antibodies (1135TB, 1153TB and Y8) and MCP21, followed by a Western blot with MCP21 to detect the HC3 subunit.

B. Immunoprecipitation with anti-Tax antibody 1135TB, followed by a Western blot with anti-Tax antibody Y8.

C= 293T control transfectants, Tax= 293T Tax transfectants, IP= immunoprecipitation, WB= Western blot, HC= heavy chain, LC=light chain.

4.7. Tax partially co-localises with proteasomes

If Tax and proteasomes interact in the nucleus, then at least partial colocalisation of the two components in the nucleus would be expected. To address this, we performed immunofluorescence confocal microscopy experiments. We detected proteasomes in both the cytoplasm and the nucleus (Figure 4.7B), with especially strong detection of proteasomes in the nuclear compartment, as has previously been observed for cultured cells (Rivett, 1998). Tax expression did not obviously alter the distribution pattern of proteasomes (Figure 4.7F). Tax was localised in the nucleus, both in defined nuclear bodies and as more diffuse staining (Figure 4.7G). Superimposition of the two staining patterns revealed a partial colocalisation of Tax with nuclear proteasomes, outside the nuclear bodies (Figure 4.7H).

Colocalisation as detected by confocal microscopy indicates that the two components detected are in close proximity, but it does not, however, prove their direct interaction. Nevertheless, together with the immunoprecipitation data, it is consistent with Tax associating with assembled nuclear proteasomes. This interaction may be transient with only a limited amount of Tax associated with proteasomes at any one time.

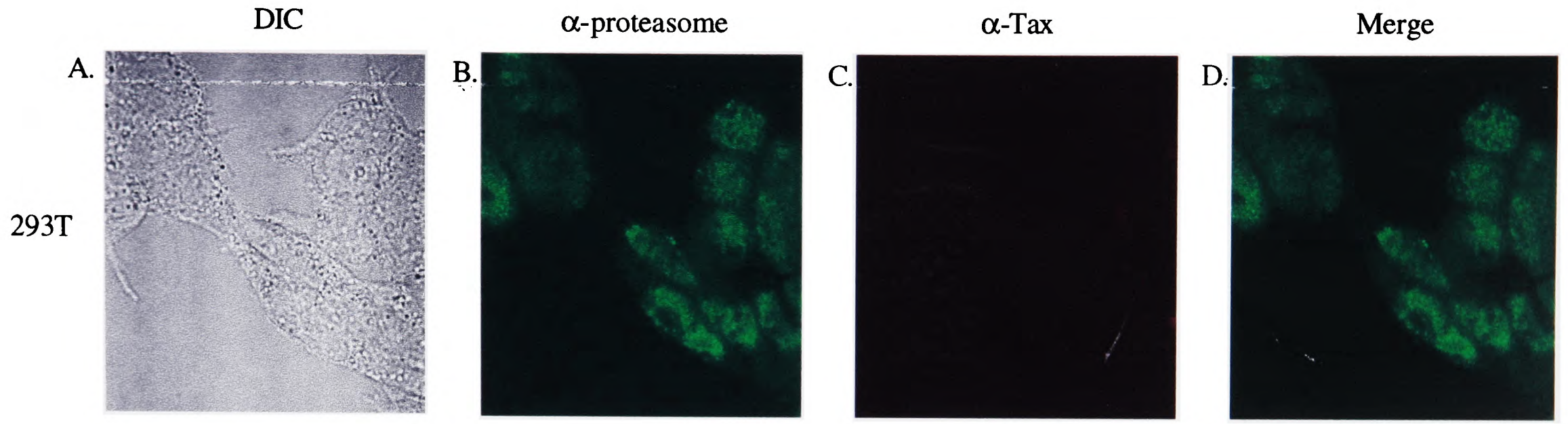


Figure 4.7. Tax partially colocalises with 20S proteasomes.

Immunofluorescence confocal microscopy as described in materials and methods. 293T cells were infected with SFV-Tax expressing Tax fused to a HA-tag. After 18 hours, cells were fixed and Tax detected with an anti-HA antibody (red) and proteasomes with α-HC3 antibody MCP21 (green). DIC: differential interference contrast. Overlap is in yellow (H.).

4.8. Tax expression stimulates the chymotryptic and tryptic activities of the 20S proteasome

Although up to five different activities have been described for the 20S proteasome, the chymotrypsin-like (cleavage after hydrophobic residues), trypsin-like (cleavage after basic residues) and caspase-like (cleavage after acidic residues) hydrolysing activities represent the three main types (Dick et al., 1998). The chymotrypsin-like activity is thought to determine the rate of protein breakdown by the proteasome (Kisselev et al., 1999).

The proteolytic properties of the 20S proteasome are modulated *in vivo* by incorporation of γ-interferon inducible subunits LMP2, LMP7 and MECL-1 and attachment of the PA28 activator to the end(s) of the 20S proteasome complex (Driscoll et al., 1993; Gaczynska et al., 1993; Groettrup et al., 1995).

Given the association of Tax with nuclear proteasomes, we wished to establish if this association altered the proteasome's proteolytic activity. Prototypic fluorogenic peptide substrates N-succinyl-LLVY-AMC (LLVY) and N-cbz-GGR-AMC (GGR) were used to assay chymotryptic and tryptic activity, respectively, in immunoprecipitated proteasome preparations from whole cell lysates. Under conditions that allowed co-precipitation of Tax with proteasomes, increased activity was seen with both substrates by proteasomes purified from Tax-transfected cells compared with control cells (Figures 4.8A & 4.9A). The relative amounts of proteasome in the different samples were determined by separating the immunoprecipitates by SDS-PAGE after the cleavage assay and immunoblotting with MCP21 antibody to detect HC3 subunit. The bands were quantified and used to normalise the fluorescence measured in the cleavage assay (Figures 4.8B & 4.9B). Cleavage of substrates was abrogated by the addition to assays of the proteasome inhibitors lactacystin or Calpain inhibitor 1 (LLnL), indicating that the proteolytic activity we measured was indeed proteasomal (Figures 4.8A & 4.9A). Because the stoichiometry of the Tax/proteasome interaction is not known, no quantitative inferences can be made from the cleavage experiments. However, given that our previous data suggested that only a fraction of proteasomes were bound by Tax at

one time (see Figure 4.5, 4.6 & 4.7 and text), detection of any enhancement of cleavage by immunoprecipitated proteasomes is significant.

We also attempted to determine the cleavage activities of proteasomes immunoprecipitated from nuclear and cytoplasmic fractions. However, reproducibility of these data from fractionated material was poor and we were unable to draw conclusions about the comparative cleavage activities. This may reflect the different conditions used during lysis and preparation of nuclear and cytoplasmic fractions (data not shown).

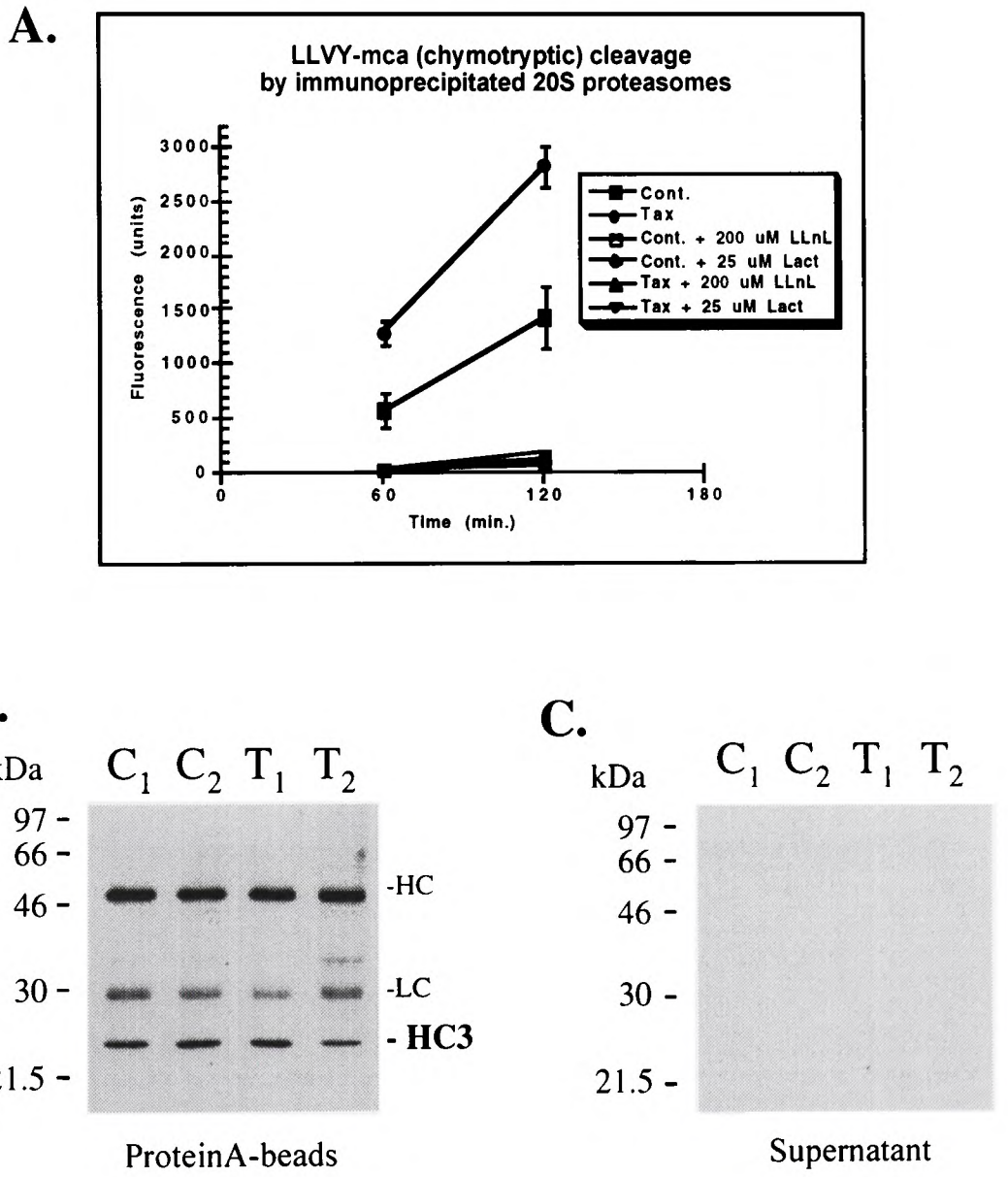


Figure 4.8. Tax expression stimulates the chymotryptic activity of 20S proteasomes.

Legend on next page.

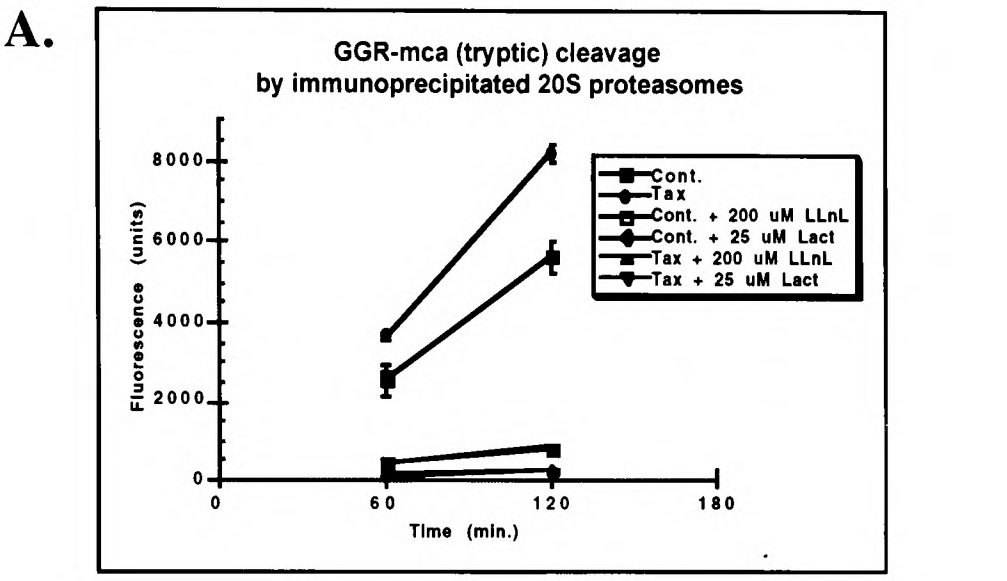


Figure 4.9. Tax expression stimulates the tryptic activity of 20S proteasomes.

Legend on next page.

Legend Figure 4.8 and 4.9.

Tax expression stimulates the chymotryptic (Fig. 4.8) and tryptic (Fig. 4.9) activities of 20S proteasomes.

A. 20S proteasomes from control and Tax transfected 293T cells were immunoprecipitated with MCP21 antibody or W6/32 (negative control) using $2x10^6$ cell equivalents per sample. Immunoprecipitates were incubated with 100 μM of fluorogenic peptide substrate N-succinyl-L-L-V-Y-mca (LLVY, Fig. 4.8) or cbz-G-G-R-mca (GGR, Fig. 4.9). Release of the fluorescent mca group was measured at 370 nm excitation / 460 nm emission and the values of the negative controls substracted from the experimental values. Subsequently, fluorescence was normalised for the amounts of proteasome in the samples (see figure B.). Lactacystin or calpain inhibitor I were added to the reactions at 25 μM or 200 μM, respectively, where indicated. Duplicates for each sample were done. One representative experiment out of 3 is shown for each substrate.

B. After the last time point was taken, the relative amounts of 20S proteasome present in the immunoprecipitates used for activity measurement (see figure A.) were determined. This was done by separation of the immunoprecipitates by SDS-PAGE, followed by Western blotting using the MCP21 antibody to detect the HC3 α-subunit. Amounts were quantified by densitometry and used to normalise the fluorescence measured in the cleavage assay.

C. After the last time point was taken, 20 μl of the reaction mix (supernatant) was separated by SDS-PAGE and processed as described in legend B. No proteasome subunits were detected in the supernatant, indicating that there was no release from the proteinA-beads. C/Cont.= control transfectants, T/Tax= Tax transfectants, HC= heavy chain, LC= light chain, Lact= lactacystin, LLnL= Calpain inhibitor I.

Note: A series of increasing amounts of proteasomes were immunoprecipitated from lysates of respectively 0.125; 0.25; 0.5; 1; 2 and $4x10^6$ cells (in duplicates). Cleavage of the fluorogenic LLVY substrate was measured as described and after the assay the amount of proteasome in each sample was determined by SDS-PAGE and Western

blotting using the MCP21 antibody (HC3 subunit specific). Whereas cleavage activity could be detected in the samples derived from $0.5x10^6$ cells upward, proteasome subunit became detectable from $1x10^6$ cell equivalents upward. Importantly, a clear correlation was found between LLVY cleavage and the amount of HC3 detected in samples used for those measurements, thereby validating the normalisation procedure used (data not shown).

4.9. Tax does not induce LMP2 and LMP7 expression in 293T cells

As Tax was shown to co-precipitate with 20S proteasomes from 293T cells, it was of interest to know the subunit composition of the proteasomes. In addition, the Tax-specific enhancement of peptide substrate cleavage we observed is similar to that reported for proteasomes containing LMP2 and LMP7 subunits (Driscoll et al., 1993; Gaczynska et al., 1993). Tax-induced expression and substitution of these subunits in cellular proteasomes could therefore explain our observations with regard to the catalytic activities of the proteasome.

However, LMP2 and LMP7 proteins were not detected by Western blot analysis of lysates from Tax-transfected or control 293T cells, indicating that these subunits were not expressed in 293T cells and that Tax did not induce their expression (Figure 4.10). Therefore, in 293T cells, Tax binds to proteasomes composed of the 'constitutive' subunits and stimulates the catalytic activities of the proteasome by a mechanism independent of the LMP2 and LMP7 subunits.

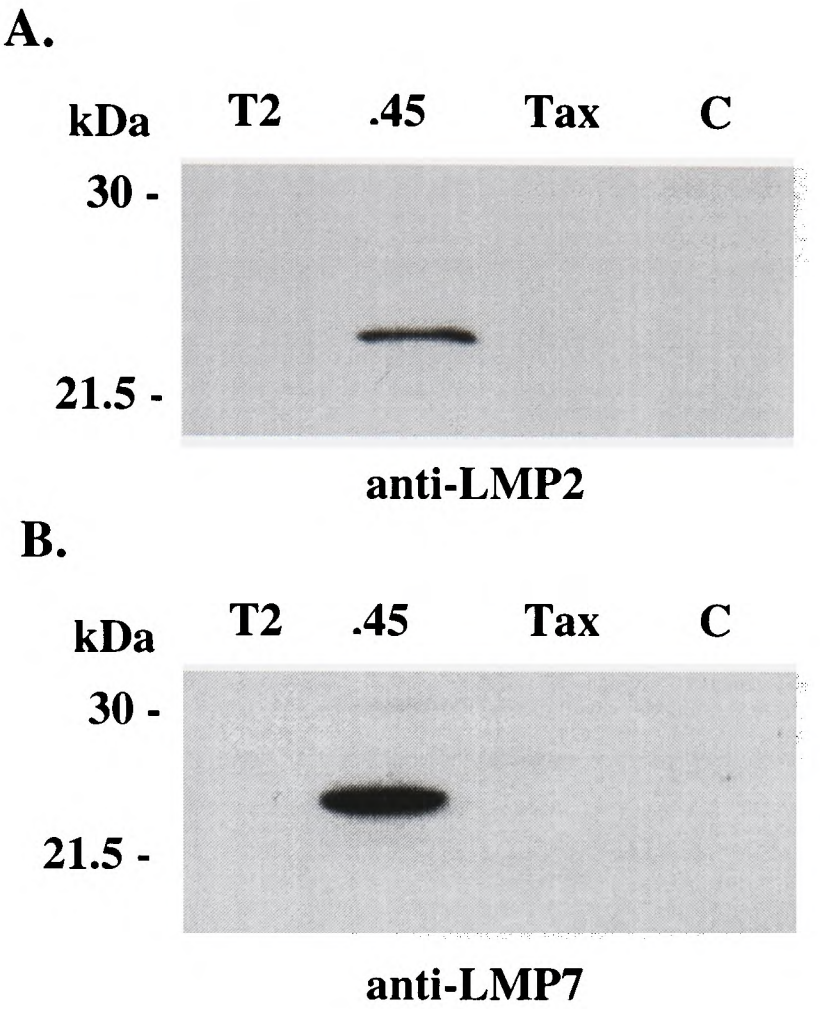


Figure 4.10. Tax does not induce expression of LMP2 and LMP7.

Cell lysates were separated by SDS-12%PAGE, followed by Western blotting using polyclonal rabbit antibodies raised against either LMP2 (A.) or LMP7 (B.).
.45= 721.45 (human B lymphoblastoid cell line), T2= 721.45 derivative with homozygous deletion in class II region encompassing LMP2 and LMP7 genes, Tax= 293T Tax transfectants, C= 293T control transfectants.

4.10. Co-precipitation of Tax with 20S proteasomes from different cell lines

We wished to confirm our data on co-precipitation of Tax with proteasomes from 293T cells with data on HTLV-1 infected and transformed cell lines, as these better represent the situation *in vivo*.

Firstly, we determined whether the LMP2 and LMP7 subunits were expressed and incorporated into 20S proteasomes of these cell lines. To this end, 20S proteasomes were

immunoprecipitated from total cell lysates, followed by a Western blot with LMP2 and LMP7 specific antibodies to detect the presence of these subunits.

Figure 4.11 shows that all 3 HTLV-1 infected cell lines (MT-2, MT-4(P) and MT-4(S)) have both LMP2 and LMP7 incorporated into their 20S proteasomes. MT-4(S) cells had relatively little LMP2 compared to MT-2 and MT-4(P) cells. Due to the unavailability of antibodies against the constitutive proteasome subunits we do not know whether, or to what extend, the constitutive counterparts, subunits delta and MB1, are expressed and incorporated. It is, however, most likely that these cells have a population of 20S proteasomes comprised of a mix of both 'constitutive' and 'immuno' proteasomes, and perhaps even proteasomes containing the four (or even six) different catalytic β subunits (Belich et al., 1994).

In the same experiment it was also confirmed that LMP2 and LMP7 were absent from proteasomes in 293T cells, also in the presence of Tax (Figure 4.11).

Subsequently, proteasomes were immunoprecipitated from HTLV-1 infected cell lines and co-precipitated Tax detected by Western blot analysis of the immunoprecipitates.

Co-precipitated 40kDa Tax could be detected in the Tax expressing MT-2 and MT-4(P) cells, whereas it was absent from MT-4(S) (control) (Figure 4.12, lanes 5, 6, 7). Tax co-precipitation was not as efficient as for 293T cells, perhaps reflecting the somewhat lower expression level of Tax. In addition, the 64kDa form of Tax (env-Tax) in MT-2 cells co-precipitated very efficiently with the 20S proteasomes (Figure 4.12, lane 5).

Furthermore, Tax expressed from vac-Tax appeared to co-precipitate with proteasomes more efficiently from lysates of 721.45 cells than from 721.174 cells (Figure 4.12, lanes 2, 4). As .45 cells express high levels of LMP2 and LMP7, and hardly any delta and MB1 subunits, and .174 cells only express the constitutive subunits (Figure 4.12, and (Belich et al., 1994)), this may indicate that LMP2 and LMP7 enhance Tax binding to proteasomes.

Taken together, these data indicate that Tax binds to 20S proteasomes in HTLV-1 infected cell lines, which express the LMP2 and LMP7 subunits and incorporate them into (at least a subset of) their proteasomes.

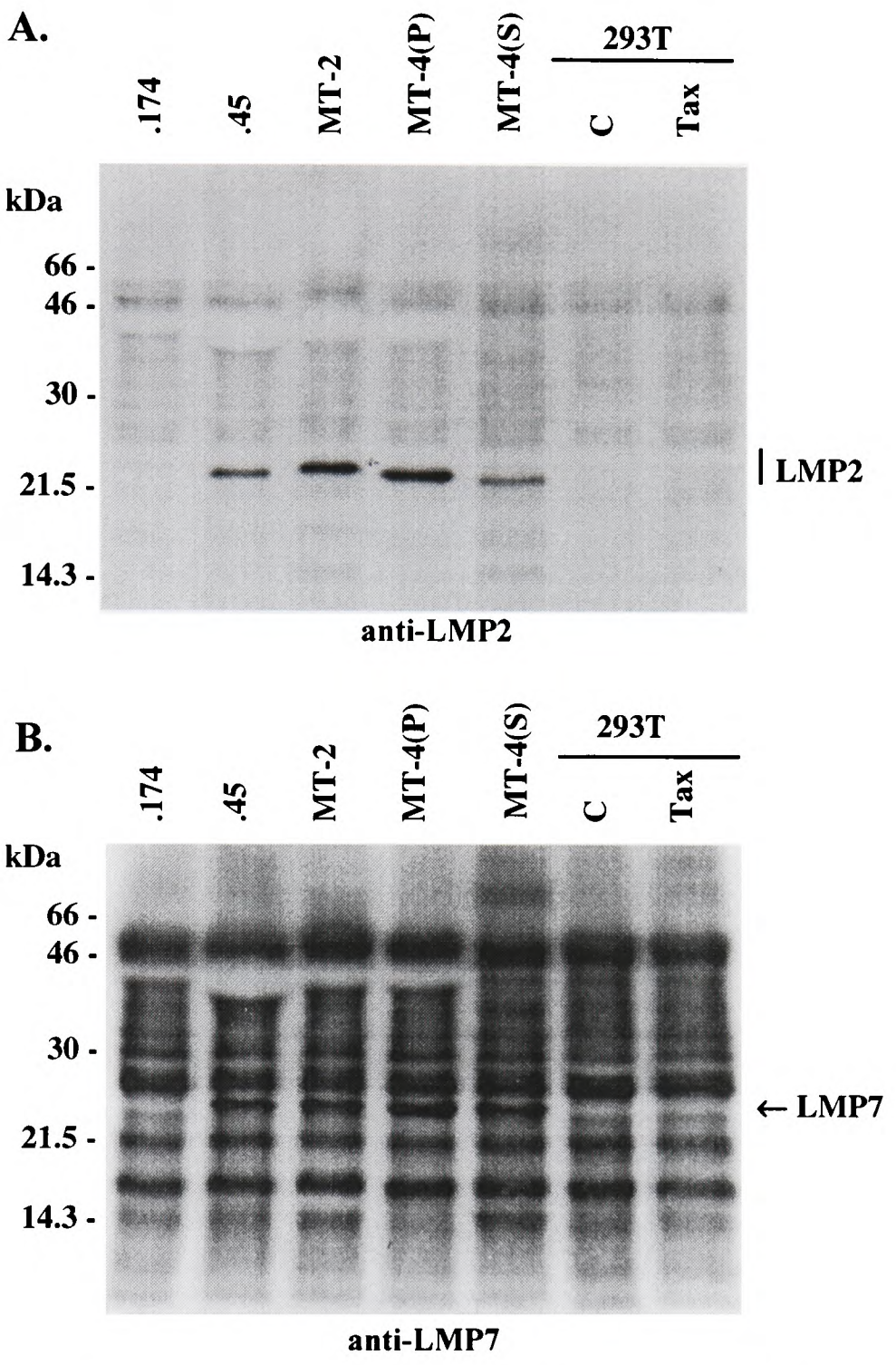


Figure 4.11. Incorporation of LMP2 and LMP7 subunits into 20S proteasomes. Total cell lysates were subjected to immunprecipitation with anti-20S proteasome antibody MCP21. Precipitates were separated by SDS-12%PAGE, transferred to nitrocellulose and probed with polyclonal rabbit anti-sera against LMP2 (**A.**) or LMP7 (**B.**).

.45= 721.45 (human B lymphoblastoid cell line; positive control), .174=721.174, a 721.45 derivative with homozygous deletion in the class II region encompassing LMP2 and LMP7 genes (negative control). MT-2, MT-4(P) and MT-4(S) are HTLV-1 infected and transformed cell lines. 293T cells were transfected with pJFE-Tax (Tax) or empty control vector (C).

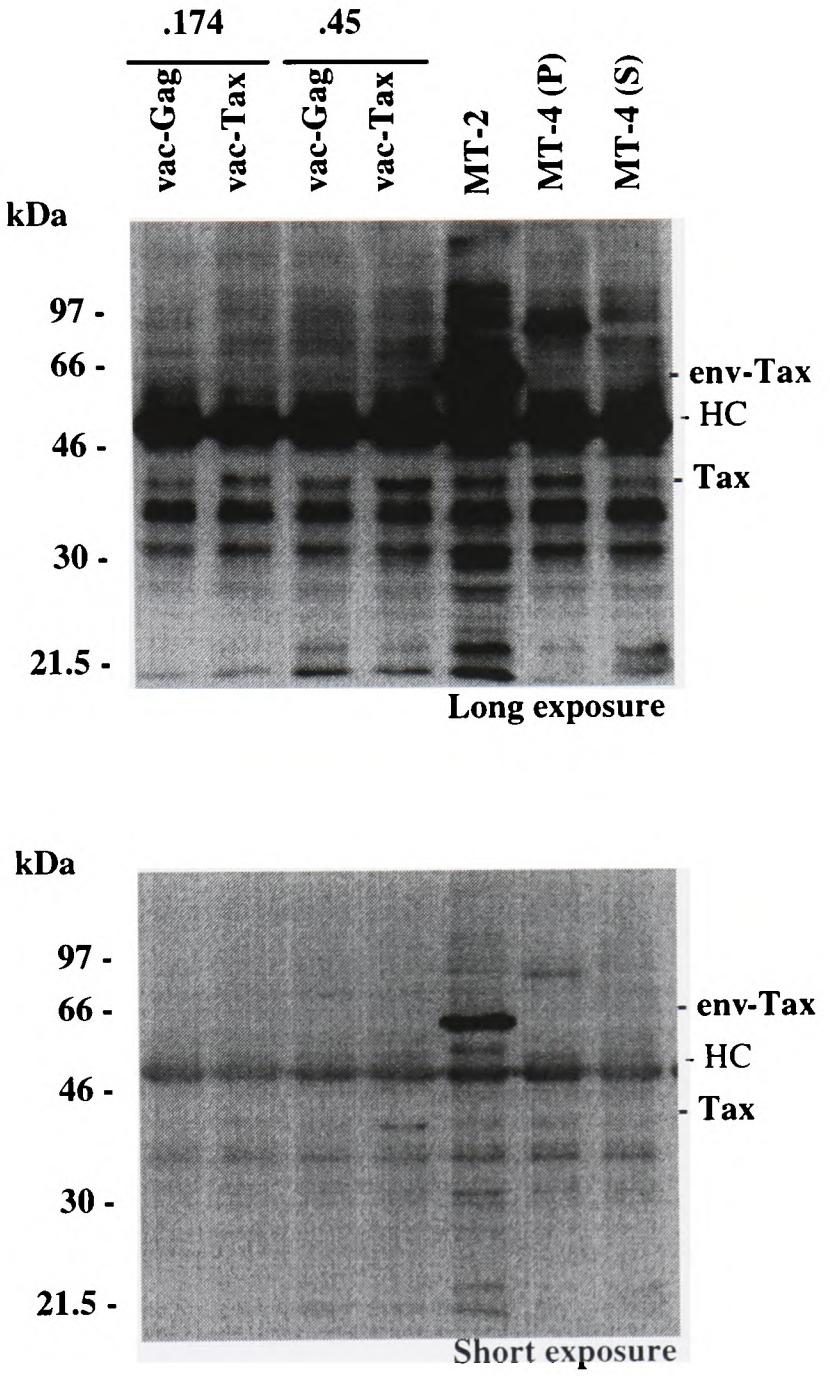


Figure 4.12. Co-precipitation of Tax with 20S proteasomes from different cell lines.

.174 and .45 cells were infected with vac-Tax or vac-Gag at a M.O.I. of 3pfu/cell and left overnight to express. Total lysates of $6x10^7$ cells of the indicated cell types were subjected to immunoprecipitation with MCP21 antibody. The precipitates were separated by SDS-PAGE and immunoblotted with anti-Tax antibody mAb1316. Tax and env-Tax are indicated on the right. HC= heavy chain. Two exposures of the same blot are shown.

4.11. Expression and partial purification of Tax-6His

With the goal of performing detailed *in vitro* studies on the interaction between Tax and the proteasome, the purification of Tax was initiated.

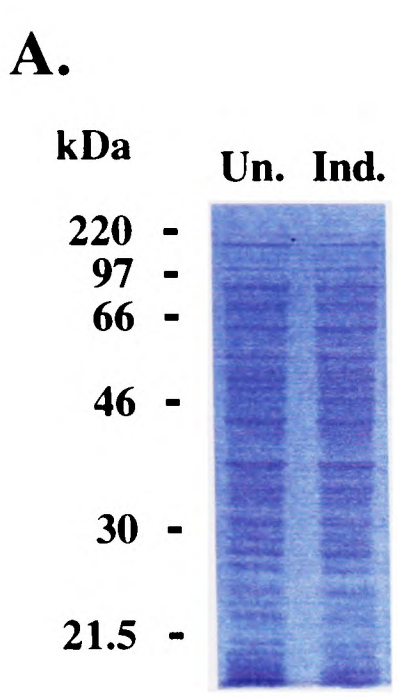
Expression in eukaryotic systems was prohibited due to the difficulty in achieving stable expression of Tax, presumably due to the induction of apoptosis by Tax (Chlichlia et al., 1995). Transient expression systems would impose restrictions on the levels of expression and the recovery of Tax from the nucleus. Therefore, it was decided to express Tax in bacteria.

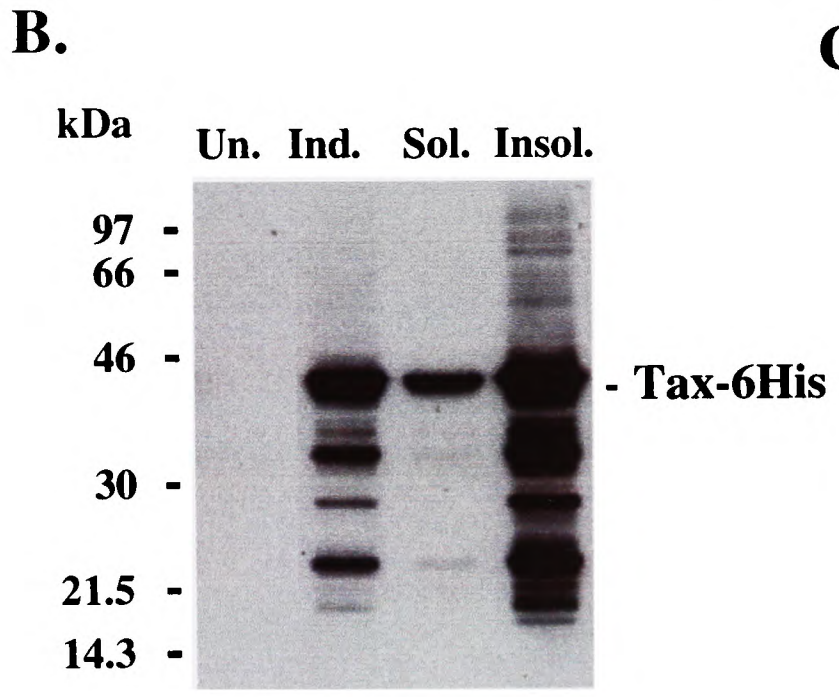
To facilitate expression of Tax in bacteria, the first seven codons of the Tax nucleotide sequence were changed into codons preferentially used in bacterial coding sequences. To allow purification over a Ni^{2+}-NTA column, a lysine followed by six histidine residues (histidine-tag) was added to the 3' end of the coding sequence.

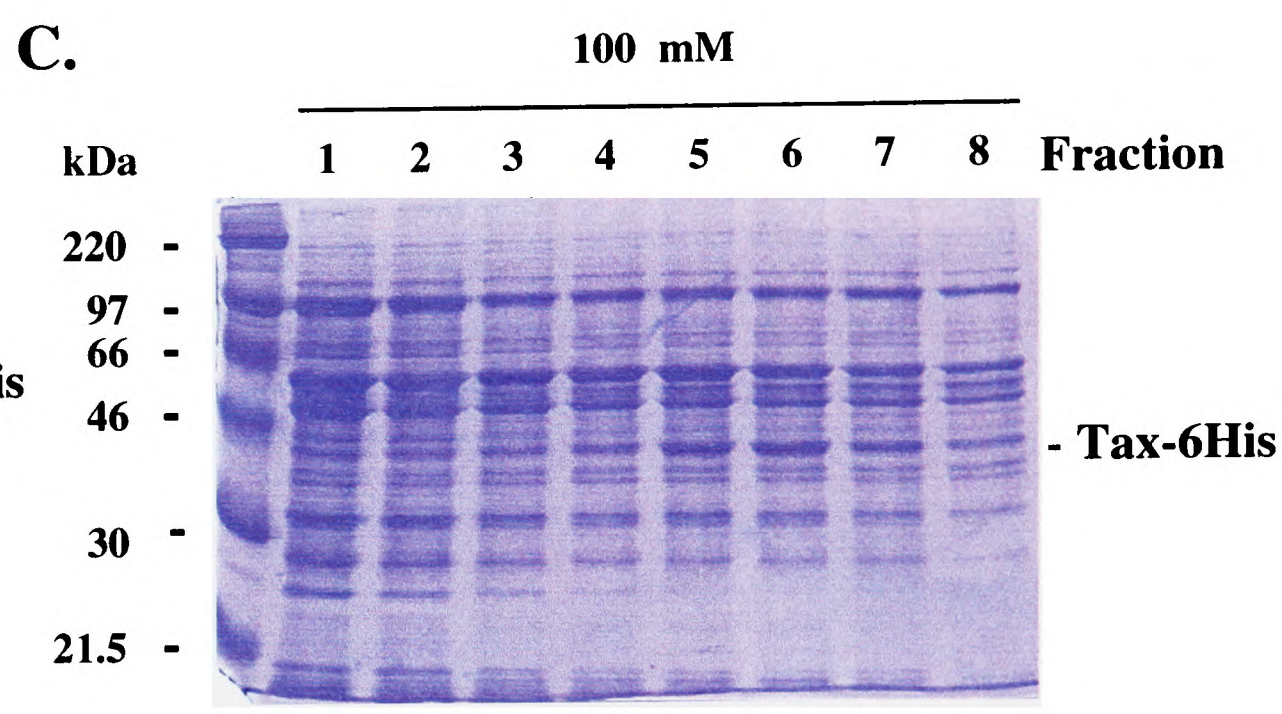
The modified Tax-sequence was cloned into the pET28c vector, which brings the expression of Tax-6His under the control of a T7*lac* promoter. As a host the *E.coli* strain BL21(DE3) was chosen. This strain carries a lysogen of bacteriophage DE3, which harbours the T7 RNA polymerase under control of a *lacUV5* promoter. When IPTG is added to the medium, expression of the T7 RNA polymerase is induced through the *lacUV5* promoter. The T7 RNA polymerase will in turn strongly activate transcription from the T7*lac* promoter, leading to expression of Tax-6His.

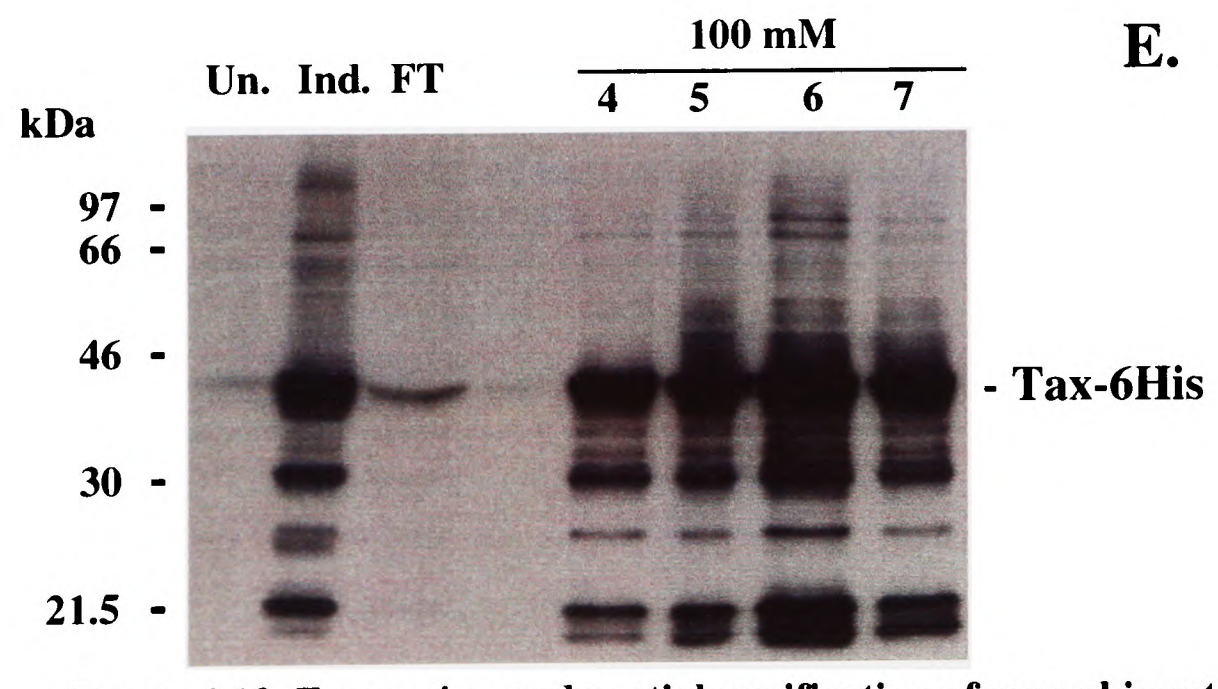
Figure 4.13B shows the induced expression of Tax-6His. The upper band represents full-length Tax-6His, whereas the smaller bands probably represent degradation fragments. Tax-6His protein could be found in the soluble as well as the insoluble fraction.

Bulk cultures were grown, expression induced, the cells lysed and the soluble fraction mixed with Ni^{2+}-NTA resin to allow binding of His-tagged proteins. The resin was settled into a column and bound protein eluted with an imidazole gradient (Figure 4.13C). The identity of the ~41kDa band in the elution fractions was confirmed to be Tax-6His by Western blotting with both an anti-penta-His antibody and an anti-Tax serum (C-terminus specific) (Figures 4.13D,E). Further Tax-6His purification was not pursued beyond this stage, as it was not made a priority.









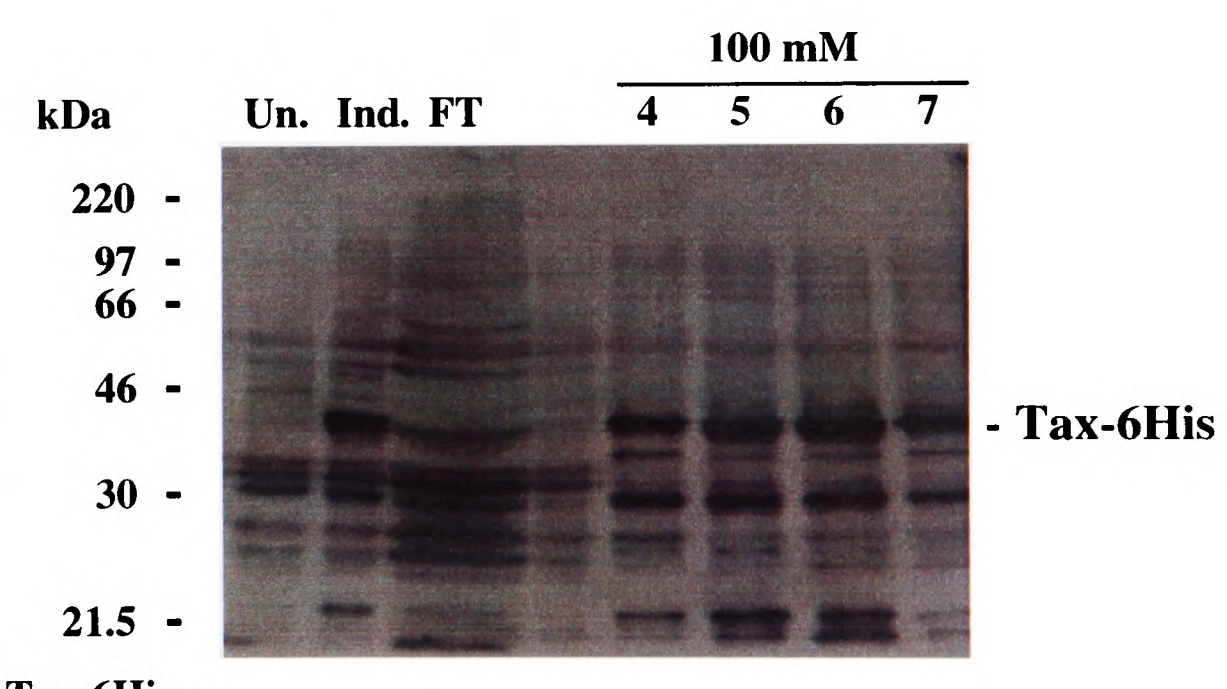


Figure 4.13. Expression and partial purification of recombinant Tax-6His.

Legend on next page.

Figure 4.13. Expression and partial purification of recombinant Tax-6His.

Expression of Tax-6His from pET28c-Tax in BL21(DE3) was induced at OD_{600}=0.6 with 1mM IPTG, for 3 hours at 37°C.

A. Total lysates of samples taken before and after induction were separated by SDS-PAGE and stained with CBB.

B. Total lysates of samples taken before and after induction and soluble and insoluble fractions of induced samples were separated by SDS-PAGE and Western blotted with a mouse anti-penta-histidine antibody. Tax elution from Ni^{2+}-NTA column.

C. 100mM imidazole elution fractions separated by SDS-PAGE, stained with Coomassie Brilliant Blue.

D. Western blot on Ni^{2+}-NTA column fractions with anti-penta-histidine antibody.

E. Western blot on Ni^{2+}-NTA column fractions with 1135TB anti-Tax antibody (C-terminus specific). Un= uninduced, Ind= induced, Sol= soluble fraction, Insol= insoluble fraction, FT= flowthrough, 100mM= 100mM imidazole elution buffer.

4.12. Summary and discussion

Summary

In the previous chapter we showed that the HTLV-1 transactivator protein Tax translocated into the nucleus very rapidly after synthesis. At steady state, nuclear Tax accounted for almost all the Tax expressed in the cell, although we could not exclude that a minor fraction of Tax was present in cytosol, where it is synthesised.

Previous studies had indicated that Tax could bind to two different 20S proteasome subunits, the α-subunit HC9 (α3) and (non-catalytic) β-subunit HsN3 (β7) (Beraud and Greene, 1996; Petropoulos and Hiscott, 1998; Rousset et al., 1996). In this chapter it was shown that Tax co-precipitated with assembled 20S proteasomes (Figure 4.2). Moreover, Tax specifically associated with assembled nuclear 20S proteasomes and we could not detect Tax bound to cytoplasmic proteasomes (Figure 4.4). The apparent molecular weight of the co-precipitated Tax was slightly higher than that of Tax present in a total cell lysate (Figures 4.3 & 4.5). We further found that Tax partially colocalised with nuclear proteasomes (Figure 4.7) and that the chymotryptic and tryptic activities of the proteasome were stimulated in the presence of Tax (Figures 4.8 & 4.9). This activation of the 20S proteasome was not due to Tax mediated induction of expression of LMP2 and LMP7 subunits (Figures 4.10 & 4.11). In addition, it was shown that Tax bound to 20S proteasomes in HTLV-1 infected cell lines MT-2 and MT-4(P), which express the LMP2 and LMP7 subunits and incorporate them into (at least a subset of) their proteasomes (Figures 4.11 & 4.12).

Localisation of Tax/proteasome interaction

The mechanism of proteasome transport into the nucleus is incompletely understood. Several of the α-subunit components contain highly conserved short nuclear localisation sequences and nuclear pore complexes appear able to translocate large protein complexes like proteasomes (Feldherr et al., 1984; Ohno et al., 1998; Reits et al., 1997; Rivett,

1998). However, subunits might also be transported individually or in subcomplexes and assemble intranuclearly (Rivett, 1998).

It has been shown that proteasomes diffuse rapidly throughout the nucleus and cytoplasm and throughout the cell during cell division. Proteasomes are contained in the nucleus upon nuclear membrane re-assembly after cell division and they are transported over the nuclear membrane very slowly and unidirectionally from the cytoplasm to the nucleus (Reits et al., 1997). As Tax is efficiently translocated to the nucleus after synthesis, it is unlikely that it binds to pre-assembled proteasomes in the cytosol and the whole complex is shuttled into the nucleus. It remains possible that Tax binds to one or more independent proteasome components prior to nuclear translocation and facilitates this process for subunits lacking a nuclear localisation signal sequence. However, the predominance of proteasome/Tax complexes in the nuclear compartment probably reflects the efficient translocation of Tax, independent of proteasome, into the nucleus following synthesis.

Tax/proteasome binding sites and the stoichiometry of the interaction

Another point relates to what actually determines/regulates the interaction between Tax and the proteasome. A number of Tax mutants was generated to map regions of Tax involved in the interaction. This work is presented in Chapter 5, and will not be discussed here.

Does subunit composition of the proteasome affect Tax binding? Tax was shown to bind 20S proteasomes containing the constitutively expressed catalytic subunits (Figure 4.2 & 4.4). In addition, it was apparent that Tax could also bind proteasomes containing the inducible subunits LMP2 and LMP7 (Figure 4.11 & 4.12). The α-subunit HC9 (α3) and (non-catalytic) β-subunit HsN3 (β7) are components of both types of proteasomes, but it remains possible that Tax binds to other subunits in addition to (or instead of) these two subunits. In addition, Tax can form dimers which could increase the number of Tax molecules bound to the proteasome at any one time (Perini et al., 1995). Therefore, although Tax seems indifferent to the presence or absence of the LMP2 and LMP7

subunits, the exact binding sites of Tax on the proteasome and the stoichiometry of the Tax/proteasome interaction remain unknown.

A role for phosphorylation in the Tax/proteasome interaction?

It is possible that phosphorylation plays an important role in the binding of Tax to the proteasome.

Phosphorylation is important in the regulation of the assembly and activity of the proteasome. The 20S proteasome was reported to be phosphorylated on serine residues of α subunits HC8 and HC9, possibly by casein kinase II (Bose et al., 1999)(Bose et al., 2001). Dephosphorylation resulted in decreased peptidase activity (Mason et al., 1996). Furthermore, interferon-γ treatment led to reduced phosphorylation of these subunits and a concomitant increase in association of PA28 complexes with the 20S proteasome (Bose et al., 1999)(Bose et al., 2001). Phosphorylation of PA28 (on serine residues) was in turn required for its stimulation of peptidase activity of 20S proteasomes (Li et al., 1996). Phosphorylation of the 19S ATPase subunit p45/Rpt6 was required for assembly of the 26S proteasome from its constituent subcomplexes (Satoh et al., 2001).

In addition, it was reported that the 20S proteasome exhibits intrinsic nucleoside diphosphate (NDP) kinase activity. This activity entails the transfer of the γ-phosphate from ATP to an NDP, with phosphohistidines as autophosphorylated intermediates. The C5 (β) and C8 (α) subunits were shown to bind ATP and to be autophosphorylated during the γ-phosphate transfer reaction (Yano et al., 1999).

Tax is phosphorylated on serines residues 300 and 301. Although phosphorylation of these residues is not required for nuclear localisation, phosphorylation of at least one of these residues is required for Tax localisation in nuclear bodies and Tax-mediated activation of gene expression via both the ATF/CREB and NFκB pathway (Bex et al., 1999). The kinase responsible for this phosphorylation is unknown. A Tax mutant which had these serines substituted for Leu-Ala (F2 mutant) displayed a slightly higher molecular weight, which is reminiscent of Tax coprecipitated with 20S proteasomes (Figure 4.5) (Bex et al., 1999). It is therefore tempting to speculate that the Tax bound to

the proteasome is dephosphorylated, although there is no direct evidence for this. As proteasome bound Tax comprises only a minority of total cellular Tax, this form of Tax would not be detected in total lysates (Figure 4.5).

This hypothesis raises the question whether Tax dephosphorylation is a prerequisite for, or perhaps a result of, the binding of Tax to the proteasome, and in general, whether the phosphorylation states of Tax and proteasome subunits determine the strength of the interaction. Also, does the NDP kinase activity of the 20S proteasome play a role in Tax phosphorylation or dephosphorylation or does Tax have an as yet uncharacterised kinase activity and modulate the activity of the 20S proteasome by influencing its phosphorylation pattern?

Mechanism of Tax mediated upregulation of proteasome activity

Although the efficiency of immunoprecipitations is unknown, a comparison of the amount of Tax detected in proteasome immunoprecipitates with the amount detected in whole cell lysates indicated that only a small proportion of the total amount of Tax is bound to proteasomes (Figures 4.5). Reciprocally, proteasome proteins were not detected in Tax immunoprecipitates (Figure 4.6), which could reflect either an incompatibility of antibody binding of Tax with proteasome association of Tax or that the amount of co-precipitated proteasome is below the detection limit (see section 4.6). However, the notion that only a limited amount of proteasomes are bound by Tax was supported by the observation that Tax only partially colocalised with nuclear proteasomes, as determined by confocal microscopy (Figure 4.7).

This brings us to the question how a limited amount of Tax may lead to the 1.3-2 fold increase of cleavage of two different fluorogenic peptide substrates by proteasomes (Figures 4.8 & 4.9). As shown, this effect was not mediated through induction of expression of the LMP2 and LMP7 proteasome subunits (Figures 4.10 & 4.11). The fact that two different proteolytic activities (the chymotryptic and tryptic activities) within the proteasome were enhanced by Tax (Figures 4.8 & 4.9), suggests that the effect is on the whole proteasomal complex rather than on single subunits. The intimate contacts seen

between adjacent subunits in the 20S proteasome crystal structure (Groll et al., 1997) are consistent with a Tax effect being transferred to the whole structure, perhaps by inducing an altered conformation. A role for phosphorylation in this cannot be excluded. Activation might be achieved through changes in the catalytic sites or by improving the entry or translocation of substrates in the proteasome.

The heterodimeric proteasome regulator PA28 modifies the activity of the proteasome in a similar way by inducing a conformational change of the 20S proteasome, which results in opening of the gate(s) in the ring of α subunits (Whitby et al., 2000). This leads to easier translocation of peptides into and out of the 20S proteasome and therefore increased activity (Stohwasser et al., 2000). PA28 can dramatically enhance the cleavage of fluorogenic peptide substrates by the proteasome (Ma et al., 1992; Groettrup et al., 1995; Song et al., 1996; Song et al., 1997). For instance, PA28 has been reported to enhance proteasomal cleavage of the chymotryptic suc-LLVY-mca substrate up to 200 fold, with a 100-fold increase at equimolar ratios of proteasome and PA28 (Ma et al., 1992). Unfortunately, we have not been able to carry out *in vitro* cleavage assays using purified proteasomes and Tax, to investigate this further for the Tax protein. However, the PA28 data show that it is in principle possible that a relatively small amount of Tax, and thereby activated proteasomes, would be able to lead to an overall increase in cleavage of peptide substrate in the order of 1.3-2 fold, as observed.

It is unknown whether Tax also binds and activates the 20S proteasome when it is complexed with PA28 or 19S caps. It also remains an open question whether Tax affects the assembly of proteasome complexes from its subcomplexes (20S, 19S and PA28), similar to the inhibitory affect on formation of 20S-PA28 complexes reported for HIV Tat protein (Seeger et al., 1997).

Possible role of Tax/proteasome interaction in transcriptional activation

An important remaining question is, of course, what the physiological function of the Tax/proteasome interaction may be.

As mentioned earlier, proteasomes have three important regulatory functions in the cell: the turnover of the bulk of proteins to maintain homeostasis; the recognition and degradation of proteins involved in transcription regulation, cell cycle and signal transduction processes and the proteolytic processing of proteins for presentation by the MHC class I pathway (Rock and Goldberg, 1999).

The possible role of the described interaction in the degradation of Tax and general protein degradation as well as the implications for MHC class I restricted processing and presentation of Tax and heterologous proteins are addressed in chapter 7.

Here we will address the role the Tax/proteasome interaction may play in Tax-mediated transcriptional activation. The proteasome has been implicated in the degradation of several transcriptional regulators (Ciechanover, 1994). Since Tax is involved in the activation of numerous genes (Yao and Wigdahl, 2000), the Tax/proteasome interaction may play a role in several of these cases, possibly explaining some of the pleiotropic effects of Tax.

Two well-described substrates for degradation and processing by the proteasome are IκBα and p105, respectively. The induced proteasomal degradation of IκBα by a phosphorylation and ubiquitination dependent pathway has been described in chapter 3. p105 is encoded by the NFκB1 gene and the N-terminal portion of p105 corresponds to the p50 subunit of the prototypical NFκB complex. The p50 subunit is generated by the processing, rather than complete degradation, of p105 by the ubiquitin-proteasome pathway (Fan and Maniatis, 1991; Lin et al., 1998; Orian et al., 1995; Palombella et al., 1994). These two processes, IκBα degradation and p105 processing, lead to the release and nuclear localisation of NFκB (Palombella et al., 1994). Tax has been shown to induce IκBα degradation, and NFκB release, by interacting with the IκB kinase (IKK) complex

(Chu et al., 1999; Harhaj and Sun, 1999; Jin et al., 1999) and to colocalise with NFκB in nuclear foci (Chapter 3) (Bex et al., 1997).

The interaction of Tax with the proteasome may provide additional mechanisms of NFκB activation. Tax was reported to strengthen the binding of p105 to proteasome subunit HC9, which correlated with a small stimulation of p105 processing into p50 by the proteasome (Hirai et al., 1992; Rousset et al., 1996). Now that we have shown that Tax can indeed interact with assembled 20S proteasomes and in addition upregulate its catalytic activity (Figures 4.2, 4.8 & 4.9), Tax may enhance p105 processing by both tethering p105 to the proteasome and enhancing the proteolytic activity of the proteasome. Where in the cell this may take place is unknown, as Tax is predominantly localised in the nucleus and p105 in the cytoplasm. One report has indicated that overexpressed p105 can relocate Tax from the nucleus to the cytoplasm (Pepin et al., 1994), suggesting that it may take place in the cytoplasm.

A similar mechanism may exist for IκBα. IκBα can translocate to the nucleus to remove NFκB from the DNA, thereby inhibiting transcriptional activation (Arenzana-Seisdedos et al., 1995; Arenzana-Seisdedos et al., 1997). In a Tax expressing cell the cytoplasmic pool of IκBα is quickly degraded by IKK-complex mediated phosphorylation of IκBα (Bex and Gaynor, 1998; Chu et al., 1999; Sun et al., 1994; Uhlik et al., 1998; Yin et al., 1998). The nuclear pool of IκBα is, however, protected from this induced signalling pathway, due to the cytoplasmic localisation of the IKK-complex (Rodriguez et al., 1999). Interestingly, Tax was reported to tether hypophosphorylated IκBα to proteasome subunit HsN3, via interaction with the ankyrin repeat of IκBα (Hirai et al., 1994; Petropoulos and Hiscott, 1998). This correlated with an increase in the constitutive phosphorylation and ubiquitination independent turnover of IκBα (Krappmann et al., 1996; Petropoulos and Hiscott, 1998). It was not determined in which cellular compartment this took place. It is conceivable that Tax mediates enhancement of constitutive phosphorylation and ubiquitin independent degradation of IκBα by tethering nuclear IκBα to nuclear proteasomes and stimulating proteasomal

proteolytic activity. This could deplete the nucleus of IκBα and contribute to the constitutive activation of NFκB seen in Tax expressing cells.

Chapter 5

Analysis of Tax mutants

5.1. Introduction

We were interested in determining which regions of Tax were important for the interaction between Tax and assembled 20S proteasomes. In addition, we wanted to know whether there was a relationship between proteasome binding and nuclear localisation of Tax and whether there was any correlation between proteasome binding of Tax mutants and observed transcriptional phenotypes, as had previously been suggested by others (Rousset et al., 1996).

A series of double amino acid mutations of Tax (M-mutants) had been previously characterised for their subcellular localisation and their ability to transactivate the HTLV-1 LTR (via CREB/ATF factors) or the HIV LTR (via the NFκB pathway) (Smith and Greene, 1990).

Mutants M7 ($^{29}C^{30}P \rightarrow AS$), M9 ($^{41}H^{42}R \rightarrow AS$) and M12 ($^{51}E^{52}H \rightarrow AS$) were reported to be localised in the cytoplasm and defective for activation of both types of promoters (Smith and Greene, 1990).

Tax mutation $^{137}G^{138}L \rightarrow AS$ (called M22) was first reported to selectively activate a CREB/ATF responsive promoter, without activating the NFκB responsive promoter (Smith and Greene, 1990), the reason why we chose to make this mutant. However, the described phenotype was later reported to belong to a different mutation ($^{130}T^{131}L \rightarrow AS$) (see erratum published (Smith and Greene, 1990)). The $^{137}G^{138}L \rightarrow AS$ mutation appeared to belong to the phenotype described for M20, which is inactive on both promoters. Despite the above, we kept this mutant in our analysis.

The mutant M47 ($^{319}L^{320}L \rightarrow RS$) selectively activated the NFκB responsive promoter, without activating the CREB/ATF responsive promoter (Smith and Greene, 1990).

Furthermore, mutant M9 ($^{41}H^{42}R \rightarrow AS$) had been reported to be deficient in binding to proteasome subunits HC9 and HsN3, whereas M47 showed enhanced binding to these subunits (Rousset et al., 1996).

We constructed this series of Tax M-mutants as they were most likely to give us information on proteasome binding and the role of nucleo-cytoplasmic localisation (Table 5.1). In addition to the M-mutants described above, we also made Tax mutants bearing combinations of these mutations, in order to look for compensatory effects between mutations.

Furthermore we made constructs in which the amino acids 2 to 58 of Tax were deleted (D2-58), as well as this deletion together with the M47 mutation (D2-58M47). Deletion of the N-terminus was reported to result in cytoplasmic localisation (Gitlin et al., 1991). Similarly, the F1 mutant was obtained, which was also reportedly localised in the cytoplasm (Bex et al., 1998).

Moreover, some Tax variants (C4, C5, C6 and C7) previously described to be CTL escape mutants were included in this analysis (Niewiesk et al., 1995).

5.2. Generation of Tax mutants

The Tax mutants were generated in the pJFE-Tax plasmid using the GeneEditor™ *in vitro* site-directed mutagenesis system (Promega). This system uses antibiotic selection to obtain a high frequency of mutants. Together with the annealing of the mutagenic oligonucleotide to the Tax sequence, a selection oligo is annealed to the ampicillin resistance gene present on the pJFE-Tax plasmid. Subsequent synthesis and ligation of the mutant strand links the two oligonucleotides. The selection oligo will alter the ampicillin gene on the newly synthesised mutant DNA strand in such a way that it will provide resistance to the GeneEditor™ antibiotic selection mix (GEASM). Therefore, resistance to GEASM encoded by this mutant strand will facilitate selection of the desired Tax mutation on the same strand. For more details please see the materials and methods chapter.

Tax mutants		Mutations: CP 29-30 AS	HR 41-42 AS	EH 51-52 AS	Del aa 77-97 Ins 12 aa	GL 137-138 AS	LL 319-320 RS		Expression
WT-Tax									**+**
M7		M7							+
M9			M9						+
M12				M12					+
M20						M20			+
M47							M47		+
M9M47			M9				M47		+
M12M47				M12			M47		+
M20M47						M20	M47		+
M7M12M47		M7		M12			M47		+
M7M20M47		M7				M20	M47		+
M9M20M47			M9			M20	M47		+
M12M47.1				M12			M47	T48S	+
M12DelM47				M12	Del/ins		M47		+
M12DelM20M47				M12	Del/ins	M20	M47		+
D2-58	Deletion 2-58, V59I								+ /-
D2-58M47	Deletion 2-58, V59I						M47		+ /-
F	I206M								+
F1	I206M,S113A,L128P,I257T								+ /-
C4.1	Y157M								+
C4.2	C23Y								+
C5	P30S,N100Y								+
C6	I31R								+
C7	D57N, T184N								+

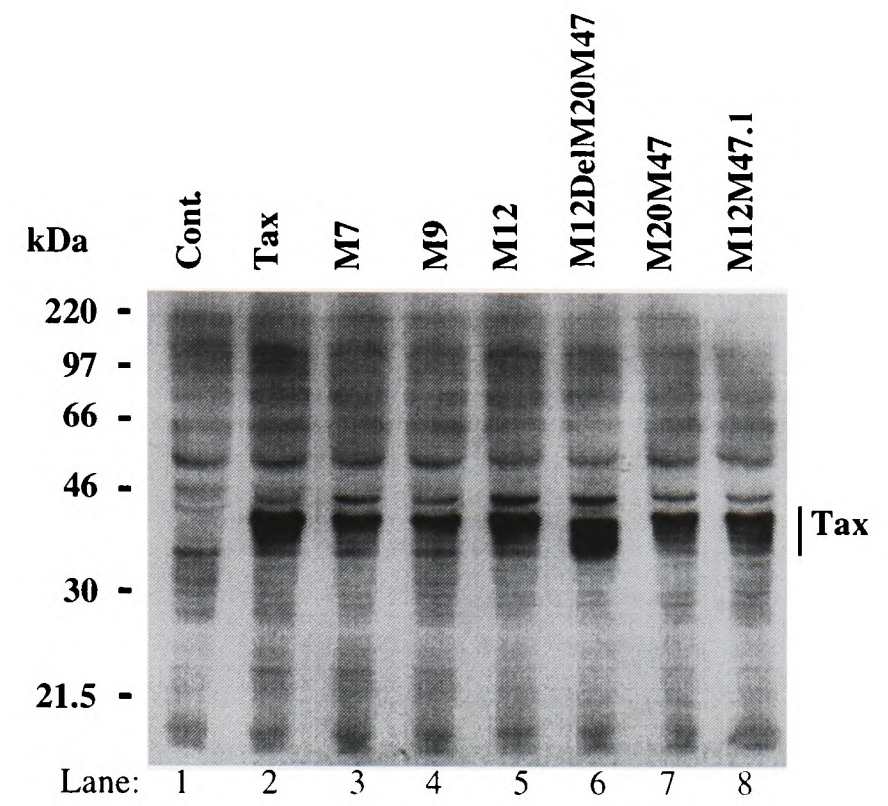
Table 5.1. Summary of mutations in Tax mutants and their expression.

All Tax mutants were constructed in the pJFE-Tax plasmid and their open reading frames completely sequenced (see appendix C). Amino acids (aa) are indicated by the single letter amino acid code. Mutations are shown in the following format: wildtype aa / aa number / new aa. For the M-mutants, the amino acid changes are shown at the top of the table and the codes (M7 etc.) were used in the columns below. For the other mutants, the changes are specified in the second column of the table. Mutants C4.1, C5, C7, F and F1 had four additional mutations compared to wild-type Tax: V109M, V172I, H232Y and E339G. Expression of the mutants was determined by Western blotting, as shown in figures 5.1 & 5.2.

The open reading frame of each mutant construct was completely sequenced. The amino acid changes present in the different mutants are described in table 5.1 and appendix C.
The Tax mutants were subsequently characterised for their expression, subcellular localisation and proteasome binding, as described in the following sections.

5.3. Expression of Tax mutants

All Tax mutants were generated in the pJFE-Tax plasmid. Expression of the mutant proteins in transiently transfected 293T cells was assessed by immunoblotting. Total lysates were separated by SDS-PAGE, blotted onto nitrocellulose and probed with a polyclonal rabbit anti-serum raised against the Tax C-terminus, which is preserved in all mutant proteins.
As shown in figures 5.1 & 5.2, most mutant proteins were expressed at levels comparable to wild-type Tax and had an apparent molecular weight indistinguishable from wild-type Tax.
However, the 2 proteins with an N-terminal deletion, D2-58 and D2-58M47, had an apparent molecular weight of around 34kDa and were expressed at lower levels (Figure 5.1, lane 15; Fig. 5.2A, lane 6). The expression of these 2 proteins was variable and their expression could not always be detected in other experiments (see Figure 5.6). The same was true for the expression level of the F1 mutant (Figure 5.6).
Due to annealing of the M12 mutagenesis oligo to a region of weak homology during mutagenesis, the mutants M12DelM47-10 and M12DelM20M47 have a deletion of amino acids 77 to 97 which is replaced by 12 other amino acids (see appendix C). This effectively disrupts the region of amino acids 77 to 99 and leaves the protein 9 amino acids shorter. Indeed, these 2 proteins appear to have a slightly higher mobility on the SDS-PA gel, indicating a lower molecular weight (Figure 5.1, lanes 6 & 12).



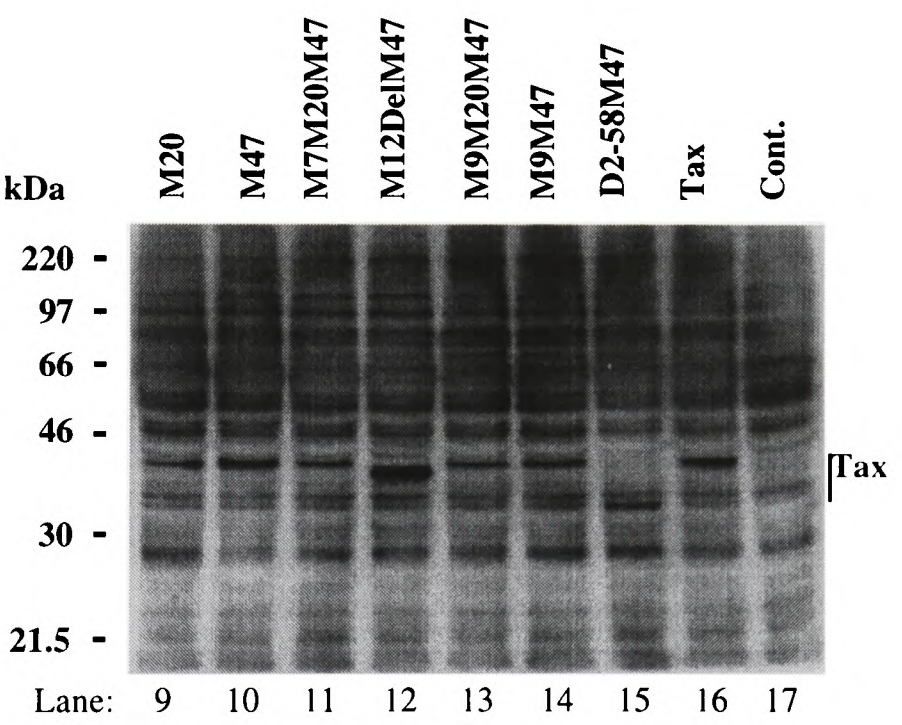


Figure 5.1. Expression of Tax mutants.

Total cell lysates of transiently transfected 293T cells were separated by SDS-PAGE, followed by a Western blot using the1135TB antiserum specific for the Tax C-terminus.

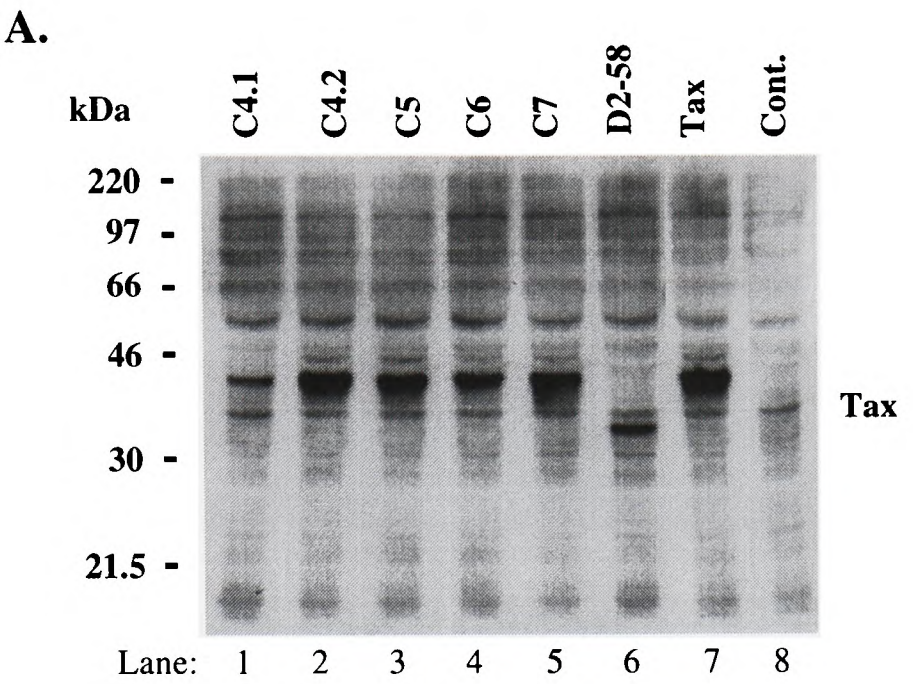


Figure 5.2. Expression of Tax mutants.

Total cell lysates of transiently transfected 293T cells were separated by SDS-PAGE, followed by a Western blot using the1135TB antiserum specific for the Tax C-terminus.

5.4. Subcellular localisation of Tax mutants

The subcellular localisation of several of the Tax mutants was determined by immunofluorescence microscopy (Figure 5.3). As shown before, wild-type Tax could be found in the nucleus, both in nuclear bodies and as more diffuse nuclear staining (Figure 5.3). The only mutant that localised, at least partially, in the nucleus was M47, which also formed nuclear bodies, presumably involved in NFκB activation (Bex et al., 1998). The N-terminal mutants M7, M9 and M12 were localised in the cytoplasm, confirming previous reports (Smith and Greene, 1990). Mutant M20 ($^{137}G^{138}L \rightarrow AS$) also failed to localise to the nucleus, thereby showing that regions outside the N-terminal nuclear localisation domain are also involved in nuclear localisation of Tax (Chapter 3, (Smith and Greene, 1992)). The double mutants (M9M47, M12M47 and M20M47) were all cytoplasmic, showing that the mutations that abrogate nuclear localisation (M9, M12, M20) are dominant (see discussion). The data on subcellular localisation of the mutants are summarised in table 5.2, where they are also compared to published data.

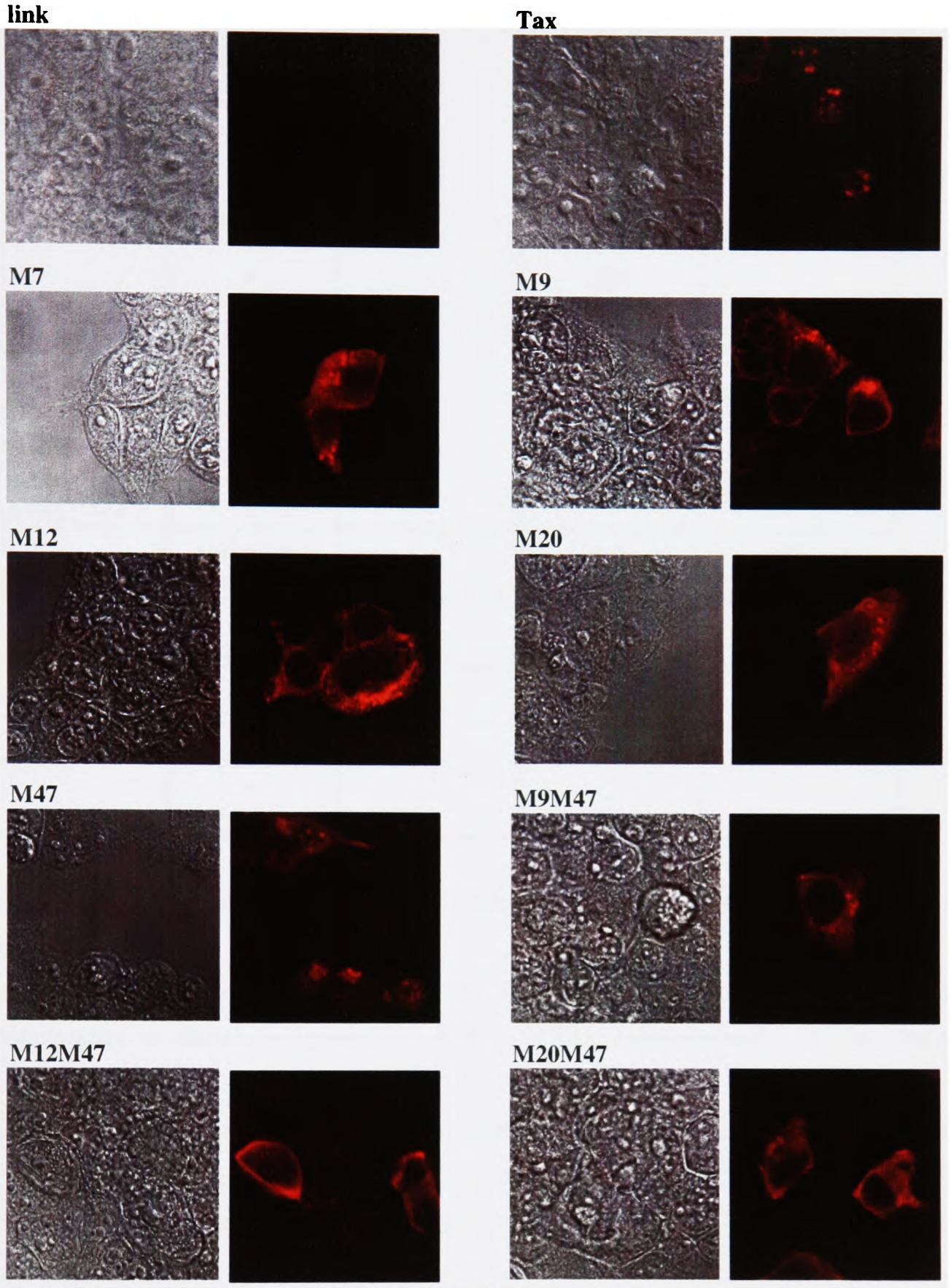


Figure 5.3. Subcellular localisation of Tax mutants.

The localisation of several Tax mutants was determined by immunofluorescence microscopy. 293T cells were fixed 48 hours post-transfection and Tax detected using a polyclonal rabbit antiserum directed against the C-terminus of Tax. For each mutant, the left panel shows a differential interference contrast picture and the right Tax detection by immuno-fluorescence.

Tax Mutant	Proteasome binding		Subcellular localisation	
	Our results	Reported (*)	Our results	Reported (**)
WT-Tax	**+**	**+**	**N**	**N**
M7	+	n.d.	C>N	C>N
M9	-	-	C>N	C>N
M12	-	n.d.	C>N	C>N
M20	+	n.d.	C>N	C>N
M47	+	+ +	N>C	N
M9M47	+		C>N	
M12M47	+		C>N	
M20M47	+		C>N	
M7M12M47	+			
M7M20M47	+			
M9M20M47	+			
M12M47.1	+			
M12DelM47	+			
M12DelM20M47	+			
D2-58	unknown		n.d.	C
D2-58M47	unknown		n.d.	n.d.
F	+		n.d.	N
F1	unknown		n.d.	C
C4.1	+			
C4.2	+			
C5	+			
C6	+			
C7	+			

Table 5.2. Summary of proteasome binding and subcellular localisation of Tax mutants.

Proteasome binding indicates the capacity of Tax mutants to co-immunoprecipitate with 20S proteasomes as shown in figures 5.1 & 5.2. +: Tax coprecipitated; -: Tax did not co-precipitate.

The subcellular localisation of Tax was determined by immunofluorescence microscopy as shown in figure 5.3. N: nuclear localisation; C: cytoplasmic localisation; N>C: more Tax was detected in the nucleus than in the cytoplasm; C>N: more Tax was detected in the cytoplasm than in the nucleus.

(*) Reported data on the binding of Tax mutants to proteasome subunits were taken from (Rousset et al., 1996).

(**) Reported data on the subcellular localisation of Tax mutants were taken from (Smith et al., 1990; Gitlin et al., 1991 and Bex et al., 1998).

n.d.: not determined

Unknown: The proteasome binding of some mutants could not be ascertained due to the variable expression of these mutants (Figure 5.6).

Clear fields: no data available.

5.5. Analysis of proteasome binding of Tax mutants

One of the chief goals of constructing the Tax mutants was to determine which regions of the Tax protein were important for the interaction with the 20S proteasome. Proteasome binding of the mutants was assessed by immunoprecipitation of 20S proteasomes with MCP21 antibody, followed by immunoblotting with anti-Tax antibody to detect co-immunoprecipitated (mutant) Tax protein. The results of these experiments are shown in figures 5.4, 5.5 & 5.6 and summarised in table 5.2.

Firstly, M9 ($^{41}H^{42}R\rightarrow AS$) and M12 ($^{51}E^{52}H\rightarrow AS$) mutants were clearly deficient in proteasome binding, implicating the Tax N-terminus in proteasome binding (Figure 5.4). The C-terminal mutant M47 ($^{319}L^{320}L\rightarrow RS$) not only maintained proteasome binding capacity as a single mutant, it was also able to compensate *in cis* for the abrogation of proteasome binding by the M9 and M12 mutations, as shown by the double mutants M9M47 and M12M47 (Figure 5.5, table 5.2 & 5.3). Maintenance of proteasome binding capacity by M7 ($^{29}C^{30}P\rightarrow AS$) and M20 ($^{137}G^{138}L\rightarrow AS$) (Figures 5.5 & 5.6), mutants localised in the cytoplasm (Figure 5.3), indicated that proteasome binding was not sufficient for nuclear localisation.

Tax mutants	HR 41-42 AS		EH 51-52 AS	21 Del 77-97 9 Ins	GL 137-138 AS	LL 319-320 RS	Proteasome binding
M12			M12				-
M12M47			M12			M47	+
M12M47.1		T48S	M12			M47	+
M12DelM20M47			M12	Del/ins	M20	M47	+
M20M47					M20	M47	+
M47						M47	+
M9	M9						-
M9M47	M9					M47	+

Table 5.3. *In cis* compensation for proteasome binding by Tax mutations.

Summary of mutations and proteasome binding of selected Tax mutants. Proteasome binding data are from figures 5.4 & 5.5. M47 compensates for M9 and M12 with respect to proteasome binding.

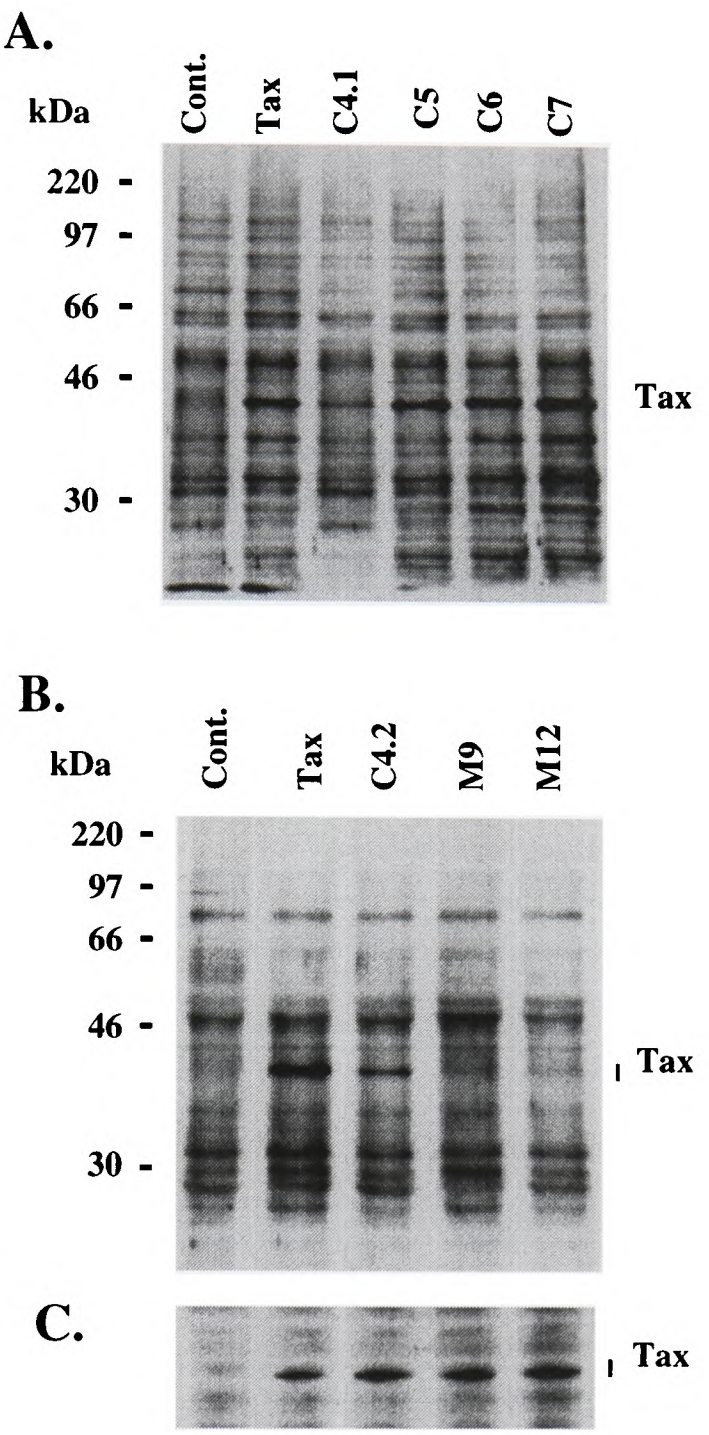
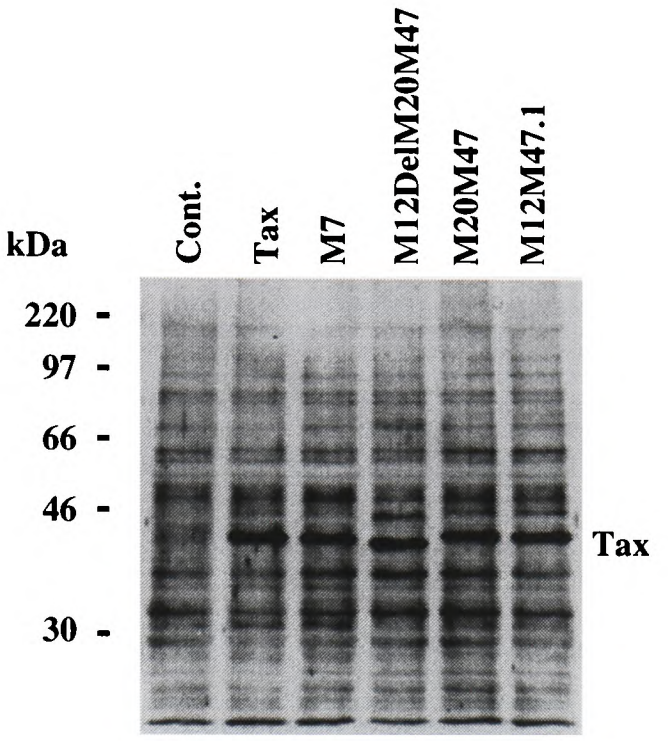


Figure 5.4. Proteasome binding of Tax mutants.

Tax mutants were expressed by transient transfection of 293T cells. **A, B.** Immuno-precipitations were performed with the proteasome specific antibody MCP21. The immunoprecipitates were subsequently separated by SDS-PAGE and Western blotted with the 1135TB anti-serum specific for the Tax C-terminus, to detect co-precipitated (mutant) Tax. **C.** Expression of mutants shown in figure B. Total cell lysates were separated by SDS-PAGE and immunoblotted with a polyclonal anti-Tax serum.



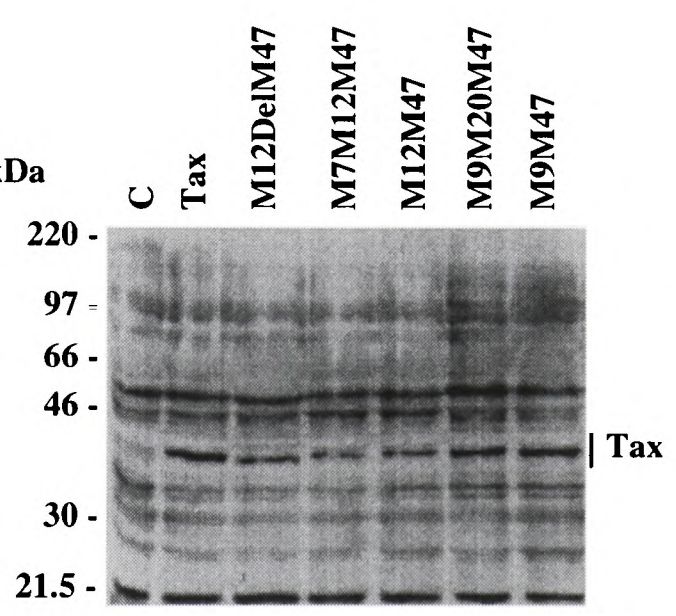


Figure 5.5. Proteasome binding of Tax mutants (continued).

Tax mutants were expressed by transient transfection of 293T cells. Immuno-precipitations were performed with the proteasome specific antibody MCP21. The immunoprecipitates were subsequently separated by SDS-PAGE and Western blotted with the 1135TB anti-serum specific for the Tax C-terminus, to detect co-precipitated (mutant) Tax.

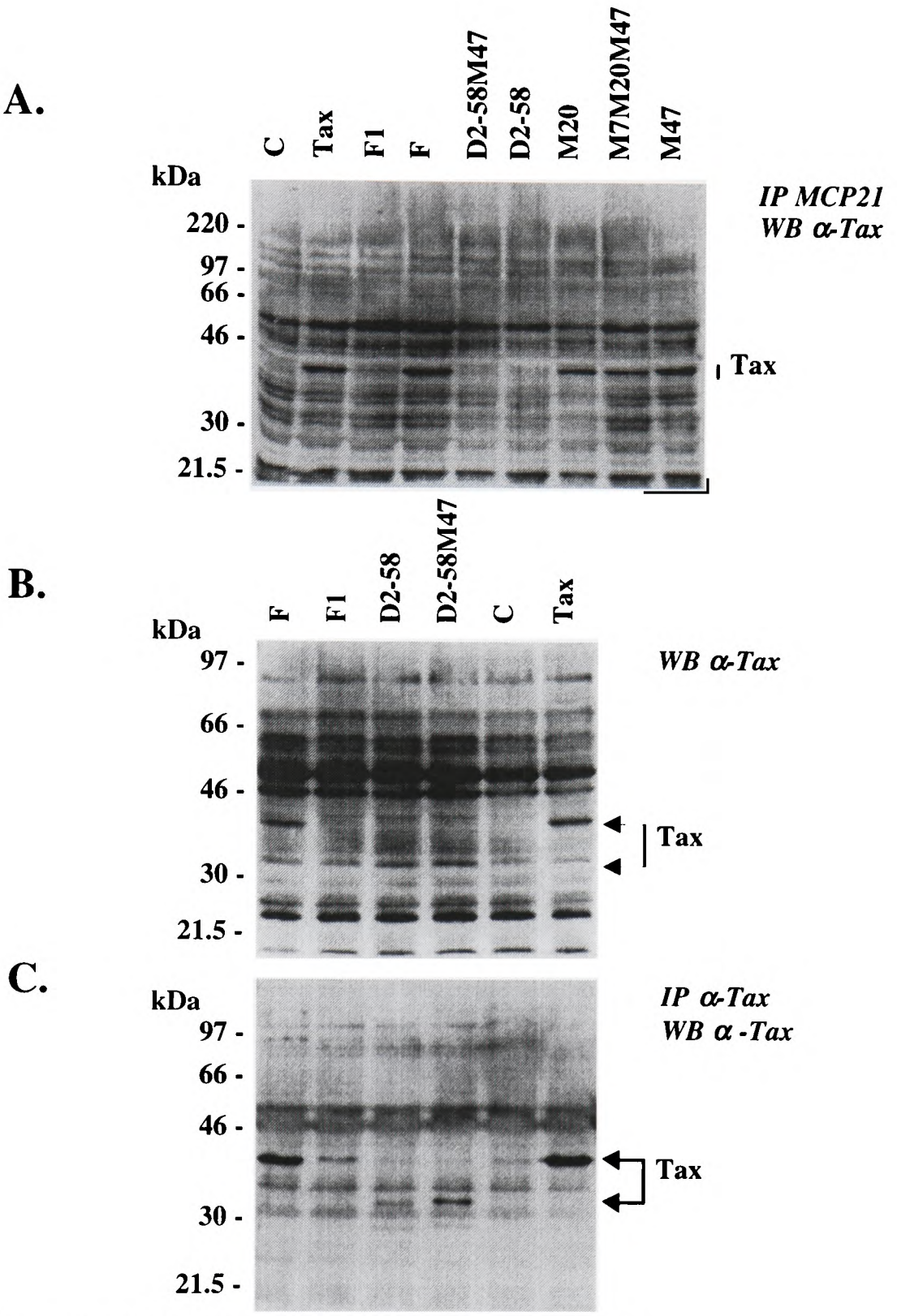


Figure 5.6. Proteasome binding of Tax mutants (continued).

Tax mutants were expressed by transient transfection of 293T cells. **A.** Immunoprecipitations were performed with the proteasome specific antibody MCP21. The immunoprecipitates were subsequently separated by SDS-PAGE and Western blotted with the 1135TB anti-serum specific for the Tax C-terminus, to detect co-precipitated (mutant) Tax. **B.** Expression of Tax mutants. Total cell lysates were separated by SDS-PAGE, blotted onto nitrocellulose and probed with an anti-Tax antibody (Y8). **C.** Immunoprecipitations were performed with the Tax specific anti-serum 1135TB. The immunoprecipitates were subsequently separated by SDS-PAGE and Western blotted with the anti-Tax antibody Y8, to detect precipitated (mutant) Tax.

However, it was noted that many mutations and combinations of mutations did not affect proteasome binding (Figures 5.4, 5.5 & 5.6, Table 5.2). For instance, mutant M12DelM20M47, carrying 3 double amino acid mutations (M12, M20 and M47) and a disruption of amino acids 77 to 97, still co-precipitated with the 20S proteasome (Figure 5.5, Tables 5.2 & 5.3). Figure 5.7 indicates all the amino acids of Tax that can be either substituted or deleted without affecting the ability of Tax to bind to 20S proteasomes. This is in contrast to the sensitivity of Tax to mutations with respect to its capacity to localise to the nucleus (Figure 5.3, (Smith and Greene, 1990)) and to transactivate promoters (Table 5.4) (Niewiesk et al., 1995; Semmes and Jeang, 1992; Smith and Greene, 1990).

Analysis of the predicted cytosolic mutants F1, D2-58 and D2-58M47 was hampered by their variable expression level (Figure 5.6). All three mutants failed to co-immunoprecipitate with 20S proteasomes (Figure 5.6A), whereas wild-type Tax and F did. However, Western blotting failed to detect expression of the mutants (Figure 5.6B) and subsequent anti-Tax immunoprecipitation indicated low-level expression of F1, D2-58 and D2-58M47 (Figure 5.6C). We can therefore not draw any conclusions about the proteasome binding capacity of these mutants.

Together, these data indicate that both the N- and C-terminus of Tax play a role in proteasome binding. The retained ability of many Tax mutants to co-precipitate with the proteasome suggested a certain degree of redundancy in proteasome binding capacity. It further appeared that proteasome binding was not sufficient for nuclear localisation of Tax. However, a full appreciation of these data will only be gained when the 3-dimensional structure of the Tax protein is known.

```
  1  MAHFPGFGQS LLFGYPVYVF GDCVQGDWCP ISGGLCSARL HRHALLATCP

 51  EHQITWDPID GRVIGSALQF LIPRLPSFPT QRTSKTLKVL TPPITHTTPN

101  IPPSFLQAVR KYSPFRNGYM EPTLGQHLPT LSFPDPGLRP QNLYTLWGGS

151  VVCMYLYQLS PPITWPLLPH VVFCHPGQLG AFLTNVPYKR IEELLYKISL

201  TTGALIILPE DCLPTTLFQP VRAPVTLTAW QHGLLPFHST LTTPGLIWTF

251  TDGTPMISGP CPKDGQPSLV LQSSSFIFHK FQTKAYHPSF LLSHGLIQYS

301  SFHNLHLLFE EYTNIPISLL FNEKEADDND HEPQISPGEL EPPSEKHFRE

351  TEV*
```

Figure 5.7. Tax amino acids dispensable and required for proteasome binding. Shown is the amino acid sequence of the Tax protein of HTLV-1. Amino acids highlighted in red can be substituted or deleted (aa77-79), either alone or in combinations, without affecting the ability of Tax to co-precipitate with 20S proteasomes (Figures 5.4, 5.5 & 5.6). Highlighted in green are the amino acids mutated in mutants M9 (^{41}H^{42}R→AS), M12 (^{51}E^{52}H→AS) and M47 (^{319}L^{320}L→RS), which appear to play a role in proteasome binding (see figures 5.4, 5.5 & 5.6 and text).

5.6 Correlation between subcellular localisation, proteasome binding and transcriptional activation of Tax mutants

For the Tax mutants for which the transcriptional phenotypes were known, the subcellular localisation, binding to 20S proteasomes and transcriptional activation properties were summarised in table 5.4. Although the sample size is small, all mutants that were active on any of the two promoter types also bound to the proteasome. However, proteasome binding did not necessarily confer transcriptional activation, as exemplified by mutants M7 and M20. All transcriptionally active mutants resided in the nucleus and all cytoplasmic mutants were inactive on both promoters. The possible implications of these correlates are discussed in the next section.

Tax Mutants	Proteasome binding	Subcellular localisation	HIV-1 LTR	HTLV-1 LTR
			Promoter activation (*)	
WT-Tax	+	N	+	+
M7	+	C>N	-	-
M9	-	C>N	-	-
M12	-	C>N	-	-
M20	+	C>N	-	-
M47	+	N>C	+	-
F	+	N	+	+
F1	n.d.	C	-	-
C4.2	+	n.d.	-	+
C5	+	n.d.	-	+
C6	+	n.d.	-	-
C7	+	n.d.	-	+

Table 5.4. Summary of proteasome binding, subcellular localisation and transcriptional activation properties of Tax mutants.

Data on the proteasome binding capacity of Tax mutants are from figure 5.4, 5.5 & 5.6. . +: Tax coprecipitated; -: Tax did not co-precipitate. Data on the subcellular localisation of Tax mutants are from figure 5.3. N: nuclear localisation; C: cytoplasmic localisation; N>C: more Tax was detected in the nucleus than in the cytoplasm; C>N: more Tax was detected in the cytoplasm than in the nucleus.

(*) Data on the activation of the HIV-LTR and HTLV-1 LTR by Tax mutants were taken from (Smith et al, 1990; Bex et al., 1998 and Niewiesk et al., 1995). +: Tax transactivation, -: no transactivation.

5.7. Summary and discussion

Summary

The transient transfection system we used for the expression of Tax protein in 293T cells allowed the generation of Tax mutants in the pJFE-Tax plasmid. In this chapter we described the characterisation of Tax mutants with respect to their expression (Figures 5.1 & 5.2), subcellular localisation (Figure 5.3) and proteasome binding (Figure 5.4, 5.5 & 5.6). Two mutations in the Tax N-terminus (M9 and M12) abrogated the ability of Tax to bind the 20S proteasome (Figure 5.4). A second mutation in the C-terminus (M47) was able to restore the proteasome binding lost by the M9 or M12 mutations (Figure 5.5, Table 5.3). Therefore, both the N- and C-terminus of Tax appear to play a role in proteasome binding. In addition it was found that several cytoplasmic mutants retained the capacity to bind to the proteasome (Figures 5.3, 5.4 & 5.5, Table 5.2). Hence, proteasome binding is not sufficient for nuclear localisation of Tax.

Compensatory mutations

N-terminal Tax mutant M9 ($^{41}H^{42}R \rightarrow AS$) had been reported to be deficient in binding to proteasome subunits HC9 and HsN3 (Rousset et al., 1996). We now confirmed that M9 is indeed deficient in binding to the assembled 20S proteasome and we found that the same applied to M12 ($^{51}E^{52}H \rightarrow AS$). Surprisingly, we found that the C-terminal mutant M47 ($^{319}L^{320}L \rightarrow RS$) not only maintained proteasome binding capacity as a single mutant, it was also able to compensate *in cis* for the abrogation of proteasome binding by the M9 and M12 mutations, as shown by the double mutants M9M47 and M12M47 (Table 5.3). The M47 mutation on its own had been reported to enhance the binding of Tax to the HC9 and HsN3 subunits (Rousset et al., 1996). It is therefore possible that both the N- and C-terminus of Tax bind to the proteasome and that the enhanced binding affinity of the C-terminal domain caused by the M47 mutation can overcome the loss of binding affinity of the N-terminal domain caused by the M9 and M12 mutations. It is

also possible that the M47 mutation affects the folding of the N-terminal domain and affects proteasome binding through an indirect effect on the N-terminal domain, rather than by a direct interaction with the proteasome. In addition, it is a possibility that the level or pattern of phosphorylation of Tax plays a role in determining the strength of the association, and that this is affected in opposite ways by the respective mutations (Bex et al., 1999)(see also Chapter 4).

Relative tolerance of Tax to mutations with respect to proteasome binding

It was remarkable that many other mutations did not affect the binding of Tax to the 20S proteasome (Figure 5.7, Table 5.2). For the double, triple and quadruple mutants, this may indicate a strong dominant effect of the M47 mutation, which is present in all of them. However, this does not apply to the M7, M20, F and C mutants. Therefore, there seems to be a degree of redundancy with respect to the capacity of Tax to associate with the proteasome, which contrasts with the sensitivity of Tax to mutations with respect to its capacity to localise to the nucleus (Figure 5.3, (Smith and Greene, 1990)) and to transactivate promoters (Table 5.4) (Niewiesk et al., 1995; Semmes and Jeang, 1992; Smith and Greene, 1990). It might be that the proteasome can recognise broad structures/folds of Tax, perhaps on the basis of hydrophobicity rather than amino acid sequence, whereas the interactions of Tax with transcription factors or a hypothetical nuclear transport receptor require more specific sequence recognition (Bex et al., 1998; Yan et al., 1998).

Proteasome binding is not sufficient for nuclear localisation

All M-mutants tested, except for M47, were localised in the cytoplasm (Figure 5.3). M47 formed the characteristic nuclear bodies, which are involved in NFκB activation (Bex et al., 1998). The N-terminal mutants M7, M9 and M12 were localised in the cytoplasm, as previously reported (Smith and Greene, 1990). It is likely that these

mutations disrupt some feature of the N-terminal nuclear localisation domain (Chapter 3, (Smith and Greene, 1992)).

Mutant M20 ($^{137}G^{138}L \rightarrow AS$) also failed to localise to the nucleus, thereby confirming that regions outside the N-terminal nuclear localisation domain are also involved in nuclear localisation of Tax (Chapter 3, (Smith and Greene, 1992)). It is unknown whether this mutation affects the conformation or accessibility of the N-terminal nuclear localisation domain or whether it directly affects the interaction with the nuclear transport receptor or a possible NLS bearing binding partner (Chapter 3 & (Smith and Greene, 1992).

The double mutants (M9M47, M12M47 and M20M47) were all cytoplasmic (Figure 5.3), showing that the mutations that abrogate nuclear localisation (M9, M12, M20) are dominant. Therefore, the M47 mutation is capable of compensating for the M9 and M12 mutations with respect to proteasome binding but not with respect to nuclear localisation. Together with the fact that the cytoplasmic mutants M7 and M20 still bound the proteasome, this indicates that nuclear localisation and proteasome binding are distinct properties of Tax, and that proteasome binding is not sufficient for nuclear localisation of Tax.

In search for correlates we summarised data on the subcellular localisation, binding to 20S proteasomes and transcriptional activation properties of Tax mutants in Table 5.4. Although the sample size was small, one could see that all mutants that were active on any of the two promoter types also bound to the proteasome. Whether proteasome binding of Tax plays a role in transcriptional activation, perhaps by inducing IκBα degradation, remains speculative (see Chapter 4). However, it was clear that proteasome binding did not necessarily confer transcriptional activation, as exemplified by mutants M7 and M20.

All transcriptionally active mutants resided in the nucleus and all cytoplasmic mutants were inactive on both promoters (Table 5.4). Tax mediated activation of transcription from the HTLV-1 LTR involves binding to members of the CREB/ATF family, thereby enhancing their dimerisation and DNA binding (Baranger et al., 1995; Perini et al., 1995;

Wagner and Green, 1993; Zhao and Giam, 1992). In addition, Tax recruits the coactivator CREB binding protein (CBP) to the transcription site in a manner independent of CREB phosphorylation (Kwok et al., 1996; Yan et al., 1998). Consequently, nuclear localisation of Tax is required for CREB/ATF mediated transcriptional activation. Therefore, it can be predicted that the Tax mutants C4.2, C5 and C7, which transactivate the HTLV-1 LTR (Table 5.4), will be localised in the nucleus.

As discussed in Chapter 3, the requirement of nuclear localisation of Tax for NFκB mediated transcriptional activation remains controversial. Tax induces increased IκBα phosphorylation and degradation by its association with the IKK complex, presumably, but not definitely, in the cytoplasm (Chu et al., 1999; Harhaj and Sun, 1999; Jin et al., 1999). Furthermore, Tax colocalised with NFκB in the nuclear bodies (Bex et al., 1997). One group reported that a cytoplasmic N-terminal deletion mutant of Tax still activated a NFκB responsive promoter (Nicot et al., 1998). On the other hand, it was shown by others that a cytoplasmic Tax mutant (F1) induced nuclear RelA expression but nevertheless failed to activate a NFκB dependent promoter (Bex et al., 1998), suggesting the need for nuclear localisation of Tax to augment nuclear NFκB. Our NFκB-active Tax proteins (WT-Tax, F and M47) were all nuclear and all inactive mutants were cytoplasmic, but they do not resolve the contradiction described above.

Chapter 6

Generation of Tax 11-19 specific CTL clones

6.1. Introduction

About 2-3% of HTLV-1 infected individuals develop an aggressive T cell tumour, adult T cell leukaemia (ATL) (Uchiyama et al., 1977), and another 2-3% develop chronic inflammatory diseases, of which the best known is HTLV-1 associated myelopathy / tropical spastic paraparesis (HAM/TSP) (Gessain et al., 1985). Ninety-five percent of infected people remain life-long asymptomatic carriers of the virus (Bangham, 2000).

HAM/TSP is a chronic inflammatory condition of the central nervous system (CNS) that results in paralysis of the legs. HAM/TSP is characterised by diffuse demyelination and mononuclear cell infiltrates in the CNS, consisting mostly of T cells. In early onset, $CD4^+$ T cells may predominate in the infiltrate, but in older lesions $CD8^+$ T cells predominate. The specificity of these infiltrating cells remains unknown (Bangham, 1993; Levin and Jacobson, 1997).

An important parameter in HTLV-1 infection is the proviral load, which generally is 10 to 100 fold higher in HAM/TSP patients than in healthy carriers (10% of PBMC in HAM/TSP patients can carry the HTLV-1 provirus) and is a strong determinant of the risk of developing HAM/TSP (Jeffery et al., 1999; Kubota et al., 2000). As a result of this higher proviral load, the anti-HTLV-1 antibody titre is typically higher in TSP/HAM patients (Lal et al., 1994).

The exact mechanism of HTLV-1 associated neurological inflammatory disease remains poorly understood. However, the existence of a strong, chronically activated CTL response which is mainly directed against the Tax protein is well established (Daenke et al., 1996; Jacobson et al., 1990, Parker et al., 1992; Parker et al., 1994). Although most

people now agree that HTLV-1 specific CTLs can be found in asymptomatic healthy carriers as well as HAM/TSP patients, there continues to be controversy about whether the frequency of HTLV-1 specific CTL is (significantly) higher in HAM/TSP patients compared to healthy carriers (Bangham, 2000; Daenke et al., 1996; Elovaara et al., 1993; Jacobson et al., 1990; Jeffery et al., 1999; Kubota et al., 1998; Parker et al., 1992; Parker et al., 1994; Ureta-Vidal et al., 2001).

Multiple MHC class I restricted epitopes have been defined in the Tax protein, spanning the whole of the protein (Daenke et al., 1996). In individuals that carry the HLA-A2 allele, the immune response is dominated by $CD8^+$ T cells that recognise the Tax 11-19 peptide (LLFGYPVYV) (Bieganowska et al., 1999; Daenke et al., 1996; Elovaara et al., 1993; Jacobson et al., 1990; Parker et al., 1992; Parker et al., 1994). The use of HLA-A2/Tax 11-19 tetramers revealed that the frequency of Tax 11-19 specific T cells was much higher than thought previously on the basis of limiting dilution analysis (LDA). The frequency approached 10% of circulation $CD8^+$ T cells in some individuals, although it was in the 1-5% range in most $HLA\text{-}A2^+$ HTLV-1 infected individuals (Bieganowska et al., 1999; Jeffery et al., 1999). It was recently shown that possession of the HLA-A2 class I allele was associated with a lower HTLV-1 proviral load and a lower risk of developing HAM/TSP (Jeffery et al., 1999), indicating a protective effect of the CTL response.

On the other hand, there is evidence that anti-HTLV-1 CTLs might contribute to the inflammation in HAM/TSP. Tax specific $CD8^+$ T cells were found in the cerebrospinal fluid of some HAM/TSP patients, sometimes at a higher frequency than in peripheral blood (Elovaara et al., 1993; Greten et al., 1998). In addition, some clones of anti-Tax CTLs were shown to secrete pro-inflammatory cytokines (IFN-γ and TNF-α) which might contribute to inflammatory demyelination processes (Biddison et al., 1997; Kubota et al., 2000). However, whether the infiltrating T cells in HAM/TSP represent HTLV-1-specific CTL remains unknown.

Tax 11-19 peptide has a very high affinity for the HLA-A2/β2microglobulin heterodimer (Parker et al., 1992) and the structure of the HLA-A2/β2m/Tax11-19 complex was among the first to be determined by X-ray crystallography (Madden et al., 1993). In addition, the structures of several T cell receptors (TCRs) in complex with HLA-A2, β2microglobulin and Tax 11-19 peptide have been determined (Ding et al., 1999; Ding et al., 1998; Garboczi et al., 1996; Hausmann et al., 1999).

T cell receptors are heterodimers of one α and one β chain. These chains are encoded by a family of gene segments that rearrange to generate the diverse TCR repertoire, estimated to consist of 10^{14} different sequences. α chains are formed by the joining of Vα and Jα segments to the Cα constant region. β chains are formed by the joining of Vβ, Dβ and Jβ segments to the Cβ constant region. The TCR chains have 3 hypervariable regions, which are located at the distal end of the molecule and are involved in recognition of the MHC/peptide complex and are therefore called complementarity-determining regions (CDRs). CDR1 and CDR2 are encoded within the (42 different) Vα and (46 different) Vβ genes, whereas the CDR3 regions are formed by the conjunction of the Vα and Jα and Vβ, Dβ and Jβ regions respectively. The joining reactions themselves generate further diversity both by removing nucleotides and by introducing non-germline bases at each junction (Davis and Bjorkman, 1988).

The resolution of crystal structures of TCR/MHC/peptide complexes (among which the TCR/HLA-A2/Tax11-19 complex) highlighted the importance of the complementarity determining regions CDR1 and, mainly, CDR3 of both the Vα and Vβ variable domains of the TCR in contacting the peptide moiety in the MHC/peptide complex. The CDR1 and CDR2 loops appeared to play a role mainly in contacting the (less variable) MHC surface (Garboczi et al., 1996; Garcia et al., 1996).

The technique developed to produce MHC/peptide complexes by refolding heavy chain and β2microglobulin around a specific peptide (Garboczi et al., 1992) has been used to make soluble tetrameric MHC/peptide complexes ("tetramers") (Altman et al., 1996). MHC/peptide complex monomers have an inherently fast dissociation rate from the T cell receptor. However, tetramerisation of these complexes resulted in a higher avidity

and consequently these tetramers were shown to bind to T cells specific for the MHC/peptide complex used (Altman et al., 1996; Whelan et al., 1999). This technology has proven very useful for the quantitation and phenotypic characterisation of cytotoxic T lymphocytes (Altman et al., 1996; Ogg et al., 1998). In addition, tetramers have been used for the rapid isolation and cloning of low frequency CTL from peripheral blood (Dunbar et al., 1999; Dunbar et al., 1998).

One of the aims of the study presented in this thesis was to determine the processes involved in the generation and presentation of epitopes from Tax for recognition by cytotoxic T lymphocytes (CTLs). Insights into these processes might help us understand the immunodominance of Tax in HTLV-1 infection (see next chapter). For this study we were in need of CTL specific for Tax epitopes. Because the Tax 11-19 epitope is so well characterised and the response against this epitope important in HTLV-1 infection, we concentrated on this epitope. Due to the variable life span and multiple specificities of the available Tax-specific CTL lines, it was desirable to obtain clones from these lines.

In this chapter we first describe the production of HLA-A2/Tax 11-19 tetramers. These tetramers were subsequently used for the characterisation of the specificity of CTL clones that were generated by limited dilution. It addition, the clones were characterised for their cytolytic activity and TCR variable domain usage. Implications of these characteristics for the role of CTL in HTLV-1 infection and inflammatory disease will be discussed.

6.2. Production of HLA-A2.01/β2m/Tax11-19 tetramer complexes

HLA-A2/Tax11-19 tetramers were produced essentially as firstly described by Altman and colleagues (Altman et al., 1996). HLA-A2.01 heavy chain and β2microglobulin (β2m) were overexpressed in *E.coli*. Both insoluble proteins, in inclusion bodies, were purified from the cell debris and resolubilised overnight in buffer containing 8M urea. The purity of both proteins was checked on an SDS-PA gel (Figure 6.1). Subsequently, a refolding of the MHC class I complex was performed. The denaturant (urea) was removed by diluting 30mg HLA-A2.01 and 10mg β2m in a large volume of refolding buffer. Also 10mg Tax 11-19 peptide was added. The refolding buffer contained a glutathione redox couple to allow formation of the disulfide bonds in the heavy chain and β2m. The refolding was allowed to proceed for 48-72 hours under gentle stirring at 4°C. After this time the refolding mixture was concentrated and the buffer exchanged for a buffer suitable for the biotinylation reaction. The HLA-A2 heavy chain expression construct had been modified in such a way that a 15 amino acid peptide recognition sequence (LHHILDAQ**K**MVWNHR) for the BirA enzyme was added to the C-terminus of the heavy chain. During the biotinylation reaction the BirA enzyme covalently linked a biotin group to the single lysine within the BirA substrate peptide (Altman et al., 1996; O'Callaghan C et al., 1999). The refolded, biotinylated complex was subsequently purified over gel-filtration and ion-exchange columns (Figure 6.2). Biotinylation of the MHC class I complex was confirmed by ELISA, before the complexes were tetramerised with extravidin-phycoerythrin (Figure 6.2). Because the biotin moiety is attached to the C-terminus of the MHC/peptide complex, this also serves to correctly orient the MHC/peptide complexes, as the site recognised by the TCR involves the N-terminal domain of the MHC-peptide complex (Altman et al., 1996; O'Callaghan C et al., 1999). The fluorochrome (phycoerythrin; PE) enabled us to detect T cells bound by the tetramer by FACS analysis.

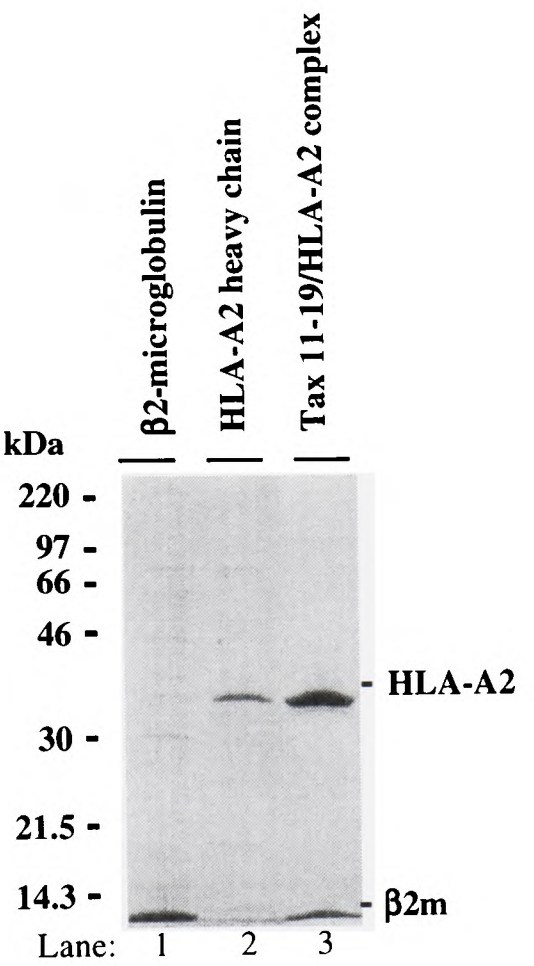
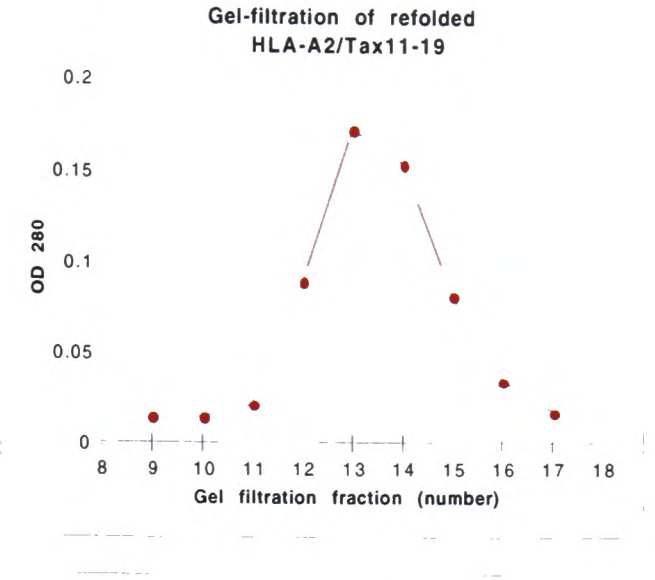


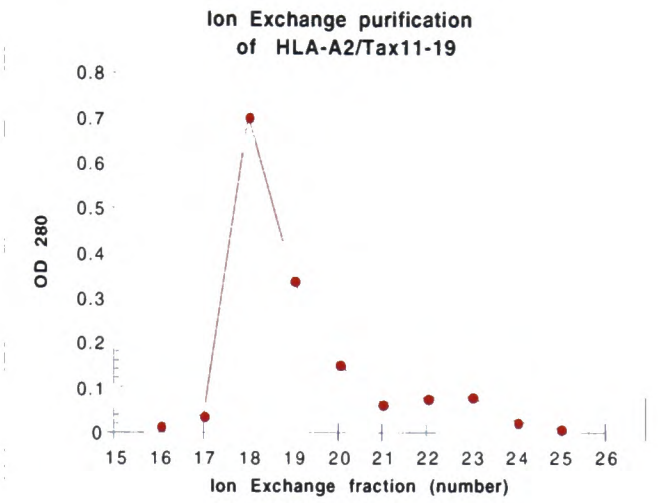
Figure 6.1. Purity of HLA-A2 heavy chain, β2m and HLA-A2/Tax11-19 tetramer complexes.

Purified proteins separated by SDS-PAGE and stained with Coomassie Brilliant Blue. Lane 1: purified β2microglobulin; lane 2: purified HLA-A2 heavy chain; lane 3: purified HLA/2m/Tax11-19 complex.

A.



B.



C.

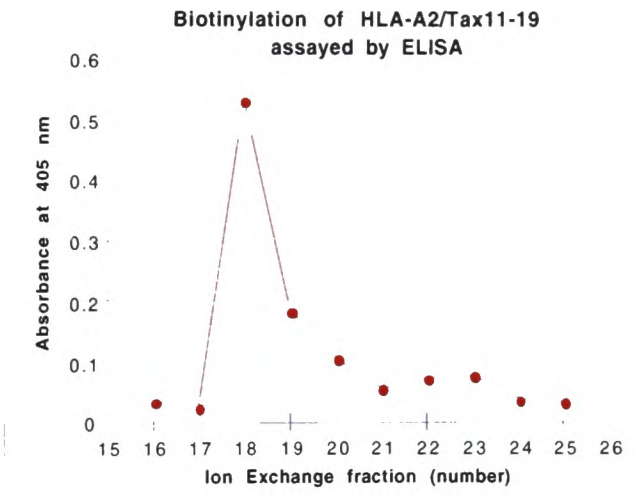


Figure 6.2. Purification of HLA-A2/Tax11-19 complexes.

A. Gel-filtration elution profile of refolded HLA-A2/Tax11-19 complex. **B.** Ion exchange elution profile of HLA-A2/Tax11-19 complex. **C.** ELISA: Samples of ion exchange fractions were immobilised on an ELISA plate and biotinylated HLA-A2/Tax11-19 complex detected with extravidin-peroxidase conjugate and chromogenic TMB reagent. Absorbance at 405 nm was measured.

6.3. Generation of Tax 11-19 specific CTL clones from a CTL line

$CD8^+$ CTL lines derived from healthy HTLV-1 infected individual HM had previously been shown to recognise Tax 11-19 peptide in the context of HLA-A2 (Daenke et al., 1996; Parker et al., 1994). One such cell line was restimulated with irradiated mixed peripheral blood mononuclear cells (PBMCs) and a peptide-pulsed $HLA\text{-}A2^+$ EBV transformed B cell line. 10 days after the restimulation, some cells were taken and analysed by FACS, using the prepared HLA-A2/Tax11-19 tetramer and an anti-CD8 antibody. This showed that ~5% of the $CD8^+$ cells stained with the HLA-A2/Tax11-19 tetramer (Figure 6.3), indicating expression of a TCR specific for this MHC/peptide complex. This growing HM CTL line was used to try and clone Tax11-19 specific CTL in two ways.

To facilitate the cloning of HLA-A2/Tax 11-19 specific CTL we would have liked to sort the specific cells with a fluorescence activated cell sorter (Dunbar et al., 1998). However, as HTLV-1 infected cells need to be dealt with in a category 3 microbiological safety environment this was not possible. Therefore, we coated streptavidin-coated magnetic beads with our HLA-A2/Tax11-19 complexes. We then incubated cells of the HM CTL line with these coated beads and pulled out cells bound to the beads (as confirmed by microscopy) (Ogg et al., 1999). These cells were subsequently plated out, at a frequency of 1 cell/well, in 96-well plates containing a 'cloning mix' consisting of RPMI, human serum, PHA, IL-2, mixed irradiated PBMCs and peptide pulsed irradiated HLA-A2+ B cells. However, no clones grew from these plates, possibly due to overstimulation, and the induction of apoptosis, by the multimeric HLA-A2/Tax11-19 complexes.

In parallel, cells from the HM CTL line were plated out by limiting dilution in the same cloning mix and several CTL clones grew from these plates. The analysis of these cultures is described in the next section.

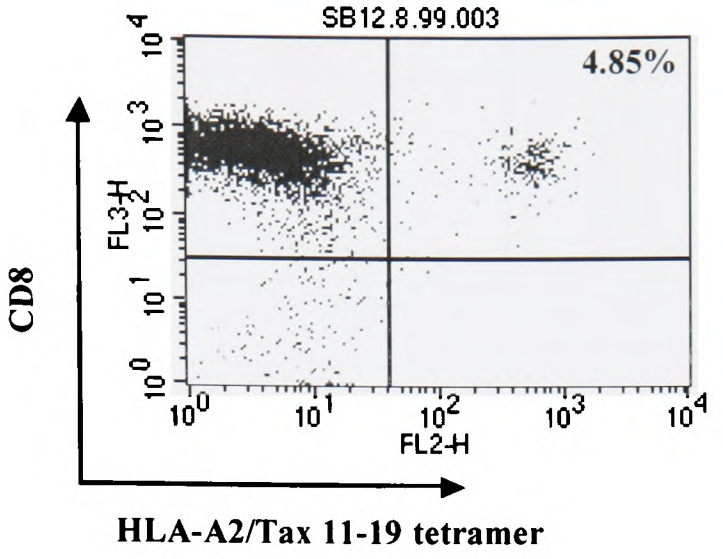


Figure 6.3. HLA-A2/Tax 11-19 tetramer staining of the HM CTL line. Cells of the HM CTL line were taken 10 days after the last restimulation and stained with the HLA-A2/Tax 11-19 tetramer (PE) and an anti-CD8 antibody (tricolour). The percentage $CD8^+$/$tetramer^+$ cells is indicated in the top right corner.

6.4. Analysis of CTL clones

6.4.1. HLA-A2/Tax11-19 tetramer staining of CTL clones

The 19 CTL cultures obtained from the limiting dilution cloning were analysed by FACS, using the HLA-A2/Tax11-19 tetramer and an anti-CD8 antibody, to assess their specificity and purity (Figures 6.4A&B). 12 out of 19 clones contained more than 70% $CD8^+$/$tetramer^+$ (see also Figure 6.5). 6 of these (A5, B2, D2, E1, E2 and E6) consisted almost exclusively (>90% $CD8^+$/$tetramer^+$) of HLA-A2/Tax 11-19 specific cells.

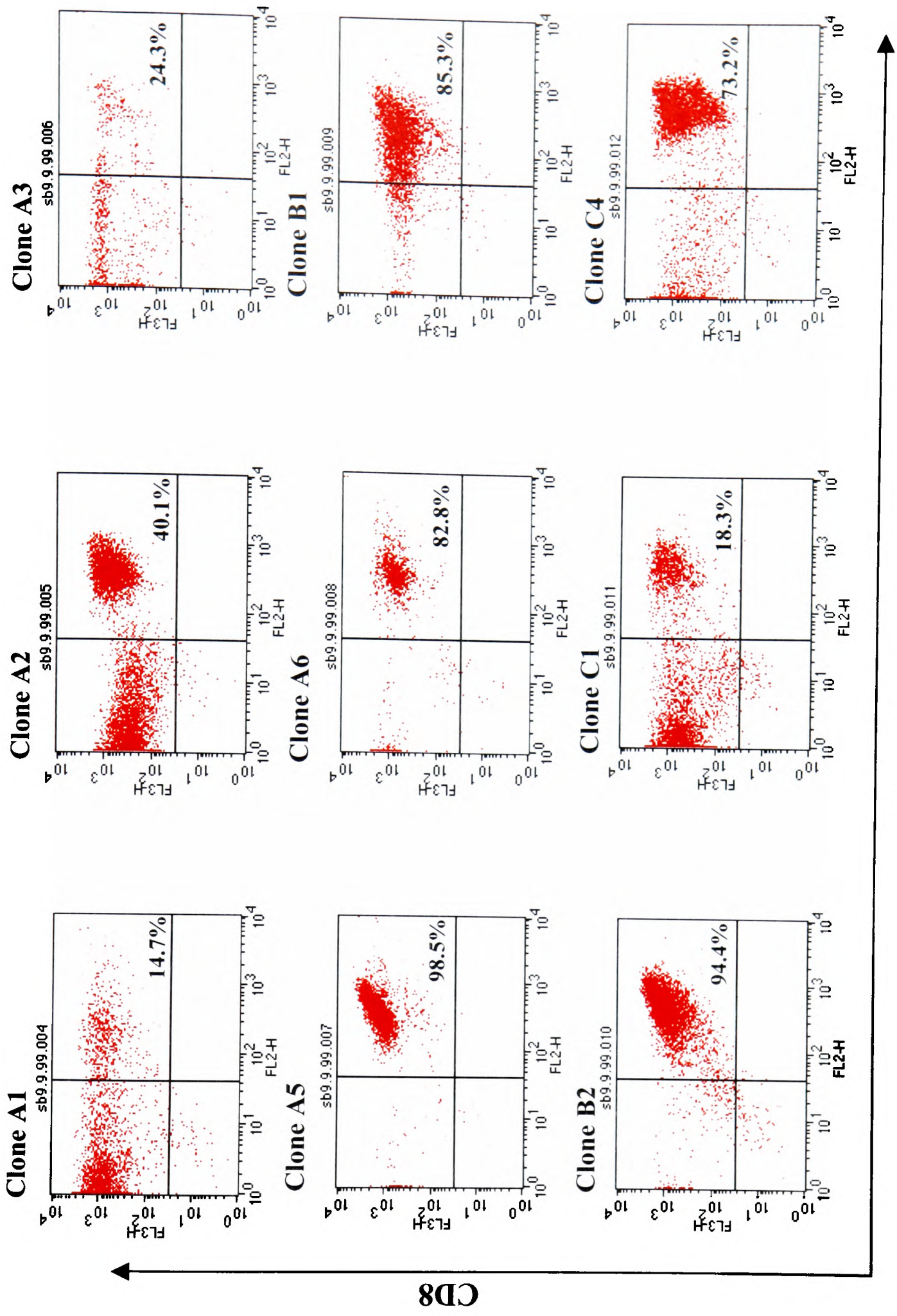


Figure 6.4A. HLA-A2/Tax 11-19 tetramer staining of CTL clones.

Cells of CTL clones were stained with the HLA-A2/Tax 11-19 tetramer (PE) and an anti-CD8 antibody (tricolour). The percentage $CD8^+$/$tetramer^+$ cells is indicated in the top right corner.

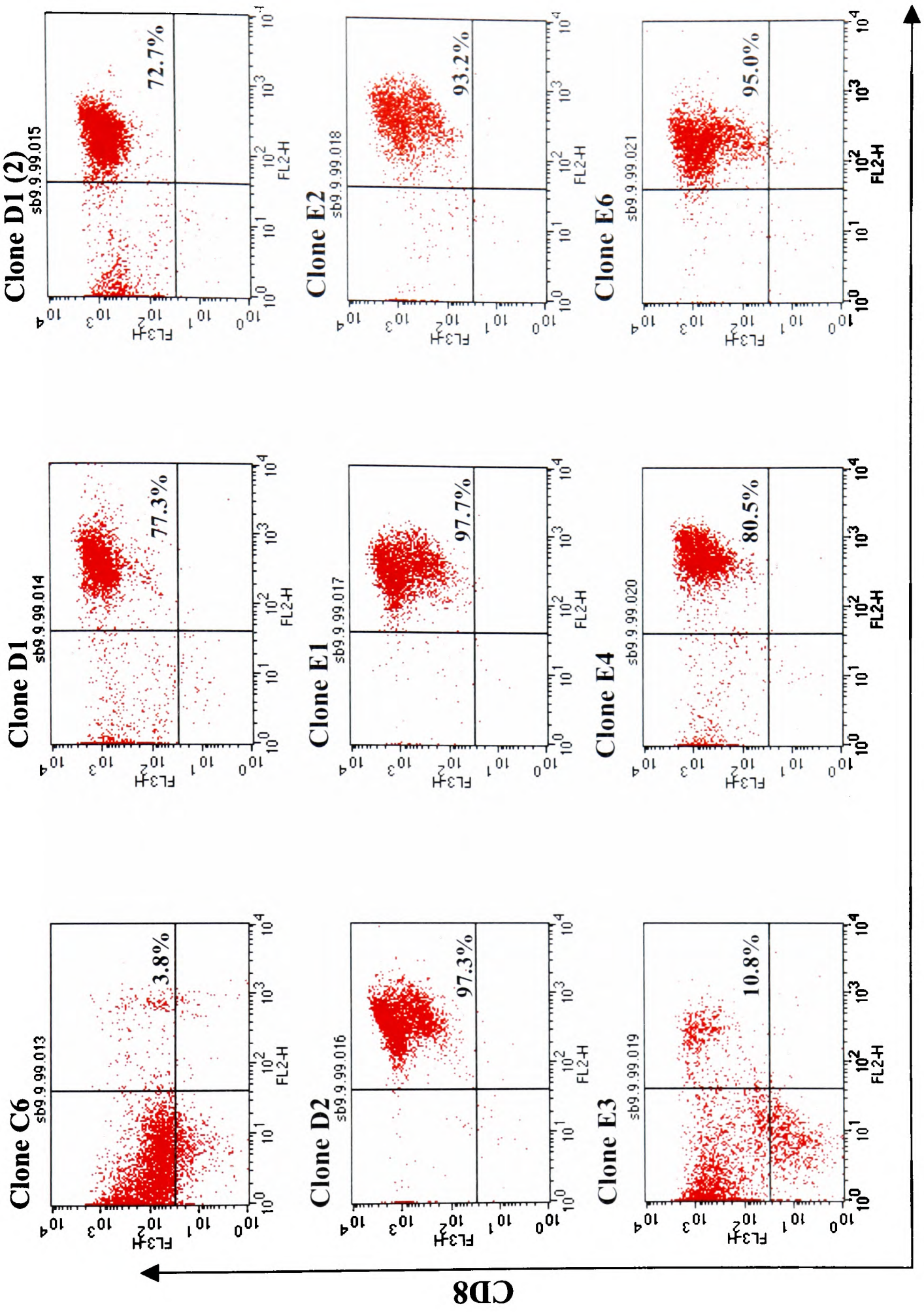


Figure 6.4B. HLA-A2/Tax 11-19 tetramer staining of CTL clones.

Cells of CTL clones were stained with the HLA-A2/Tax 11-19 tetramer (PE) and an anti-CD8 antibody (tricolour). The percentage $CD8^+$/$tetramer^+$ cells is indicated in the top right corner.

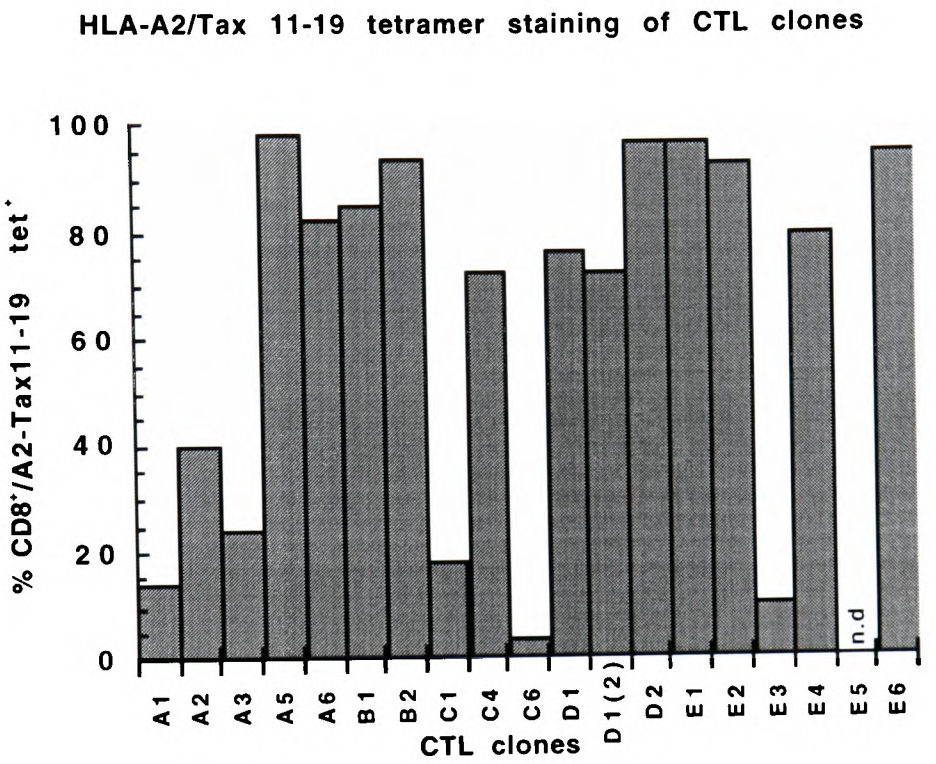


Figure 6.5. HLA-A2/Tax 11-19 tetramer staining of CTL clones. Graphic representation of the percentages of $CD8^+$/A2/Tax11-19tet^+ cells of the CTL clones. Data are from figures 6.4A & B.

6.4.2. Cytolytic activity of CTL clones

Tetramer staining gave us information about the specificity of the TCR expressed on the surface of the CD8+ cells, but did not give us any information on the activity of these cells. The ability of the clones to lyse target cells was therefore tested in a standard chromium release CTL assay, using peptide (Tax 11-19) pulsed and unpulsed autologous cells (HM B cell line) as targets. The effector to target ratio used was 5:1. Almost all tested CTL clones displayed substantial cytolytic activity towards peptide pulsed targets. 11 out of 19 cultures showed more than 24% (and as high as 63%) specific lysis with less than 5% non-specific killing. 5 others displayed more than 45% (and up to 72%) specific lysis, but also killed non-specifically at a rate of more than 5% (Figure 6.6).

All the 12 cultures that contained more than 70% $CD8^+$/$tetramer^+$ cells by FACS staining (Figure 6.5) displayed more than 45% specific lysis of peptide pulsed targets (Figure 6.6). Therefore, a good correlation existed between the tetramer positivity of the CTL cultures and their capacity to lyse target cells displaying the Tax 11-19 peptide.

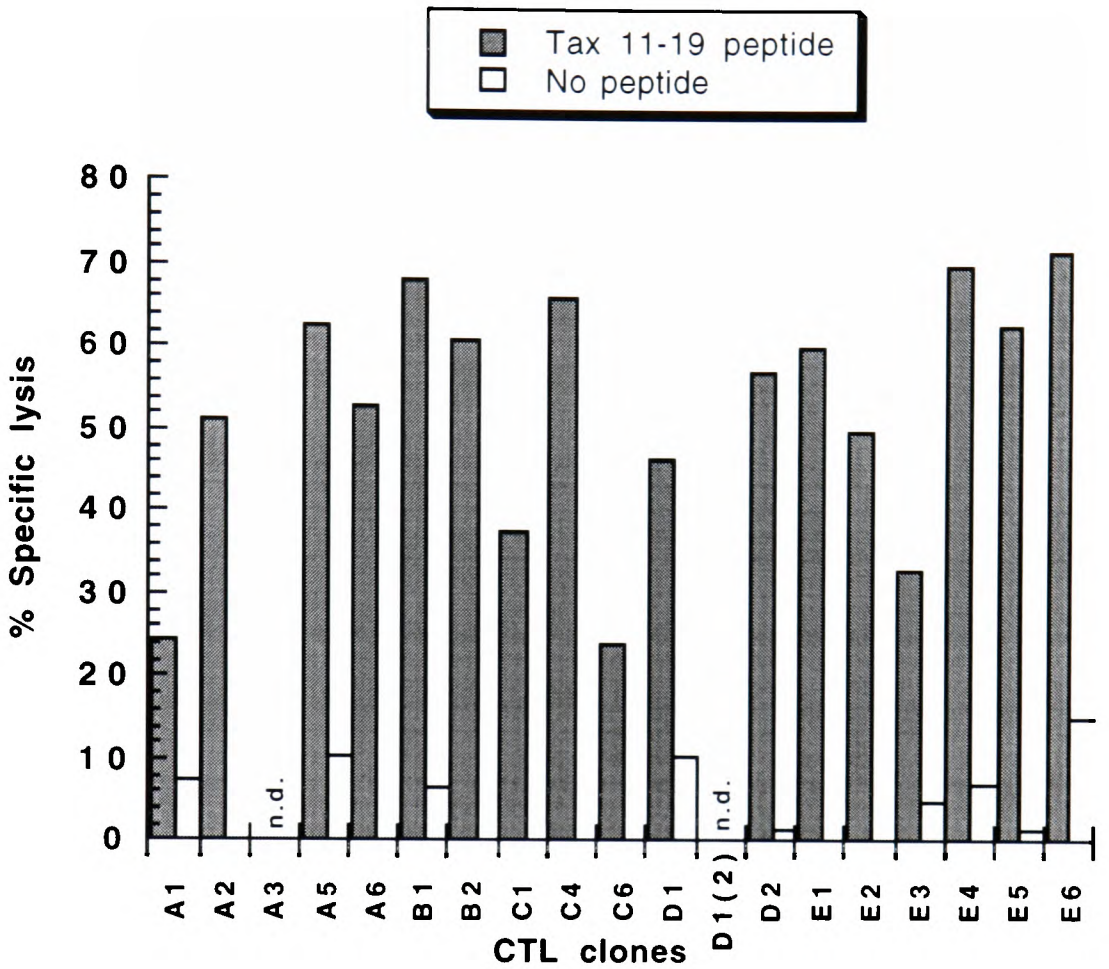


Figure 6.6. Cytolytic activity of Tax 11-19 specific CTL clones. Standard chromium release CTL assays were performed using the Tax 11-19 specific CTL clones generated (Figure 6.5.). Targets cells were peptide pulsed or unpulsed autologous BCL, as indicated. Effector to target ratio was 5:1. The percentage specific lysis after a 4 hour incubation is plotted (y-axis).

6.4.3. Characterisation of Vα and Vβ usage of two Tax 11-19 specific CTL clones

Since the vast majority of virus specific CTL from HTLV-1 infected HLA-A2-positive individuals recognise the Tax 11-19 epitope, it was of interest to define whether these CTL were dominated by a single, limited or heterogeneous set of TCRs. In addition, although tetramer staining indicated that several of the CTL clones we generated consisted almost exclusively of cells bearing TCRs specific for the HLA-A2/Tax 11-19 complex (Figures 6.4 & 6.5), this did not exclude that the cultures were comprised of more than one T cell clone, with more than one different TCR.

One rough, but relatively easy, way to determine the clonality of a T cell population, is by determining the Vα and Vβ usage within the T cell population.

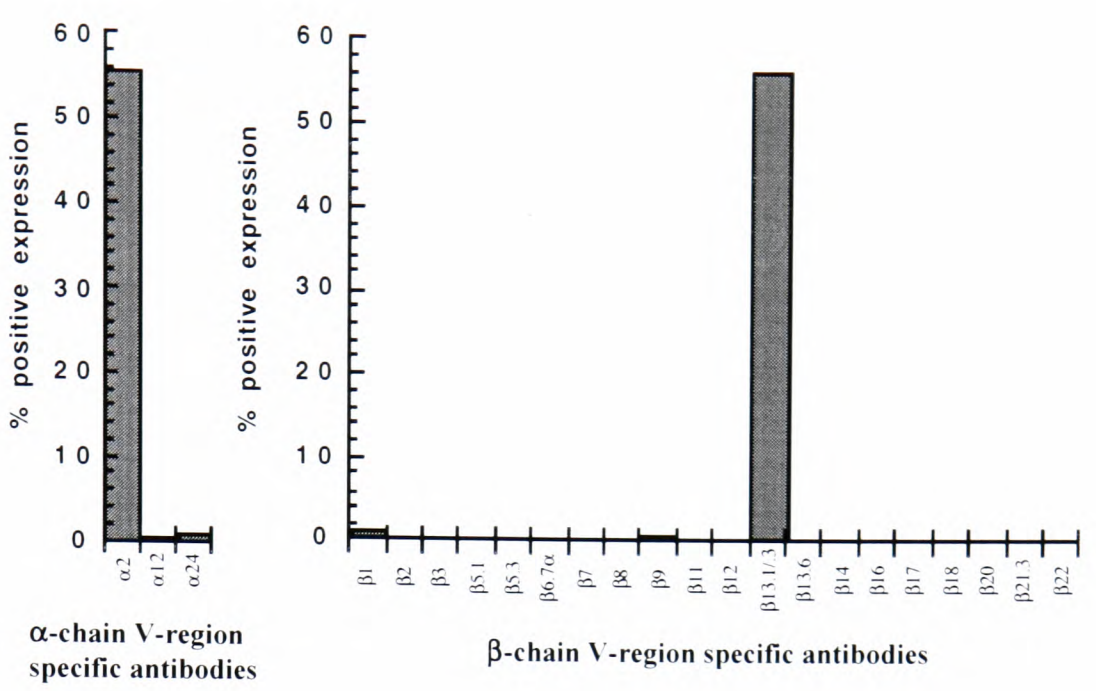
Clones E2 and E4 were chosen for analysis of the Vα and Vβ usage of their TCRs, as these clones grew well and displayed high levels of tetramer positive $CD8^+$ cells and high cytolytic activity (Figures 6.5 & 6.6). None of the other clones grew to sufficiently high number to allow such an analysis. The E2 and E4 cells were stained with an (incomplete) panel of monoclonal antibodies specific for different variable regions of the TCR α and β chains, Vα and Vβ, in order to characterise their TCRs. Results of this analysis are shown in figure 6.7.

Clone E2 (93% $CD8^+/tet^+$; 50% specific lysis) showed 56% Vα2 and 57% Vβ13-1/3 staining and was negative for all other antibodies tested. Because of the similar percentages of positivity for these chains, it seems likely that these two variable regions pair to form a functional TCR.

Clone E4 (80% $CD8^+/tet^+$; 70% specific lysis) showed 87% Vβ13-1/3 staining as well as 13% for Vβ5.3. The identity of the accompanying Vα regions remains unknown.

Therefore we concluded that both these clones, E2 and E4, were in fact mixed clones. Further implications of the Vα and Vβ usage are discussed below.

E2



E4

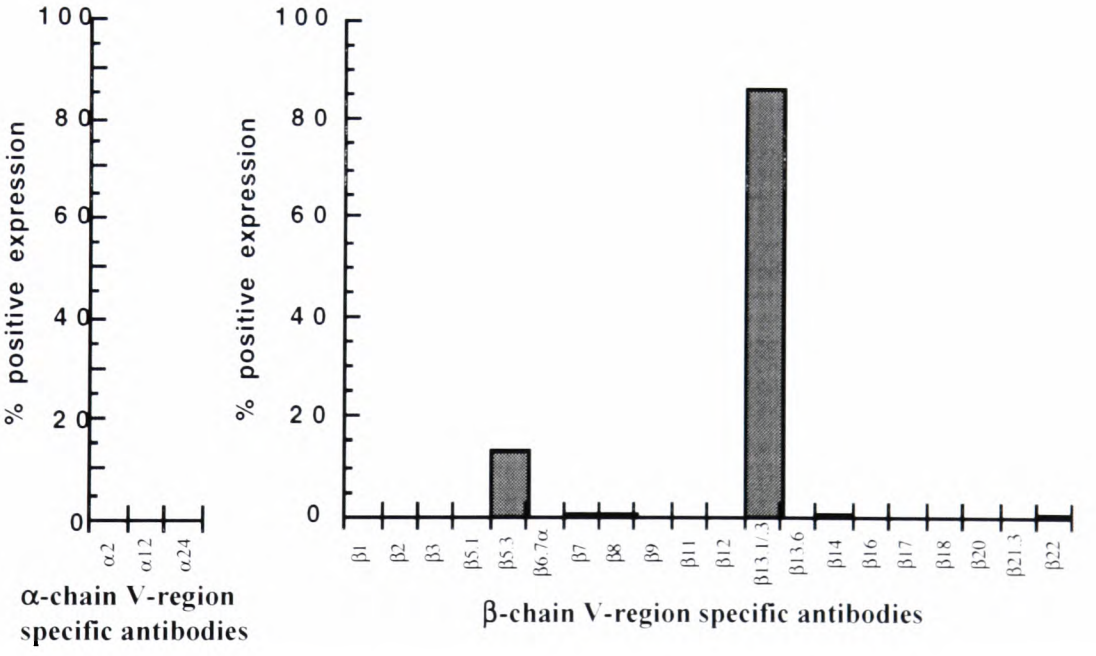


Figure 6.7. Characterisation of Vα and Vβ usage of E2 and E4 CTL clones.

Two CTL clones (E2-top panel and E4-lower panel) were analysed with a panel of monoclonal antibodies specific for Vα and Vβ segments. Cells were incubated with antibodies and analysed by FACS.

6.5. Summary and discussion

Summary

In this chapter we described the production of HLA-A2/β2m/Tax 11-19 tetramer complexes (Figures 6.1, 6.2 & 6.3) and their subsequent use for the characterisation of the specificity of CTL clones which were generated by limited dilution (Figure 6.4). In addition these clones were characterised for their cytolytic activity and TCR Vα and Vβ usage (Figures 6.6 & 6.7).

Recognition of HLA-A2/Tax 11-19 by TCRs

Several CTL clones were generated that were specific for the HLA-A2/Tax 11-19 complex and also displayed cytolytic activity towards Tax 11-19 peptide pulsed autologous targets. The capacity of HLA-A2/Tax 11-19 specific T cells to lyse (peptide pulsed) target cells is well documented (Daenke et al., 1996; Elovaara et al., 1993; Jacobson et al., 1990; Parker et al., 1994). These CTL clones proved useful in studies on the processes involved in the generation and presentation of epitopes from Tax for recognition by CTLs (see next chapter). Although TCR variable domain usage analysis revealed that at least two of these clones were in fact mixed clones, this did not matter for this purpose.

The vast majority of virus specific CTL from HTLV-1 infected HLA-A2-positive individuals recognise the Tax 11-19 epitope (Daenke et al., 1996; Elovaara et al., 1993; Parker et al., 1994). Here we tried to define the Vα and Vβ usage of the CTL clones we generated in order to see whether the Tax 11-19 specific CTL response was dominated by a single, limited or heterogeneous set of TCRs. This question has been addressed in several studies in addition to our own limited analysis (Biddison et al., 1997; Bieganowska et al., 1999; Elovaara et al., 1995; Utz et al., 1996).

We found that Vα2, Vβ13-1/3 and Vβ5.3 were used by the 2 CTL clones we analysed (Figure 6.7). Usage of the Vα2 chain (Biddison et al., 1997; Elovaara et al., 1995; Utz et al., 1996), the Vβ13-1/3 chain (Biddison et al., 1997) and the Vβ5 chain (Bieganowska et al., 1999; Utz et al., 1996) by HLA-A2/Tax 11-19 specific $CD8^+$ T cells in HAM/TSP patients have been described. The pairing of Vα2 with Vβ13-1/3 has also been reported (Biddison et al., 1997). We now confirm that these chains are also used for HLA-A2/Tax 11-19 recognition in HTLV-1 infected healthy $HLA\text{-}A2^+$ individuals (Daenke et al., 1996; Parker et al., 1994).

Oligoclonal expansion of a limited number of distinct Tax specific founder T cells has been observed in HAM/TSP patients. These T cells use various different TCR Vα/Vβ combinations between as well as within individual subjects. TCRs with quite diverse V-region combinations and no apparent amino acid sequence similarities were found to recognise the HLA-A2/Tax 11-19 complex (Biddison et al., 1997; Bieganowska et al., 1999; Elovaara et al., 1995; Utz et al., 1996). This recognition of a single MHC/peptide complex by various distinct TCRs, indicates that the primary TCR contact residues may vary between different TCRs. The flexibility in the positioning of the CDR loops plays an important role in this. This notion has been confirmed with the crystal structures of two different TCRs complexed with HLA-A2/Tax 11-19. Although both TCRs bound in a diagonal mode, 16 out of 17 amino acids that made contacts with the HLA-A2/Tax 11-19 were different between the two TCRs (Ding et al., 1998). Furthermore, it was shown that a TCR specific for the HLA-A2/Tax 11-19 complex, could accommodate substantial amino acid changes in the peptide. However, two different clones showed major differences in specificity for several peptide residues (Ding et al., 1999; Hausmann et al., 1999). Moreover, although the overall binding of a TCR to MHC complexes with mutant peptides may be very similar, the signals generated might be very different (Ding et al., 1999). Nevertheless, this potential for crossreactivity of TCR clones may result in crossreactivity with self-antigens, lending some support to the autoimmune hypothesis for HTLV-1 induced CNS damage. This phenomenon, known as molecular mimicry, is thought to play a role in the recognition of myelin basic protein derived peptides by T cells in multiple sclerosis patients (Wucherpfennig and Strominger, 1995).

Overall, these data show that the human TCR repertoire is sufficiently diverse to allow selection of multiple different HLA-A2/Tax 11-19 specific T cell clones with completely different Vα and Vβ usage. This ability to recognise HLA-A2/Tax 11-19 through the usage of different TCRs may contribute to the immunodominance of this MHC/peptide complex in HTLV-1 infected HLA-$A2^+$ individuals.

Chapter 7

Tax and MHC class I antigen processing and presentation

7.1. Introduction

HAM/TSP patients (2-3% of infected individuals) as well as healthy carriers have a strong chronically activated cytotoxic T cell (CTL) response against the virus, which is mainly directed against the Tax protein (Daenke et al., 1996; Parker et al., 1992; Parker et al., 1994). It is still very much under debate whether the role of the CTL response in HTLV-1 infection is protective or contributing to inflammatory disease, or both (Bangham et al., 1996; Levin and Jacobson, 1997). However, it was recently shown that possession of the HLA-A2 class I allele was associated with a lower HTLV-1 proviral load and a lower risk of developing HAM/TSP (Jeffery et al., 1999), indicating a protective effect of the CTL response.

In the past, multiple MHC class I restricted epitopes have been defined in the Tax protein, spanning the whole of the protein. It was further shown that multiple epitopes of Tax can be recognised simultaneously by CTLs within an individual (Daenke et al., 1996; Parker et al., 1994). Therefore, the Tax protein appears to be very immunogenic. In individuals that carry the MHC class I HLA-A2 allele, the immune response is dominated by $CD8^+$ T cells that recognise the Tax 11-19 peptide (Bieganowska et al., 1999; Daenke et al., 1996; Elovaara et al., 1993; Jacobson et al., 1990; Parker et al., 1992; Parker et al., 1994).

HTLV-1 specific CTLs appear to be chronically activated, as indicated by the cytolytic activity of HTLV-1 specific CTLs in freshly isolated peripheral blood mononuclear cells. These CTL are mainly directed against the Tax protein and their chronic activation implies that they have recently been exposed to antigen (Daenke et al., 1996; Parker et al., 1992; Parker et al., 1994). In addition, antibodies recognising Tax (and Rex) can be

found (Lal et al., 1994). These immunological data indicate that there is chronic expression of the Tax protein. In line with this, the only viral mRNA that is reproducibly found in peripheral blood mononuclear cells of infected people is the doubly spliced mRNA encoding Tax and Rex proteins, which is the first viral mRNA to be produced in an infected cell (Kinoshita et al., 1989). More recently, direct evidence was obtained that naturally infected cells *in vivo* are capable of expressing the Tax protein. It was shown that a large proportion of HTLV-1 infected PBMCs (10-80%) isolated from infected individuals became positive for Tax protein after only 6 hours of cultivation *in vitro*, as determined by a sensitive flow cytometric technique (Hanon et al., 2000). These cells were mostly $CD4^+$, but, surprisingly, also HTLV-1 infected and Tax expressing $CD8^+$ cells were detected (Hanon et al., 2000). In addition, evidence was provided that $CD8^+$ lymphocytes rapidly killed autologous Tax-expressing $CD4^+$ and $CD8^+$ cells by a perforin-dependent mechanism (Hanon et al., 2000; Hanon et al., 2000). It therefore appears that Tax expression in HTLV-1 infected cells continuously stimulates Tax specific CD8+ T lymphocytes, which subsequently efficiently destroy those Tax expressing cells.

Presentation of peptide epitopes on the cell surface of an infected cell for recognition by $CD8^+$ T lymphocytes is performed by MHC class I molecules (Germain, 1994; Rammensee et al., 1993; Townsend et al., 1986). The presented peptides (8-11 amino acids long) are generated by the degradation of endogenously synthesised proteins (Townsend et al., 1988; Townsend et al., 1985). The multicatalytic proteinase complex called proteasome has been implicated in the degradation of most cellular proteins and the generation of the majority of the antigenic peptides (Craiu et al., 1997; Rock et al., 1994). After their generation, the peptides are transported into the lumen of the endoplasmic reticulum (ER) by the transporter associated with antigen presentation (TAP) (Kelly et al., 1992; Momburg et al., 1994; Neefjes et al., 1993; Spies et al., 1992). Inside the ER, the peptides form a complex with MHC class I molecules and β2 microglobulin and this tri-molecular complex is then transported from the ER through

the Golgi apparatus to the plasma membrane, where it is displayed for recognition by surveying CTL (Townsend et al., 1989).

It has been shown that proteasomes diffuse rapidly throughout nucleus and cytoplasm and throughout the cell during cell division (Reits et al., 1997). Changes in local distribution during the cell cycle have been reported, which correlated with time points of cyclin degradation (Amsterdam et al., 1993; Palmer et al., 1994). In general, it seems most likely that proteasomes distribute within the cell according to the location of their protein substrates within the cell (Hirsch and Ploegh, 2000).

However, recently evidence has been accumulating about the role of centrosomes, or microtubule-organizing centres (MTOCs) and promyelocytic leukaemia (PML) oncogenic domains (PODs; also know as PML bodies) as sites of proteasomal degradation of cellular proteins (Anton et al., 1999; Fabunmi et al., 2000; Fabunmi et al., 2001; Garcia-Mata et al., 1999; Johnston et al., 1998; Mattsson et al., 2001; Wigley et al., 1999).

MTOCs are localised in the cytoplasm and have a central role in nucleating the assembly of most cytosolic microtubules. PML bodies are localised in the nucleus and contain several other proteins in addition to PML, such as Sp100, HAUSP and SUMO-1. PML bodies have been implicated in many different cellular functions such as transcriptional regulation, tumorigenicity and apoptosis.

However, overexpression of a misfolded protein or inhibition of proteasome activity leads to the accumulation of aggregates of misfolded protein at the MTOCs and PML bodies. These inclusions are stable, detergent-insoluble and have been called "aggresomes". Depending on the identity of the accumulated protein it could be polyubiquitinated. Furthermore, molecular chaperones (such as Hsp70) and, importantly, proteasomes can be found to localise at these sites (Anton et al., 1999; Fabunmi et al., 2001; Garcia-Mata et al., 1999; Johnston et al., 1998; Mattsson et al., 2001; Wigley et al., 1999).

Current evidence indicates that MTOCs and PML bodies may be general sites of deposition of misfolded proteins and proteasomal degradation under basal conditions (Fabunmi et al., 2001; Garcia-Mata et al., 1999). These sites then become more visible when the system is overloaded with misfolded protein, either through overexpression of misfolded proteins, proteasome inhibition or by defects in the ubiquitin-proteasome pathway.

In addition to the role of MTOCs and PML bodies in protein degradation, there are also indications that they may be the sites of the generation of antigenic peptides for MHC class I restricted antigen presentation. Firstly, the proteasome regulator PA28, which has been implicated in antigen presentation (Groettrup et al., 1996; Preckel et al., 1999), was shown to localise to both locales (Fabunmi et al., 2000; Fabunmi et al., 2001; Wigley et al., 1999). Furthermore, interferon-γ increased the number and size of PML and PA28 containing bodies and promoted the accumulation of immunoproteasomes at these bodies (Wigley et al., 1999). It was also reported that a correlation was found between the disappearance of a misfolded protein from MTOC and PML and the surface expression of MHC class I bound peptide generated from the same protein (Anton et al., 1999). It is important to keep in mind that the nuclear envelope forms part of the ER and contains TAP transporters (Reits et al., 2000). It is therefore not necessary for peptides produced in the nucleus to be delivered to the cytoplasm before entering the ER for binding to MHC class I molecules.

As indicated above, the proteasome is held responsible for the degradation of most cytoplasmic and nuclear proteins and the generation of the majority of peptides for presentation via the MHC class I pathway (Rock and Goldberg, 1999; Rock et al., 1994). Since Tax associates with the 20S proteasome (Chapter 4 and (Rousset et al., 1996)) and is the immunodominant antigen in the CTL response mounted against HTLV-1 (Jacobson et al., 1990; Parker et al., 1994), we hypothesised that Tax might be efficiently targeted to the proteasome for degradation and concomitant peptide epitope generation. In other

words, we wondered whether efficient generation of epitopes from Tax contributed to the immunodominance of Tax in HTLV-1 infection.

As we showed that Tax stimulated the chymotryptic and tryptic activities of the 20S proteasome, we further hypothesised that Tax might affect the proteasomal generation of epitopes from heterologous (viral) proteins, by modifying the cleavage specificity of the proteasome (see Chapter 2). This could also contribute to the immunodominance of Tax, by diminishing the generation of epitopes from other antigens.

Therefore, we studied the intracellular degradation of the Tax protein and the requirements for the presentation of a Tax epitope for recognition by CTL. In addition, we studied the effect of Tax expression on the processing and presentation of heterologous proteins. Insights into these processes might help us understand the immunodominance of Tax in HTLV-1 infection.

7.2. Processing and presentation of Tax protein

7.2.1. Tax is a long-lived protein

A link between the rate of degradation of an antigen and the efficiency of presentation of epitopes to CTL had been previously suggested (Grant et al., 1995; Tobery and Siliciano, 1997; Townsend et al., 1988). As Tax associates with the 20S proteasome (Chapter 4 and (Rousset et al., 1996)) and is the immunodominant antigen in the CTL response mounted against HTLV-1 (Jacobson et al., 1990; Parker et al., 1994) it was of interest to determine the metabolic stability of the Tax protein. To this end, transiently transfected 293T cells were metabolically labelled for 1 hour and chased with unlabelled medium for various times. Tax was immunoprecipitated from the samples taken at the different time points and immunoprecipitates separated by SDS-PAGE (Figure 7.1). Autoradiography and subsequent densitometric analysis revealed that Tax was a stable, long-lived protein with a half-life of around 15 hours. Similar stability of Tax was seen in the HTLV-1 transformed cell line MT-2 (personal communication, Katie Jeffery). These results indicate that the association of Tax with the proteasome does not target it for rapid degradation.

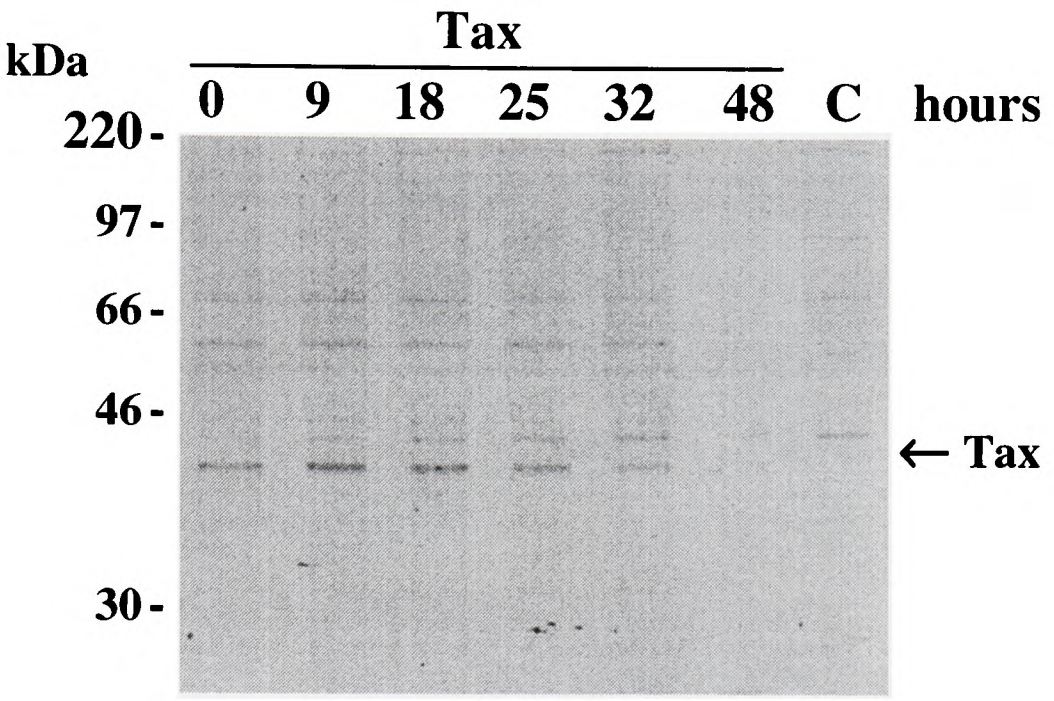


Figure 7.1. Tax is a long-lived protein.

Transfected 293T cells were metabolically labelled for 1 hour and either harvested immediately, or chased for the indicated amount of time (9, 18, 25, 32, 48 hours). Immunoprecipitations on whole cell lysates were performed with anti-Tax antibody BR-76. An autoradiograph of the immunoprecipitates separated by SDS-PAGE is shown. Densitometry performed on the auto-radiograph indicated a half-life of Tax of 15 hours.

7.2.2. Tax degradation is only marginally affected by treatment with proteasome inhibitor

The proteasome has been implicated in the degradation of short-lived as well as long-lived proteins (Craiu et al., 1997; Rock et al., 1994). As Tax associates with the 20S proteasome we wondered whether Tax degradation was performed by the proteasome. We therefore performed a pulse-chase metabolic labelling experiment similar to the one described in the previous section and incubated the cells with 50μM N-acetyl-L-leucinyl-N-leucinyl-L-norleucinal (LLnL) (Figure 7.2A). LLnL reversibly inhibits the proteasome, but also some other proteases such as lysosomal cathepsins and calpains (Bogyo et al., 1997; Craiu et al., 1997; Rock et al., 1994). 50μM LLnL had been shown to potently inhibit the degradation of long-lived proteins in several different cell lines (Craiu et al., 1997; Rock et al., 1994). In our experiment, incubation of the cells with 50μM LLnL led only to a marginal extension of the half-life of Tax from 15 hours to 16.6 hours (Figure 7.2B). However, the significance of this finding remains uncertain. Because of the long half-life of Tax we needed to incubate cells with the inhibitor for prolonged periods. As the proteasome has an essential role in cell survival (Heinemeyer et al., 1991), and high inhibitor concentrations are toxic to the cell (Schwarz et al., 2000), it was not possible to use the inhibitor at higher concentrations. Although the literature indicates that 50μM LLnL should lead to substantial inhibition of proteasome activity, this was not tested in our experiment.

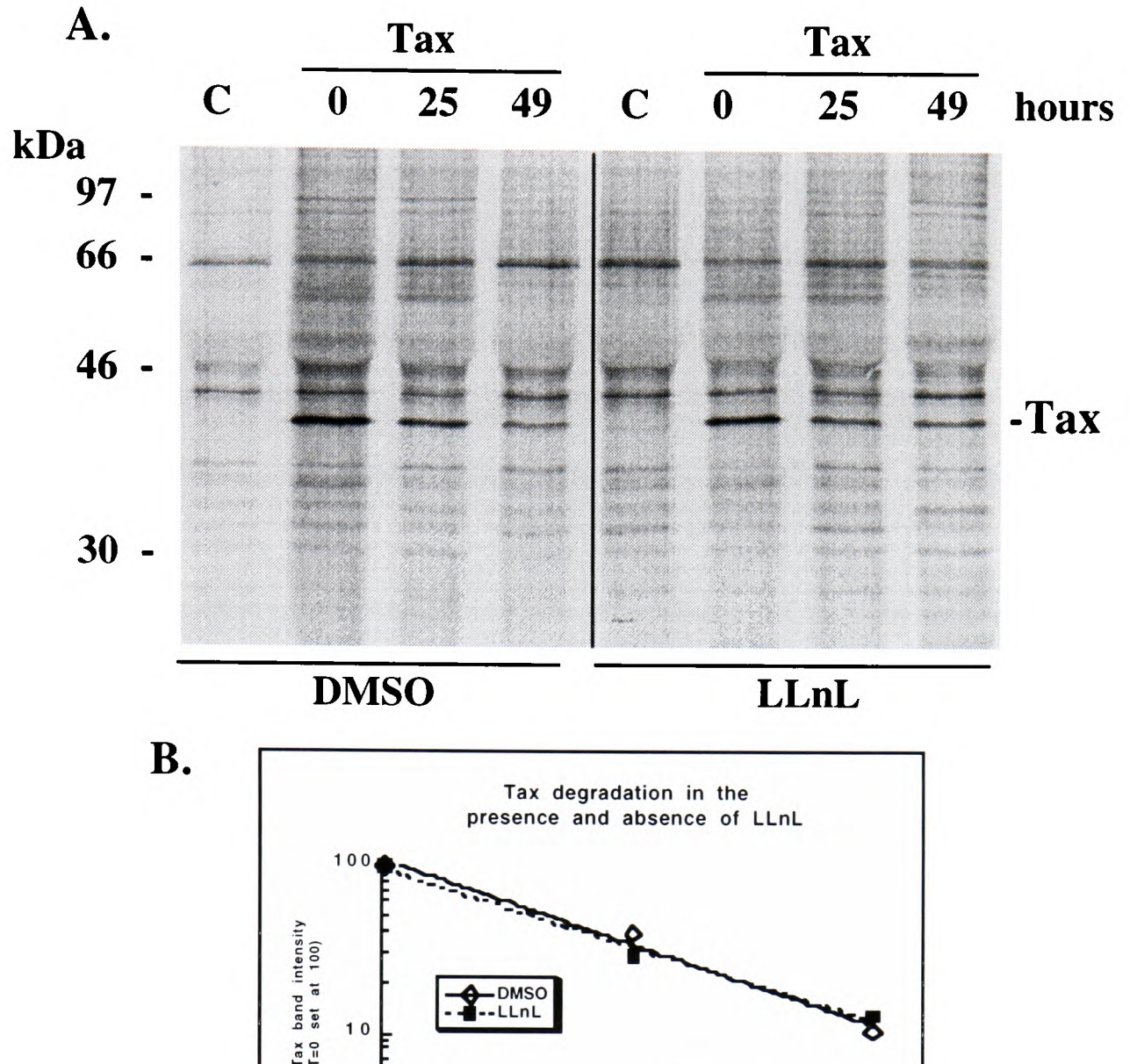


Figure 7.2. Tax degradation is not substantially affected by 50 μM Calpain inhibitor I (LLnL).

A. Transfected 293T cells were metabolically labelled for 1 hour and either harvested immediately, or chased in medium containing 50 μM calpain inhibitor I (LLnL) or DMSO control for the indicated amount of time (25 or 49 hours). Immunoprecipitations on whole cell lysates were performed with anti-Tax antibody BR-76. An autoradiograph of the immunoprecipitates separated by SDS-PAGE is shown. Tax= Tax transfected 293T cells; C= control transfected 293T cells.

B. Densitometric analysis of the gels shown in figure (A.) lead to the generation of degradation curves as shown in the graph. Band intensity at T=0 was set at 100. Calculated half-lives (T1/2) are shown in the graph.

7.2.3. Tax mobility on SDS-PAGE is affected by proteasome and isopeptidase inhibitors

Although the proteasome has been implicated in the degradation of long-lived proteins, it remains unknown whether this degradation is ubiquitin dependent (Rock and Goldberg, 1999). Ubiquitin conjugates are very difficult to detect due to the activity of deubiquitination enzymes and efficient targeting to and degradation by the proteasome (Hershko and Ciechanover, 1998).

In order to detect Tax-polyubiquitin conjugates, we incubated cells with the proteasome inhibitors lactacystin and LLnL to inhibit proteasome mediated protein degradation and added N-ethylmaleimide (NEM) to inhibit the activity of isopeptidases, among which are the deubiquitination enzymes (Schubert et al., 2000; Sharipo et al., 1998).

In a preliminary experiment we harvested treated cells immediately in SDS-sample buffer, separated the proteins by SDS-PAGE and performed a Western blot with anti-Tax antibody.

No higher molecular weight conjugates were detected, possibly due to the limited sensitivity of this method of detection. However, it was a surprise to find that, for all cell lines tested, the Tax protein displayed an upward shift in apparent molecular weight (Figure 7.3). This was the case for the 40kDa form of Tax as well as the higher molecular weight form of Tax (env-Tax) in MT-2 cells. This shift in apparent size was reminiscent of the shift in size observed for the Tax protein co-immunoprecipitated with the 20S proteasome (Chapter 4). Therefore, this Tax protein may represent the same form of Tax co-immunoprecipitated with 20S proteasomes. As discussed in Chapter 4, this Tax protein is possibly modified by phosphorylation or dephosphorylation (see also discussion). In addition, it was observed that in the MT-4(P) and MT-2 cell lines there was an increase in the (steady-state) amount of Tax detected. As mentioned before, the half-life of Tax in MT-2 cells was determined to be around 12 hours (Katie Jeffreys, personal communication). The half-life of Tax in MT-4(P) cells is not known, and may be shorter than that observed in 293T cells, similar to Tax in the HTLV-1 transformed cell line SLB (Slamon et al., 1985). Therefore, the increase in the amount of Tax detected

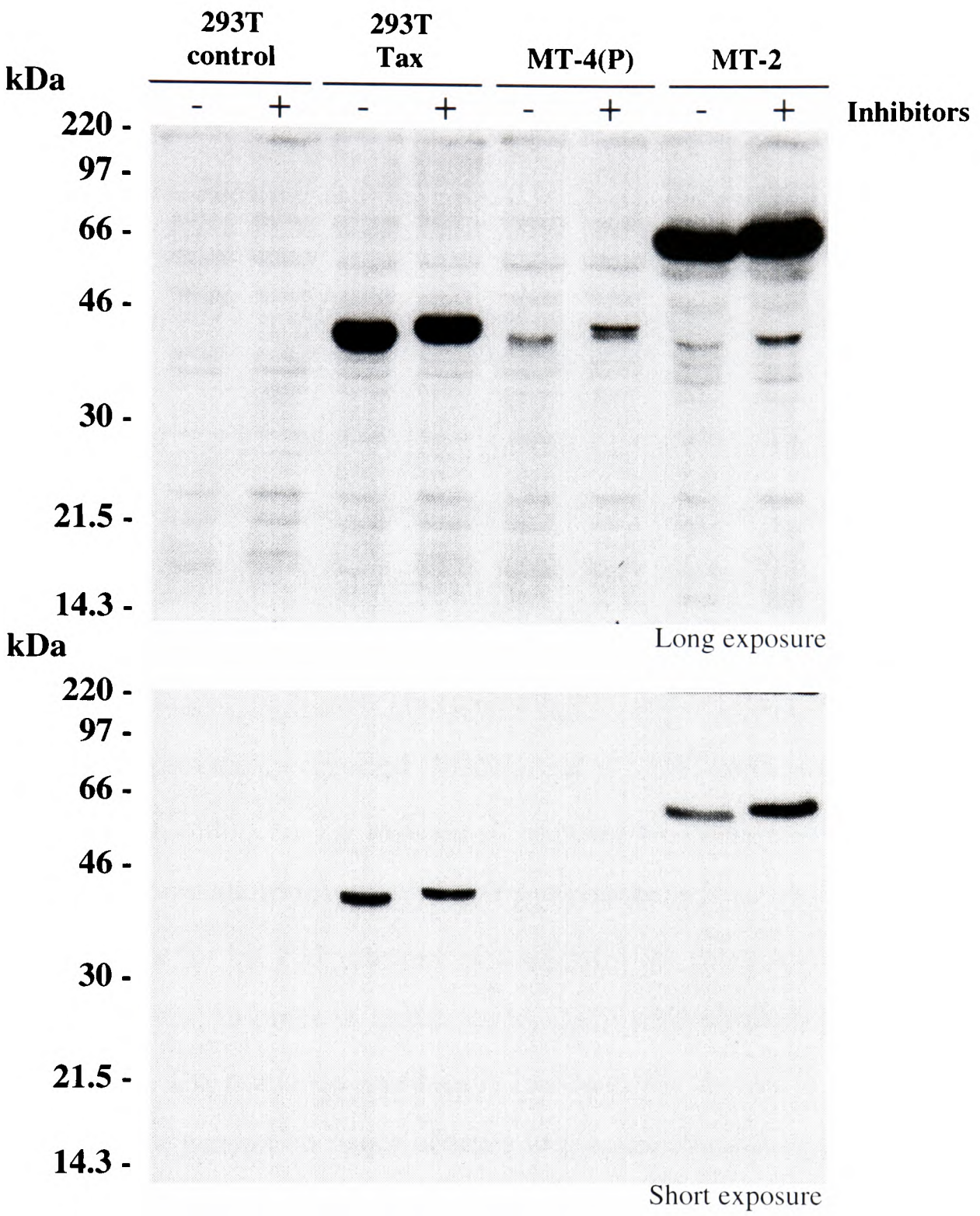


Figure 7.3. Tax mobility on SDS-PAGE is affected by proteasome and isopeptidase inhibitors

Cells were incubated for 3 hours in medium with (+) or without (-) inhibitors lactacystin (25 μM), calpain inhibitor I (LLnL; 50 μM) and N-ethylmaleimide (NEM; 5 mM). Cells were harvested directly in SDS-sample buffer (with β-mercaptoethanol). Equal amounts of protein were loaded per lane. Samples were separated by SDS-PAGE and subjected to Western blotting with the monoclonal anti-Tax antibody mAb1316. Two exposures are shown to better present differences between bands of different intensity. 293T cells were transfected with pJFE-Tax (Tax) or empty control vector (control). MT-2 and MT-4(P) are HTLV-1 infected and transformed cell lines.

the amount of Tax detected could indicate stabilisation of Tax, due to inhibition of proteasome mediated degradation in these cells.

Together, these data suggest a possible link between association with the proteasome, Tax modification and Tax degradation.

7.2.4. Tax can be recruited to PML bodies during proteasome inhibition

Overnight incubation of 293T cells with 5μM proteasome inhibitor MG132 (a regimen previously described by others (Lee and Goldberg, 1998; Mattsson et al., 2001)) led to the accumulation of proteasomes in the nucleus. In addition, the intensity of the staining increased dramatically (Figure 7.4). For comparison, the distribution and intensity of staining remained unchanged for NFκB. This redistribution and increase in the amount of proteasomes has been previously reported (Mattsson et al., 2001) and is possibly due to homeostatic mechanism leading to the increase of proteasome synthesis when misfolded protein substrates accumulate in the presence of proteasome inhibitors. The settings of the confocal microscope for MCP21 staining were adjusted for the other samples treated with proteasome inhibitor, in order to enable us to study colocalisation of proteasomes with other components. Tax remained localised in bodies in the nucleus in the presence of MG132 (Figure 7.5). In general no major changes in the distribution of proteasomes in relation to Tax were observed. However, in a minority of cells (~5%) Tax was found to colocalise with both proteasomes and PML protein in the nucleus (Figure 7.5). Only in the presence of proteasome inhibitor we observed such localisation of proteasomes inside the Tax bodies, rather than surrounding them. Proteasomes have been previously reported to localise to PML bodies, especially under conditions of proteasome inhibition, and PML bodies have been implicated in the degradation of nuclear proteins (Anton et al., 1999; Fabunmi et al., 2001; Mattsson et al., 2001). It is therefore tempting to speculate that at least some degradation of Tax takes place in these bodies.

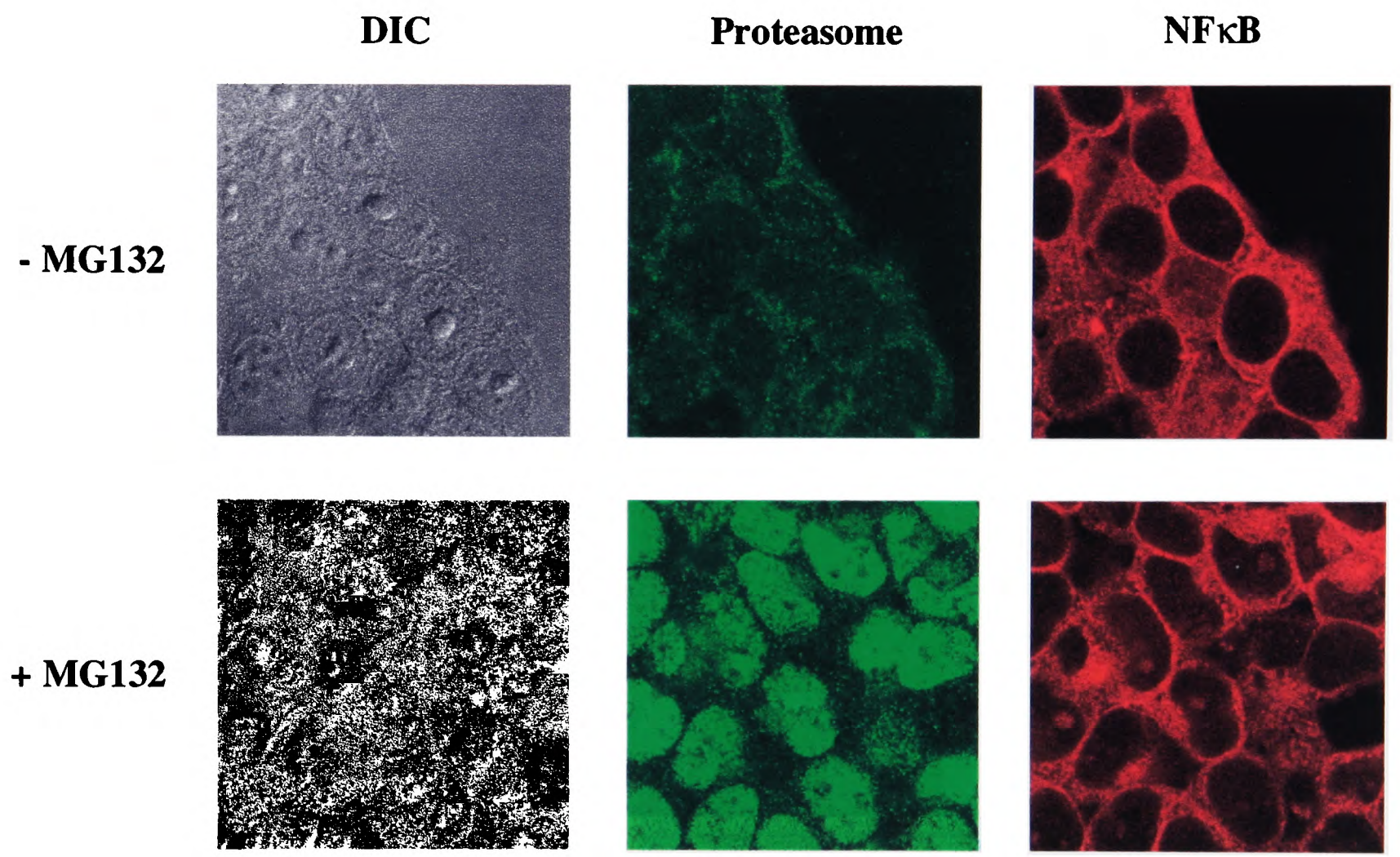


Figure 7.4. Proteasome inhibition causes nuclear accumulation of proteasomes.

293T cells were treated (or mock treated) overnight with 5μM proteasome inhibitor MG132 (Mattson et al., 2001). Cells were examined by immunofluoresence microscopy.. Proteasomes were detected using MCP21 antibody (green), NKκB was detected using a p65-specific antibody (red).

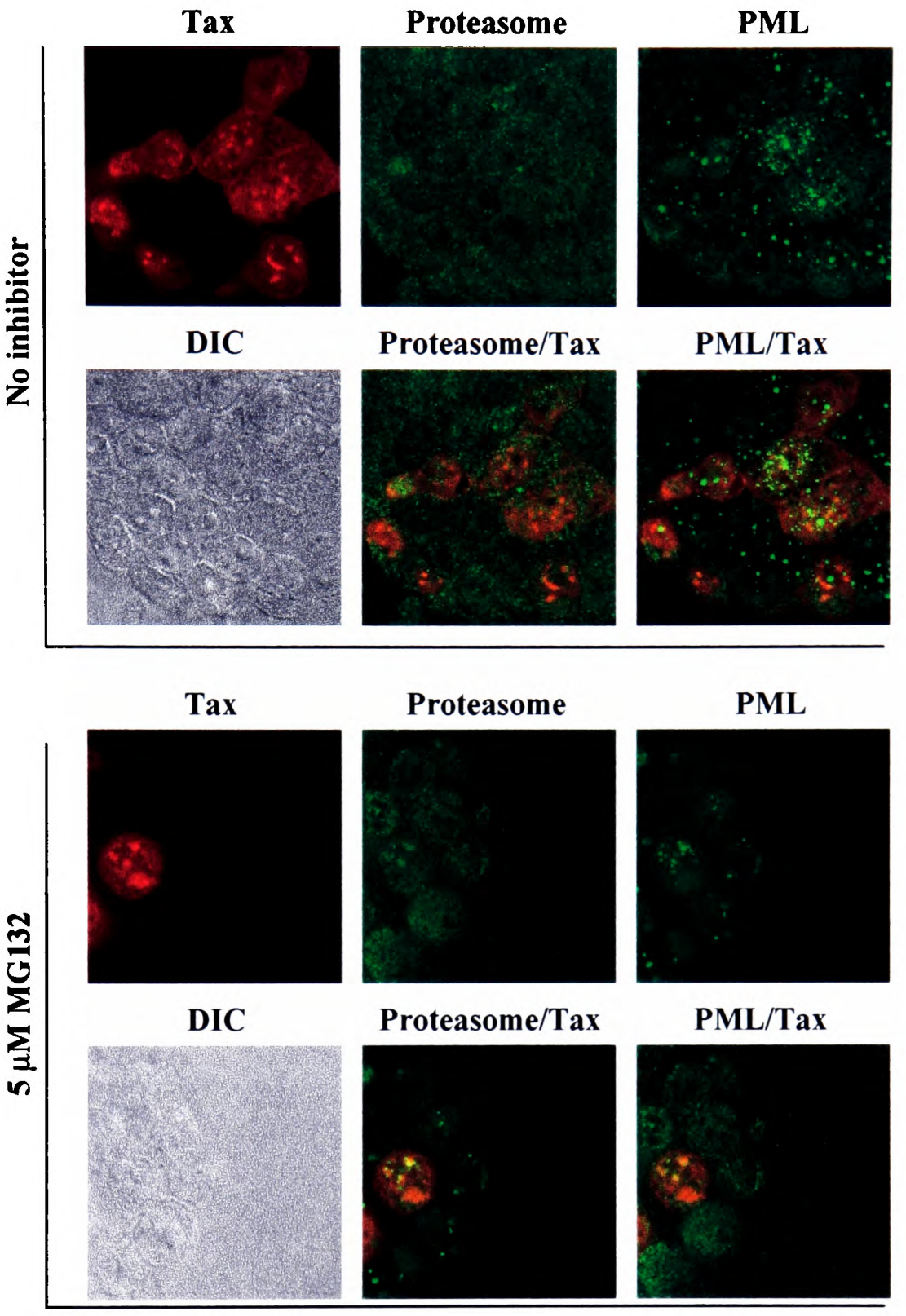


Figure 7.5. Tax recruitment to PML bodies during proteasome inhibition. Transiently transfected 293T cells were incubated overnight with 5μM MG132 or mock-treated. Shown is confocal microscopical analysis of cells. Tax was detected with a monoclonal antibody against the Tax C-terminus (red), proteasomes with MCP21 antibody (green) and PML protein with a polyclonal rabbit anti-serum (green). In the panels showing dual staining, yellow indicates overlap.

7.2.5. Tax can be found to colocalise with proteasomes in perinuclear structures

We also occasionally found Tax, in the absence of proteasome inhibitors, to be localised in perinuclear structures, in addition to the presence of Tax in nuclear bodies (Figure 7.6). Tax strongly colocalised with proteasomes in these structures (Figure 7.6). This perinuclear colocalisation was also, more frequently, observed for the cytoplasmic mutant M12 (Figure 7.6). These inclusions are reminiscent of the "aggresomes" that have been reported to form at the microtubule organising centres (MTOCs) (Anton et al., 1999; Garcia-Mata et al., 1999; Johnston et al., 1998; Wigley et al., 1999). Aggresomes are thought to consist of aggregated misfolded protein and recruited components of the proteasome machinery. Although proteasomal localisation at MTOCs has been reported to occur under basal conditions (Wigley et al., 1999), the structures increased in size when a misfolded protein was overexpressed or when the proteasome was inhibited. We may therefore observe these structures as part of normal physiology or because of protein misfolding. It remains unknown what caused these structures to form in the Tax expressing cells shown (see discussion).

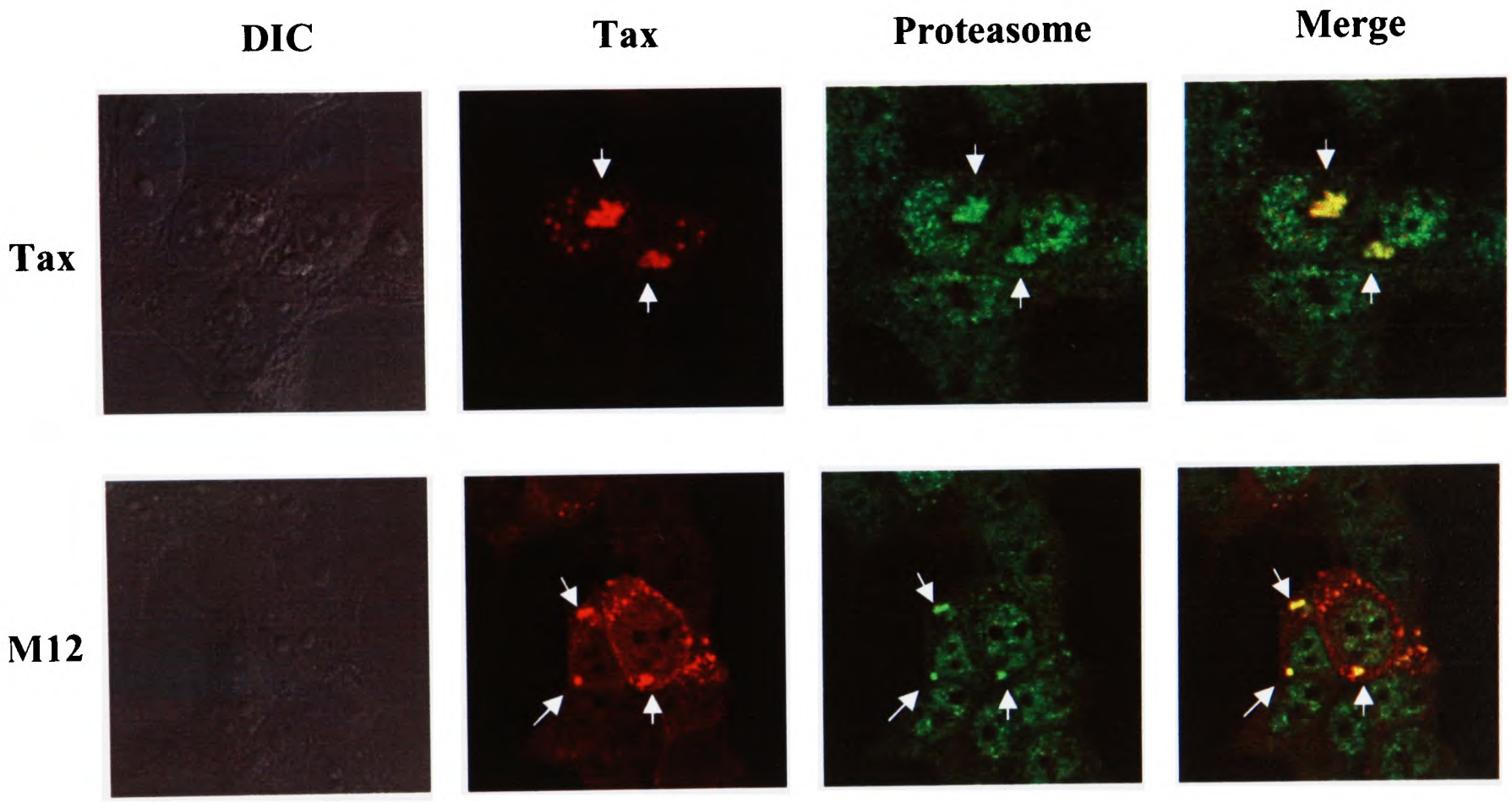


Figure 7.6. Colocalisation of Tax with proteasomes in perinuclear structures.

Confocal microscopy. Transiently transfected 293T cells were fixed 48 hours posttransfection and stained with a polyclonal rabbit anti-Tax serum (red) and the monoclonal antibody MCP21 (anti-proteasome; green). In the right panel both stainings are superimposed with overlap shown in yellow.

7.2.6. Presentation of Tax 11-19 epitope to CTL is dependent on the TAP transporter and independent of LMP2 and LMP7 proteasome subunits

Ultimately we were interested in establishing the requirements for the presentation of epitopes from the Tax protein to CTL. As discussed in the previous chapter, we chose to investigate the processing and presentation of the Tax 11-19 epitope, as it is well characterised and highly immunodominant (Chapter 6) (Bieganowska et al., 1999; Daenke et al., 1996; Ding et al., 1999; Ding et al., 1998; Elovaara et al., 1993; Garboczi et al., 1996; Hausmann et al., 1999; Jacobson et al., 1990; Madden et al., 1993; Parker et al., 1992; Parker et al., 1994; Parker et al., 1992). We used a set of different target cell lines to determine whether the presentation of the Tax 11-19 epitope was TAP dependent and whether the generation of the Tax 11-19 peptide in the cell was dependent on expression of the LMP2 and LMP7 subunits.

Figure 7.7 shows that the Tax 11-19 epitope was presented well by the wild-type B cell line 721.45. In contrast, presentation was abrogated in the cell line 721.174, which lacks the genes for both TAP1 and TAP2 and proteasome subunits LMP2 and LMP7 (DeMars et al., 1984). However, expression of both TAP subunits in this cell line (721.174/TAPs) restored the presentation of the Tax 11-19 epitope. This indicates that the presentation of the Tax 11-19 epitope is dependent on the TAP transporter and that the generation of the epitope does not require the LMP2 and LMP7 subunits of the proteasome. Expression of the LMP7 subunit in the 721.174/TAPs cell line did not further affect the presentation of the Tax 11-19 epitope.

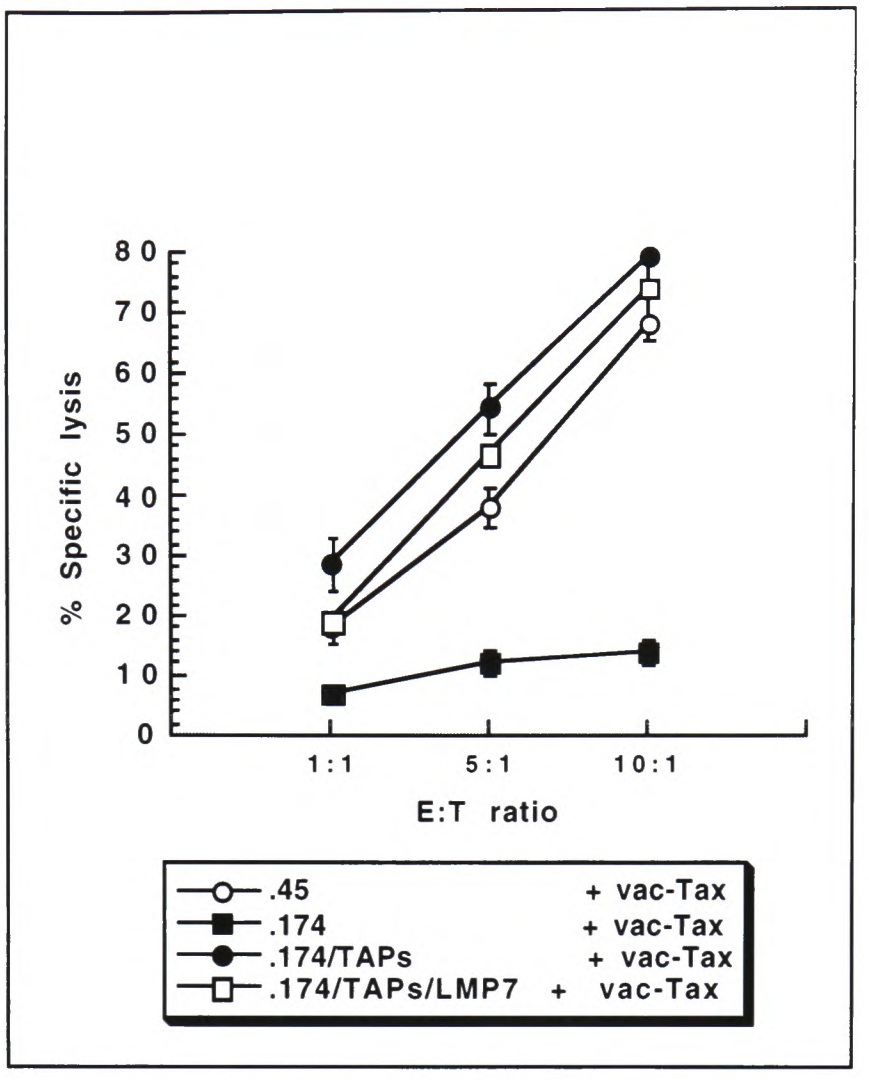


Figure 7.7. Presentation of Tax 11-19 epitope to CTL is dependent on TAP transporter, but independent of expression of LMP2 and LMP7.

Indicated target cells were infected with vac-Tax at a M.O.I. of 5 pfu/cell. Infected cells were left overnight to express Tax. The next day a standard 4 hour chromium release assay was performed using the Tax11-19 specific CTL clone E4.

Target cells:

.45: 721.45 cells (human B lymphoblastoid cell line);

.174: 721.174 cells: 721.45 derivative with only one copy of chromosome 6 containing a deletion in the class II region of the MHC locus, thereby lacking TAP1 and 2 and the LMP2 and LMP7 genes (DeMars et al., 1984):

.174/TAPs: .174 cells stably transfected with plasmids containing the human TAP1 and TAP2 genes (Cerundolo et al., 1995);

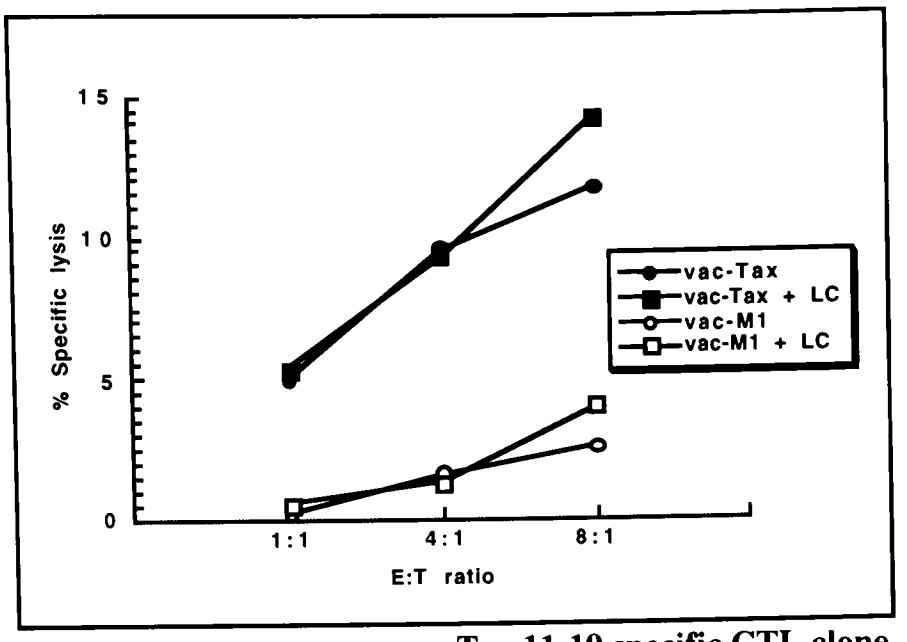
.174/TAPs/LMP7: .174/TAPs cells stably transfected with plasmid containing the LMP7b gene (Sewell et al., 1999).

7.2.7. Lactacystin does not block presentation of Tax 11-19 epitope to CTL

Although the presentation of Tax11-19 was shown not to depend on the LMP2 and LMP7 subunits (Figure 7.7), it left open the possibility that the epitope was generated by the constitutive proteasome. To investigate the role of the proteasome in the generation of the Tax 11-19 epitope, we incubated 721.174/TAPs cells with the specific and irreversible proteasome inhibitor lactacystin in a CTL lysis assay. The inhibitor was added before infection with vac-Tax and kept in the medium throughout the rest of the CTL assay. Figure 7.8A shows that incubation with lactacystin did not result in a reduction in the specific lysis by the Tax11-19 specific CTL clone, suggesting a proteasome independent mechanism of epitope generation. Although the efficiency of lysis was not very high in this experiment, an increase of specific lysis was observed with increasing E:T ratios. The same result was obtained in a separate experiment in which higher levels of lysis were observed (Figure 7.9), although for this experiment no control for the effect of lactacystin was performed (see below).

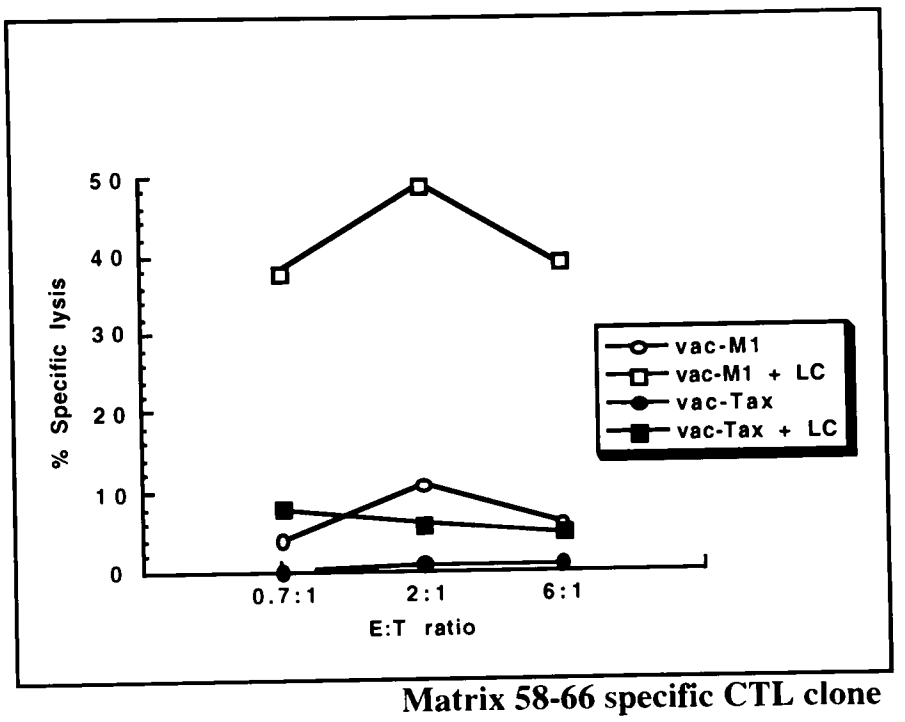
The effectiveness of lactacystin was confirmed in a parallel CTL assay using an influenza matrix 58-66 specific CTL clone and exactly the same treated and infected target cells as used for the Tax CTL assay. This matrix epitope is not generated by constitutive proteasomes (and probably destroyed by it) and is only presented when the LMP7 subunit is expressed or when proteasomes are inhibited with lactacystin (Gileadi et al., 1999). Here, the matrix 58-66 epitope is clearly presented only in the presence of lactacystin, confirming the effectiveness of the lactacystin treatment (Figure 7.8B).

A.



Tax 11-19 specific CTL clone

B.



Matrix 58-66 specific CTL clone

Figure 7.8. Lactacystin does not block presentation of Tax11-19 epitope to CTL

.174/TAPs cells were treated or mock treated with 100 μM lactacystin for 1 hour prior to infection with vac-Tax or vac-M1 (expressing influenza matrix protein) at a M.O.I. of 5 pfu/cell. 1 μM lactacystin was kept in the medium of the relevant samples for the rest of the experiment. Infected cells were left overnight to express. The next day a standard 5 hour chromium release assay was performed using either the HLA-A2 restricted Tax 11-19 specific CTL clone B2 (figure **A.**) or the Cer-43 CTL clone specific for the HLA-A2 restricted Matrix 58-66 epitope (figure **B.**).

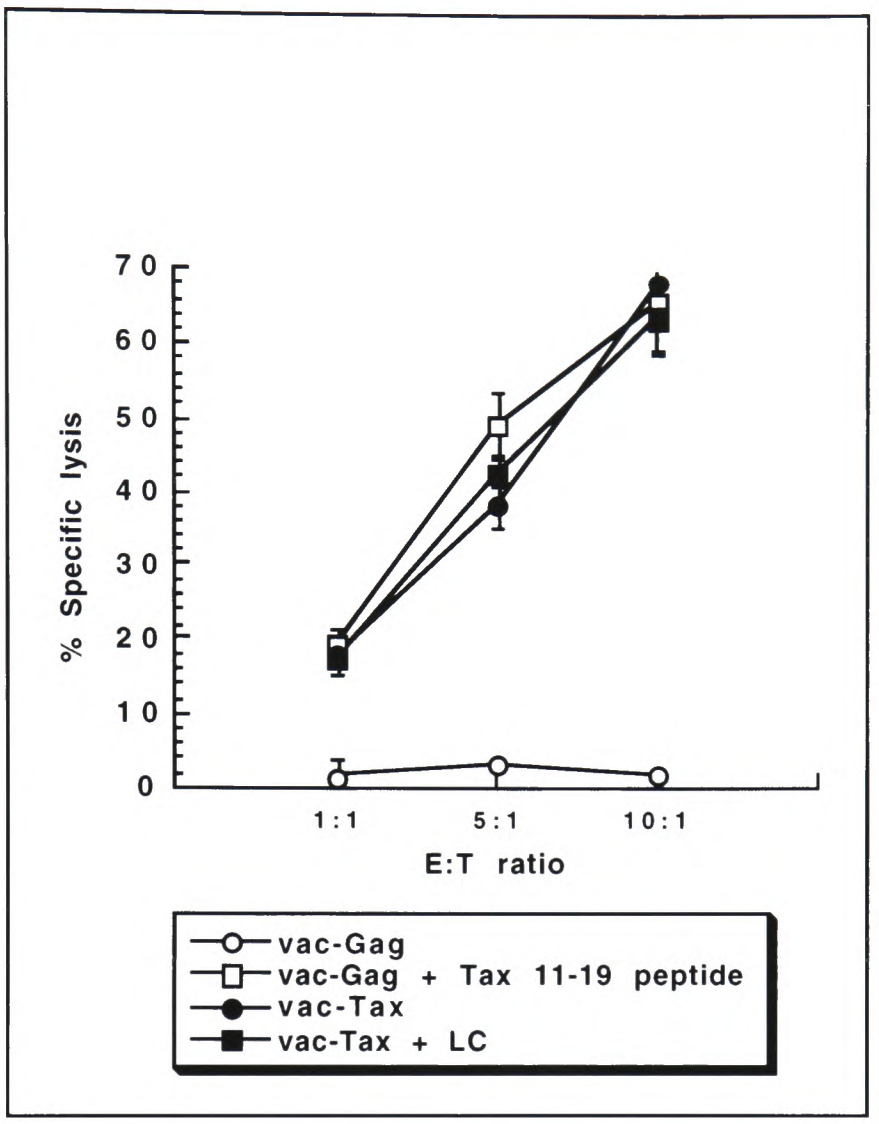


Figure 7.9. Lactacystin does not block presentation of Tax 11-19 epitope to CTL

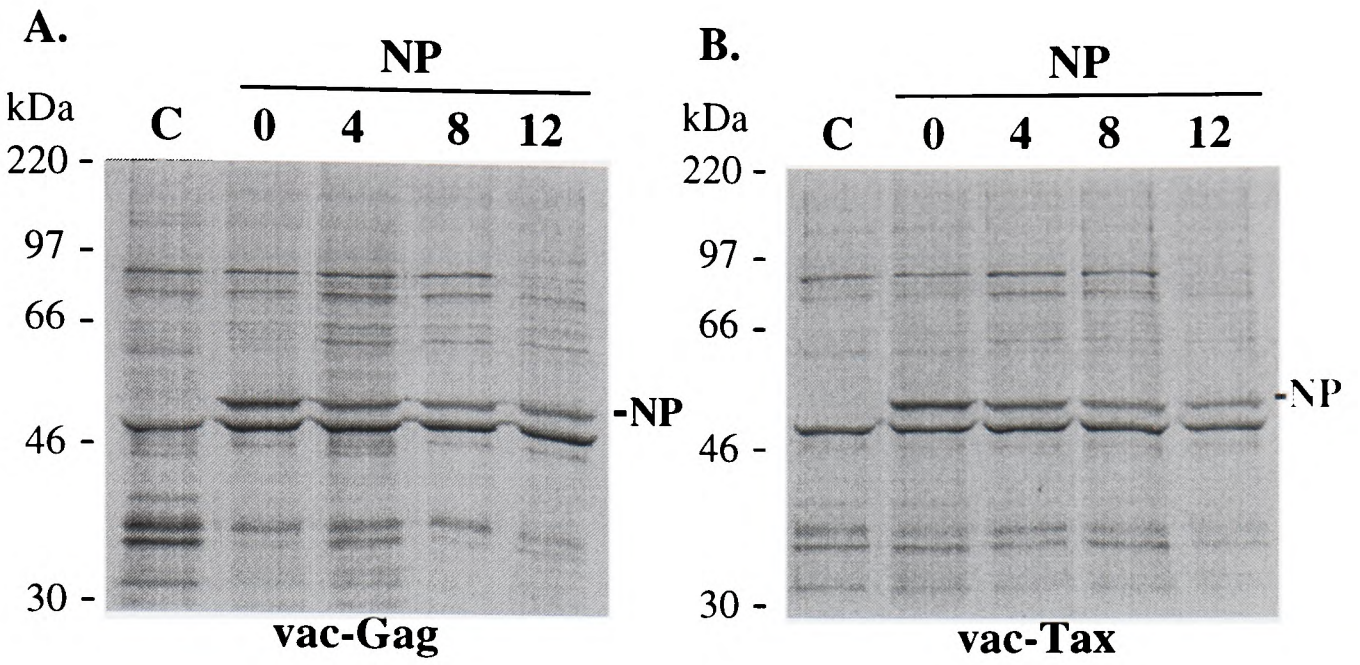
.45 cells were treated or mock treated with 100 μM lactacystin for 1 hour prior to infection with vac-Tax or vac-Gag at a M.O.I. of 5 pfu/cell. 1 μM lactacystin was kept in the medium of the relevant sample for the rest of the experiment. Infected cells were left overnight to express. The next day a standard 4 hour chromium release assay was performed using the Tax11-19 specific CTL clone E4. Tax 11-19 peptide was added to the relevant sample during labelling of target cells with chromium. .45 cells: 721.45 cells. LC= lactacystin.

7.3. Tax has no apparent effect on the MHC class I antigen presentation pathway

7.3.1. Tax expression does not affect the degradation of influenza nucleoprotein

As we had shown that Tax associated with 20S proteasomes and stimulated their chymotryptic and tryptic activities (Chapter 4), and the proteasome is responsible for the majority of intracellular protein degradation (Craiu et al., 1997; Rock et al.. 1994). we wondered whether Tax had an effect on the rate of degradation of whole proteins in the cell. To address this we chose influenza nucleoprotein (NP) as a model protein as it is a well-characterised nuclear protein. NP is a relatively stable protein which was reported to be degraded by nuclear proteasomes in PML bodies (Anton et al., 1999).

We measured the turnover of NP expressed from vac-NP in the presence and absence of Tax (expressed from vac-Tax). However, no effect of Tax co-expression on the degradation of NP was observed (Figure 7.10). This may indicate that the interaction of Tax with the proteasome does not affect the rate of proteasomal degradation of whole proteins *in vivo*.



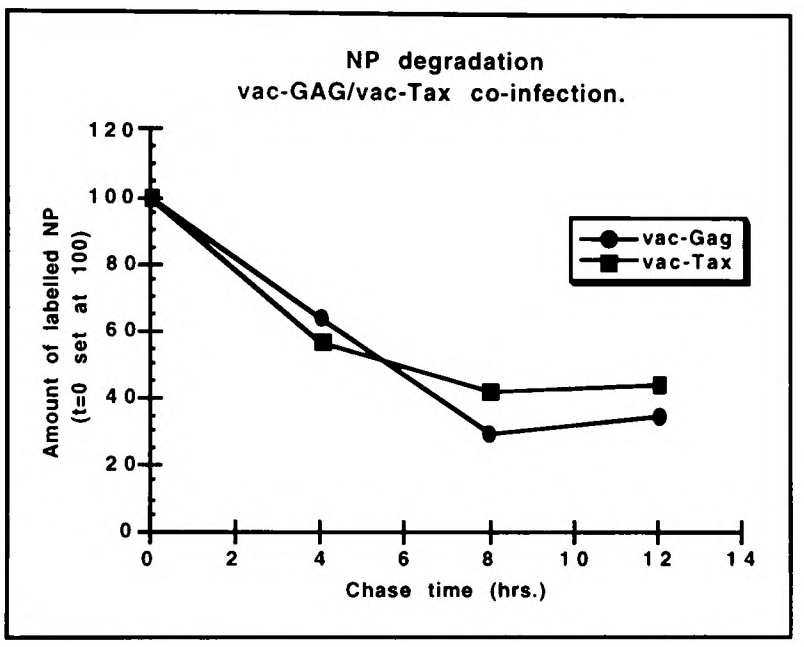


Figure 7.10 Tax expression does not affect the degradation of influenza nucleoprotein.

A, B. 293T cells were infected with either vac-Gag or vac-Tax and co-infected with either vac-NP or vac-Gag (C; control). Cells were metabolically labelled for 1 hour and either harvested immediately or chased with cold medium for the indicated time (4, 8, 12 hours). NP was immunoprecipitated from whole cell lysates with antibody 4-7-18. Autoradiographs of immunoprecipitates separated by SDS-PAGE are shown.

C. The result of densitometric analysis of the autoradiographs in (A.) and (B.) is shown.

7.3.2. Tax does not affect the presentation of the 265-273 epitope of influenza nucleoprotein to CTL

LMP2, LMP7 and PA28 have been shown to be required for the efficient presentation of specific epitopes to CTL (Cerundolo et al., 1995; Fehling et al., 1994; Gileadi et al., 1999; Schwarz et al., 2000; Schwarz et al., 2000; Sibille et al., 1995; Sijts et al., 2000; Van Kaer et al., 1994). These modulators do, however, not affect the rate of degradation of protein substrates by the proteasome (Gaczynska et al., 1993; Groettrup et al., 1996; Van Kaer et al., 1994), but rather seem to act by changing the cleavage pattern and the release of peptide fragments by the proteasome (Driscoll et al., 1993; Gaczynska et al., 1993; Gaczynska et al., 1994; Gileadi et al., 1999; Groettrup et al., 1995; Schwarz et al., 2000). Specifically, LMP2 and LMP7 incorporation lead to enhanced cleavage after hydrophobic and basic residues (Driscoll et al., 1993; Gaczynska et al., 1993).

As we had shown that Tax could stimulate the chymotryptic and tryptic activities of the proteasome (Chapter 4), we wondered whether Tax could act in a similar way and enhance the presentation of (viral) antigens to CTL. We choose to look at the presentation of the HLA-A3 restricted NP epitope 265-273 (ILRGSVAHK) that had previously been shown to be prevented from recognition by CTL when target cells were treated with 100μM lactacystin, indicating proteasome dependency of epitope generation (Cerundolo et al., 1997).

Figure 7.11 shows excellent recognition by CTL of peptide pulsed target cells. vac-NP infected cells expressing NP endogenously were also recognised well, although at a lower level than peptide pulsed target cells. However, co-infection with vac-Tax did not further enhance the recognition of this epitope.

Although this experiment suggests that Tax does not play a role in modulation of antigen processing, it might be the case that the CTL assay is not sensitive enough to detect an increase in presentation, when NP alone is recognised so well. It remains possible that Tax has an effect on poorly generated and presented epitopes (Gileadi et al., 1999; Groettrup et al., 1996).

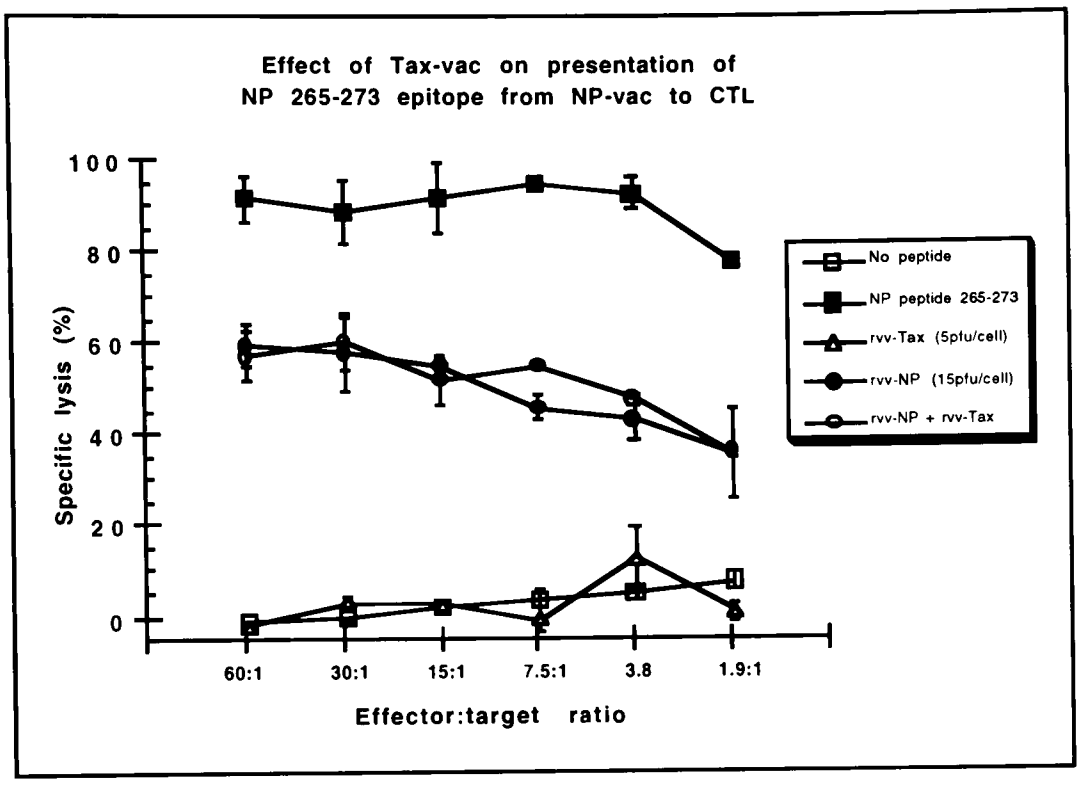


Figure 7.11. Tax does not affect the presentation of the 265-273 epitope of influenza nucleoprotein to CTL.

Target cells (HLA-A3$^+$ B cell line) were either infected overnight with recombinant vaccinia viruses vac-Tax (5 pfu/cell) or vac-NP (15 pfu/cell) or both or pulsed with peptide in the morning. Subsequently, a standard chromium release assay was performed using a NP265-273 specific CTL line.

7.3.3. Transient Tax expression in 293T cells does not affect class I cell surface expression

Although we didn't detect an effect of Tax on the presentation of a specific epitope (previous section), we wondered whether Tax expression would lead to the generation of more high affinity ligands for MHC class I molecules and hence higher levels of expression of these molecules on the cell surface. Similar effects on the stability and cell surface expression of class I molecules have been observed for the proteasome modulators LMP2, LMP7 and PA28 (Fehling et al., 1994; Preckel et al., 1999; Van Kaer et al., 1994).

We therefore transiently transfected 293T cells with pJFE-Tax, and two Tax mutants deficient for proteasome binding, M9 and M12, and measured the level of MHC class I cell surface expression by FACS analysis. For this we used the monoclonal antibody W6/32 which recognises conformationally correct peptide bound MHC class I molecules. As can be seen in figure 7.12, at 24 hours post-transfection there was an increase in MHC class I detected on the surface which is attributed to the liposome transfection method. At later time points, for all constructs tested, the mean level of class I returns to the level seen on untransfected 293T cells.

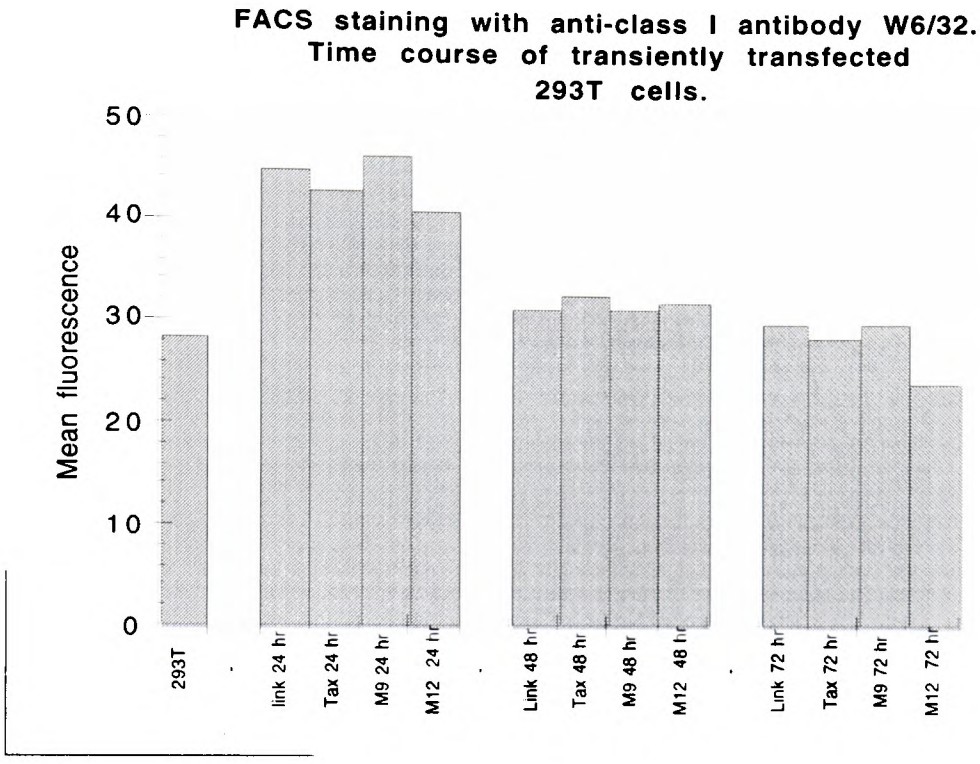


Figure 7.12. Transient Tax expression does not affect MHC class I cell surface expression.

293T cells were transiently transfected (at T=0 hours) with Tax,Tax-M9, Tax-M12 or empty vector (link). Class I surface expression was measured by staining with the class I conformational antibody W6/32 and subsequent FACS analysis. Cells were analysed 24 hours, 48 hours and 72 hours post-transfection, as indicated.

7.3.4. Normal levels of MHC class I cell surface expression on HTLV-1 infected cell lines

We next looked at the MHC class I surface levels on HTLV-1 transformed cell lines as these cells constitutively express Tax and better resemble the *in vivo* situation.

HTLV-1 infected and Tax expressing cell lines MT-2 and MT-4(P) displayed very similar levels of class I molecules on the cell surface as the HTLV-1 infected but Tax negative cell line MT-4(S) (see figure 7.13).

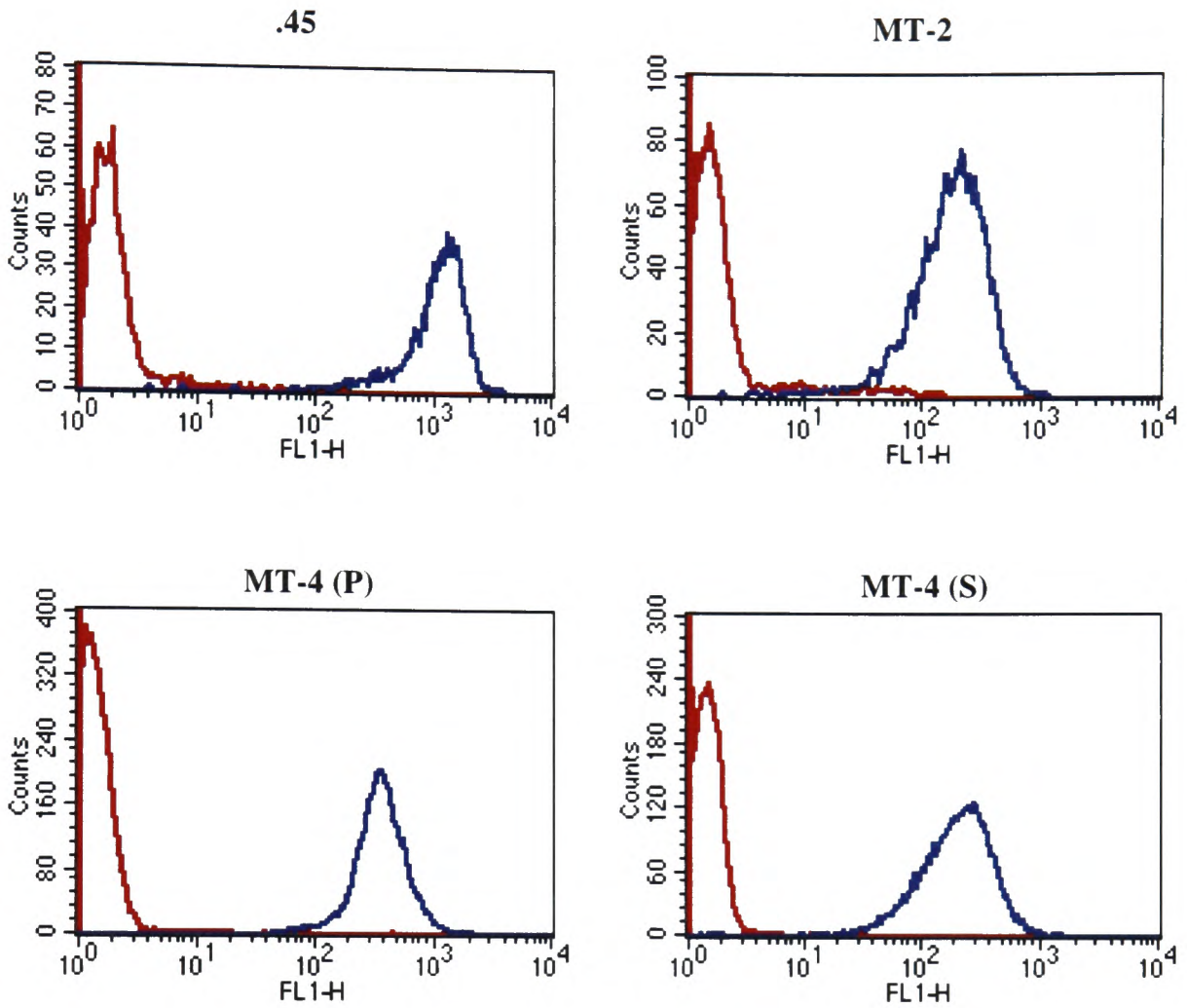


Figure 7.13. Normal levels of MHC class I cell surface expression on HTLV-1 infected cell lines.

MHC class I surface expression on HTLV-1 infected cell lines MT-2, MT-4(P) and MT-4(S) was determined by FACS analysis using the MHC class I conformation specific antibody W6/32. The red graphs represent the negative control (no secondary antibody) for each cell type and the blue graph represents staining with W6/32 antibody. 721.45 cells were used a s a positive control.

7.4. Discussion

In this chapter we set out to find evidence for the hypothesis that efficient processing and presentation of Tax contributed to the immunodominance of Tax in the CTL response against HTLV-1. We were prompted to do so by the observation that Tax associated with the 20S proteasome and enhanced its chymotryptic and tryptic activities (Chapter 4) and the fact that the proteasome has been implicated in the degradation of most cellular proteins and the generation of the majority of peptides for presentation via the MHC class I pathway (Rock and Goldberg, 1999; Rock et al., 1994). We therefore studied the intracellular degradation of the Tax protein and presentation of the Tax 11-19 epitope for recognition by CTL. In addition, we studied the effect of Tax expression on the processing and presentation of heterologous proteins.

Degradation of Tax

We found that Tax was a very stable protein with a metabolic half-life of around 15 hours (Figure 7.1). Its proximity to the proteasome and the activation of the proteasome's catalytic activity apparently didn't target it for rapid degradation. Furthermore, we only observed a marginal effect of the proteasome inhibitor LLnL on the half-life of Tax (Figure 7.2). However, this latter finding has to be treated with caution, as the long half-life of Tax required long incubations with the inhibitor, which forced us to use moderate concentrations of the inhibitor (50μM). Although strong inhibition of degradation of long-lived proteins with 50μM LLnL has been reported (Craiu et al., 1997; Rock et al., 1994), proteasome inhibition was not confirmed in our experiments. Nevertheless, the long half-life of Tax indicates that Tax is not targeted for rapid degradation by the proteasome. Although similar stability of Tax was seen in the HTLV-1 transformed cell line MT-2 (personal communication, Katie Jeffery), others have reported a relatively rapid turnover of Tax (T1/2 ~2 hours) in the HTLV-1 transformed cell line SLB-1 (Slamon et al., 1985). Therefore, cell type specific differences in Tax turnover may exist.

However. Tax appeared not to be completely unaffected by proteasome inhibitors. When cells were treated with proteasome and isopeptidase inhibitors we observed that the (steady state) amount of Tax increased in the MT-4(P) and MT-2 cell lines (Figure 7.3), suggesting stabilisation of Tax due to inhibition of proteasome mediated degradation in these cells. Furthermore, we found that Tax displayed a slightly higher molecular weight in treated cells. This shift in apparent size was reminiscent of the shift in size observed for the Tax protein co-immunoprecipitated with the 20S proteasome (Chapter 4). Therefore, this Tax protein may represent the same form of Tax co-immunoprecipitated with 20S proteasomes. As discussed in Chapter 4, this Tax protein is possibly modified by phosphorylation or dephosphorylation. Together, these data suggest a possible link between association with the proteasome, Tax modification and Tax degradation. Phosphorylation of proteins as a signal for degradation is well established. Regions rich in prolines, glutamic acid, serine and threonine (PEST-sequences), which form consensus phosphorylation motifs for several kinases, have been implicated in the degradation of some proteins (Rogers et al., 1986). Furthermore, the best studied example of ubiquitin-proteasome mediated degradation, IκBα, is phosphorylated on serine residues 32 and 36, which marks it out for ubiquitination and subsequent proteasome mediated degradation (Chen et al., 1995; Palombella et al., 1994). This phosphorylated form can only be detected in the presence of proteasome inhibitors (as they prevent it from being degraded) and appears as a slightly higher molecular weight form of IκBα (Chen et al., 1995; Palombella et al., 1994). Inversely, phosphorylation has also been reported to stabilise certain proteins that are normally degraded by the ubiquitin-proteasome pathway (Musti et al., 1997). However, as we haven't shown that the observed change in mobility of Tax in an SDS-PAGE gel indeed represents a change in its phosphorylation status, these considerations remain speculative.

Localisation of Tax in MTOCs and PML bodies

Overnight incubation of 293T cells with 5μM MG132 led to the accumulation of proteasomes in the nucleus and a dramatic increase in the intensity of the staining (Figure 7.4). This effect had been previously observed by others (Mattsson et al., 2001). This is possibly due to homeostatic mechanism leading to the increase of proteasome synthesis when misfolded protein substrates accumulate in the presence of proteasome inhibitors. Recently, an interesting mechanism has been proposed which involves RPN4, a transcriptional activator of genes encoding proteasomal subunits which is required for normal levels of these subunits. RPN4 was shown to be extremely short-lived and its degradation proteasome dependent. Therefore, when the activity of the proteasome is compromised, this protein rapidly accumulates and activates transcription of proteasome components leading to higher levels of assembled proteasomes (Xie and Varshavsky, 2001). Nuclear localisation of proteasomes might be explained by an accumulation of substrates in the nuclear compartment, perhaps cyclins, which recruit proteasomes.

Tax remained localised in bodies in the nucleus in the presence of MG132 (Figure 7.5) and in general no major changes in the distribution of proteasomes in relation to Tax were observed. In light of the stability of Tax (Figure 7.1), no major differences in intensity of staining were expected. However, in a minority of cells (~5%) Tax was found to colocalise with both proteasomes and PML protein (Figure 7.5). Only in the presence of proteasome inhibitor we observed such localisation of proteasomes inside the Tax bodies. In addition, we occasionally found Tax, in the absence of proteasome inhibitors, to be localised in perinuclear structures (MTOCs/aggresomes), in addition to the presence of Tax in nuclear bodies (Figure 7.6). We saw localisation at perinuclear structures more frequently for M12 (Figure 7.6).

Recently, microtubule-organising centres (MTOCs) and PML bodies have been identified as sites of proteasomal degradation of cellular proteins (Anton et al., 1999; Fabunmi et al., 2001; Garcia-Mata et al., 1999; Johnston et al., 1998; Mattsson et al., 2001; Wigley et al., 1999). Misfolded proteins accumulate at the MTOCs and PML bodies, where

they form stable detergent-insoluble aggregates and have been reported to colocalise with molecular chaperones, polyubiquitin, PA28 and proteasomes.

Tax accumulation at proteasome containing PML bodies in the presence of proteasome inhibitors strongly resembled the described accumulation of NP at those sites (Anton et al., 1999). This may therefore indicate that at least some of Tax is degraded in those structures.

It remains unknown what caused the perinuclear structures to form in the untreated Tax expressing cells. Some stress condition may have induced the accumulation of misfolded protein, resulting in aggresome formation. Tax might be misfolded itself and be a substrate, as has been reported for a mutated form of influenza nucleoprotein (Anton et al., 1999). Alternatively, Tax could be recruited to these structures by its association with the proteasome. The fact that aggresomes were more frequently seen with the M12 mutant suggests that the mutation might lead to increased instability and aggregation of Tax.

Generation and presentation of the Tax11-19 epitope

Our CTL lysis assays clearly showed that the presentation of the Tax 11-19 epitope was dependent on the transporter associated with antigen presentation (TAP) (Figure 7.7). This shows that the epitope, or its precursor fragment, is generated in the nucleocytoplasmic compartment and is subsequently transported into endoplasmic reticulum (ER) by the TAP transporter. In this respect Tax therefore conforms to the classical MHC class I presentation pathway (Kelly et al., 1992; Spies et al., 1992).

These experiments further demonstrated that the generation of the epitope did not require the LMP2 and LMP7 subunits of the proteasome (Figure 7.7). This findings also seems to fit in with previous findings suggesting that the majority of peptides can be generated in the absence of these subunits (Arnold et al., 1992; Momburg et al., 1992). However, mice deficient for any of these subunits have shown their importance in the presentation of certain peptide epitopes and the immune response in general (Fehling et al., 1994; Van Kaer et al., 1994).

Furthermore, we showed that the presentation of the Tax 11-19 epitope could not be inhibited with the proteasome specific inhibitor lactacystin (Figures 7.8 & 7.9). The effectiveness of lactacystin was confirmed in a parallel CTL assay where the presentation of the influenza matrix 58-66 epitope was detected. This matrix epitope is not generated by constitutive proteasomes (and probably destroyed by it) and is only presented when the LMP7 subunit is expressed or when proteasomes are inhibited with lactacystin (Gileadi et al., 1999). We showed that the matrix 58-66 epitope was clearly presented only in the presence of lactacystin, confirming the effectiveness of the lactacystin treatment.

These results indicate therefore that the generation of the Tax 11-19 epitope does not require the proteasome, although we cannot rule out that a proteasome subset or a subset of its activities is resistant to the lactacystin treatment.

Lactacystin resistant/proteasome independent presentation of epitopes is not unprecedented. An epitope of tumour antigen NY-ESO-1 displayed exactly the same presentation characteristics as described for Tax 11-19, i.e. TAP dependency, indifference to the presence or absence of the proteasome subunits LMP2 and LMP7 and resistance to lactacystin treatment (Chen et al., 2000). In addition, several groups have reported enhanced presentation of certain epitopes in the presence of proteasome inhibitors (Gileadi et al., 1999; Luckey et al., 1998; Schwarz et al., 2000; Sewell et al., 1999; Vinitsky et al., 1997). These observations have led to the proposition and identification of other cytoplasmic and ER-resident proteases with a role in antigen processing, such as tri-peptidyl peptidase II (TPPII) (Geier et al., 1999; Glas et al., 1998; Wang et al., 2000), puromycin-sensitive aminopeptidase (PSA) and bleomycin hydrolase (BH) (Stoltze et al., 2000), cysteine and metallo-proteases (Lopez and Del Val, 1997; Lopez et al., 2000) and leucine aminopeptidase (LAP) (Beninga et al., 1998). In many cases these proteases have been proposed to play a role in post-proteasomal trimming of fragments. Several studies have indicated that the proteasome was required for the generation of the C-terminus of a peptide epitope, whereas the generation of the N-terminus was performed by another cytoplasmic protease (Beninga et al., 1998; Craiu et al., 1997; Mo et al., 1999; Stoltze et al., 2000). However, also proteasome independent

trimming of the C-terminus of a relatively short peptide fragment has been reported (Yang et al., 1996). In addition, several studies have shown the involvement of ER-resident (amino-)proteases in the trimming of antigenic peptides (Elliott et al., 1995; Snyder et al., 1994), which might even dependent on the presence of the correct MHC class I molecule (Paz et al., 1999). In this respect it is important to note that the TAP transporter can translocate peptides up to 40 amino acids long (Momburg et al., 1994) and that trimming of at least 40 N-terminal amino acids in the ER has been reported (Elliott et al., 1995).

Altogether, any of these proteases with reported involvement in the MHC class I restricted antigen presentation pathway may play a role in the generation of the Tax 11-19 epitope. Such processing in the nucleus or cytoplasm does not need to produce the final Tax 11-19 peptide and may be transported into the ER as an extended precursor, which is then further trimmed in the ER.

DRiPs as a source of antigenic Tax peptides?

A related question is the apparent discrepancy between the long half-life and stability of Tax and the apparently efficient generation of the Tax 11-19 epitope. It was long held that peptides were generated from mature proteins and that the rate of degradation (half-life) of the protein was an important determinant of the efficiency of epitope generation (Gileadi et al., 1999; Grant et al., 1995; Tobery and Siliciano, 1997; Townsend et al., 1988; Vijh et al., 1998). However, many immunodominant antigens, such as influenza NP and matrix proteins (Gileadi et al., 1999; Townsend et al., 1985) or HIV Gag protein (Schubert et al., 2000), are in fact long-lived. In addition, several reports showed that the stability of endogenously synthesised antigens did not correlate with the generation of peptide/MHC complexes (Anton et al., 1998; Goth et al., 1996). This discrepancy was recently resolved by the demonstration that a large fraction of newly synthesised proteins are either not completely synthesised and are cotranslationally degraded (Turner and Varshavsky, 2000) or are completed but never attain their native structure and are rapidly degraded (Schubert et al., 2000). Both these classes of misfolded proteins are

collectively called defective ribosomal products (DRiPs) (Yewdell et al., 1996). In addition to this, it was elegantly shown that the majority of substrates for the TAP transporter are also derived from newly synthesised proteins (Reits et al., 2000). These data suggest that the majority of Tax peptide epitopes may also be derived from DRiPs rather than from the long-lived native protein.

Tax and the antigen presentation pathway

No evidence was found for an effect of Tax on the degradation of heterologous proteins or the presentation of other epitopes to CTL (Figures 7.10 & 7.11). However, it remains possible that Tax has an effect on the degradation of specific proteins, such as IκBα or p105, by tethering them to the proteasome in addition to enhancing the activity of the proteasome (Chapter 4 and (Petropoulos and Hiscott, 1998; Rousset et al., 1996)). Moreover, Tax appeared to be associated with only a small fraction of proteasomes at any one time (Chapter 4), perhaps making an effect on total protein degradation unlikely. Similarly, no effect of Tax was detected on the presentation to CTL of a proteasome dependent epitope from influenza nucleoprotein (Figure 7.11). Again, this could reflect the fact that Tax is associated with only a subset of proteasomes. Moreover, the effects of LMP2, LMP7 and PA28 on antigen presentation were only detectable for certain specific epitopes that were not efficiently presented without these components (Gileadi et al., 1999; Groettrup et al., 1996; Schwarz et al., 2000). Therefore, the possibility remains that Tax can affect the processing and presentation of poorly presented epitopes.

Together with the fact that cell surface expression of MHC class I molecules is not detectably altered by the expression of Tax (Figures 7.12 & 7.13), this indicates that the MHC class I processing and presentation pathway is largely unaffected by Tax expression. However, it remains possible that Tax has more subtle effects on this pathway.

Chapter 8

Summary and Discussion

8.1. Summary

In this thesis the interaction between the HTLV-1 Tax protein and the 20S proteasome was characterised and the role of this interaction in cellular processes and the cytotoxic T cell (CTL) response against HTLV-1 investigated.

We described the rapid translocation of Tax into the nucleus, where it was stable and formed unique bodies involved in transcriptional activation (Chapter 1).

It was further found that Tax associated with assembled nuclear 20S proteasomes and stimulated the chymotryptic and tryptic activities of the 20S proteasome, independent of the induction of the LMP2 and LMP7 proteasome subunits. Confocal microscopy revealed a partial colocalisation of Tax with nuclear proteasomes (Chapter 2).

The analysis of a panel of Tax mutants revealed that both the Tax N- and C-terminus play a role in the interaction of Tax with the proteasome and further showed that proteasome binding was not sufficient for nuclear localisation of Tax. Therefore, Tax probably translocates into the nucleus prior to and independent of proteasome association (Chapter 3).

Tax specific cytotoxic T cell (CTL) clones were generated and characterised using tetrameric MHC class I/peptide complexes. The TCR repertoire appeared sufficiently diverse to allow recognition of the HLA-A2/Tax11-19 complex using multiple different Vα and Vβ segments (Chapter 4).

The generated CTL clones were used to investigate the requirements for processing and presentation of Tax for recognition by CTL. It was found that Tax was a very stable protein and that the presentation of the immunodominant Tax11-19 epitope was dependent on the TAP peptide transporter, independent of the expression of LMP2 and LMP7 proteasome subunits and resistant to treatment with the proteasome inhibitor lactacystin (Chapter 5).

It was proposed that the interaction between Tax and the 20S proteasome plays a role in Tax mediated transcriptional activation, leading to cellular activation and proliferation, and may not determine the immunodominance of Tax in the CTL response against HTLV-1.

8.2. Discussion

Most of the implications of the findings presented in this thesis have been discussed at the end of each individual results chapter. Here the findings are integrated into the current picture of HTLV-1 infection. In addition, the findings regarding the interaction between Tax and the proteasome will be compared with other viral proteins that have been reported to interact with proteasome subunits.

8.2.1. The role of Tax in HTLV-1 infection

The immune response against HTLV-1 is of interest as the virus persists at high levels in the face of a strong cellular immune response (Bangham, 2000). Furthermore, HTLV-1 has been associated with a neurological inflammatory disease, HAM/TSP (Gessain et al., 1985). There is strong evidence that the CTL response plays an important role in reducing the HTLV-1 viral load, and thereby the risk of developing HAM/TSP (Hanon et al., 2000; Jeffery et al., 1999). The balance between viral replication and the elimination of infected cells by the CTL response is therefore of crucial importance to the outcome of HTLV-1 infection. It appears that the viral transactivator protein Tax plays an important role in both these processes and is therefore central to HTLV-1 infection.

The Tax protein is essential for viral replication and is expressed early in the infected cell. Tax activates transcription from the viral LTR as well as many cellular genes involved in cellular activation and proliferation (Chen et al., 1985; Sodroski et al., 1985; Yao and Wigdahl, 2000). It was shown that a high proportion of infected cells is capable of expressing Tax protein (Hanon et al., 2000). We found that Tax translocated into the nucleus very efficiently after synthesis, a property that may speed up viral replication

and cellular activation (Chapter 3). In the nucleus, Tax was localised in transcriptional bodies together with NFκB (Chapter 3). Furthermore, we have suggested that the association of Tax with the proteasome and the resulting stimulation of the proteasome's catalytic activity may be involved in the enhanced degradation and processing of specific inhibitors, IκBα and p105, which could contribute to the constitutive activation of NFκB and thereby cellular activation and proliferation (Chapter 4). These Tax-mediated transcriptional activation processes may therefore play a role in the production of new virions (infectious spread) as well as the transmission of provirus by cell division ('mitotic' spread).

On the other hand, Tax is the immunodominant target antigen in the CTL response against HTLV-1. Multiple MHC class I restricted epitopes have been defined in the Tax protein, spanning the whole of the protein, which may be recognised simultaneously (Daenke et al., 1996; Parker et al., 1994). In individuals carrying the HLA-A2 allele, the immune response is dominated by $CD8^+$ T cells that recognise the Tax 11-19 peptide (Bieganowska et al., 1999; Daenke et al., 1996; Elovaara et al., 1993; Jacobson et al., 1990; Jeffery et al., 1999; Parker et al., 1992; Parker et al., 1994). As indicated in chapter 1, the restrictive selection of CTL epitopes is an aggregate effect of several steps in the MHC class I antigen processing and presentation pathway. Peptides need to be liberated from their precursor proteins, transported into the ER by the TAP transporter, bind to class I molecules and ultimately be recognised by a T cell receptor (TCR) on a T cell and trigger an immune response (Chen et al., 2000; Yewdell and Bennink, 1999).

Firstly, Tax is expressed early in an infected cell and it was shown that a high proportion of infected cells are capable of doing so *in vivo* (Hanon et al., 2000). We initially hypothesised that Tax, by its association with the 20S proteasome and the activation of the proteasome's activity, was efficiently targeted for degradation and concomitant peptide epitope generation. However, we found that Tax was in fact a stable, long-lived protein, indicating that this was not the case (Chapter 7). Moreover, the presentation of the immunodominant Tax11-19 epitope to CTL could not be inhibited by the proteasome inhibitor lactacystin (Chapter 7). However, metabolic stability of

immunodominant antigens and failure to inhibit presentation of immunodominant epitopes with proteasome inhibitors are not uncommon (Chen et al., 2000; Gileadi et al., 1999; Luckey et al., 1998; Schubert et al., 2000; Schwarz et al., 2000; Vinitsky et al., 1997). We propose that the majority of Tax peptide epitopes may be derived not from native Tax protein, but from defective ribosomal product (DRiPs) (Schubert et al., 2000; Yewdell et al., 1996). In the case of the Tax11-19 epitope, short N-terminal fragments of Tax may be generated by the premature termination of Tax synthesis during ribosomal translation of the *tax/rex* mRNA (Turner and Varshavsky, 2000; Yewdell et al., 1996). Such an epitope containing peptide could either be trimmed in the cytosol (Beninga et al., 1998; Craiu et al., 1997; Mo et al., 1999; Stoltze et al., 2000), or transported as a precursor by TAP and further trimmed in the ER (Elliott et al., 1995; Paz et al., 1999; Snyder et al., 1994). The TAP transporter is known to be able to translocate peptides up to 40 amino acids long (Momburg et al., 1994) and also trimming of at least 40 N-terminal amino acids in the ER has been reported (Elliott et al., 1995). Such a scenario would explain the paradox of the metabolic stability of Tax, the TAP dependency, the indifference to the presence or absence of LMP2/LMP7 and the lactacystin resistance of the presentation of Tax11-19 to CTL (Chapter 7). In addition, deriving the peptide epitope from DRiPs, rather than native protein, would allow the very rapid generation and presentation of the epitope after the start of viral gene expression, giving the CTL response a head start (Reits et al., 2000).

After the generation of the epitope and the transport into the ER, the peptide needs to associate with a MHC class I molecule. The affinity of the Tax11-19 peptide for HLA-A2 is known to be very high (Parker et al., 1992). For other Tax epitopes the optimum peptide length and affinity has not been determined, but binding affinity is likely to exceed the required threshold level (Deng et al., 1997), as indicated by the fact that CTL specific for these epitopes can be found (Daenke et al., 1996; Parker et al., 1992; Parker et al., 1994).

Lastly, the presented peptide needs to be recognised by a T cell receptor and trigger an immune response. Our analysis of Vα and Vβ usage of HLA-A2/Tax11-19 specific T cells clones (Chapter 6) and reports by others (Biddison et al., 1997; Bieganowska et al.,

1999; Elovaara et al., 1995; Utz et al., 1996) have shown that the human TCR repertoire is sufficiently diverse to allow selection of multiple different HLA-A2/Tax11-19 specific T cell clones with completely different Vα and Vβ usage. This ability to recognise HLA-A2/Tax11-19 through the usage of different TCRs may also contribute to the immunodominance of this MHC/peptide complex in HTLV-1 infected HLA-$A2^+$ individuals.

Therefore, the early expression of Tax, the efficient generation of peptide epitopes, possibly from DRiPs, the high affinity of Tax11-19 for HLA-A2 and the flexibility of the TCR repertoire to recognise the HLA-A2/Tax11-19 complex may all contribute to the immunodominance of Tax in general, and the Tax11-19 epitope in particular.

These consideration lead to the following picture of the dynamics of HTLV-1 infection. A high proportion of HTLV-1 infected cells start to express the Tax protein (Hanon et al., 2000). DRiPs generated during translation lead to the efficient and fast generation of Tax peptide epitopes, which are presented on the cell surface for recognition by CTL. Native Tax protein translocates into the nucleus very rapidly after completion of its synthesis (Chapter 3). In the nucleus Tax is very stable and localises in transcriptional bodies, leading to activation of viral transcription and cellular activation and proliferation (Chapters 3). The association of Tax with the proteasome may play a role in these transcriptional activation processes, as indicated above and chapter 4. The efficient generation and presentation of Tax epitopes leads to the activation of CTL, which become chronically activated and persistently destroy Tax-expressing HTLV-1 infected $CD4^+$, and some $CD8^+$, cells (Daenke et al., 1996; Hanon et al., 2000; Hanon et al., 2000; Parker et al., 1992; Parker et al., 1994). The rapid CTL mediated lysis of HTLV-1 infected cells restricts the ability of HTLV-1 to complete full-cycle viral replication, which has two major consequences: Firstly, the proviral load is mainly maintained by mitotic transmission, i.e. proliferation of cells with integrated provirus. This also explains the relatively little sequence variation of HTLV-1, when compared with for instance HIV, which depends more on transmission of virions, and thus error prone reverse transcription. Secondly, the rapid clearance of Tax expressing cells, before other viral

proteins can be expressed and epitopes presented, limits the generation of CTL specific for other HTLV-1 antigens. Therefore, the efficient CTL response against Tax contributes to the immunodominance of Tax by preventing the expression of other viral antigens (Bangham, 2000).

The competition between viral propagation and the elimination of infected cells by the CTL response will lead to a dynamic equilibrium viral load. The viral load is generally 10 to 100 fold higher in HAM/TSP patients than in healthy carriers and is a strong determinant of the risk of developing HAM/TSP (Jeffery et al., 1999; Kubota et al., 2000). Host genetic factors are likely to play an important role in the outcome of HTLV-1 infection. These factors can be involved in determining the efficiency of the CTL response (such as the HLA-A2 allele) or factors affecting the efficiency of Tax mediated cellular proliferation, although the latter are less likely to be polymorphic (Jeffery et al., 1999). Similarly, differences between viral isolates may play a role. Tax variants more active in transcriptional activation could more effectively stimulate proliferation of infected cells, leading to a higher viral load. In addition, the mutation of Tax CTL epitopes could give a selective advantage in evading the CTL response. However, natural mutations in Tax epitopes leading to abrogation of CTL recognition were found to severely compromise the transactivation function of Tax. Therefore, functional impairment of Tax may balance any selective advantage conferred by an amino acid change that abolishes CTL recognition (Niewiesk et al., 1995). In addition, no HTLV-1 strain/sequence has so-far been associated with higher viral load or HAM/TSP (Bangham et al., 1988; Daenke et al., 1990), although more subtle and heterogeneous contributions of sequence variation cannot be excluded.

8.2.2. Viral interference with the proteasome

In this thesis the interaction between HTLV-1 Tax protein and the 20S proteasome was described. This interaction was shown to occur in the nucleus and to result in stimulation of the chymotryptic and tryptic activities of the proteasome. We have proposed that this interaction plays a role in Tax-mediated transcriptional activation, by enhancing the degradation of inhibitors of transcriptional activation such as IκBα and p105 (Chapter 4). We further found that Tax itself was not targeted for rapid proteasomal degradation and that Tax expression did not enhance the presentation to CTL of a proteasome dependent epitope of another viral protein (Chapter 7).

Tax is not the only viral protein able to interact with the proteasome and to modulate its activity. Biochemical evidence for a direct interaction with proteasome subunits has been obtained for hepatitis B virus X (Hbx) protein (Fischer et al., 1995; Hu et al., 1999; Huang et al., 1996; Zhang et al., 2000), human immunodeficiency virus type (HIV-1) Tat and Nef proteins (Rossi et al., 1997; Seeger et al., 1997) and the E1A protein of adenovirus type 5 (Ad5) (Turnell et al., 2000) (Table 7.1).

Viral proteins appear to interact with 20S subunits (Tax, Nef) as well as 19S cap subunits (E1A) and sometimes with both (Hbx, Tat). Viral proteins interact with α as well as β subunits of the 20S proteasome, but so-far no direct interaction between a viral protein and a catalytic β subunit has been reported. Within the 19S cap complexes viral proteins have been shown to bind the ATPase subunits (S4, S6, S6'and S8) in the base of the 19S complex. The ATPases play a crucial role in the unfolding and translocation of substrates for proteasomal degradation (Baumeister et al., 1998; Braun et al., 1999; Ortega et al., 2000).

Virus	Protein	Interacting proteasome subunits	Effect on proteasome activity	Proposed functional effect
HTLV-1	Tax	HC9 (20S, α3) HsN3 (20S, β7)	Stimulation of chymotryptic and tryptic activity	NFκB activation
HBV	Hbx	HC9 (20S, α4) PSMC1 (19S ATPase, S4)	Inhibition of all 20S catalytic activities	Hbx mediated transcriptional activation
HIV-1	Tat	α-ring of 20S TBP1 (19S ATPase, S6') TBP7 (19S ATPase, S6)	- Inhibition of chymotryptic activity of 20S - Inhibition of PA28 association with 20S - Stimulation of chymotryptic activity of 26S	N.D.
HIV-1	Nef	HsN3 (20S, β7)	N.D.	N.D.
Ad5	E1A	Sug1 (19S ATPase, S8) PSMC1 (19S ATPase, S4)	Reduction in ATPase activity	N.D.

Table 7.1. Viral proteins interacting with proteasome subunits.

The data summarised in the table are from the following references: HTLV-1 Tax (Rousset et al., 1996), HBV Hbx (Huang et al., 1996; Zhang et al., 2000), HIV-1 Tat (Seeger et al., 1997), HIV-1 Nef (Rossi et al., 1997) and Ad5 E1A (Turnell et al., 2000). N.D. not determined.

As the proteasome is essential for cell survival, viral proteins modulate proteasome activity, rather than completely blocking it. The different viral proteins have various effects on the activity of the proteasome. Whereas Tax stimulated the chymotryptic and tryptic activity of the 20S proteasome (Chapter 4), HIV Tat and Hbx protein were reported to inhibit the chymotryptic (Tat) or all three different catalytic activities (Hbx) of the 20S proteasome.

The interaction of E1A with S4 and S8 ATPase subunits was shown to result in decreased ATPase activity and a reduction in ubiquitin-proteasome mediated p53 degradation (Turnell et al., 2000). The effect of Hbx and HIV Tat on the ATPase activity of the 19S cap was not determined. However, Tat stimulated *in vitro* hydrolysis by the 26S proteasome of both a fluorogenic peptide substrate as well as ubiquitin-lysozyme, suggesting stimulation of ATPase activity (Seeger et al., 1997). Hbx protein inhibited *in vitro* hydrolysis of ubiquitinated lysozyme (Hu et al., 1999) as well as the *in vivo* degradation of two substrates of the ubiquitin-proteasome pathway (Zhang et al., 2000). However, it was not determined whether these effects were due to effects on the 20S proteasome core or the 19S regulator complexes.

Although the proteasome has been identified as a target for all these viral proteins, the information about the functional consequences of the interactions is still limited. For some factors it has been proposed that the interaction may explain (some of) the pleiotropic effects observed during viral infection, such as transcriptional activation, cellular activation, proliferation and transformation (Hu et al., 1999; Turnell et al., 2000). In particular for Hbx protein it was shown that sequences involved in the interaction with the proteasome, were also important for its transcriptional activation function (Zhang et al., 2000). In addition, proteasome inhibitors blocked Hbx mediated transactivation of AP-1, AP-2 and SP1 site containing promoters, suggesting that proteasome function was required for the transactivation function of Hbx (Hu et al., 1999). As mentioned earlier, for HTLV-1 Tax the interaction with the proteasome has been implicated in the stimulation of p105 processing and phosphorylation and ubiquitination independent IκBα degradation (Beraud and Greene, 1996; Petropoulos and Hiscott, 1998; Rousset et al., 1996)(Chapter 4).

Although a role of these viral proteins in stabilising other (viral) proteins and thereby suppressing MHC class I antigen presentation has been suggested by many, no evidence is currently available to support this hypothesis (Beraud and Greene, 1996; Hu et al., 1999; Seeger et al., 1997; Turnell et al., 2000)(Chapter 7).

Appendix A

Abbreviations

ATP	adenosine triphosphate
Ab	antibody
AMC	aminomethylcoumarin
β2m	beta-2-microglobulin
bp	base pairs
BUdR	5'bromo-2'deoxyuridine
BSA	bovine serum albumin
°C	degrees Celsius
CNS	central nervous system
CTL	cytotoxic T cell
Da	Dalton
DMEM	Dulbecco's Modified Eagle medium
DMSO	dimethylsulfoxide
DNA	deoxyribonucleic acid
dNTP	deoxynucleoside triphosphate
EBV	Epstein-Barr Virus
E.coli	*Escherichia coli*
EDTA	ethylenediaminetetraacetic acid
ELISA	enzyme-linked immunosorbent assay
ER	endoplasmic reticulum
E:T	effector (CTL) to target ratio
FACS	fluorescence activated cell sorter
FCS	foetal calf serum
FITC	fluorescein isothiocyanate
FPLC	fast performance liquid chromatography
g	gram
GGR	N-cbz-GGR-AMC
HC	heavy chain
HLA	human leukocyte antigen
hr(s)	hour(s)
HTLV-1	human T cell lymphotropic virus type 1
Ig	immunoglobulin
IL-2	interleukin-2
IP	immunoprecipitation
IPTG	isopropyl-β-D-thiogalactoside
kb	kilo base pairs
kDa	kilo Dalton
L	litre
LB	Luria-Bertani
LLnL	N-acetyl-L-leucinyl-L-leucinyl-L-norleucinal calpain inhibitor 1
LLVY	N-succinyl-LLVY-AMC

LRSC	lissamine rhodamine sulfchloride
M	molar
mAb	monoclonal antibody
MG132	cbz-L-leucinyl-L-leucinyl-L-leucinal
MHC	major histocompatibility complex
mg	milligram
min (or ')	minutes
ml	millilitre
mM	millimolar
M.O.I.	multiplicity of infection
mRNA	messenger RNA
MW	molecular weight
µg	microgram
µl	microlitre
µM	micromolar
ng	nanogram
nM	nanomolar
NP	influenza nucleoprotein
NP-40	nonidet P-40 detergent
OD	optical density
o/n	overnight
PAGE	polyacrylamide gelelectrophoresis
PBMCs	peripheral blood mononuclear cells
PBS	phosphate buffered saline
PCR	polymerase chain reaction
PE	phycoerythrin
PEG	polyethylene glycol
pfu	plaque forming units
PHA	phytohemaglutinin
RNA	ribonucleic acid
rpm	rotations (revolutions) per minute
RPMI	Rosell Park Memorial Institute medium
RT	room temperature
RT	reverse transcriptase
SDS-PA	SDS polyacrylamide
Sec (or ")	seconds
T1/2	half-life
TBE	Tris/Boric acid/EDTA buffer
TE	Tris/EDTA buffer
Tet^+	tetramer positive
Tween-20	polyoxyethylene sorbitan monolaurate
Ub	ubiquitin
UV	ultraviolet
V	volts
Vac	recombinant vaccinia virus (rVV)
W	watts

Appendix B

Oligonucleotides

Sequencing primers:

JFE5-PRI 5'-TGG ATG TTG CCT TTA CTT CTA G Tm=59.8°C
JFE3-PRI 5'-TCT AGT TGT GGT TTG TCC AAA C Tm=60.5°C

Mutagenesis oligos:

M7 5'-CTG TGT ACA AGG CGA CTG G**GC TAG** CAT CTC TGG GGG ACT--ATG TTC
NheI

M12 5'-CCC TAC TGG CCA CCT GTC CAG **CTA GC**C AGA TCA CCT GGG--ACC CCA TC
NheI

M22 5'-CCC TGT CTT TTC CAG ACC CCG **CTA GC**C GGC CCC AGA ACC TGT ACA C
NheI

M47 5'-GAA TAC ACC AAC ATC CCC ATT TCT **AGA TC**T TTT AAC GAA--AAA GAG GCA GAT G
Bgl II

C4 5'-GTC TAC GTG TTT GGA GAC **TAC GTA** CAA GGC GAC TGG
SnaB I

C6 5'-GGC GAC TGG TGC CCC **AGA** TCT GGG GGA CTA TG
Bgl II

C7 5'-CAA TCA CTC ATA CAA CCC CCA ACA TTC C**CT TAA G**CT TCC TCC AGG CCG TGC GCA AAT ACT C
Afl II

Underlined: Restriction site.
Bold: Nucleotides different from wild-type Tax sequence.

Oligos for Tax-6His construct (PCR primers)

5'-Nco I 5'-GTC CTG CCA TGG CTC ATT TCC CGG GTT TTG GTC AGA-

Nco I

-GTC TTC TTT TCG GAT ACC CAG

3'-BamHI+His 5'-TAG CGC GGA TCC GAT CAG TGA TGG TGA TGG-

Bam HI

-TGA TGT TTG ACT TCT GTT TCG CGG AAA TGT-

-TTT TC

Oligos for Δ2-58

5'-Δ2-58 5'-CAT TGA AGA TCT GCC ATG GTG GAC GGC AGA-

Bgl II

-GTG ATC GGC TCA GCT CTA CAG TTC C

3'-EcoRI 5'-TAG-CCG-GAA-TTC CTC AGA CTT CTG TTT CGC-

-GGA *EcoRI*

Underlined: Restriction site.

```
m12delm47orf      MAHFPGFGQS LLFGYPVYVF GDCVQGDWCP ISGGLCSARL HRHALLATCP ASQITT 55
m12delm20m47orf   MAHFPGFGQS LLFGYPVYVF GDCVQGDWCP ISGGLCSARL HRHALLATCP ASQITT 55
m12m47orf         MAHFPGFGQS LLFGYPVYVF GDCVQGDWCP ISGGLCSARL HRHALLATCP ASQITT 55
m12m47_1orf       MAHFPGFGQS LLFGYPVYVF GDCVQGDWCP ISGGLCSARL HRHALLASCP ASQITT 55
m12orf            MAHFPGFGQS LLFGYPVYVF GDCVQGDWCP ISGGLCSARL HRHALLATCP ASQITT 55
m7m12m47orf       MAHFPGFGQS LLFGYPVYVF GDCVQGDWCP ISGGLCSARL HRHALLATCP ASQITT 55
m47orf            MAHFPGFGQS LLFGYPVYVF GDCVQGDWAS ISGGLCSARL HRHALLATCP ASQITT 55
m20m47orf         MAHFPGFGQS LLFGYPVYVF GDCVQGDWCP ISGGLCSARL HRHALLATCP EHQITT 55
taxorf            MAHFPGFGQS LLFGYPVYVF GDCVQGDWCP ISGGLCSARL HRHALLATCP EHQITT 55
m20orf            MAHFPGFGQS LLFGYPVYVF GDCVQGDWCP ISGGLCSARL HRHALLATCP EHQITT 55
m9m47orf          MAHFPGFGQS LLFGYPVYVF GDCVQGDWCP ISGGLCSARL HRHALLATCP EHQITT 55
m9m20m47orf       MAHFPGFGQS LLFGYPVYVF GDCVQGDWCP ISGGLCSARL ASHALLATCP EHQITT 55
m9orf             MAHFPGFGQS LLFGYPVYVF GDCVQGDWCP ISGGLCSARL ASHALLATCP EHQITT 55
m7orf             MAHFPGFGQS LLFGYPVYVF GDCVQGDWAS ISGGLCSARL HRHALLATCP EHQITT 55
m7m20m47orf       MAHFPGFGQS LLFGYPVYVF GDCVQGDWAS ISGGLCSARL HRHALLATCP EHQIT  55

m12delm47orf      WDPIDGRVIG SALQFLIPRL PYWPPVQLAR S......P..  .GTPNIPPSF LQAVR 101
m12delm20m47orf   WDPIDGRVIG SALQFLIPRL PYWPPVQLAR S......P..  .GTPNIPPSF LQAVR 101
m12m47orf         WDPIDGRVIG SALQFLIPRL PSFPTQRTSK TLKVLTPPIT HTTPNIPPSF LQAVR 110
m12m47_1orf       WDPIDGRVIG SALQFLIPRL PSFPTQRTSK TLKVLTPPIT HTTPNIPPSF LQAVR 110
m12orf            WDPIDGRVIG SALQFLIPRL PSFPTQRTSK TLKVLTPPIT HTTPNIPPSF LQAVR 110
m7m12m47orf       WDPIDGRVIG SALQFLIPRL PSFPTQRTSK TLKVLTPPIT HTTPNIPPSF LQAVR 110
m47orf            WDPIDGRVIG SALQFLIPRL PSFPTQRTSK TLKVLTPPIT HTTPNIPPSF LQAVR 110
m20m47orf         WDPIDGRVIG SALQFLIPRL PSFPTQRTSK TLKVLTPPIT HTTPNIPPSF LQAVR 110
taxorf            WDPIDGRVIG SALQFLIPRL PSFPTQRTSK TLKVLTPPIT HTTPNIPPSF LQAVR 110
m20orf            WDPIDGRVIG SALQFLIPRL PSFPTQRTSK TLKVLTPPIT HTTPNIPPSF LQAVR 110
m9m47orf          WDPIDGRVIG SALQFLIPRL PSFPTQRTSK TLKVLTPPIT HTTPNIPPSF LQAVR 110
m9m20m47orf       WDPIDGRVIG SALQFLIPRL PSFPTQRTSK TLKVLTPPIT HTTPNIPPSF LQAVR 110
m9orf             WDPIDGRVIG SALQFLIPRL PSFPTQRTSK TLKVLTPPIT HTTPNIPPSF LQAVR 110
m7orf             WDPIDGRVIG SALQFLIPRL PSFPTQRTSK TLKVLTPPIT HTTPNIPPSF LQAVR 110
m7m20m47orf       WDPIDGRVIG SALQFLIPRL PSFPTQRTSK TLKVLTPPIT HTTPNIPPSF LQAVR 110

m12delm47orf      KYSPFRNGYM EPTLGQHLPT LSFPDPGLRP QNLYTLWGGS VVCMYLYQLS PPITW 156
m12delm20m47orf   KYSPFRNGYM EPTLGQHLPT LSFPDPASRP QNLYTLWGGS VVCMYLYQLS PPITW 156
m12m47orf         KYSPFRNGYM EPTLGQHLPT LSFPDPGLRP QNLYTLWGGS VVCMYLYQLS PPITW 165
m12m47_1orf       KYSPFRNGYM EPTLGQHLPT LSFPDPGLRP QNLYTLWGGS VVCMYLYQLS PPITW 165
m12orf            KYSPFRNGYM EPTLGQHLPT LSFPDPGLRP QNLYTLWGGS VVCMYLYQLS PPITW 165
m7m12m47orf       KYSPFRNGYM EPTLGQHLPT LSFPDPGLRP QNLYTLWGGS VVCMYLYQLS PPITW 165
m47orf            KYSPFRNGYM EPTLGQHLPT LSFPDPGLRP QNLYTLWGGS VVCMYLYQLS PPITW 165
m20m47orf         KYSPFRNGYM EPTLGQHLPT LSFPDPASRP QNLYTLWGGS VVCMYLYQLS PPITW 165
taxorf            KYSPFRNGYM EPTLGQHLPT LSFPDPGLRP QNLYTLWGGS VVCMYLYQLS PPITW 165
m20orf            KYSPFRNGYM EPTLGQHLPT LSFPDPASRP QNLYTLWGGS VVCMYLYQLS PPITW 165
m9m47orf          KYSPFRNGYM EPTLGQHLPT LSFPDPGLRP QNLYTLWGGS VVCMYLYQLS PPITW 165
m9m20m47orf       KYSPFRNGYM EPTLGQHLPT LSFPDPASRP QNLYTLWGGS VVCMYLYQLS PPITW 165
m9orf             KYSPFRNGYM EPTLGQHLPT LSFPDPGLRP QNLYTLWGGS VVCMYLYQLS PPITW 165
m7orf             KYSPFRNGYM EPTLGQHLPT LSFPDPGLRP QNLYTLWGGS VVCMYLYQLS PPITW 165
m7m20m47orf       KYSPFRNGYM EPTLGQHLPT LSFPDPASRP QNLYTLWGGS VVCMYLYQLS PPITW 165
```

```
m12delm47orf      PLLPHVVFCH PGQLGAFLTN VPYKRIEELL YKISLTTGAL IILPEDCLPT TLFQP 211
m12delm20m47orf   PLLPHVVFCH PGQLGAFLTN VPYKRIEELL YKISLTTGAL IILPEDCLPT TLFQP 211
m12m47orf         PLLPHVVFCH PGQLGAFLTN VPYKRIEELL YKISLTTGAL IILPEDCLPT TLFQP 220
m12m47_1orf       PLLPHVVFCH PGQLGAFLTN VPYKRIEELL YKISLTTGAL IILPEDCLPT TLFQP 220
m12orf            PLLPHVVFCH PGQLGAFLTN VPYKRIEELL YKISLTTGAL IILPEDCLPT TLFQP 220
m7m12m47orf       PLLPHVVFCH PGQLGAFLTN VPYKRIEELL YKISLTTGAL IILPEDCLPT TLFQP 220
m47orf            PLLPHVVFCH PGQLGAFLTN VPYKRIEELL YKISLTTGAL IILPEDCLPT TLFQP 220
m20m47orf         PLLPHVVFCH PGQLGAFLTN VPYKRIEELL YKISLTTGAL IILPEDCLPT TLFQP 220
taxorf            PLLPHVVFCH PGQLGAFLTN VPYKRIEELL YKISLTTGAL IILPEDCLPT TLFQP 220
m20orf            PLLPHVVFCH PGQLGAFLTN VPYKRIEELL YKISLTTGAL IILPEDCLPT TLFQP 220
m9m47orf          PLLPHVVFCH PGQLGAFLTN VPYKRIEELL YKISLTTGAL IILPEDCLPT TLFQP 220
m9m20m47orf       PLLPHVVFCH PGQLGAFLTN VPYKRIEELL YKISLTTGAL IILPEDCLPT TLFQP 220
m9orf             PLLPHVVFCH PGQLGAFLTN VPYKRIEELL YKISLTTGAL IILPEDCLPT TLFQP 220
m7orf             PLLPHVVFCH PGQLGAFLTN VPYKRIEELL YKISLTTGAL IILPEDCLPT TLFQP 220
m7m20m47orf       PLLPHVVFCH PGQLGAFLTN VPYKRIEELL YKISLTTGAL IILPEDCLPT TLFQP 220

m12delm47orf      VRAPVTLTAW QHGLLPFHST LTTPGLIWTF TDGTPMISGP CPKDGQPSLV LQSSS 266
m12delm20m47orf   VRAPVTLTAW QHGLLPFHST LTTPGLIWTF TDGTPMISGP CPKDGQPSLV LQSSS 266
m12m47orf         VRAPVTLTAW QHGLLPFHST LTTPGLIWTF TDGTPMISGP CPKDGQPSLV LQSSS 275
m12m47_1orf       VRAPVTLTAW QHGLLPFHST LTTPGLIWTF TDGTPMISGP CPKDGQPSLV LQSSS 275
m12orf            VRAPVTLTAW QHGLLPFHST LTTPGLIWTF TDGTPMISGP CPKDGQPSLV LQSSS 275
m7m12m47orf       VRAPVTLTAW QHGLLPFHST LTTPGLIWTF TDGTPMISGP CPKDGQPSLV LQSSS 275
m47orf            VRAPVTLTAW QHGLLPFHST LTTPGLIWTF TDGTPMISGP CPKDGQPSLV LQSSS 275
m20m47orf         VRAPVTLTAW QHGLLPFHST LTTPGLIWTF TDGTPMISGP CPKDGQPSLV LQSSS 275
taxorf            VRAPVTLTAW QHGLLPFHST LTTPGLIWTF TDGTPMISGP CPKDGQPSLV LQSSS 275
m20orf            VRAPVTLTAW QHGLLPFHST LTTPGLIWTF TDGTPMISGP CPKDGQPSLV LQSSS 275
m9m47orf          VRAPVTLTAW QHGLLPFHST LTTPGLIWTF TDGTPMISGP CPKDGQPSLV LQSSS 275
m9m20m47orf       VRAPVTLTAW QHGLLPFHST LTTPGLIWTF TDGTPMISGP CPKDGQPSLV LQSSS 275
m9orf             VRAPVTLTAW QHGLLPFHST LTTPGLIWTF TDGTPMISGP CPKDGQPSLV LQSSS 275
m7orf             VRAPVTLTAW QHGLLPFHST LTTPGLIWTF TDGTPMISGP CPKDGQPSLV LQSSS 275
m7m20m47orf       VRAPVTLTAW QHGLLPFHST LTTPGLIWTF TDGTPMISGP CPKDGQPSLV LQSSS 275

m12delm47orf      FIFHKFQTKA YHPSFLLSHG LIQYSSFHNL HLLFEEYTNI PISRSFNEKE ADDND 321
m12delm20m47orf   FIFHKFQTKA YHPSFLLSHG LIQYSSFHNL HLLFEEYTNI PISRSFNEKE ADDND 321
m12m47orf         FIFHKFQTKA YHPSFLLSHG LIQYSSFHNL HLLFEEYTNI PISRSFNEKE ADDND 330
m12m47_1orf       FIFHKFQTKA YHPSFLLSHG LIQYSSFHNL HLLFEEYTNI PISRSFNEKE ADDND 330
m12orf            FIFHKFQTKA YHPSFLLSHG LIQYSSFHNL HLLFEEYTNI PISLLFNEKE ADDND 330
m7m12m47orf       FIFHKFQTKA YHPSFLLSHG LIQYSSFHNL HLLFEEYTNI PISRSFNEKE ADDND 330
m47orf            FIFHKFQTKA YHPSFLLSHG LIQYSSFHNL HLLFEEYTNI PISRSFNEKE ADDND 330
m20m47orf         FIFHKFQTKA YHPSFLLSHG LIQYSSFHNL HLLFEEYTNI PISRSFNEKE ADDND 330
taxorf            FIFHKFQTKA YHPSFLLSHG LIQYSSFHNL HLLFEEYTNI PISLLFNEKE ADDND 330
m20orf            FIFHKFQTKA YHPSFLLSHG LIQYSSFHNL HLLFEEYTNI PISLLFNEKE ADDND 330
m9m47orf          FIFHKFQTKA YHPSFLLSHG LIQYSSFHNL HLLFEEYTNI PISRSFNEKE ADDND 330
m9m20m47orf       FIFHKFQTKA YHPSFLLSHG LIQYSSFHNL HLLFEEYTNI PISRSFNEKE ADDND 330
m9orf             FIFHKFQTKA YHPSFLLSHG LIQYSSFHNL HLLFEEYTNI PISLLFNEKE ADDND 330
m7orf             FIFHKFQTKA YHPSFLLSHG LIQYSSFHNL HLLFEEYTNI PISLLFNEKE ADDND 330
m7m20m47orf       FIFHKFQTKA YHPSFLLSHG LIQYSSFHNL HLLFEEYTNI PISRSFNEKE ADDND 330
```

```
m12delm47orf      HEPQISPGEL  EPPSEKHFRE  TEV*344
m12delm20m47orf   HEPQISPGEL  EPPSEKHFRE  TEV*344
m12m47orf         HEPQISPGEL  EPPSEKHFRE  TEV*353
m12m47_1orf       HEPQISPGEL  EPPSEKHFRE  TEV*353
m12orf            HEPQISPGEL  EPPSEKHFRE  TEV*353
m7m12m47orf       HEPQISPGEL  EPPSEKHFRE  TEV*353
m47orf            HEPQISPGEL  EPPSEKHFRE  TEV*353
m20m47orf         HEPQISPGEL  EPPSEKHFRE  TEV*353
taxorf            HEPQISPGEL  EPPSEKHFRE  TEV*353
m20orf            HEPQISPGEL  EPPSEKHFRE  TEV*353
m9m47orf          HEPQISPGEL  EPPSEKHFRE  TEV*353
m9m20m47orf       HEPQISPGEL  EPPSEKHFRE  TEV*353
m9orf             HEPQISPGEL  EPPSEKHFRE  TEV*353
m7orf             HEPQISPGEL  EPPSEKHFRE  TEV*353
m7m20m47orf       HEPQISPGEL  EPPSEKHFRE  TEV*353
```

```
taxorf       MAHFPGFGQS LLFGYPVYVF GDCVQGDWCP ISGGLCSARL HRHALLATCP EHQITWDPID 60
c6orf        MAHFPGFGQS LLFGYPVYVF GDCVQGDWCP RSGGLCSARL HRHALLATCP EHQITWDPID 60
c4_2orf      MAHFPGFGQS LLFGYPVYVF GDYVQGDWCP ISGGLCSARL HRHALLATCP EHQITWDPID 60
forf         MAHFPGFGQS LLFGYPVYVF GDCVQGDWCP ISGGLCSARL HRHALLATCP EHQITWDPID 60
c4_1orf      MAHFPGFGQS LLFGYPVYVF GDCVQGDWCP ISGGLCSARL HRHALLATCP EHQITWDPID 60
c7orf        MAHFPGFGQS LLFGYPVYVF GDCVQGDWCP ISGGLCSARL HRHALLATCP EHQITWNPID 60
f1orf        MAHFPGFGQS LLFGYPVYVF GDCVQGDWCP ISGGLCSARL HRHALLATCP EHQITWDPID 60
c5orf        MAHFPGFGQS LLFGYPVYVF GDCVQGDWCS ISGGLCSARL HRHALLATCP EHQITWDPID 60
d2-58orf     ~~~~~~~~~~ ~~~~~~~~~~ ~~~~~~~~~~ ~~~~~~~~~~ ~~~~~~~~~~ ~~~~~~~~MV D 3
d2-58m47orf  ~~~~~~~~~~ ~~~~~~~~~~ ~~~~~~~~~~ ~~~~~~~~~~ ~~~~~~~~~~ ~~~~~~~~MV D 3

taxorf       GRVIGSALQF LIPRLPSFPT QRTSKTLKVL TPPITHTTPN IPPSFLQAVR KYSPFRNGYM 1
c6orf        GRVIGSALQF LIPRLPSFPT QRTSKTLKVL TPPITHTTPN IPPSFLQAVR KYSPFRNGYM 1
c4_2orf      GRVIGSALQF LIPRLPSFPT QRTSKTLKVL TPPITHTTPN IPPSFLQAVR KYSPFRNGYM 1
forf         GRVIGSALQF LIPRLPSFPT QRTSKTLKVL TPPITHTTPN IPPSFLQAMR KYSPFRNGYM 1
c4_1orf      GRVIGSALQF LIPRLPSFPT QRTSKTLKVL TPPITHTTPN IPPSFLQAMR KYSPFRNGYM 1
c7orf        GRVIGSALQF LIPRLPSFPT QRTSKTLKVL TPPITHTTPN IPPSFLQAMR KYSPFRNGYM 1
f1orf        GRVIGSALQF LIPRLPSFPT QRTSKTLKVL TPPITHTTPN IPPSFLQAMR KYAPFRNGYM 1
c5orf        GRVIGSALQF LIPRLPSFPT QRTSKTLKVL TPPITHTTPY IPPSFLQAMR KYSPFRNGYM 1
d2-58orf     GRVIGSALQF LIPRLPSFPT QRTSKTLKVL TPPITHTTPN IPPSFLQAVR KYSPFRNGYM 6
d2-58m47orf  GRVIGSALQF LIPRLPSFPT QRTSKTLKVL TPPITHTTPN IPPSFLQAVR KYSPFRNGYM 6

taxorf       EPTLGQHLPT LSFPDPGLRP QNLYTLWGGS VVCMYLYQLS PPITWPLLPH VVFCHPGQLG 1
c6orf        EPTLGQHLPT LSFPDPGLRP QNLYTLWGGS VVCMYLYQLS PPITWPLLPH VVFCHPGQLG 1
c4_2orf      EPTLGQHLPT LSFPDPGLRP QNLYTLWGGS VVCMYLYQLS PPITWPLLPH VVFCHPGQLG 1
forf         EPTLGQHLPT LSFPDPGLRP QNLYTLWGGS VVCMYLYQLS PPITWPLLPH VIFCHPGQLG 1
c4_1orf      EPTLGQHLPT LSFPDPGLRP QNLYTLWGGS VVCMYLCQLS PPITWPLLPH VIFCHPGQLG 1
c7orf        EPTLGQHLPT LSFPDPGLRP QNLYTLWGGS VVCMYLYQLS PPITWPLLPH VIFCHPGQLG 1
f1orf        EPTLGQHPPT LSFPDPGLRP QNLYTLWGGS VVCMYLYQLS PPITWPLLPH VIFCHPGQLG 1
c5orf        EPTLGQHLPT LSFPDPGLRP QNLYTLWGGS VVCMYLYQLS PPITWPLLPH VIFCHPGQLG 1
d2-58orf     EPTLGQHLPT LSFPDPGLRP QNLYTLWGGS VVCMYLYQLS PPITWPLLPH VVFCHPGQLG 1
d2-58m47orf  EPTLGQHLPT LSFPDPGLRP QNLYTLWGGS VVCMYLYQLS PPITWPLLPH VVFCHPGQLG 1

taxorf       AFLTNVPYKR IEELLYKISL TTGALIILPE DCLPTTLFQP VRAPVTLTAW QHGLLPFHST 2
c6orf        AFLTNVPYKR IEELLYKISL TTGALIILPE DCLPTTLFQP VRAPVTLTAW QHGLLPFHST 2
c4_2orf      AFLTNVPYKR IEELLYKISL TTGALIILPE DCLPTTLFQP VRAPVTLTAW QHGLLPFHST 2
forf         AFLTNVPYKR IEELLYKISL TTGALMILPE DCLPTTLFQP VRAPVTLTAW QNGLLPFHST 2
c4_1orf      AFLTNVPYKR IEELLYKISL TTGALIILPE DCLPTTLFQP VRAPVTLTAW QNGLLPFHST 2
c7orf        AFLNNVPYKR IEELLYKISL TTGALIILPE DCLPTTLFQP VRAPVTLTAW QNGLLPFHST 2
f1orf        AFLTNVPYKR IEELLYKISL TTGALMILPE DCLPTTLFQP VRAPVTLTAW QNGLLPFHST 2
c5orf        AFLTNVPYKR IEELLYKISL TTGALIILPE DCLPTTLFQP VRAPVTLTAW QNGLLPFHST 2
d2-58orf     AFLTNVPYKR IEELLYKISL TTGALIILPE DCLPTTLFQP VRAPVTLTAW QHGLLPFHST 1
d2-58m47orf  AFLTNVPYKR IEELLYKISL TTGALIILPE DCLPTTLFQP VRAPVTLTAW QHGLLPFHST 1
```

```
taxorf     LTTPGLIWTF TDGTPMISGP CPKDGQPSLV LQSSSFIFHK FQTKAYHPSF LLSHGLIQYS 30
c6orf      LTTPGLIWTF TDGTPMISGP CPKDGQPSLV LQSSSFIFHK FQTKAYHPSF LLSHGLIQYS 30
c4_2orf    LTTPGLIWTF TDGTPMISGP CPKDGQPSLV LQSSSFIFHK FQTKAYHPSF LLSHGLIQYS 30
forf       LTTPGLIWTF TDGTPMISGP CPKDGQPSLV LQSSSFIFHK FQTKAYHPSF LLSHGLIQYS 30
c4_1orf    LTTPGLIWTF TDGTPMISGP CPKDGQPSLV LQSSSFIFHK FQTKAYHPSF LLSHGLIQYS 30
c7orf      LTTPGLIWTF TDGTPMISGP CPKDGQPSLV LQSSSFIFHK FQTKAYHPSF LLSHGLIQYS 30
f1orf      LTTPGLIWTF TDGTPMISGP CPKDGQPSLV LQSSSFIFHK FQTKAYHPSF LLSHGLIQYS 30
c5orf      LTTPGLIWTF TDGTPMISGP CPKDGQPSLV LQSSSFIFHK FQTKAYHPSF LLSHGLIQYS 30
d2-58orf   LTTPGLIWTF TDGTPMISGP CPKDGQPSLV LQSSSFIFHK FQTKAYHPSF LLSHGLIQYS 24
d2-58m47orf LTTPGLIWTF TDGTPMISGP CPKDGQPSLV LQSSSFIFHK FQTKAYHPSF LLSHGLIQYS 24

taxorf     SFHNLHLLFE EYTNIPISLL FNEKEADDND HEPQISPGEL EPPSEKHFRE TEV* 353
c6orf      SFHNLHLLFE EYTNIPISLL FNEKEADDND HEPQISPGEL EPPSEKHFRE TEV* 353
c4_2orf    SFHNLHLLFE EYTNIPISLL FNEKEADDND HEPQISPGEL EPPSEKHFRE TEV* 353
forf       SFHNLHLLFE EYTNIPISLL FNEKEADDND HEPQISPGGL EPPSEKHFRE TEV* 353
c4_1orf    SFHNLHLLFE EYTNIPISLL FNEKEADDND HEPQISPGGL EPPSEKHFRE TEV* 353
c7orf      SFHNLHLLFE EYTNIPISLL FNEKEADDND HEPQISPGGL EPPSEKHFRE TEV* 353
f1orf      SFHNLHLLFE EYTNIPISLL FNEKEADDND HEPQISPGGL EPPSEKHFRE TEV* 353
c5orf      SFHNLHLLFE EYTNIPISLL FNEKEADDND HEPQISPGGL EPPSEKHFRE TEV* 353
d2-58orf   SFHNLHLLFE EYTNIPISLL FNEKEADDND HEPQISPGEL EPPSEKHFRE TEV* 296
d2-58m47orf SFHNLHLLFE EYTNIPISRS FNEKEADDND HEPQISPGEL EPPSEKHFRE TEV* 296
```

References:

Ahn, K., Erlander, M., Leturcq, D., Peterson, P. A., Fruh, K., and Yang, Y. (1996). In vivo characterization of the proteasome regulator PA28. J Biol Chem *271*, 18237-42.

Ahn, K., Gruhler, A., Galocha, B., Jones, T. R., Wiertz, E. J., Ploegh, H. L., Peterson, P. A., Yang, Y., and Fruh, K. (1997). The ER-luminal domain of the HCMV glycoprotein US6 inhibits peptide translocation by TAP. Immunity *6*, 613-21.

Akopian, T. N., Kisselev, A. F., and Goldberg, A. L. (1997). Processive degradation of proteins and other catalytic properties of the proteasome from Thermoplasma acidophilum. J Biol Chem *272*, 1791-8.

Altman, J. D., Moss, P. A., Goulder, P. J., Barouch, D. H., McHeyzer-Williams, M. G., Bell, J. I., McMichael, A. J., and Davis, M. M. (1996). Phenotypic analysis of antigen-specific T lymphocytes. Science *274*, 94-6.

Amsterdam, A., Pitzer, F., and Baumeister, W. (1993). Changes in intracellular localization of proteasomes in immortalized ovarian granulosa cells during mitosis associated with a role in cell cycle control. Proc Natl Acad Sci U S A *90*, 99-103.

Anton, L. C., Schubert, U., Bacik, I., Princiotta, M. F., Wearsch, P. A., Gibbs, J., Day, P. M., Realini, C., Rechsteiner, M. C., Bennink, J. R., and Yewdell, J. W. (1999). Intracellular localization of proteasomal degradation of a viral antigen. J Cell Biol *146*, 113-24.

Anton, L. C., Snyder, H. L., Bennink, J. R., Vinitsky, A., Orlowski, M., Porgador, A., and Yewdell, J. W. (1998). Dissociation of proteasomal degradation of biosynthesized viral proteins from generation of MHC class I-associated antigenic peptides. J Immunol *160*, 4859-68.

Arendt, C. S., and Hochstrasser, M. (1999). Eukaryotic 20S proteasome catalytic subunit propeptides prevent active site inactivation by N-terminal acetylation and promote particle assembly. Embo J *18*, 3575-85.

Arenzana-Seisdedos, F., Thompson, J., Rodriguez, M. S., Bachelerie, F., Thomas, D., and Hay, R. T. (1995). Inducible nuclear expression of newly synthesized I kappa B alpha negatively regulates DNA-binding and transcriptional activities of NF-kappa B. Mol Cell Biol *15*, 2689-96.

Arenzana-Seisdedos, F., Turpin, P., Rodriguez, M., Thomas, D., Hay, R. T., Virelizier, J. L., and Dargemont, C. (1997). Nuclear localization of I kappa B alpha promotes active transport of NF-kappa B from the nucleus to the cytoplasm. J Cell Sci *110*, 369-78.

Arnold, D., Driscoll, J., Androlewicz, M., Hughes, E., Cresswell, P., and Spies, T. (1992). Proteasome subunits encoded in the MHC are not generally required for the processing of peptides bound by MHC class I molecules. Nature *360*, 171-4.

Aviel, S., Winberg, G., Massucci, M., and Ciechanover, A. (2000). Degradation of the epstein-barr virus latent membrane protein 1 (LMP1) by the ubiquitin-proteasome

pathway. Targeting via ubiquitination of the N-terminal residue. J Biol Chem *275*, 23491-9.

Baeuerle, P. A., and Baltimore, D. (1988). I kappa B: a specific inhibitor of the NF-kappa B transcription factor. Science *242*, 540-6.

Baeuerle, P. A., and Baltimore, D. (1996). NF-kappa B: ten years after. Cell *87*, 13-20.

Ballard, D. W., Bohnlein, E., Lowenthal, J. W., Wano, Y., Franza, B. R., and Greene, W. C. (1988). HTLV-I tax induces cellular proteins that activate the kappa B element in the IL-2 receptor alpha gene. Science *241*, 1652-5.

Bangham, C. R. (1993). Human T-cell leukaemia virus type I and neurological disease. Curr Opin Neurobiol *3*, 773-8.

Bangham, C. R. (2000). The immune response to HTLV-I. Curr Opin Immunol *12*, 397-402.

Bangham, C. R., Daenke, S., Phillips, R. E., Cruickshank, J. K., and Bell, J. I. (1988). Enzymatic amplification of exogenous and endogenous retroviral sequences from DNA of patients with tropical spastic paraparesis. Embo J *7*, 4179-84.

Bangham, C. R., Kermode, A. G., Hall, S. E., and Daenke, S. (1996). The cytotoxic T-lymphocyte response to HTLV-1: the main determinant of disease? Seminars in Virology *7*, 41-48.

Baranger, A. M., Palmer, C. R., Hamm, M. K., Giebler, H. A., Brauweiler, A., Nyborg, J. K., and Schepartz, A. (1995). Mechanism of DNA-binding enhancement by the human T-cell leukaemia virus transactivator Tax. Nature *376*, 606-8.

Baumeister, W., Walz, J., Zuhl, F., and Seemuller, E. (1998). The proteasome: paradigm of a self-compartmentalizing protease. Cell *92*, 367-80.

Beekman, N. J., van Veelen, P. A., van Hall, T., Neisig, A., Sijts, A., Camps, M., Kloetzel, P. M., Neefjes, J. J., Melief, C. J., and Ossendorp, F. (2000). Abrogation of CTL epitope processing by single amino acid substitution flanking the C-terminal proteasome cleavage site. J Immunol *164*, 1898-905.

Beg, A. A., Sha, W. C., Bronson, R. T., and Baltimore, D. (1995). Constitutive NF-kappa B activation, enhanced granulopoiesis, and neonatal lethality in I kappa B alpha-deficient mice. Genes Dev *9*, 2736-46.

Belich, M. P., Glynne, R. J., Senger, G., Sheer, D., and Trowsdale, J. (1994). Proteasome components with reciprocal expression to that of the MHC-encoded LMP proteins. Curr Biol *4*, 769-76.

Belich, M. P., Salmeron, A., Johnston, L. H., and Ley, S. C. (1999). TPL-2 kinase regulates the proteolysis of the NF-kappaB-inhibitory protein NF-kappaB1 p105. Nature *397*, 363-8.

Ben-Shahar, S., Komlosh, A., Nadav, E., Shaked, I., Ziv, T., Admon, A., DeMartino, G. N., and Reiss, Y. (1999). 26 S proteasome-mediated production of an authentic major histocompatibility class I-restricted epitope from an intact protein substrate. J Biol Chem *274*, 21963-72.

Bence, N. F., Sampat, R. M., and Kopito, R. R. (2001). Impairment of the ubiquitin-proteasome system by protein aggregation. Science *292*, 1552-5.

Benham, A. M., Gromme, M., and Neefjes, J. (1998). Allelic differences in the relationship between proteasome activity and MHC class I peptide loading. J Immunol *161*, 83-9.

Benham, A. M., and Neefjes, J. J. (1997). Proteasome activity limits the assembly of MHC class I molecules after IFN-gamma stimulation. J Immunol *159*, 5896-904.

Beninga, J., Rock, K. L., and Goldberg, A. L. (1998). Interferon-gamma can stimulate post-proteasomal trimming of the N terminus of an antigenic peptide by inducing leucine aminopeptidase. J Biol Chem *273*, 18734-42.

Beraud, C., and Greene, W. C. (1996). Interaction of HTLV-I Tax with the human proteasome: implications for NF-kappa B induction. J Acquir Immune Defic Syndr Hum Retrovirol *13*, S76-84.

Beraud, C., Lombard-Platet, G., Michal, Y., and Jalinot, P. (1991). Binding of the HTLV-I Tax1 transactivator to the inducible 21 bp enhancer is mediated by the cellular factor HEB1. Embo J *10*, 3795-803.

Beraud, C., Sun, S. C., Ganchi, P., Ballard, D. W., and Greene, W. C. (1994). Human T-cell leukemia virus type I Tax associates with and is negatively regulated by the NF-kappa B2 p100 gene product: implications for viral latency. Mol Cell Biol *14*, 1374-82.

Bex, F., McDowall, A., Burny, A., and Gaynor, R. (1997). The human T-cell leukemia virus type 1 transactivator protein Tax colocalizes in unique nuclear structures with NF-kappaB proteins. J Virol *71*, 3484-97.

Bex, F., Murphy, K., Wattiez, R., Burny, A., and Gaynor, R. B. (1999). Phosphorylation of the human T-cell leukemia virus type 1 transactivator tax on adjacent serine residues is critical for tax activation. J Virol *73*, 738-45.

Bex, F., Yin, M. J., Burny, A., and Gaynor, R. B. (1998). Differential transcriptional activation by human T-cell leukemia virus type 1 Tax mutants is mediated by distinct interactions with CREB binding protein and p300. Mol Cell Biol *18*, 2392-405.

Biddison, W. E., Kubota, R., Kawanishi, T., Taub, D. D., Cruikshank, W. W., Center, D. M., Connor, E. W., Utz, U., and Jacobson, S. (1997). Human T cell leukemia virus type I (HTLV-I)-specific CD8+ CTL clones from patients with HTLV-I-associated neurologic disease secrete proinflammatory cytokines, chemokines, and matrix metalloproteinase. J Immunol *159*, 2018-25.

Bieganowska, K., Hollsberg, P., Buckle, G. J., Lim, D. G., Greten, T. F., Schneck, J., Altman, J. D., Jacobson, S., Ledis, S. L., Hanchard, B., Chin, J., Morgan, O., Roth, P. A., and Hafler, D. A. (1999). Direct analysis of viral-specific CD8+ T cells with soluble HLA- A2/Tax11-19 tetramer complexes in patients with human T cell lymphotropic virus-associated myelopathy. J Immunol *162*, 1765-71.

Boes, B., Hengel, H., Ruppert, T., Multhaup, G., Koszinowski, U. H., and Kloetzel, P. M. (1994). Interferon gamma stimulation modulates the proteolytic activity and cleavage site preference of 20S mouse proteasomes. J Exp Med *179*, 901-9.

Bogyo, M., Gaczynska, M., and Ploegh, H. L. (1997). Proteasome inhibitors and antigen presentation. Biopolymers *43*, 269-80.

Bose, S., Brooks, P., Mason, G. G., and Rivett, A. J. (2001). gamma-Interferon decreases the level of 26 S proteasomes and changes the pattern of phosphorylation. Biochem J *353*, 291-7.

Bose, S., Mason, G. G., and Rivett, A. J. (1999). Phosphorylation of proteasomes in mammalian cells. Mol Biol Rep *26*, 11-4.

Braun, B. C., Glickman, M., Kraft, R., Dahlmann, B., Kloetzel, P. M., Finley, D., and Schmidt, M. (1999). The base of the proteasome regulatory particle exhibits chaperone-like activity. Nat Cell Biol *1*, 221-6.

Brockman, J. A., Scherer, D. C., McKinsey, T. A., Hall, S. M., Qi, X., Lee, W. Y., and Ballard, D. W. (1995). Coupling of a signal response domain in I kappa B alpha to multiple pathways for NF-kappa B activation. Mol Cell Biol *15*, 2809-18.

Brown, K., Park, S., Kanno, T., Franzoso, G., and Siebenlist, U. (1993). Mutual regulation of the transcriptional activator NF-kappa B and its inhibitor, I kappa B-alpha. Proc Natl Acad Sci U S A *90*, 2532-6.

Burgert, H. G., and Kvist, S. (1985). An adenovirus type 2 glycoprotein blocks cell surface expression of human histocompatibility class I antigens. Cell *41*, 987-97.

Burri, L., Hockendorff, J., Boehm, U., Klamp, T., Dohmen, R. J., and Levy, F. (2000). Identification and characterization of a mammalian protein interacting with 20S proteasome precursors. Proc Natl Acad Sci U S A *97*, 10348-53.

Burton, M., Upadhyaya, C. D., Maier, B., Hope, T. J., and Semmes, O. J. (2000). Human T-cell leukemia virus type 1 Tax shuttles between functionally discrete subcellular targets. J Virol *74*, 2351-64.

Cerundolo, V., Benham, A., Braud, V., Mukherjee, S., Gould, K., Macino, B., Neefjes, J., and Townsend, A. (1997). The proteasome-specific inhibitor lactacystin blocks presentation of cytotoxic T lymphocyte epitopes in human and murine cells. Eur J Immunol *27*, 336-41.

Cerundolo, V., Kelly, A., Elliott, T., Trowsdale, J., and Townsend, A. (1995). Genes encoded in the major histocompatibility complex affecting the generation of peptides for

TAP transport [published erratum appears in Eur J Immunol 1995 May:25(5):1485]. Eur J Immunol *25*, 554-62.

Chau, V., Tobias, J. W., Bachmair, A., Marriott, D., Ecker, D. J., Gonda, D. K., and Varshavsky, A. (1989). A multiubiquitin chain is confined to specific lysine in a targeted short-lived protein. Science *243*, 1576-83.

Chen, I. S., Slamon, D. J., Rosenblatt, J. D., Shah, N. P., Quan, S. G., and Wachsman, W. (1985). The x gene is essential for HTLV replication. Science *229*, 54-8.

Chen, J. L., Dunbar, P. R., Gileadi, U., Jager, E., Gnjatic, S., Nagata, Y., Stockert, E., Panicali, D. L., Chen, Y. T., Knuth, A., Old, L. J., and Cerundolo, V. (2000). Identification of NY-ESO-1 peptide analogues capable of improved stimulation of tumor-reactive CTL. J Immunol *165*, 948-55.

Chen, P., and Hochstrasser, M. (1996). Autocatalytic subunit processing couples active site formation in the 20S proteasome to completion of assembly. Cell *86*, 961-72.

Chen, W., Anton, L. C., Bennink, J. R., and Yewdell, J. W. (2000). Dissecting the multifactorial causes of immunodominance in class I- restricted T cell responses to viruses. Immunity *12*, 83-93.

Chen, Z., Hagler, J., Palombella, V. J., Melandri, F., Scherer, D., Ballard, D., and Maniatis, T. (1995). Signal-induced site-specific phosphorylation targets I kappa B alpha to the ubiquitin-proteasome pathway. Genes Dev *9*, 1586-97.

Chen, Z. J., Parent, L., and Maniatis, T. (1996). Site-specific phosphorylation of IkappaBalpha by a novel ubiquitination- dependent protein kinase activity. Cell *84*, 853-62.

Chlichlia, K., Moldenhauer, G., Daniel, P. T., Busslinger, M., Gazzolo, L., Schirrmacher, V., and Khazaie, K. (1995). Immediate effects of reversible HTLV-1 tax function: T-cell activation and apoptosis. Oncogene *10*, 269-77.

Chu, Z. L., DiDonato, J. A., Hawiger, J., and Ballard, D. W. (1998). The tax oncoprotein of human T-cell leukemia virus type 1 associates with and persistently activates IkappaB kinases containing IKKalpha and IKKbeta. J Biol Chem *273*, 15891-4.

Chu, Z. L., Shin, Y. A., Yang, J. M., DiDonato, J. A., and Ballard, D. W. (1999). IKKgamma mediates the interaction of cellular IkappaB kinases with the tax transforming protein of human T cell leukemia virus type 1. J Biol Chem *274*, 15297-300.

Chun, A. C., Zhou, Y., Wong, C. M., Kung, H. F., Jeang, K. T., and Jin, D. Y. (2000). Coiled-coil motif as a structural basis for the interaction of HTLV type 1 Tax with cellular cofactors. AIDS Res Hum Retroviruses *16*, 1689-94.

Ciechanover, A. (1994). The ubiquitin-proteasome proteolytic pathway. Cell *79*, 13-21.

Ciechanover, A., Finley, D., and Varshavsky, A. (1984). Ubiquitin dependence of selective protein degradation demonstrated in the mammalian cell cycle mutant ts85. Cell *37*, 57-66.

Ciminale, V., Pavlakis, G. N., Derse, D., Cunningham, C. P., and Felber, B. K. (1992). Complex splicing in the human T-cell leukemia virus (HTLV) family of retroviruses: novel mRNAs and proteins produced by HTLV type I. J Virol *66*, 1737-45.

Cohen, L., Henzel, W. J., and Baeuerle, P. A. (1998). IKAP is a scaffold protein of the IkappaB kinase complex [see comments]. Nature *395*, 292-6.

Coscoy, L., Gonzalez-Dunia, D., Tangy, F., Syan, S., Brahic, M., and Ozden, S. (1998). Molecular mechanism of tumorigenesis in mice transgenic for the human T cell leukemia virus Tax gene. Virology *248*, 332-41.

Craiu, A., Akopian, T., Goldberg, A., and Rock, K. L. (1997). Two distinct proteolytic processes in the generation of a major histocompatibility complex class I-presented peptide. Proc Natl Acad Sci U S A *94*, 10850-5.

Craiu, A., Gaczynska, M., Akopian, T., Gramm, C. F., Fenteany, G., Goldberg, A. L., and Rock, K. L. (1997). Lactacystin and clasto-lactacystin beta-lactone modify multiple proteasome beta-subunits and inhibit intracellular protein degradation and major histocompatibility complex class I antigen presentation. J Biol Chem *272*, 13437-45.

Daenke, S., and Bangham, C. R. (1994). Do T cells cause HTLV-1-associated disease?: a taxing problem [editorial]. Clin Exp Immunol *96*, 179-81.

Daenke, S., Kermode, A. G., Hall, S. E., Taylor, G., Weber, J., Nightingale, S., and Bangham, C. R. (1996). High activated and memory cytotoxic T-cell responses to HTLV-1 in healthy carriers and patients with tropical spastic paraparesis. Virology *217*, 139-46.

Daenke, S., McCracken, S. A., and Booth, S. (1999). Human T-cell leukaemia/lymphoma virus type 1 syncytium formation is regulated in a cell-specific manner by ICAM-1, ICAM-3 and VCAM-1 and can be inhibited by antibodies to integrin beta2 or beta7. J Gen Virol *80*, 1429-36.

Daenke, S., Nightingale, S., Cruickshank, J. K., and Bangham, C. R. (1990). Sequence variants of human T-cell lymphotropic virus type I from patients with tropical spastic paraparesis and adult T-cell leukemia do not distinguish neurological from leukemic isolates. J Virol *64*, 1278-82.

Davis, M. M., and Bjorkman, P. J. (1988). T-cell antigen receptor genes and T-cell recognition. Nature *334*, 395-402.

DeMars, R., Chang, C. C., Shaw, S., Reitnauer, P. J., and Sondel, P. M. (1984). Homozygous deletions that simultaneously eliminate expressions of class I and class II antigens of EBV-transformed B-lymphoblastoid cells. I. Reduced proliferative responses of autologous and allogeneic T cells to mutant cells that have decreased expression of class II antigens. Hum Immunol *11*, 77-97.

Deng, Y., Yewdell, J. W., Eisenlohr, L. C., and Bennink, J. R. (1997). MHC affinity, peptide liberation, T cell repertoire, and immunodominance all contribute to the paucity of MHC class I-restricted peptides recognized by antiviral CTL. J Immunol *158*, 1507-15.

Deveraux, Q., Ustrell, V., Pickart, C., and Rechsteiner, M. (1994). A 26 S protease subunit that binds ubiquitin conjugates. J Biol Chem *269*, 7059-61.

Dick, L. R., Aldrich, C., Jameson, S. C., Moomaw, C. R., Pramanik, B. C., Doyle, C. K., DeMartino, G. N., Bevan, M. J., Forman, J. M., and Slaughter, C. A. (1994). Proteolytic processing of ovalbumin and beta-galactosidase by the proteasome to a yield antigenic peptides. J Immunol *152*, 3884-94.

Dick, L. R., Cruikshank, A. A., Destree, A. T., Grenier, L., McCormack, T. A., Melandri, F. D., Nunes, S. L., Palombella, V. J., Parent, L. A., Plamondon, L., and Stein, R. L. (1997). Mechanistic studies on the inactivation of the proteasome by lactacystin in cultured cells. J Biol Chem *272*, 182-8.

Dick, T. P., Nussbaum, A. K., Deeg, M., Heinemeyer, W., Groll, M., Schirle, M., Keilholz, W., Stevanovic, S., Wolf, D. H., Huber, R., Rammensee, H. G., and Schild, H. (1998). Contribution of proteasomal beta-subunits to the cleavage of peptide substrates analyzed with yeast mutants. J Biol Chem *273*, 25637-46.

Dick, T. P., Ruppert, T., Groettrup, M., Kloetzel, P. M., Kuehn, L., Koszinowski, U. H., Stevanovic, S., Schild, H., and Rammensee, H. G. (1996). Coordinated dual cleavages induced by the proteasome regulator PA28 lead to dominant MHC ligands. Cell *86*, 253-62.

DiDonato, J. A., Hayakawa, M., Rothwarf, D. M., Zandi, E., and Karin, M. (1997). A cytokine-responsive IkappaB kinase that activates the transcription factor NF-kappaB [see comments]. Nature *388*, 548-54.

Ding, Y. H., Baker, B. M., Garboczi, D. N., Biddison, W. E., and Wiley, D. C. (1999). Four A6-TCR/peptide/HLA-A2 structures that generate very different T cell signals are nearly identical. Immunity *11*, 45-56.

Ding, Y. H., Smith, K. J., Garboczi, D. N., Utz, U., Biddison, W. E., and Wiley, D. C. (1998). Two human T cell receptors bind in a similar diagonal mode to the HLA-A2/Tax peptide complex using different TCR amino acids. Immunity *8*, 403-11.

Driscoll, J., Brown, M. G., Finley, D., and Monaco, J. J. (1993). MHC-linked LMP gene products specifically alter peptidase activities of the proteasome [see comments]. Nature *365*, 262-4.

Dunbar, P. R., Chen, J. L., Chao, D., Rust, N., Teisserenc, H., Ogg, G. S., Romero, P., Weynants, P., and Cerundolo, V. (1999). Cutting edge: rapid cloning of tumor-specific CTL suitable for adoptive immunotherapy of melanoma. J Immunol *162*, 6959-62.

Dunbar, P. R., Ogg, G. S., Chen, J., Rust, N., van der Bruggen, P., and Cerundolo, V. (1998). Direct isolation, phenotyping and cloning of low-frequency antigen-specific cytotoxic T lymphocytes from peripheral blood. Curr Biol *8*, 413-6.

Elias, S., Bercovich, B., Kahana, C., Coffino, P., Fischer, M., Hilt, W., Wolf, D. H., and Ciechanover, A. (1995). Degradation of ornithine decarboxylase by the mammalian and yeast 26S proteasome complexes requires all the components of the protease. Eur J Biochem *229*, 276-83.

Elliott, T., Willis, A., Cerundolo, V., and Townsend, A. (1995). Processing of major histocompatibility class I-restricted antigens in the endoplasmic reticulum. J Exp Med *181*, 1481-91.

Elovaara, I., Koenig, S., Brewah, A. Y., Woods, R. M., Lehky, T., and Jacobson, S. (1993). High human T cell lymphotropic virus type 1 (HTLV-1)-specific precursor cytotoxic T lymphocyte frequencies in patients with HTLV-1-associated neurological disease. J Exp Med *177*, 1567-73.

Elovaara, I., Utz, U., Smith, S., and Jacobson, S. (1995). Limited T cell receptor usage by HTLV-I tax-specific, HLA class I restricted cytotoxic T lymphocytes from patients with HTLV-I associated neurological disease. J Neuroimmunol *63*, 47-53.

Etlinger, J. D., and Goldberg, A. L. (1977). A soluble ATP-dependent proteolytic system responsible for the degradation of abnormal proteins in reticulocytes. Proc Natl Acad Sci U S A *74*, 54-8.

Ey, P. L., Prowse, S. J., and Jenkin, C. R. (1978). Isolation of pure IgG1, IgG2a and IgG2b immunoglobulins from mouse serum using protein A-sepharose. Immunochemistry *15*, 429-36.

Eytan, E., Armon, T., Heller, H., Beck, S., and Hershko, A. (1993). Ubiquitin C-terminal hydrolase activity associated with the 26 S protease complex. J Biol Chem *268*, 4668-74.

Fabunmi, R. P., Wigley, W. C., Thomas, P. J., and DeMartino, G. N. (2000). Activity and regulation of the centrosome-associated proteasome. J Biol Chem *275*, 409-13.

Fabunmi, R. P., Wigley, W. C., Thomas, P. J., and DeMartino, G. N. (2001). Interferon gamma regulates accumulation of the proteasome activator PA28 and immunoproteasomes at nuclear PML bodies. J Cell Sci *114*, 29-36.

Falk, K., Rotzschke, O., and Rammensee, H. G. (1990). Cellular peptide composition governed by major histocompatibility complex class I molecules [see comments]. Nature *348*, 248-51.

Fan, C. M., and Maniatis, T. (1991). Generation of p50 subunit of NF-kappa B by processing of p105 through an ATP-dependent pathway. Nature *354*, 395-8.

Fehling, H. J., Swat, W., Laplace, C., Kuhn, R., Rajewsky, K., Muller, U., and von Boehmer, H. (1994). MHC class I expression in mice lacking the proteasome subunit LMP-7. Science *265*, 1234-7.

Feldherr, C. M., Kallenbach, E., and Schultz, N. (1984). Movement of a karyophilic protein through the nuclear pores of oocytes. J Cell Biol *99*, 2216-22.

Fenteany, G., Standaert, R. F., Lane, W. S., Choi, S., Corey, E. J., and Schreiber, S. L. (1995). Inhibition of proteasome activities and subunit-specific amino-terminal threonine modification by lactacystin. Science *268*, 726-31.

Fischer, M., Runkel, L., and Schaller, H. (1995). HBx protein of hepatitis B virus interacts with the C-terminal portion of a novel human proteasome alpha-subunit. Virus Genes *10*, 99-102.

Fujii, M., Sassone-Corsi, P., and Verma, I. M. (1988). c-fos promoter trans-activation by the tax1 protein of human T-cell leukemia virus type I. Proc Natl Acad Sci U S A *85*, 8526-30.

Fujii, M., Tsuchiya, H., Chuhjo, T., Akizawa, T., and Seiki, M. (1992). Interaction of HTLV-1 Tax1 with p67SRF causes the aberrant induction of cellular immediate early genes through CArG boxes. Genes Dev *6*, 2066-76.

Gaczynska, M., Rock, K. L., and Goldberg, A. L. (1993). Gamma-interferon and expression of MHC genes regulate peptide hydrolysis by proteasomes [see comments] [published erratum appears in Nature 1995 Mar 16;374(6519):290]. Nature *365*, 264-7.

Gaczynska, M., Rock, K. L., Spies, T., and Goldberg, A. L. (1994). Peptidase activities of proteasomes are differentially regulated by the major histocompatibility complex-encoded genes for LMP2 and LMP7. Proc Natl Acad Sci U S A *91*, 9213-7.

Garboczi, D. N., Ghosh, P., Utz, U., Fan, Q. R., Biddison, W. E., and Wiley, D. C. (1996). Structure of the complex between human T-cell receptor, viral peptide and HLA-A2. Nature *384*, 134-41.

Garboczi, D. N., Hung, D. T., and Wiley, D. C. (1992). HLA-A2-peptide complexes: refolding and crystallization of molecules expressed in Escherichia coli and complexed with single antigenic peptides. Proc Natl Acad Sci U S A *89*, 3429-33.

Garcia, K. C., Degano, M., Stanfield, R. L., Brunmark, A., Jackson, M. R., Peterson, P. A., Teyton, L., and Wilson, I. A. (1996). An alphabeta T cell receptor structure at 2.5 A and its orientation in the TCR-MHC complex. Science *274*, 209-19.

Garcia-Mata, R., Bebok, Z., Sorscher, E. J., and Sztul, E. S. (1999). Characterization and dynamics of aggresome formation by a cytosolic GFP- chimera. J Cell Biol *146*, 1239-54.

Geier, E., Pfeifer, G., Wilm, M., Lucchiari-Hartz, M., Baumeister, W., Eichmann, K., and Niedermann, G. (1999). A giant protease with potential to substitute for some functions of the proteasome. Science *283*, 978-81.

Geleziunas, R., Ferrell, S., Lin, X., Mu, Y., Cunningham, E. T., Jr., Grant, M., Connelly, M. A., Hambor, J. E., Marcu, K. B., and Greene, W. C. (1998). Human T-cell leukemia

virus type 1 Tax induction of NF-kappaB involves activation of the IkappaB kinase alpha (IKKalpha) and IKKbeta cellular kinases. Mol Cell Biol *18*, 5157-65.

Germain, R. N. (1994). MHC-dependent antigen processing and peptide presentation: providing ligands for T lymphocyte activation. Cell *76*, 287-99.

Gessain, A., Barin, F., Vernant, J. C., Gout, O., Maurs, L., Calender, A., and de The, G. (1985). Antibodies to human T-lymphotropic virus type-I in patients with tropical spastic paraparesis. Lancet *2*, 407-10.

Ghislain, M., Udvardy, A., and Mann, C. (1993). S. cerevisiae 26S protease mutants arrest cell division in G2/metaphase. Nature *366*, 358-62.

Ghosh, G., van Duyne, G., Ghosh, S., and Sigler, P. B. (1995). Structure of NF-kappa B p50 homodimer bound to a kappa B site [see comments]. Nature *373*, 303-10.

Gileadi, U., Moins-Teisserenc, H. T., Correa, I., Booth, B. L., Dunbar, P. R., Sewell, A. K., Trowsdale, J., Phillips, R. E., and Cerundolo, V. (1999). Generation of an immunodominant CTL epitope is affected by proteasome subunit composition and stability of the antigenic protein. J Immunol *163*, 6045-52.

Gitlin, S. D., Lindholm, P. F., Marriott, S. J., and Brady, J. N. (1991). Transdominant human T-cell lymphotropic virus type I TAX1 mutant that fails to localize to the nucleus. J Virol *65*, 2612-21.

Glas, R., Bogyo, M., McMaster, J. S., Gaczynska, M., and Ploegh, H. L. (1998). A proteolytic system that compensates for loss of proteasome function. Nature *392*, 618-22.

Glickman, M. H., Rubin, D. M., Coux, O., Wefes, I., Pfeifer, G., Cjeka, Z., Baumeister, W., Fried, V. A., and Finley, D. (1998). A subcomplex of the proteasome regulatory particle required for ubiquitin-conjugate degradation and related to the COP9-signalosome and eIF3. Cell *94*, 615-23.

Glotzer, M., Murray, A. W., and Kirschner, M. W. (1991). Cyclin is degraded by the ubiquitin pathway [see comments]. Nature *349*, 132-8.

Goth, S., Nguyen, V., and Shastri, N. (1996). Generation of naturally processed peptide/MHC class I complexes is independent of the stability of endogenously synthesized precursors. J Immunol *157*, 1894-904.

Grant, E. P., Michalek, M. T., Goldberg, A. L., and Rock, K. L. (1995). Rate of antigen degradation by the ubiquitin-proteasome pathway influences MHC class I presentation. J Immunol *155*, 3750-8.

Greten, T. F., Slansky, J. E., Kubota, R., Soldan, S. S., Jaffee, E. M., Leist, T. P., Pardoll, D. M., Jacobson, S., and Schneck, J. P. (1998). Direct visualization of antigen-specific T cells: HTLV-1 Tax11-19- specific CD8(+) T cells are activated in peripheral blood and accumulate in cerebrospinal fluid from HAM/TSP patients. Proc Natl Acad Sci U S A *95*, 7568-73.

Grassmann, R., Dengler, C., Muller-Fleckenstein, I., Fleckenstein, B., McGuire, K., Dokhelar, M. C., Sodroski, J. G., and Haseltine, W. A. (1989). Transformation to continuous growth of primary human T lymphocytes by human T-cell leukemia virus type I X-region genes transduced by a Herpesvirus saimiri vector. Proc Natl Acad Sci U S A *86*, 3351-5.

Greten, T. F., Slansky, J. E., Kubota, R., Soldan, S. S., Jaffee, E. M., Leist, T. P., Pardoll, D. M., Jacobson, S., and Schneck, J. P. (1998). Direct visualization of antigen-specific T cells: HTLV-1 Tax11-19- specific CD8(+) T cells are activated in peripheral blood and accumulate in cerebrospinal fluid from HAM/TSP patients. Proc Natl Acad Sci U S A *95*, 7568-73.

Griffin, T. A., Nandi, D., Cruz, M., Fehling, H. J., Kaer, L. V., Monaco, J. J., and Colbert, R. A. (1998). Immunoproteasome assembly: cooperative incorporation of interferon gamma (IFN-gamma)-inducible subunits. J Exp Med *187*, 97-104.

Groettrup, M., Kraft, R., Kostka, S., Standera, S., Stohwasser, R., and Kloetzel, P. M. (1996). A third interferon-gamma-induced subunit exchange in the 20S proteasome. Eur J Immunol *26*, 863-9.

Groettrup, M., Ruppert, T., Kuehn, L., Seeger, M., Standera, S., Koszinowski, U., and Kloetzel, P. M. (1995). The interferon-gamma-inducible 11 S regulator (PA28) and the LMP2/LMP7 subunits govern the peptide production by the 20 S proteasome in vitro. J Biol Chem *270*, 23808-15.

Groettrup, M., Soza, A., Eggers, M., Kuehn, L., Dick, T. P., Schild, H., Rammensee, H. G., Koszinowski, U. H., and Kloetzel, P. M. (1996). A role for the proteasome regulator PA28alpha in antigen presentation. Nature *381*, 166-8.

Groettrup, M., Standera, S., Stohwasser, R., and Kloetzel, P. M. (1997). The subunits MECL-1 and LMP2 are mutually required for incorporation into the 20S proteasome. Proc Natl Acad Sci U S A *94*, 8970-5.

Groll, M., Bajorek, M., Kohler, A., Moroder, L., Rubin, D. M., Huber, R., Glickman, M. H., and Finley, D. (2000). A gated channel into the proteasome core particle. Nat Struct Biol *7*, 1062-7.

Groll, M., Ditzel, L., Lowe, J., Stock, D., Bochtler, M., Bartunik, H. D., and Huber, R. (1997). Structure of 20S proteasome from yeast at 2.4 A resolution [see comments]. Nature *386*, 463-71.

Groll, M., Heinemeyer, W., Jager, S., Ullrich, T., Bochtler, M., Wolf, D. H., and Huber, R. (1999). The catalytic sites of 20S proteasomes and their role in subunit maturation: a mutational and crystallographic study. Proc Natl Acad Sci U S A *96*, 10976-83.

Gronostajski, R. M., Pardee, A. B., and Goldberg, A. L. (1985). The ATP dependence of the degradation of short- and long-lived proteins in growing fibroblasts. J Biol Chem *260*, 3344-9.

Grossman, W. J., Kimata, J. T., Wong, F. H., Zutter, M., Ley, T. J., and Ratner, L. (1995). Development of leukemia in mice transgenic for the tax gene of human T- cell leukemia virus type I. Proc Natl Acad Sci U S A *92*, 1057-61.

Gui, J. F., Tronchere, H., Chandler, S. D., and Fu, X. D. (1994). Purification and characterization of a kinase specific for the serine- and arginine-rich pre-mRNA splicing factors. Proc Natl Acad Sci U S A *91*, 10824-8.

Hanly, S. M., Rimsky, L. T., Malim, M. H., Kim, J. H., Hauber, J., Duc Dodon, M., Le, S. Y., Maizel, J. V., Cullen, B. R., and Greene, W. C. (1989). Comparative analysis of the HTLV-I Rex and HIV-1 Rev trans-regulatory proteins and their RNA response elements. Genes Dev *3*, 1534-44.

Hanon, E., Hall, S., Taylor, G. P., Saito, M., Davis, R., Tanaka, Y., Usuku, K., Osame, M., Weber, J. N., and Bangham, C. R. (2000). Abundant tax protein expression in CD4+ T cells infected with human T- cell lymphotropic virus type I (HTLV-I) is prevented by cytotoxic T lymphocytes. Blood *95*, 1386-92.

Hanon, E., Stinchcombe, J. C., Saito, M., Asquith, B. E., Taylor, G. P., Tanaka, Y., Weber, J. N., Griffiths, G. M., and Bangham, C. R. (2000). Fratricide among CD8(+) T lymphocytes naturally infected with human T cell lymphotropic virus type I. Immunity *13*, 657-64.

Harada, S., Koyanagi, Y., and Yamamoto, N. (1985). Infection of HTLV-III/LAV in HTLV-I-carrying cells MT-2 and MT-4 and application in a plaque assay. Science *229*, 563-6.

Harhaj, E. W., and Sun, S. C. (1999). IKKgamma serves as a docking subunit of the IkappaB kinase (IKK) and mediates interaction of IKK with the human T-cell leukemia virus Tax protein. J Biol Chem *274*, 22911-4.

Hausmann, S., Biddison, W. E., Smith, K. J., Ding, Y. H., Garboczi, D. N., Utz, U., Wiley, D. C., and Wucherpfennig, K. W. (1999). Peptide recognition by two HLA-A2/Tax11-19-specific T cell clones in relationship to their MHC/peptide/TCR crystal structures. J Immunol *162*, 5389-97.

Heinemeyer, W., Fischer, M., Krimmer, T., Stachon, U., and Wolf, D. H. (1997). The active sites of the eukaryotic 20 S proteasome and their involvement in subunit precursor processing. J Biol Chem *272*, 25200-9.

Heissmeyer, V., Krappmann, D., Wulczyn, F. G., and Scheidereit, C. (1999). NF-kappaB p105 is a target of IkappaB kinases and controls signal induction of Bcl-3-p50 complexes. Embo J *18*, 4766-78.

Hendil, K. B., Kristensen, P., and Uerkvitz, W. (1995). Human proteasomes analysed with monoclonal antibodies. Biochem J *305*, 245-52.

Hershko, A., and Ciechanover, A. (1998). The ubiquitin system. Annu Rev Biochem *67*, 425-79.

Hidaka, M., Inoue, J., Yoshida, M., and Seiki, M. (1988). Post-transcriptional regulator (rex) of HTLV-1 initiates expression of viral structural proteins but suppresses expression of regulatory proteins. Embo J *7*, 519-23.

Hill, A., Jugovic, P., York, I., Russ, G., Bennink, J., Yewdell, J., Ploegh, H., and Johnson, D. (1995). Herpes simplex virus turns off the TAP to evade host immunity. Nature *375*, 411-5.

Hirai, H., Fujisawa, J., Suzuki, T., Ueda, K., Muramatsu, M., Tsuboi, A., Arai, N., and Yoshida, M. (1992). Transcriptional activator Tax of HTLV-1 binds to the NF-kappa B precursor p105. Oncogene *7*, 1737-42.

Hirai, H., Suzuki, T., Fujisawa, J., Inoue, J., and Yoshida, M. (1994). Tax protein of human T-cell leukemia virus type I binds to the ankyrin motifs of inhibitory factor kappa B and induces nuclear translocation of transcription factor NF-kappa B proteins for transcriptional activation. Proc Natl Acad Sci U S A *91*, 3584-8.

Hirsch, C., and Ploegh, H. L. (2000). Intracellular targeting of the proteasome. Trends Cell Biol *10*, 268-72.

Hisamatsu, H., Shimbara, N., Saito, Y., Kristensen, P., Hendil, K. B., Fujiwara, T., Takahashi, E., Tanahashi, N., Tamura, T., Ichihara, A., and Tanaka, K. (1996). Newly identified pair of proteasomal subunits regulated reciprocally by interferon gamma. J Exp Med *183*, 1807-16.

Hochstrasser, M., and Varshavsky, A. (1990). In vivo degradation of a transcriptional regulator: the yeast alpha 2 repressor. Cell *61*, 697-708.

Hu, Z., Zhang, Z., Doo, E., Coux, O., Goldberg, A. L., and Liang, T. J. (1999). Hepatitis B virus X protein is both a substrate and a potential inhibitor of the proteasome complex. J Virol *73*, 7231-40.

Huang, J., Kwong, J., Sun, E. C., and Liang, T. J. (1996). Proteasome complex as a potential cellular target of hepatitis B virus X protein. J Virol *70*, 5582-91.

Huxford, T., Huang, D. B., Malek, S., and Ghosh, G. (1998). The crystal structure of the IkappaBalpha/NF-kappaB complex reveals mechanisms of NF-kappaB inactivation [see comments]. Cell *95*, 759-70.

Inoue, J., Seiki, M., Taniguchi, T., Tsuru, S., and Yoshida, M. (1986). Induction of interleukin 2 receptor gene expression by p40x encoded by human T-cell leukemia virus type 1. Embo J *5*, 2883-8.

Inoue, J., Yoshida, M., and Seiki, M. (1987). Transcriptional (p40x) and post-transcriptional (p27x-III) regulators are required for the expression and replication of human T-cell leukemia virus type I genes. Proc Natl Acad Sci U S A *84*, 3653-7.

Jacobs, M. D., and Harrison, S. C. (1998). Structure of an IkappaBalpha/NF-kappaB complex [see comments]. Cell *95*, 749-58.

Jacobson, S., Shida, H., McFarlin, D. E., Fauci, A. S., and Koenig, S. (1990). Circulating CD8+ cytotoxic T lymphocytes specific for HTLV-I pX in patients with HTLV-I associated neurological disease. Nature *348*, 245-8.

Jeffery, K. J., Usuku, K., Hall, S. E., Matsumoto, W., Taylor, G. P., Procter, J., Bunce, M., Ogg, G. S., Welsh, K. I., Weber, J. N., Lloyd, A. L., Nowak, M. A., Nagai, M., Kodama, D., Izumo, S., Osame, M., and Bangham, C. R. (1999). HLA alleles determine human T-lymphotropic virus-I (HTLV-I) proviral load and the risk of HTLV-I-associated myelopathy. Proc Natl Acad Sci U S A *96*, 3848-53.

Jin, D. Y., Giordano, V., Kibler, K. V., Nakano, H., and Jeang, K. T. (1999). Role of adapter function in oncoprotein-mediated activation of NF- kappaB. Human T-cell leukemia virus type I Tax interacts directly with IkappaB kinase gamma. J Biol Chem *274*, 17402-5.

Jin, D. Y., Spencer, F., and Jeang, K. T. (1998). Human T cell leukemia virus type 1 oncoprotein Tax targets the human mitotic checkpoint protein MAD1. Cell *93*, 81-91.

Johnston, J. A., Ward, C. L., and Kopito, R. R. (1998). Aggresomes: a cellular response to misfolded proteins. J Cell Biol *143*, 1883-98.

Jones, T. R., Wiertz, E. J., Sun, L., Fish, K. N., Nelson, J. A., and Ploegh, H. L. (1996). Human cytomegalovirus US3 impairs transport and maturation of major histocompatibility complex class I heavy chains. Proc Natl Acad Sci U S A *93*, 11327-33.

Karin, M., and Ben-Neriah, Y. (2000). Phosphorylation meets ubiquitination: the control of NF-[kappa]B activity. Annu Rev Immunol *18*, 621-63.

Kelly, A., Powis, S. H., Kerr, L. A., Mockridge, I., Elliott, T., Bastin, J., Uchanska-Ziegler, B., Ziegler, A., Trowsdale, J., and Townsend, A. (1992). Assembly and function of the two ABC transporter proteins encoded in the human major histocompatibility complex. Nature *355*, 641-4.

Kinoshita, T., Shimoyama, M., Tobinai, K., Ito, M., Ito, S., Ikeda, S., Tajima, K., Shimotohno, K., and Sugimura, T. (1989). Detection of mRNA for the tax1/rex1 gene of human T-cell leukemia virus type I in fresh peripheral blood mononuclear cells of adult T-cell leukemia patients and viral carriers by using the polymerase chain reaction. Proc Natl Acad Sci U S A *86*, 5620-4.

Kisselev, A. F., Akopian, T. N., Castillo, V., and Goldberg, A. L. (1999). Proteasome active sites allosterically regulate each other, suggesting a cyclical bite-chew mechanism for protein breakdown. Mol Cell *4*, 395-402.

Kisselev, A. F., Akopian, T. N., and Goldberg, A. L. (1998). Range of sizes of peptide products generated during degradation of different proteins by archaeal proteasomes. J Biol Chem *273*, 1982-9.

Kisselev, A. F., Akopian, T. N., Woo, K. M., and Goldberg, A. L. (1999). The sizes of peptides generated from protein by mammalian 26 and 20 S proteasomes. Implications

for understanding the degradative mechanism and antigen presentation. J Biol Chem *274*, 3363-71.

Kiyokawa, T., Seiki, M., Iwashita, S., Imagawa, K., Shimizu, F., and Yoshida, M. (1985). p27x-III and p21x-III, proteins encoded by the pX sequence of human T- cell leukemia virus type I. Proc Natl Acad Sci U S A *82*, 8359-63.

Kleijnen, M. F., Shih, A. H., Zhou, P., Kumar, S., Soccio, R. E., Kedersha, N. L., Gill, G., and Howley, P. M. (2000). The hPLIC proteins may provide a link between the ubiquitination machinery and the proteasome. Mol Cell *6*, 409-19.

Knowlton, J. R., Johnston, S. C., Whitby, F. G., Realini, C., Zhang, Z., Rechsteiner, M., and Hill, C. P. (1997). Structure of the proteasome activator REGalpha (PA28alpha). Nature *390*, 639-43.

Kobayashi, N., Konishi, H., Sabe, H., Shigesada, K., Noma, T., Honjo, T., and Hatanaka, M. (1984). Genomic structure of HTLV (human T-cell leukemia virus): detection of defective genome and its amplification in MT-2 cells. Embo J *3*, 1339-43.

Koegl, M., Hoppe, T., Schlenker, S., Ulrich, H. D., Mayer, T. U., and Jentsch, S. (1999). A novel ubiquitination factor, E4, is involved in multiubiquitin chain assembly. Cell *96*, 635-44.

Koralnik, I. J., Gessain, A., Klotman, M. E., Lo Monico, A., Berneman, Z. N., and Franchini, G. (1992). Protein isoforms encoded by the pX region of human T-cell leukemia/lymphotropic virus type I. Proc Natl Acad Sci U S A *89*, 8813-7.

Krappmann, D., Wulczyn, F. G., and Scheidereit, C. (1996). Different mechanisms control signal-induced degradation and basal turnover of the NF-kappaB inhibitor IkappaB alpha in vivo. Embo J *15*, 6716-26.

Kubota, R., Kawanishi, T., Matsubara, H., Manns, A., and Jacobson, S. (1998). Demonstration of human T lymphotropic virus type I (HTLV-I) tax- specific CD8+ lymphocytes directly in peripheral blood of HTLV-I- associated myelopathy/tropical spastic paraparesis patients by intracellular cytokine detection. J Immunol *161*, 482-8.

Kubota, R., Nagai, M., Kawanishi, T., Osame, M., and Jacobson, S. (2000). Increased HTLV type 1 tax specific CD8+ cells in HTLV type 1-asociated myelopathy/tropical spastic paraparesis: correlation with HTLV type 1 proviral load. AIDS Res Hum Retroviruses *16*, 1705-9.

Kuby. (1994). Immunology, Second Edition (New York: W.H Freeman and company).

Kwok, R. P., Laurance, M. E., Lundblad, J. R., Goldman, P. S., Shih, H., Connor, L. M., Marriott, S. J., and Goodman, R. H. (1996). Control of cAMP-regulated enhancers by the viral transactivator Tax through CREB and the co-activator CBP. Nature *380*, 642-6.

Lal, R. B., Giam, C. Z., Coligan, J. E., and Rudolph, D. L. (1994). Differential immune responsiveness to the immunodominant epitopes of regulatory proteins (tax and rex) in

human T cell lymphotropic virus type I-associated myelopathy. J Infect Dis *169*, 496-503.

Lee, D. H., and Goldberg, A. L. (1998). Proteasome inhibitors: valuable new tools for cell biologists. Trends Cell Biol *8*, 397-403.

Lee, F. S., Hagler, J., Chen, Z. J., and Maniatis, T. (1997). Activation of the IkappaB alpha kinase complex by MEKK1, a kinase of the JNK pathway. Cell *88*, 213-22.

Lemasson, I., and Nyborg, J. K. (2001). Human T-cell Leukemia Virus Type I Tax Repression of p73beta Is Mediated through Competition for the C/H1 Domain of CBP. J Biol Chem *276*, 15720-7.

Levin, M. C., and Jacobson, S. (1997). HTLV-I associated myelopathy/tropical spastic paraparesis (HAM/TSP): a chronic progressive neurologic disease associated with immunologically mediated damage to the central nervous system. J Neurovirol *3*, 126-40.

Levitskaya, J., Coram, M., Levitsky, V., Imreh, S., Steigerwald-Mullen, P. M., Klein, G., Kurilla, M. G., and Masucci, M. G. (1995). Inhibition of antigen processing by the internal repeat region of the Epstein-Barr virus nuclear antigen-1. Nature *375*, 685-8.

Levitskaya, J., Sharipo, A., Leonchiks, A., Ciechanover, A., and Masucci, M. G. (1997). Inhibition of ubiquitin/proteasome-dependent protein degradation by the Gly-Ala repeat domain of the Epstein-Barr virus nuclear antigen 1. Proc Natl Acad Sci U S A *94*, 12616-21.

Li, N., Lerea, K. M., and Etlinger, J. D. (1996). Phosphorylation of the proteasome activator PA28 is required for proteasome activation. Biochem Biophys Res Commun *225*, 855-60.

Lin, L., DeMartino, G. N., and Greene, W. C. (1998). Cotranslational biogenesis of NF-kappaB p50 by the 26S proteasome. Cell *92*, 819-28.

Lin, L., and Ghosh, S. (1996). A glycine-rich region in NF-kappaB p105 functions as a processing signal for the generation of the p50 subunit. Mol Cell Biol *16*, 2248-54.

Lopez, D., and Del Val, M. (1997). Selective involvement of proteasomes and cysteine proteases in MHC class I antigen presentation. J Immunol *159*, 5769-72.

Lopez, D., Gil-Torregrosa, B. C., Bergmann, C., and Del Val, M. (2000). Sequential cleavage by metallopeptidases and proteasomes is involved in processing HIV-1 ENV epitope for endogenous MHC class I antigen presentation. J Immunol *164*, 5070-7.

Luckey, C. J., King, G. M., Marto, J. A., Venketeswaran, S., Maier, B. F., Crotzer, V. L., Colella, T. A., Shabanowitz, J., Hunt, D. F., and Engelhard, V. H. (1998). Proteasomes can either generate or destroy MHC class I epitopes: evidence for nonproteasomal epitope generation in the cytosol. J Immunol *161*, 112-21.

Ma, C. P., Slaughter, C. A., and DeMartino, G. N. (1992). Identification, purification, and characterization of a protein activator (PA28) of the 20 S proteasome (macropain). J Biol Chem *267*, 10515-23.

Madden, D. R., Garboczi, D. N., and Wiley, D. C. (1993). The antigenic identity of peptide-MHC complexes: a comparison of the conformations of five viral peptides presented by HLA-A2. Cell *75*, 693-708.

Maggirwar, S. B., Harhaj, E., and Sun, S. C. (1995). Activation of NF-kappa B/Rel by Tax involves degradation of I kappa B alpha and is blocked by a proteasome inhibitor. Oncogene *11*, 993-8.

Mason, G. G., Hendil, K. B., and Rivett, A. J. (1996). Phosphorylation of proteasomes in mammalian cells. Identification of two phosphorylated subunits and the effect of phosphorylation on activity. Eur J Biochem *238*, 453-62.

Matsuoka, E., Takenouchi, N., Hashimoto, K., Kashio, N., Moritoyo, T., Higuchi, I., Isashiki, Y., Sato, E., Osame, M., and Izumo, S. (1998). Perivascular T cells are infected with HTLV-I in the spinal cord lesions with HTLV-I-associated myelopathy/tropical spastic paraparesis: double staining of immunohistochemistry and polymerase chain reaction in situ hybridization. Acta Neuropathol (Berl) *96*, 340-6.

Mattaj, I. W., and Englmeier, L. (1998). Nucleocytoplasmic transport: the soluble phase. Annu Rev Biochem *67*, 265-306.

Mattsson, K., Pokrovskaja, K., Kiss, C., Klein, G., and Szekely, L. (2001). Proteins associated with the promyelocytic leukemia gene product (PML)-containing nuclear body move to the nucleolus upon inhibition of proteasome-dependent protein degradation. Proc Natl Acad Sci U S A *98*, 1012-7.

May, M. J., and Ghosh, S. (1999). IkappaB kinases: kinsmen with different crafts [comment]. Science *284*, 271-3.

McKinsey, T. A., Brockman, J. A., Scherer, D. C., Al-Murrani, S. W., Green, P. L., and Ballard, D. W. (1996). Inactivation of IkappaBbeta by the tax protein of human T-cell leukemia virus type 1: a potential mechanism for constitutive induction of NF- kappaB. Mol Cell Biol *16*, 2083-90.

Mercurio, F., DiDonato, J. A., Rosette, C., and Karin, M. (1993). p105 and p98 precursor proteins play an active role in NF-kappa B- mediated signal transduction. Genes Dev *7*, 705-18.

Mercurio, F., Zhu, H., Murray, B. W., Shevchenko, A., Bennett, B. L., Li, J., Young, D. B., Barbosa, M., Mann, M., Manning, A., and Rao, A. (1997). IKK-1 and IKK-2: cytokine-activated IkappaB kinases essential for NF- kappaB activation [see comments]. Science *278*, 860-6.

Michalek, M. T., Grant, E. P., Gramm, C., Goldberg, A. L., and Rock, K. L. (1993). A role for the ubiquitin-dependent proteolytic pathway in MHC class I- restricted antigen presentation. Nature *363*, 552-4.

Miwa, M., Shimotohno, K., Hoshino, H., Fujino, M., and Sugimura, T. (1984). Detection of pX proteins in human T-cell leukemia virus (HTLV)-infected cells by using antibody against peptide deduced from sequences of X-IV DNA of HTLV-I and Xc DNA of HTLV-II proviruses. Gann *75*, 752-5.

Miyoshi, I., Kubonishi, I., Yoshimoto, S., Akagi, T., Ohtsuki, Y., Shiraishi, Y., Nagata, K., and Hinuma, Y. (1981). Type C virus particles in a cord T-cell line derived by co-cultivating normal human cord leukocytes and human leukaemic T cells. Nature *294*, 770-1.

Mo, A. X., van Lelyveld, S. F., Craiu, A., and Rock, K. L. (2000). Sequences that flank subdominant and cryptic epitopes influence the proteolytic generation of MHC class I-presented peptides. J Immunol *164*, 4003-10.

Mo, X. Y., Cascio, P., Lemerise, K., Goldberg, A. L., and Rock, K. (1999). Distinct proteolytic processes generate the C and N termini of MHC class I-binding peptides. J Immunol *163*, 5851-9.

Momburg, F., Ortiz-Navarrete, V., Neefjes, J., Goulmy, E., van de Wal, Y., Spits, H., Powis, S. J., Butcher, G. W., Howard, J. C., Walden, P., and et al. (1992). Proteasome subunits encoded by the major histocompatibility complex are not essential for antigen presentation. Nature *360*, 174-7.

Momburg, F., Roelse, J., Hammerling, G. J., and Neefjes, J. J. (1994). Peptide size selection by the major histocompatibility complex-encoded peptide transporter. J Exp Med *179*, 1613-23.

Monaco, J. J. (1992). A molecular model of MHC class-I-restricted antigen processing. Immunol Today *13*, 173-9.

Murakami, T., Hirai, H., Suzuki, T., Fujisawa, J., and Yoshida, M. (1995). HTLV-1 Tax enhances NF-kappa B2 expression and binds to the products p52 and p100, but does not suppress the inhibitory function of p100. Virology *206*, 1066-74.

Murakami, Y., Matsufuji, S., Kameji, T., Hayashi, S., Igarashi, K., Tamura, T., Tanaka, K., and Ichihara, A. (1992). Ornithine decarboxylase is degraded by the 26S proteasome without ubiquitination. Nature *360*, 597-9.

Musti, A. M., Treier, M., and Bohmann, D. (1997). Reduced ubiquitin-dependent degradation of c-Jun after phosphorylation by MAP kinases. Science *275*, 400-2.

Myung, J., Kim, K. B., Lindsten, K., Dantuma, N. P., and Crews, C. M. (2001). Lack of proteasome active site allostery as revealed by subunit-specific inhibitors. Mol Cell *7*, 411-20.

Nagashima, K., Yoshida, M., and Seiki, M. (1986). A single species of pX mRNA of human T-cell leukemia virus type I encodes trans-activator p40x and two other phosphoproteins. J Virol *60*, 394-9.

Nandi, D., Woodward, E., Ginsburg, D. B., and Monaco, J. J. (1997). Intermediates in the formation of mouse 20S proteasomes: implications for the assembly of precursor beta subunits. Embo J *16*, 5363-75.

Nakielny, S., and Dreyfuss, G. (1999). Transport of proteins and RNAs in and out of the nucleus. Cell *99*, 677-90.

Naumann, M., Nieters, A., Hatada, E. N., and Scheidereit, C. (1993). NF-kappa B precursor p100 inhibits nuclear translocation and DNA binding of NF-kappa B/rel-factors. Oncogene *8*, 2275-81.

Neefjes, J. J., Momburg, F., and Hammerling, G. J. (1993). Selective and ATP-dependent translocation of peptides by the MHC- encoded transporter [published erratum appears in Science 1994 Apr 1;264(5155):16]. Science *261*, 769-71.

Neisig, A., Roelse, J., Sijts, A. J., Ossendorp, F., Feltkamp, M. C., Kast, W. M., Melief, C. J., and Neefjes, J. J. (1995). Major differences in transporter associated with antigen presentation (TAP)-dependent translocation of MHC class I-presentable peptides and the effect of flanking sequences. J Immunol *154*, 1273-9.

Nicot, C., Tie, F., and Giam, C. Z. (1998). Cytoplasmic forms of human T-cell leukemia virus type 1 Tax induce NF- kappaB activation. J Virol *72*, 6777-84.

Niedermann, G., Butz, S., Ihlenfeldt, H. G., Grimm, R., Lucchiari, M., Hoschutzky, H., Jung, G., Maier, B., and Eichmann, K. (1995). Contribution of proteasome-mediated proteolysis to the hierarchy of epitopes presented by major histocompatibility complex class I molecules. Immunity *2*, 289-99.

Niedermann, G., Grimm, R., Geier, E., Maurer, M., Realini, C., Gartmann, C., Soll, J., Omura, S., Rechsteiner, M. C., Baumeister, W., and Eichmann, K. (1997). Potential immunocompetence of proteolytic fragments produced by proteasomes before evolution of the vertebrate immune system. J Exp Med *186*, 209-20.

Niewiesk, S., Daenke, S., Parker, C. E., Taylor, G., Weber, J., Nightingale, S., and Bangham, C. R. (1995). Naturally occurring variants of human T-cell leukemia virus type I Tax protein impair its recognition by cytotoxic T lymphocytes and the transactivation function of Tax. J Virol *69*, 2649-53.

Niewiesk, S., Daenke, S., Parker, C. E., Taylor, G., Weber, J., Nightingale, S., and Bangham, C. R. (1994). The transactivator gene of human T-cell leukemia virus type I is more variable within and between healthy carriers than patients with tropical spastic paraparesis. J Virol *68*, 6778-81.

O'Callaghan C. A., Byford, M. F., Wyer, J. R., Willcox, B. E., Jakobsen, B. K., McMichael, A. J., and Bell, J. I. (1999). BirA enzyme: production and application in the study of membrane receptor-ligand interactions by site-specific biotinylation. Anal Biochem *266*, 9-15.

Ogg, G. S., Jin, X., Bonhoeffer, S., Dunbar, P. R., Nowak, M. A., Monard, S., Segal, J. P., Cao, Y., Rowland-Jones, S. L., Cerundolo, V., Hurley, A., Markowitz, M., Ho, D. D.,

Nixon, D. F., and McMichael, A. J. (1998). Quantitation of HIV-1-specific cytotoxic T lymphocytes and plasma load of viral RNA. Science *279*, 2103-6.

Ogg, G. S., King, A. S., Dunbar, P. R., and McMichael, A. J. (1999). Isolation of HIV-1-specific cytotoxic T lymphocytes using human leukocyte antigen-coated beads. Aids *13*, 1991-3.

Ohno, M., Fornerod, M., and Mattaj, I. W. (1998). Nucleocytoplasmic transport: the last 200 nanometers. Cell *92*, 327-36.

Orian, A., Whiteside, S., Israel, A., Stancovski, I., Schwartz, A. L., and Ciechanover, A. (1995). Ubiquitin-mediated processing of NF-kappa B transcriptional activator precursor p105. Reconstitution of a cell-free system and identification of the ubiquitin-carrier protein, E2, and a novel ubiquitin-protein ligase, E3, involved in conjugation. J Biol Chem *270*, 21707-14.

Orlowski, M., Cardozo, C., and Michaud, C. (1993). Evidence for the presence of five distinct proteolytic components in the pituitary multicatalytic proteinase complex. Properties of two components cleaving bonds on the carboxyl side of branched chain and small neutral amino acids. Biochemistry *32*, 1563-72.

Ortega, J., Singh, S. K., Ishikawa, T., Maurizi, M. R., and Steven, A. C. (2000). Visualization of Substrate Binding and Translocation by the ATP- Dependent Protease, ClpXP. Mol Cell *6*, 1515-1521.

Ossendorp, F., Eggers, M., Neisig, A., Ruppert, T., Groettrup, M., Sijts, A., Mengede, E., Kloetzel, P. M., Neefjes, J., Koszinowski, U., and Melief, C. (1996). A single residue exchange within a viral CTL epitope alters proteasome- mediated degradation resulting in lack of antigen presentation. Immunity *5*, 115-24.

Ozes, O. N., Mayo, L. D., Gustin, J. A., Pfeffer, S. R., Pfeffer, L. M., and Donner, D. B. (1999). NF-kappaB activation by tumour necrosis factor requires the Akt serine-threonine kinase [see comments]. Nature *401*, 82-5.

Palmer, A., Mason, G. G., Paramio, J. M., Knecht, E., and Rivett, A. J. (1994). Changes in proteasome localization during the cell cycle. Eur J Cell Biol *64*, 163-75.

Palombella, V. J., Rando, O. J., Goldberg, A. L., and Maniatis, T. (1994). The ubiquitin-proteasome pathway is required for processing the NF- kappa B1 precursor protein and the activation of NF-kappa B. Cell *78*, 773-85.

Pamer, E., and Cresswell, P. (1998). Mechanisms of MHC class I--restricted antigen processing. Annu Rev Immunol *16*, 323-58.

Papa, F. R., Amerik, A. Y., and Hochstrasser, M. (1999). Interaction of the Doa4 deubiquitinating enzyme with the yeast 26S proteasome. Mol Biol Cell *10*, 741-56.

Parker, C. E., Daenke, S., Nightingale, S., and Bangham, C. R. (1992). Activated, HTLV-1-specific cytotoxic T-lymphocytes are found in healthy seropositives as well as in patients with tropical spastic paraparesis. Virology *188*, 628-36.

Parker, C. E., Nightingale, S., Taylor, G. P., Weber, J., and Bangham, C. R. (1994). Circulating anti-Tax cytotoxic T lymphocytes from human T-cell leukemia virus type I-infected people, with and without tropical spastic paraparesis, recognize multiple epitopes simultaneously. J Virol *68*, 2860-8.

Parker, K. C., DiBrino, M., Hull, L., and Coligan, J. E. (1992). The beta 2-microglobulin dissociation rate is an accurate measure of the stability of MHC class I heterotrimers and depends on which peptide is bound. J Immunol *149*, 1896-904.

Paz, P., Brouwenstijn, N., Perry, R., and Shastri, N. (1999). Discrete proteolytic intermediates in the MHC class I antigen processing pathway and MHC I-dependent peptide trimming in the ER. Immunity *11*, 241-51.

Pepin, N., Roulston, A., Lacoste, J., Lin, R., and Hiscott, J. (1994). Subcellular redistribution of HTLV-1 Tax protein by NF-kappa B/Rel transcription factors. Virology *204*, 706-16.

Perini, G., Wagner, S., and Green, M. R. (1995). Recognition of bZIP proteins by the human T-cell leukaemia virus transactivator Tax. Nature *376*, 602-5.

Peters, J. M. (1994). Proteasomes: protein degradation machines of the cell. Trends Biochem Sci *19*, 377-82.

Petropoulos, L., and Hiscott, J. (1998). Association between HTLV-1 Tax and I kappa B alpha is dependent on the I kappa B alpha phosphorylation state. Virology *252*, 189-99.

Phair, R. D., and Misteli, T. (2000). High mobility of proteins in the mammalian cell nucleus. Nature *404*, 604-9.

Preckel, T., Fung-Leung, W. P., Cai, Z., Vitiello, A., Salter-Cid, L., Winqvist, O., Wolfe, T. G., Von Herrath, M., Angulo, A., Ghazal, P., Lee, J. D., Fourie, A. M., Wu, Y., Pang, J., Ngo, K., Peterson, P. A., Fruh, K., and Yang, Y. (1999). Impaired immunoproteasome assembly and immune responses in PA28-/- mice. Science *286*, 2162-5.

Rammensee, H. G., Falk, K., and Rotzschke, O. (1993). Peptides naturally presented by MHC class I molecules. Annu Rev Immunol *11*, 213-44.
Rammensee, H. G., Friede, T., and Stevanoviic, S. (1995). MHC ligands and peptide motifs: first listing. Immunogenetics *41*, 178-228.

Ramos, P. C., Hockendorff, J., Johnson, E. S., Varshavsky, A., and Dohmen, R. J. (1998). Ump1p is required for proper maturation of the 20S proteasome and becomes its substrate upon completion of the assembly. Cell *92*, 489-99.

Reits, E. A., Vos, J. C., Gromme, M., and Neefjes, J. (2000). The major substrates for TAP in vivo are derived from newly synthesized proteins. Nature *404*, 774-8.

Reits, E. A. J., Benham, A. M., Plougastel, B., Neefjes, J., and Trowsdale, J. (1997). Dynamics of proteasome distribution in living cells. Embo J *16*, 6087-94.

Renard, P., Percherancier, Y., Kroll, M., Thomas, D., Virelizier, J. L., Arenzana-Seisdedos, F., and Bachelerie, F. (2000). Inducible NF-kappaB activation is permitted by simultaneous degradation of nuclear IkappaBalpha. J Biol Chem *275*, 15193-9.

Reusch, U., Muranyi, W., Lucin, P., Burgert, H. G., Hengel, H., and Koszinowski, U. H. (1999). A cytomegalovirus glycoprotein re-routes MHC class I complexes to lysosomes for degradation. Embo J *18*, 1081-91.

Richardson, J. H., Edwards, A. J., Cruickshank, J. K., Rudge, P., and Dalgleish, A. G. (1990). In vivo cellular tropism of human T-cell leukemia virus type 1. J Virol *64*, 5682-7.

Rietsch, A., and Beckwith, J. (1998). The genetics of disulfide bond metabolism. Annu Rev Genet *32*, 163-84.

Rivett, A. J. (1998). Intracellular distribution of proteasomes. Curr Opin Immunol *10*, 110-4.

Robek, M. D., and Ratner, L. (1999). Immortalization of CD4(+) and CD8(+) T lymphocytes by human T-cell leukemia virus type 1 Tax mutants expressed in a functional molecular clone. J Virol *73*, 4856-65.

Rock, K. L., and Goldberg, A. L. (1999). Degradation of cell proteins and the generation of MHC class I- presented peptides. Annu Rev Immunol *17*, 739-79.

Rock, K. L., Gramm, C., Rothstein, L., Clark, K., Stein, R., Dick, L., Hwang, D., and Goldberg, A. L. (1994). Inhibitors of the proteasome block the degradation of most cell proteins and the generation of peptides presented on MHC class I molecules. Cell *78*, 761-71.

Rodriguez, M. S., Thompson, J., Hay, R. T., and Dargemont, C. (1999). Nuclear retention of IkappaBalpha protects it from signal-induced degradation and inhibits nuclear factor kappaB transcriptional activation. J Biol Chem *274*, 9108-15.

Rodriguez, M. S., Wright, J., Thompson, J., Thomas, D., Baleux, F., Virelizier, J. L., Hay, R. T., and Arenzana-Seisdedos, F. (1996). Identification of lysine residues required for signal-induced ubiquitination and degradation of I kappa B-alpha in vivo. Oncogene *12*, 2425-35.

Rogers, S., Wells, R., and Rechsteiner, M. (1986). Amino acid sequences common to rapidly degraded proteins: the PEST hypothesis. Science *234*, 364-8.

Rossi, F., Evstafieva, A., Pedrali-Noy, G., Gallina, A., and Milanesi, G. (1997). HsN3 proteasomal subunit as a target for human immunodeficiency virus type 1 Nef protein. Virology *237*, 33-45.

Roth, M. B., Zahler, A. M., and Stolk, J. A. (1991). A conserved family of nuclear phosphoproteins localized to sites of polymerase II transcription. J Cell Biol *115*, 587-96.

Rothwarf, D. M., Zandi, E., Natoli, G., and Karin, M. (1998). IKK-gamma is an essential regulatory subunit of the IkappaB kinase complex [see comments]. Nature *395*, 297-300.

Rousset, R., Desbois, C., Bantignies, F., and Jalinot, P. (1996). Effects on NF-kappa B1/p105 processing of the interaction between the HTLV-1 transactivator Tax and the proteasome. Nature *381*, 328-31.

Satoh, K., Sasajima, H., Nyoumura, K. I., Yokosawa, H., and Sawada, H. (2001). Assembly of the 26S proteasome is regulated by phosphorylation of the p45/Rpt6 ATPase subunit. Biochemistry *40*, 314-9.

Scherer, D. C., Brockman, J. A., Chen, Z., Maniatis, T., and Ballard, D. W. (1995). Signal-induced degradation of I kappa B alpha requires site-specific ubiquitination. Proc Natl Acad Sci U S A *92*, 11259-63.

Schmidtke, G., Emch, S., Groettrup, M., and Holzhutter, H. G. (2000). Evidence for the existence of a non-catalytic modifier site of peptide hydrolysis by the 20 S proteasome. J Biol Chem *275*, 22056-63.

Schubert, U., Anton, L. C., Gibbs, J., Norbury, C. C., Yewdell, J. W., and Bennink, J. R. (2000). Rapid degradation of a large fraction of newly synthesized proteins by proteasomes. Nature *404*, 770-4.

Schwarz, K., de Giuli, R., Schmidtke, G., Kostka, S., van den Broek, M., Kim, K. B., Crews, C. M., Kraft, R., and Groettrup, M. (2000). The selective proteasome inhibitors lactacystin and epoxomicin can be used to either up- or down-regulate antigen presentation at nontoxic doses. J Immunol *164*, 6147-57.

Schwarz, K., Eggers, M., Soza, A., Koszinowski, U. H., Kloetzel, P. M., and Groettrup, M. (2000). The proteasome regulator PA28alpha/beta can enhance antigen presentation without affecting 20S proteasome subunit composition. Eur J Immunol *30*, 3672-9.

Schwarz, K., van Den Broek, M., Kostka, S., Kraft, R., Soza, A., Schmidtke, G., Kloetzel, P. M., and Groettrup, M. (2000). Overexpression of the proteasome subunits LMP2, LMP7, and MECL-1, but not PA28 alpha/beta, enhances the presentation of an immunodominant lymphocytic choriomeningitis virus T cell epitope. J Immunol *165*, 768-78.

Seeger, M., Ferrell, K., Frank, R., and Dubiel, W. (1997). HIV-1 tat inhibits the 20 S proteasome and its 11 S regulator-mediated activation. J Biol Chem *272*, 8145-8.

Semmes, O. J., and Jeang, K. T. (1992). HTLV-I Tax is a zinc-binding protein: role of zinc in Tax structure and function. Virology *188*, 754-64.

Semmes, O. J., and Jeang, K. T. (1992). Mutational analysis of human T-cell leukemia virus type I Tax: regions necessary for function determined with 47 mutant proteins. J Virol *66*, 7183-92.

Seufert, W., Futcher, B., and Jentsch, S. (1995). Role of a ubiquitin-conjugating enzyme in degradation of S- and M-phase cyclins. Nature *373*, 78-81.

Sewell, A. K., Price, D. A., Teisserenc, H., Booth, B. L., Gileadi, U., Flavin, F. M., Trowsdale, J., Phillips, R. E., and Cerundolo, V. (1999). IFN-gamma exposes a cryptic cytotoxic T lymphocyte epitope in HIV-1 reverse transcriptase. J Immunol *162*, 7075-9.

Sharipo, A., Imreh, M., Leonchiks, A., Imreh, S., and Masucci, M. G. (1998). A minimal glycine-alanine repeat prevents the interaction of ubiquitinated I kappaB alpha with the proteasome: a new mechanism for selective inhibition of proteolysis [see comments]. Nat Med *4*, 939-44.

Sheaff, R. J., Singer, J. D., Swanger, J., Smitherman, M., Roberts, J. M., and Clurman, B. E. (2000). Proteasomal turnover of p21Cip1 does not require p21Cip1 ubiquitination. Mol Cell *5*, 403-10.

Sibille, C., Gould, K. G., Willard-Gallo, K., Thomson, S., Rivett, A. J., Powis, S., Butcher, G. W., and De Baetselier, P. (1995). LMP2+ proteasomes are required for the presentation of specific antigens to cytotoxic T lymphocytes. Curr Biol *5*, 923-30.

Siekevitz, M., Feinberg, M. B., Holbrook, N., Wong-Staal, F., and Greene, W. C. (1987). Activation of interleukin 2 and interleukin 2 receptor (Tac) promoter expression by the trans-activator (tat) gene product of human T-cell leukemia virus, type I. Proc Natl Acad Sci U S A *84*, 5389-93.

Siekevitz, M., Josephs, S. F., Dukovich, M., Peffer, N., Wong-Staal, F., and Greene, W. C. (1987). Activation of the HIV-1 LTR by T cell mitogens and the trans-activator protein of HTLV-I [published erratum appears in Science 1988 Jan 29;239(4839):451]. Science *238*, 1575-8.

Sijts, A. J., Ruppert, T., Rehermann, B., Schmidt, M., Koszinowski, U., and Kloetzel, P. M. (2000). Efficient generation of a hepatitis B virus cytotoxic T lymphocyte epitope requires the structural features of immunoproteasomes. J Exp Med *191*, 503-14.

Slamon, D. J., Boyle, W. J., Keith, D. E., Press, M. F., Golde, D. W., and Souza, L. M. (1988). Subnuclear localization of the trans-activating protein of human T-cell leukemia virus type I. J Virol *62*, 680-6.

Slamon, D. J., Press, M. F., Souza, L. M., Murdock, D. C., Cline, M. J., Golde, D. W., Gasson, J. C., and Chen, I. S. (1985). Studies of the putative transforming protein of the type I human T-cell leukemia virus. Science *228*, 1427-30.

Smith, M. R., and Greene, W. C. (1992). Characterization of a novel nuclear localization signal in the HTLV-I tax transactivator protein. Virology *187*, 316-20.

Smith, M. R., and Greene, W. C. (1990). Identification of HTLV-I tax trans-activator mutants exhibiting novel transcriptional phenotypes [published errata appear in Genes Dev 1991 Jan;5(1):150 and 1995 Sep 15;9(18):2324]. Genes Dev *4*, 1875-85.

Smith, M. R., and Greene, W. C. (1991). Molecular biology of the type I human T-cell leukemia virus (HTLV-I) and adult T-cell leukemia. J Clin Invest *87*, 761-6.

Snyder, H. L., Yewdell, J. W., and Bennink, J. R. (1994). Trimming of antigenic peptides in an early secretory compartment. J Exp Med *180*, 2389-94.

Sodroski, J., Rosen, C., Goh, W. C., and Haseltine, W. (1985). A transcriptional activator protein encoded by the x-lor region of the human T-cell leukemia virus. Science *228*, 1430-4.

Sommerfelt, M. A., Williams, B. P., Clapham, P. R., Solomon, E., Goodfellow, P. N., and Weiss, R. A. (1988). Human T cell leukemia viruses use a receptor determined by human chromosome 17. Science *242*, 1557-9.

Song, X., Mott, J. D., von Kampen, J., Pramanik, B., Tanaka, K., Slaughter, C. A., and DeMartino, G. N. (1996). A model for the quaternary structure of the proteasome activator PA28. J Biol Chem *271*, 26410-7.

Song, X., von Kampen, J., Slaughter, C. A., and DeMartino, G. N. (1997). Relative functions of the alpha and beta subunits of the proteasome activator, PA28. J Biol Chem *272*, 27994-8000.

Spies, T., Cerundolo, V., Colonna, M., Cresswell, P., Townsend, A., and DeMars, R. (1992). Presentation of viral antigen by MHC class I molecules is dependent on a putative peptide transporter heterodimer. Nature *355*, 644-6.

Stohwasser, R., Salzmann, U., Giesebrecht, J., Kloetzel, P. M., and Holzhutter, H. G. (2000). Kinetic evidences for facilitation of peptide channelling by the proteasome activator PA28. Eur J Biochem *267*, 6221-30.

Stoltze, L., Nussbaum, A. K., Sijts, A., Emmerich, N. P., Kloetzel, P. M., and Schild, H. (2000). The function of the proteasome system in MHC class I antigen processing. Immunol Today *21*, 317-9.

Sun, S. C., Elwood, J., Beraud, C., and Greene, W. C. (1994). Human T-cell leukemia virus type I Tax activation of NF-kappa B/Rel involves phosphorylation and degradation of I kappa B alpha and RelA (p65)-mediated induction of the c-rel gene. Mol Cell Biol *14*, 7377-84.

Sun, S. C., Ganchi, P. A., Ballard, D. W., and Greene, W. C. (1993). NF-kappa B controls expression of inhibitor I kappa B alpha: evidence for an inducible autoregulatory pathway. Science *259*, 1912-5.

Sun, S. C., Ganchi, P. A., Beraud, C., Ballard, D. W., and Greene, W. C. (1994). Autoregulation of the NF-kappa B transactivator RelA (p65) by multiple cytoplasmic inhibitors containing ankyrin motifs. Proc Natl Acad Sci U S A *91*, 1346-50.

Suzuki, T., Fujisawa, J. I., Toita, M., and Yoshida, M. (1993). The trans-activator tax of human T-cell leukemia virus type 1 (HTLV-1) interacts with cAMP-responsive element (CRE) binding and CRE modulator proteins that bind to the 21-base-pair enhancer of HTLV-1. Proc Natl Acad Sci U S A *90*, 610-4.

Suzuki, T., Hirai, H., Fujisawa, J., Fujita, T., and Yoshida, M. (1993). A trans-activator Tax of human T-cell leukemia virus type 1 binds to NF- kappa B p50 and serum response factor (SRF) and associates with enhancer DNAs of the NF-kappa B site and CArG box. Oncogene *8*, 2391-7.

Suzuki, T., Hirai, H., Murakami, T., and Yoshida, M. (1995). Tax protein of HTLV-1 destabilizes the complexes of NF-kappa B and I kappa B-alpha and induces nuclear translocation of NF-kappa B for transcriptional activation. Oncogene *10*, 1199-207.

Suzuki, T., Hirai, H., and Yoshida, M. (1994). Tax protein of HTLV-1 interacts with the Rel homology domain of NF- kappa B p65 and c-Rel proteins bound to the NF-kappa B binding site and activates transcription. Oncogene *9*, 3099-105.

Takebe, Y., Seiki, M., Fujisawa, J., Hoy, P., Yokota, K., Arai, K., Yoshida, M., and Arai, N. (1988). SR alpha promoter: an efficient and versatile mammalian cDNA expression system composed of the simian virus 40 early promoter and the R-U5 segment of human T-cell leukemia virus type 1 long terminal repeat. Mol Cell Biol *8*, 466-72.

Tanaka, A., Takahashi, C., Yamaoka, S., Nosaka, T., Maki, M., and Hatanaka, M. (1990). Oncogenic transformation by the tax gene of human T-cell leukemia virus type I in vitro. Proc Natl Acad Sci U S A *87*, 1071-5.

Thrower, J. S., Hoffman, L., Rechsteiner, M., and Pickart, C. M. (2000). Recognition of the polyubiquitin proteolytic signal. Embo J *19*, 94-102.

Tobery, T. W., and Siliciano, R. F. (1997). Targeting of HIV-1 antigens for rapid intracellular degradation enhances cytotoxic T lymphocyte (CTL) recognition and the induction of de novo CTL responses in vivo after immunization. J Exp Med *185*, 909-20.

Tojima, Y., Fujimoto, A., Delhase, M., Chen, Y., Hatakeyama, S., Nakayama, K., Kaneko, Y., Nimura, Y., Motoyama, N., Ikeda, K., Karin, M., and Nakanishi, M. (2000). NAK is an IkappaB kinase-activating kinase. Nature *404*, 778-82.

Tomazin, R., Hill, A. B., Jugovic, P., York, I., van Endert, P., Ploegh, H. L., Andrews, D. W., and Johnson, D. C. (1996). Stable binding of the herpes simplex virus ICP47 protein to the peptide binding site of TAP. Embo J *15*, 3256-66.

Tongaonkar, P., Chen, L., Lambertson, D., Ko, B., and Madura, K. (2000). Evidence for an interaction between ubiquitin-conjugating enzymes and the 26S proteasome. Mol Cell Biol *20*, 4691-8.

Tortorella, D., Gewurz, B. E., Furman, M. H., Schust, D. J., and Ploegh, H. L. (2000). Viral subversion of the immune system. Annu Rev Immunol *18*, 861-926.

Townsend, A., Bastin, J., Gould, K., Brownlee, G., Andrew, M., Coupar, B., Boyle, D., Chan, S., and Smith, G. (1988). Defective presentation to class I-restricted cytotoxic T lymphocytes in vaccinia-infected cells is overcome by enhanced degradation of antigen. J Exp Med *168*, 1211-24.

Townsend, A., Ohlen, C., Bastin, J., Ljunggren, H. G., Foster, L., and Karre, K. (1989). Association of class I major histocompatibility heavy and light chains induced by viral peptides [see comments]. Nature *340*, 443-8.

Townsend, A. R., Gotch, F. M., and Davey, J. (1985). Cytotoxic T cells recognize fragments of the influenza nucleoprotein. Cell *42*, 457-67.

Townsend, A. R., Rothbard, J., Gotch, F. M., Bahadur, G., Wraith, D., and McMichael, A. J. (1986). The epitopes of influenza nucleoprotein recognized by cytotoxic T lymphocytes can be defined with short synthetic peptides. Cell *44*, 959-68.

Turnell, A. S., Grand, R. J., Gorbea, C., Zhang, X., Wang, W., Mymryk, J. S., and Gallimore, P. H. (2000). Regulation of the 26S proteasome by adenovirus E1A. Embo J *19*, 4759-73.

Turner, G. C., and Varshavsky, A. (2000). Detecting and measuring cotranslational protein degradation in vivo. Science *289*, 2117-20.

Uchiyama, T., Yodoi, J., Sagawa, K., Takatsuki, K., and Uchino, H. (1977). Adult T-cell leukemia: clinical and hematologic features of 16 cases. Blood *50*, 481-92.

Uhlik, M., Good, L., Xiao, G., Harhaj, E. W., Zandi, E., Karin, M., and Sun, S. C. (1998). NF-kappaB-inducing kinase and IkappaB kinase participate in human T- cell leukemia virus I Tax-mediated NF-kappaB activation. J Biol Chem *273*, 21132-6.

Ureta-Vidal, A., Pique, C., Garcia, Z., Dehee, A., Tortevoye, P., Desire, N., Gessain, A., Chancerel, B., Gout, O., Lemonnier, F. A., and Cochet, M. (2001). Human T cell leukemia virus Type I (HTLV-I) infection induces greater expansions of CD8 T lymphocytes in persons with HTLV-I-associated myelopathy/tropical spastic paraparesis than in asymptomatic carriers. J Infect Dis *183*, 857-64.

Utz, U., Banks, D., Jacobson, S., and Biddison, W. E. (1996). Analysis of the T-cell receptor repertoire of human T-cell leukemia virus type 1 (HTLV-1) Tax-specific CD8+ cytotoxic T lymphocytes from patients with HTLV-1-associated disease: evidence for oligoclonal expansion. J Virol *70*, 843-51.

Van Kaer, L., Ashton-Rickardt, P. G., Eichelberger, M., Gaczynska, M., Nagashima, K., Rock, K. L., Goldberg, A. L., Doherty, P. C., and Tonegawa, S. (1994). Altered peptidase and viral-specific T cell response in LMP2 mutant mice. Immunity *1*, 533-41.

van Nocker, S., Sadis, S., Rubin, D. M., Glickman, M., Fu, H., Coux, O., Wefes, I., Finley, D., and Vierstra, R. D. (1996). The multiubiquitin-chain-binding protein Mcb1 is a component of the 26S proteasome in Saccharomyces cerevisiae and plays a nonessential, substrate-specific role in protein turnover. Mol Cell Biol *16*, 6020-8.

Verma, I. M., Stevenson, J. K., Schwarz, E. M., Van Antwerp, D., and Miyamoto, S. (1995). Rel/NF-kappa B/I kappa B family: intimate tales of association and dissociation. Genes Dev *9*, 2723-35.

Vijh, S., Pilip, I. M., and Pamer, E. G. (1998). Effect of antigen-processing efficiency on in vivo T cell response magnitudes. J Immunol *160*, 3971-7.

Vinitsky, A., Anton, L. C., Snyder, H. L., Orlowski, M., Bennink, J. R., and Yewdell, J. W. (1997). The generation of MHC class I-associated peptides is only partially inhibited by proteasome inhibitors: involvement of nonproteasomal cytosolic proteases in antigen processing? J Immunol *159*, 554-64.

Wagner, S., and Green, M. R. (1993). HTLV-I Tax protein stimulation of DNA binding of bZIP proteins by enhancing dimerization. Science *262*, 395-9.

Wang, E. W., Kessler, B. M., Borodovsky, A., Cravatt, B. F., Bogyo, M., Ploegh, H. L., and Glas, R. (2000). Integration of the ubiquitin-proteasome pathway with a cytosolic oligopeptidase activity. Proc Natl Acad Sci U S A *97*, 9990-5.

Wenzel, T., and Baumeister, W. (1995). Conformational constraints in protein degradation by the 20S proteasome. Nat Struct Biol *2*, 199-204.

Whelan, J. A., Dunbar, P. R., Price, D. A., Purbhoo, M. A., Lechner, F., Ogg, G. S., Griffiths, G., Phillips, R. E., Cerundolo, V., and Sewell, A. K. (1999). Specificity of CTL interactions with peptide-MHC class I tetrameric complexes is temperature dependent. J Immunol *163*, 4342-8.

Whitby, F. G., Masters, E. I., Kramer, L., Knowlton, J. R., Yao, Y., Wang, C. C., and Hill, C. P. (2000). Structural basis for the activation of 20S proteasomes by 11S regulators. Nature *408*, 115-20.

Wiertz, E. J., Jones, T. R., Sun, L., Bogyo, M., Geuze, H. J., and Ploegh, H. L. (1996). The human cytomegalovirus US11 gene product dislocates MHC class I heavy chains from the endoplasmic reticulum to the cytosol. Cell *84*, 769-79.

Wiertz, E. J., Tortorella, D., Bogyo, M., Yu, J., Mothes, W., Jones, T. R., Rapoport, T. A., and Ploegh, H. L. (1996). Sec61-mediated transfer of a membrane protein from the endoplasmic reticulum to the proteasome for destruction [see comments]. Nature *384*, 432-8.

Wigley, W. C., Fabunmi, R. P., Lee, M. G., Marino, C. R., Muallem, S., DeMartino, G. N., and Thomas, P. J. (1999). Dynamic association of proteasomal machinery with the centrosome. J Cell Biol *145*, 481-90.

Winston, J. T., Strack, P., Beer-Romero, P., Chu, C. Y., Elledge, S. J., and Harper, J. W. (1999). The SCFbeta-TRCP-ubiquitin ligase complex associates specifically with phosphorylated destruction motifs in IkappaBalpha and beta-catenin and stimulates IkappaBalpha ubiquitination in vitro [published erratum appears in Genes Dev 1999 Apr 15;13(8):1050]. Genes Dev *13*, 270-83.

Woronicz, J. D., Gao, X., Cao, Z., Rothe, M., and Goeddel, D. V. (1997). IkappaB kinase-beta: NF-kappaB activation and complex formation with IkappaB kinase-alpha and NIK [see comments]. Science *278*, 866-9.

Wucherpfennig, K. W., and Strominger, J. L. (1995). Molecular mimicry in T cell-mediated autoimmunity: viral peptides activate human T cell clones specific for myelin basic protein. Cell *80*, 695-705.

Xie, Y., and Varshavsky, A. (2000). Physical association of ubiquitin ligases and the 26S proteasome. Proc Natl Acad Sci U S A *97*, 2497-502.

Xie, Y., and Varshavsky, A. (2001). RPN4 is a ligand, substrate, and transcriptional regulator of the 26S proteasome: A negative feedback circuit. Proc Natl Acad Sci U S A *98*, 3056-61.

Yamaoka, S., Courtois, G., Bessia, C., Whiteside, S. T., Weil, R., Agou, F., Kirk, H. E., Kay, R. J., and Israel, A. (1998). Complementation cloning of NEMO, a component of the IkappaB kinase complex essential for NF-kappaB activation. Cell *93*, 1231-40.

Yamaoka, S., Inoue, H., Sakurai, M., Sugiyama, T., Hazama, M., Yamada, T., and Hatanaka, M. (1996). Constitutive activation of NF-kappa B is essential for transformation of rat fibroblasts by the human T-cell leukemia virus type I Tax protein. Embo J *15*, 873-87.

Yan, J. P., Garrus, J. E., Giebler, H. A., Stargell, L. A., and Nyborg, J. K. (1998). Molecular interactions between the coactivator CBP and the human T-cell leukemia virus Tax protein. J Mol Biol *281*, 395-400.

Yang, B., Hahn, Y. S., Hahn, C. S., and Braciale, T. J. (1996). The requirement for proteasome activity class I major histocompatibility complex antigen presentation is dictated by the length of preprocessed antigen. J Exp Med *183*, 1545-52.

Yang, Y., Fruh, K., Ahn, K., and Peterson, P. A. (1995). In vivo assembly of the proteasomal complexes, implications for antigen processing. J Biol Chem *270*, 27687-94.

Yano, M., Mori, S., and Kido, H. (1999). Intrinsic nucleoside diphosphate kinase-like activity is a novel function of the 20 S proteasome. J Biol Chem *274*, 34375-82.

Yao, J., and Wigdahl, B. (2000). Human T cell lymphotropic virus type I genomic expression and impact on intracellular signaling pathways during neurodegenerative disease and leukemia. Front Biosci *5*, D138-68.

Yaron, A., Hatzubai, A., Davis, M., Lavon, I., Amit, S., Manning, A. M., Andersen, J. S., Mann, M., Mercurio, F., and Ben-Neriah, Y. (1998). Identification of the receptor component of the IkappaBalpha-ubiquitin ligase. Nature *396*, 590-4.

Yellen-Shaw, A. J., Wherry, E. J., Dubois, G. C., and Eisenlohr, L. C. (1997). Point mutation flanking a CTL epitope ablates in vitro and in vivo recognition of a full-length viral protein. J Immunol *158*, 3227-34.

Yewdell, J. W., Anton, L. C., and Bennink, J. R. (1996). Defective ribosomal products (DRiPs): a major source of antigenic peptides for MHC class I molecules? J Immunol *157*, 1823-6.

Yewdell, J. W., and Bennink, J. R. (1999). Immunodominance in major histocompatibility complex class I-restricted T lymphocyte responses. Annu Rev Immunol *17*, 51-88.

Yin, M. J., Christerson, L. B., Yamamoto, Y., Kwak, Y. T., Xu, S., Mercurio, F., Barbosa, M., Cobb, M. H., and Gaynor, R. B. (1998). HTLV-I Tax protein binds to MEKK1 to stimulate IkappaB kinase activity and NF-kappaB activation. Cell *93*, 875-84.

Yoshida, M. (2001). Multiple viral strategies of htlv-1 for dysregulation of cell growth control. Annu Rev Immunol *19*, 475-96.

Yoshida, M., Miyoshi, I., and Hinuma, Y. (1982). Isolation and characterization of retrovirus from cell lines of human adult T-cell leukemia and its implication in the disease. Proc Natl Acad Sci U S A *79*, 2031-5.

Zandi, E., Rothwarf, D. M., Delhase, M., Hayakawa, M., and Karin, M. (1997). The IkappaB kinase complex (IKK) contains two kinase subunits, IKKalpha and IKKbeta, necessary for IkappaB phosphorylation and NF-kappaB activation. Cell *91*, 243-52.

Zhang, Z., Torii, N., Furusaka, A., Malayaman, N., Hu, Z., and Liang, T. J. (2000). Structural and functional characterization of interaction between hepatitis B virus X protein and the proteasome complex. J Biol Chem *275*, 15157-65.

Zhao, L. J., and Giam, C. Z. (1992). Human T-cell lymphotropic virus type I (HTLV-I) transcriptional activator, Tax, enhances CREB binding to HTLV-I 21-base-pair repeats by protein-protein interaction. Proc Natl Acad Sci U S A *89*, 7070-4.

Zhao, L. J., and Giam, C. Z. (1991). Interaction of the human T-cell lymphotrophic virus type I (HTLV-I) transcriptional activator Tax with cellular factors that bind specifically to the 21-base-pair repeats in the HTLV-I enhancer. Proc Natl Acad Sci U S A *88*, 11445-9.

Zhao, L. J., and Padmanabhan, R. (1988). Nuclear transport of adenovirus DNA polymerase is facilitated by interaction with preterminal protein. Cell *55*, 1005-15.

Zheng, P., Guo, Y., Niu, Q., Levy, D. E., Dyck, J. A., Lu, S., Sheiman, L. A., and Liu, Y. (1998). Proto-oncogene PML controls genes devoted to MHC class I antigen presentation. Nature *396*, 373-6.

Ziegler, H., Thale, R., Lucin, P., Muranyi, W., Flohr, T., Hengel, H., Farrell, H., Rawlinson, W., and Koszinowski, U. H. (1997). A mouse cytomegalovirus glycoprotein retains MHC class I complexes in the ERGIC/cis-Golgi compartments. Immunity *6*, 57-66.

Zinkernagel, R. M., Bachmann, M. F., Kundig, T. M., Oehen, S., Pirchet, H., and Hengartner, H. (1996). On immunological memory. Annu Rev Immunol *14*, 333-67.